The progression of epileptogenesis in cultured juvenile rodent slices

Ellen Black

Doctor of Philosophy

Aston University

September 2023

Aston University

The Progression of Epileptogenesis in Cultured Juvenile Rodent Slices

Ellen Black

Doctor of Philosophy, 2023

Abstract

The investigation of the brain's physiological activity is subject to a range of compromises; the fidelity and spatial resolution of data from cells and networks must be balanced with maintaining as natural an environment and as much connectivity as possible. This is further complicated when measuring aberrant cellular and network activity in models of neurological conditions such as epilepsy or performing longitudinal studies looking at drug treatment or the development of recurrent seizure-like events.

This thesis will present the deployment and optimisation of an organotypic slice culture preparation, using both rodent tissue and slices created from tissue blocks taken from human paediatric epilepsy patients experiencing refractory seizures. The naïve rodent tissue can be maintained relatively easily in a physiological state or provoked into exhibiting spontaneous recurrent seizure-like events which are responsive to a variety of pharmacological treatments both acutely and over days/weeks of treatment. This approach in rodent slice cultures allows for experimental manipulation of brain tissue rapidly, repeatably and over a longer time-period than an acute slice preparation would allow as slices were viable for testing for up to 2 weeks post extraction. However, human tissue slices were more difficult to obtain and to maintain in culture, making them significantly more difficult to obtain results of pharmacological activity from.

The process of optimisation, including the assessment of various culture mediums, different ages of animal, antibiotic testing, and experimenting with new materials for culture substrates, is discussed and the preparation tested with a range of common anti-epileptic drugs, as well as the development of epileptiform activity being followed via cellular and network-level *in vitro* electrophysiology.

The novel antiepileptic drugs that will be tested the tricyclic antidepressant tianeptine and the anorectic dexfenfluramine, as they have both shown potential to be. These drugs were tested both acutely and at a low concentration applied chronically to the organotypic cultures. The results obtained from these studies illustrate the advantage of the culture approach with longitudinal dosing showing promising results in our hands. The finding in this thesis suggest that dexfenfluramine shows promise as a therapeutic treatment for epilepsy, results obtained when testing tianeptine were much more variable, but they do indicate that at administered chronically at low doses tianeptine suppresses seizure activity.

Acknowledgements

I would like to thank my supervisors, Dr Stuart Greenhill and Professor Gavin Woodhall, for all of their help and support throughout the duration of this project – they really went above and beyond, and I cannot thank them enough. I also need to give a big thank you to the various members of lab 351, specifically Nicole Marley, Beth Rees, Divya Dhangar, Max Wilson, Laura Harvey and Hannah Somerfield for their encouragement, patience and friendship through the good times and the hard times.

Another thanks must go to the staff of the Aston Biomedical Unit – Wayne, Matt and Kat – for their tireless work in supporting research here and to all the support staff in the office and technical teams who helped us with purchasing, maintenance and all the other things that a PhD depends upon.

Finally, none of this would have been possible without the love and support of my family and friends, so a big thank you must go out to my Mum, Dad, and sisters (Laura, Rebecca, and Cathy) for their belief in me and words of encouragement throughout. To my friends thanks for putting up with me on the bad days and cheering me on through the good ones, and a special thank you to Alice for always being there for me and giving me a place to stay when visits to Birmingham were required. Lastly, I want to thank my partner, Lewis, for all of the patience and kindness he has shown throughout this PhD.

Abbreviations

aCSF – artificial cerebrospinal fluid

AD – Alzheimer's disease

AED – anti-epileptic drug

AMC – aged-matched control

AMPA(r) – α-amino-3-hydroxy-5-methyl-4-isoxazolepropionic acid (receptor)

BBB – blood-brain barrier

CA1 – cornu ammonis subfield 1

CA3 - cornu ammonis subfield 3

CNS – central nervous system

DG – dentate gyrus

DS – Dravet Syndrome

(m)EC – (medial) entorhinal cortex

(s)EPSC – (spontaneous) excitatory postsynaptic current

(s) EPSP – (spontaneous) excitatory postsynaptic potential

GABA(r) – gamma-aminobutyric acid (receptor)

HT – human tissue

IEI – inter-event interval

ING – interneuron network gamma

(s)IPSC – (spontaneous) inhibitory postsynaptic current

(s)IPSP - (spontaneous) inhibitory postsynaptic potential

KA(r) – kainic acid (receptor)

LFP – local field potential

LGS – Lennox Gastaut Syndrome

LTD – long term depression

LTP – long term potentiation

MOA – mechanism of action

NMDA(r) – N-methyl-D-aspartate (receptor)

PING – pyramidal network interneuron gamma

SE – status epilepticus

SEM – standard error of the mean

SLE – seizure-like events

SMA – supplementary motor area

SRS – spontaneous recurrent seizures

TLE – temporal lobe epilepsy

Table of Contents

Table of Figures

Chapter 1: Introduction

The mammalian brain is one of the most complex objects known to humankind. Within its structures and networks, a wide variety of neurons are constantly communicating with one another via the transfer of neurotransmitters and electrical impulses, integrating this information and responding to its summation over time, leading to emergent network activity. This emergent activity presents itself as rhythmic patterns of neural activity known as neuronal oscillations, created by thousands of individual electrical impulses which work together to create complex waveforms that neurons within the brain use to communicate over long distances and co-ordinate their activity. These oscillations are produced in the brain, spinal cord and autonomic nervous system and reflect a balance of interactions between excitation and inhibition with the brain, where, during an oscillation cycle excitation and inhibition occur at different phases. Depending on their type and frequency, neuronal oscillations are driven by intrinsic mechanisms within individual neurons, such as ionic currents, or by interactions between populations of neurons, and thus enable the synchronisation of neuronal activity across brain regions to promote precise coordination of the neural processes which underpin the basis of cognition, memory, behaviour, and movement. Yet, despite being so integral to the fundamental function of the brain, very little is currently known about the molecular and even cellular basis of mechanisms fundamental to the generation and control of neuronal oscillations.

The concept of 'brain waves' predates the notion of neuronal oscillations, posited originally in the 19th century as the basis of non-verbal communication, or even as a mystical telepathic link. The first human brain oscillations were recorded by Hans Berger and colleagues in the late 1920s using an electroencephalograph (EEG) and following this discovery more scientifically based phenomena have come to be referred to as brain waves. Throughout the last 100 years, there has been an increasing body of evidence that neurons within the brain act collectively as groups of networks at various levels of organisation, which oscillate synchronously to facilitate cognitive function, known as neuronal networks (Jermakowwicz et al., 2007; Lisman, 2015). Neuronal networks can in turn define cellular-level activity via interactions between inhibitory and excitatory neurons (Gansel, 2022). Excitatory neurons mediate increased excitability by releasing neurotransmitters such as glutamate, provoking membrane depolarisation. Inhibitory neurons act in opposition to this, decreasing postsynaptic excitability via the release of gamma aminobutyric acid (GABA) which binds to GABA receptors at the synapse causing activation and opening of chloride or potassium channels, leading to a hyperpolarisation of the membrane and a lower likelihood of action potential threshold being reached. Neuronal networks within the brain communicate locally, but they also have the ability to facilitate communication between distal regions of the brain. The activity of neuronal networks is

highly dynamic and varies depending on which class of neurons are involved and their localisation within the brain, along with the state of the brain itself (movement, concentration, sleep, memory formation etc.) and the stage of organismal development; only select sub-populations of neurons contribute to the function of a network in any given system.

Disruptions to cellular or network neuronal activity can cause oscillations to become desynchronised which can lead to the development of abnormal neurological processes. Excessive or irregular synchrony of neurons can lead to the generation of epilepsy, a neurological disorder characterised by recurrent seizure activity. Seizures are characterized by abnormal, synchronized electrical activity in the brain, during a seizure neurons fire in a hyper-synchronised manner leading to intense bursts of oscillatory activity that can manifest as high-frequency waves (80-500Hz) and are typically localized to specific brain regions. Seizures disrupt normal brain function and can result in numerous different symptoms depending on the brain area affected and the underlying pathology, including uncontrolled movement of the body, loss of consciousness or sensory disturbances (Aur et al., 2010; Liu et al., 2018). The root cause of this network dysfunction can be genetic, environmental or developmental, and dictates the type, severity and age-dependence of the epileptic activity.

Both the electrical and behavioural aspects of seizure activity and epilepsy are complex and our understanding of the cellular and network processes that cause them are limited. Much of the research that has been carried out to aid our understanding of these processes has involved the use of animal models of epilepsy that make use of several tools including electrical stimulation, traumatic brain injury, genetic manipulation, or the use of chemoconvulsants to induce seizure-like activity and allow these processes to be investigated. Organotypic brain slice cultures represent a physiologically relevant 3D model of the brain as they contain all CNS cell types and can be produced from brain areas involved in neurodegenerative disorders, such as epilepsy. These cultures provide a valuable ex vivo platform for studying the mechanisms of neurological diseases and screening potential therapeutics prior to in vivo experiments (Croft et al., 2019). Carrying out experiments in models like this reduces the number of animals needed for experimentation and allows for rapid manipulation of the experimental environment without requiring a consideration of the metabolism or bioavailability of the pharmacological tools used. *In vitro* studies have also been carried out on resected human brain tissue taken from patients with intractable epilepsies. Such studies provide a valuable indication of what happens *in vivo* in epilepsy patients on both a cellular and local network level, though, this tissue is difficult to access and can be highly variable or sparsely populated with neurons depending on the

pathology of the patient.

This thesis will work to optimise the culture conditions of organotypic brain slices to induce spontaneous seizure like events in these cultures. *In vitro* electrophysiology techniques to explore the process of epileptogenesis in organotypic slice cultures, assess their usefulness in the drug screening process and culture human brain tissue using the same methodology. This research is focused on giving a better insight into the development of epilepsy in humans, whilst working towards reducing the number of animals necessary for neuroscience research.

1.1 Glutamatergic and GABAergic mechanisms of oscillation:

Glutamate and GABA are two neurotransmitters that play a key role in the emergence of neuronal oscillations, they are chemical messengers that facilitate communication between neurons by travelling across synapses to allow signals to pass from one neuron to another. Glutamate receptors shape neuronal oscillations by regulating synaptic strength and excitability, while GABA receptors contribute to maintaining the balance of inhibitory and excitatory networks. The interactions between glutamate and GABA shape brain function and imbalances in glutamatergic and GABAergic signaling are associated with a variety of neurological disorders.

1.1.1 Glutamate:

Glutamate is the most abundant excitatory neurotransmitter in the mammalian central nervous system (CNS), with the majority of excitatory neurons in the CNS being glutamatergic (Curtis & Watkins, 1960; Rioult-Pedotti *et al.*, 1998). An excitatory neurotransmitter excites or stimulates a nerve cell, making it more likely that the chemical message will continue to move from nerve cell to nerve cell and not be stopped. Glutamate is essential for proper brain function.

Glutamate is an amino acid that is synthesised from Krebs cycle intermediates, and is found ubiquitously throughout the body; however, it cannot pass through the blood-brain barrier (BBB) and it must therefore be synthesised within the brain, so that it is available for neurotransmission. Glutamate plays a number of disparate roles including prevention of apoptosis via promotion of Ca^{2+} influx. (Yano *et al.*, 1998). However, excessive glutamate stimulation can cause a large cation influx which results in a cascade of events leading to neuronal lysis and death via excitotoxicity (Rothman, 1985). Excess extracellular glutamate has been shown to cause excitotoxicity as the increased Ca^{2+}

influx leads to increased generation of reactive oxygen species (ROS) from mitochondria, thus impairing the ability of a neuron to maintain cellular energy levels, leading to neuronal cell death (Purves *et al.*, 2001; Gleichmann & Mattson, 2011). This process is thought to play a role in various neurological disorders such as stroke and ischemia, which can in turn result in dementia, disability and in many cases death. During an ischemic stroke blood flow to the brain is disrupted leading to a decreased delivery of nutrients and oxygen to neurons which can result in the release of excessive amounts of glutamate due to the breakdown in cells' ability to maintain normal membrane polarisation, leading to a spiral of neuronal excitotoxicity and cell death (Ugalde- Triviño & Díaz-Guerra, 2021). Glutamate levels within the brain influence oscillations, low micromolar concentrations of glutamate can alter neuronal firing patterns and affect LFPS (Rawal et al., 2022). Imbalances in glutamate can lead to overexcitation, potentially causing cell damage or death. Glutamate impacts energy levels, neuroplasticity and overall neural function, its intricate interactions contribute to the brains adaptability and resilience. In epilepsy there is an imbalance of excitatory and inhibitory conductance in nerve cells within the brain, and dysregulation of glutamate receptors can contribute the epilepsy pathogenesis (Chen et al., 2023). Glutamate dysregulation leads to cellular and network hyperactivity, contributing to seizure initiation and the development of chronic epilepsy. Understanding glutamatergic mechanisms is crucial for improving epilepsy management strategies and there is currently promising ongoing research that explores the sue of glutamate receptor antagonists as epilepsy treatment (Chen et al., 2023).

There are two major classes of glutamatergic receptors found in the CNS: ionotropic (iGluRs) and metabotropic (mGluRs) glutamatergic receptors. iGluRs consist of a cation-specific ion channel which undergoes a conformational change when glutamate binds, allowing an influx of Na^+ and Ca^{2+} ions into the neuron. There are three categories of iGluRs: N-methyl D-aspartate receptors (NMDArs), α-amino-3-hydroxy-5-methyl-4-isoxazolepropionic acid receptors (AMPArs) and kainate receptors (KARs) (Eccles & McGeer, 1979). iGluRs are involved in fast, excitatory synaptic transmission, most commonly via the influx of Na^+ ions into the post-synapsic cell. mGluRs are G-protein coupled receptors (GPCRs), there are three groups of mGluR containing eight receptor subtypes (mGluR1-8): group I (mGluR1/5, via G_q and G_s), group II (mGluR2/3, via $G_{i/o}$) and group III (mGluR4/6-8, via $G_{i/o}$). When glutamate binds to mGluRs, intracellular signal transduction pathways are triggered dependent on the type of G-protein linked to the receptor. These can be phospholipase C and/or adenylate cyclase dependent and can include protein kinase pathways such as the mitogen-activated protein kinase/extracellular receptor kinase (MAPK/ERK) and mammalian target of rapamycin (mTOR) pathways. This can lead to

the modification of other proteins, such as ion channels (Lee *et al.*, 2012). mGluRs are generally slower to activate than iGluRs, but they have a wide range of effects both pre- and postsynaptically and are assumed to be involved in modulatory functions such as altering the excitability of neuronal activity, or regulating mood, concentration or appetite (Sherman, 2014).

1.1.1.1 NMDArs:

NMDArs are ionotropic glutamate receptors which play an important role in excitatory neurotransmission. They are di-heteromeric transmembrane ligand-gated ion channels which are highly permeable to Ca^{2+}, these receptors are activated by when both glutamate and glycine bind to the receptor. The binding of two glutamate molecules and two glycine molecules drives channel gating and allows Ca^{2+} ions to flow through the channel (Rajani et al., 2020), At resting membrane potentials, NMDArs are blocked by an ion of Mg^{2+} which must be removed in order for glutamatergic excitatory signaling to take place. The Mg^{2+} block is voltage dependant, so for the block to be removed the membrane must become depolarised (Hou et al., 2020). NMDArs consist of four subunits from three families GluN1, GluN2 (A-D) and GluN3 (A-B). GluN1 contains the glycine-binding site while the glutamate-binding site is found on GluN2 subunits; these two subunits combine to form a fully functional receptor. Each NMDAR is formed from different combinations of the GluN1 subunit with various GluN2 subunits (and to a lesser extent GluN3 subunits) (Dingledine *et al*., 1999; Matsuda *et al.*, 2002). The expression of subunits that makeup NMDArs varies significantly during development, which in turn affects the properties of NMDArs at the synapse. Changes also occur according to neuronal activity, and even the composition of the lipid membrane surrounding NMDArs or the levels of available co-agonist can affect their function (Kleckner & Dingledine, 1998; Traynelis *et al.*, 2010, Liu et al., 2019). Excitatory postsynaptic events produced by NMDArs allow entry of Ca^{2+} and Na^{+} into the neuron, and K^{+} out of the neuron, inducing further depolarisation and activating a range of intracellular processes (Kampa *et al.*, 2004; Hunt & Castillo, 2012).

NMDArs are crucial for generating and maintaining gamma oscillations as they contribute to the synchronization of fast-spiking inhibitory interneurons, particularly parvalbumin-expressing (PV+) GABAergic neurons (Susin & Destexhe, 2023). PV+ neurons are inhibitory interneurons which mediate feedforward and feedback inhibition. They are central to gamma oscillations and play a major role in separating excitatory principal cells into functional groups. PV+ cells receive feedback excitation from local pyramidal neurons and NMDArs underlie the integration of this feedback, this incorporation of NMDArs at feedback connections onto PV+ cells allow cooperative recruitment of other PV+ interneurons, which strengthens and stabilises cell assemblies within neural networks.

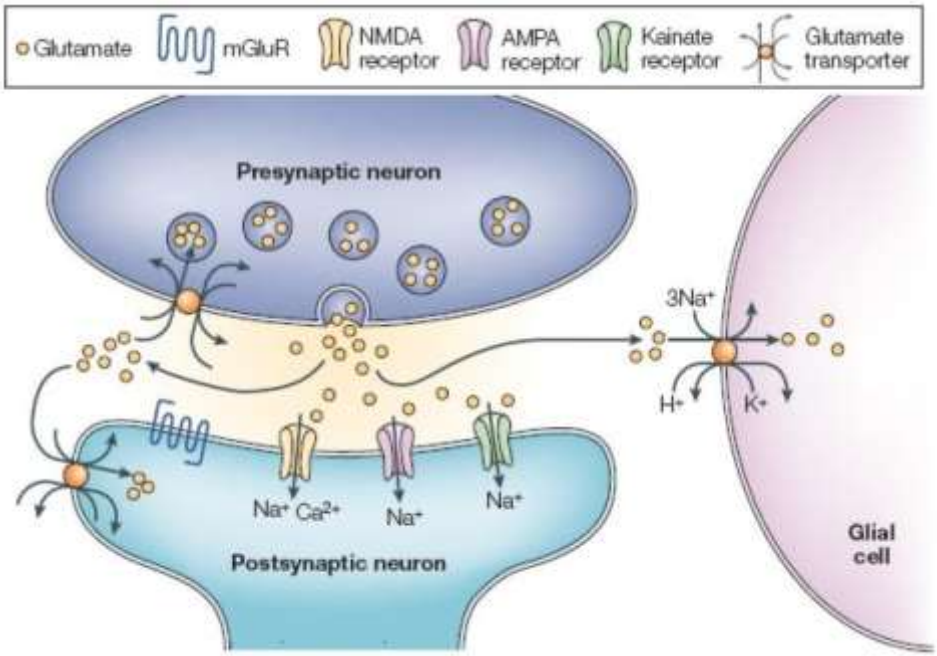

Figure 1.1: Schematic drawing of a glutamatergic synapse (Attwell & Gibb, 2005).

Illustration demonstrates the different variations of glutamate receptors and transporters present on pre- and postsynaptic membranes.

In early development NMDArs are mainly GluN2B-containing receptors which remain open to allow for relatively long excitatory postsynaptic currents (EPSCs). During synaptic maturation, the composition of the NMDAr subunits switches from predominantly GluN2B-containing to GluN2A-containing receptors, leading to shorter EPSCs as incorporation of GluN2A into GluN2B-dominant synapses results in faster decay kinetics and decreased channel open time (Visini *et al*., 1998; Liu *et al.*, 2004; Sanz-Clemente *et al.*, 2013). The predominance of GluN2B-containing NMDArs during early neurodevelopment allows for non-synchronous synaptic inputs to be integrated with other inputs due to the receptors staying open for longer and allowing a broader integration of EPSCs at the synapse, when the switch to predominantly GluN2A-containing NMDArs happens more precise timings with fast synchronous synaptic function are favoured and the integrative capacity of the synapse reduces (Chen *et al*., 1999; Bellone & Nicoll, 2007).

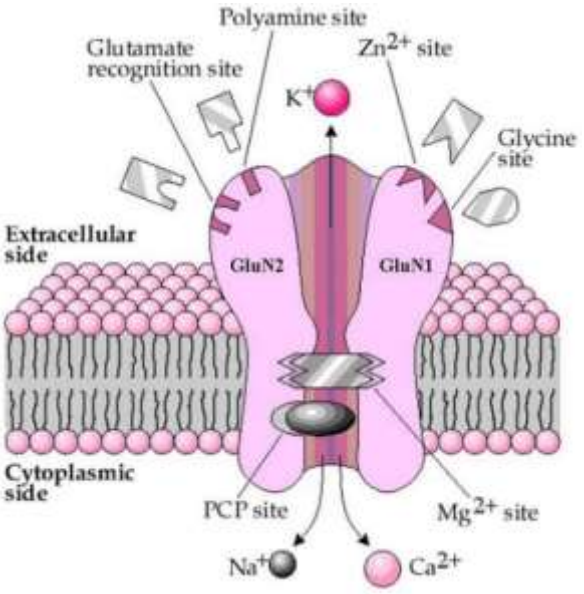

Figure 1.2: Schematic diagram demonstrating the subunit composition of Glun1/GluN2 containing NMDArs (Furukawa *et al.*, 2005).

A schematic representation of the major NMDAr subunits and binding sites including the glutamate and glycine binding sites. In the lumen of the channel the Mg^{2+} site for both binding and blocking can be seen, this is where the direct flow of ions (Na^+, Ca^{2+} and K^+) occurs.

NMDArs also play an important role in synaptic plasticity, during synaptic maturation the subunit composition of these receptors' changes in accordance with neuronal activity. Sanz-Clemente *et al.* (2013) demonstrated that NMDAr composition becomes predominantly GluN2A-containing during synaptic maturation and in response to stimuli during neonatal development. GluN2B-containing NMDArs are predominant in early development as they allow for longer EPSP duration, when GluN2A is then incorporated shorter EPSCs are produced due to faster decay kinetics (Liu *et al.*, 2004).

1.1.1.2 AMPArs:

AMPArs are ionotropic glutamate receptors responsible for mediating fast excitatory synaptic transmission which are voltage-insensitive and have faster kinetics than NMDArs (Jeun *et al.*, 2009). They are tetrameric assemblies of various combinations of the subunits GluA1-4 which follow a dimer-to-dimer formation (Dingledine *et al.*, 1999; Traynelis *et al.*, 2010). AMPArs allow Na^+ and K^+ to pass through the membrane, if no GluA2 subunit is present they will also allow passage of Ca^{2+}. These

receptors are expressed in both neurons and glia and are most vitally found postsynaptically at glutamatergic synapses (Henley & Wilkinson, 2016). GluA2-lacking AMPARs are important for Ca^{2+}-mediated depolarisation as they are Ca^{2+}-permeable, these are typically found in the postnatal brain during early development. However, most AMPARs in the developed brain contain the GluA2 subunit making them impermeable to Ca^{2+} (Wenthold *et al.*, 1996; Wright & Vissel, 2012).

AMPARs are abundant and widely distributed throughout the CNS, they are located on both the pre- and post-synaptic membranes of neurons found in the hippocampus, cortex, basal ganglia, amygdala, thalamus and more. Dysfunction or dysregulation of AMPARs has been found to contribute to the pathology of epilepsy (Beneyto & Meador-Woodruff, 2004). A 2003 study showed downregulation of AMPAR subunits, GluN1 & GluN2A/B, could help to prevent excitotoxicity from glutamatergic overstimulation (Wyneken *et al.*, 2003). It has been suggested that seizures potentiate AMPAR-mediated neurotransmission via the removal of Ca^{2+}-impermeable AMPARs and subsequent insertion of Ca^{2+}-permeable AMPARs, causing enhanced neurotransmission (Prasad *et al.*, 2002; Martin & Kapur, 2008). The 'Glu2A hypothesis' is a theory that suggests neurological insult causes a decrease in GluA2 expression resulting in more Ca^{2+}-permeable AMPARs, which causes the onset of seizures (Joshi *et al*., 2018).

There is evidence to suggest that AMPARs demonstrate neuron specific subunit configurations, principal neurons in the neocortex and hippocampus exhibit low Ca^{2+}-permeability resulting in slow desensitisation which suggests principal neurons contain predominantly GluA2-containing AMPARs. In comparison GABAergic interneurons desensitise much faster, indicating increasing Ca^{2+}-permeability and a lack of GluA2-containing AMPARs (Geiger *et al*., 1995; Koh *et al*., 1995; Wenthold *et al*., 1996).

Desensitisation is a reduced response to a sustained stimulus which occurs in all glutamate receptors, however AMPARs exhibit particularly fast desensitisation (Traynelis *et al*., 2010). AMPARs are constantly moving between synaptic and extrasynaptic sites via Brownian diffusion. There is evidence that AMPARs exhibit rapid desensitisation in the sustained presence of glutamate, this desensitisation leads to an increased diffusion rate and allows desensitised AMPARs to diffuse to extrasynaptic sites and be exchanged for naïve AMPARs. This process of glutamate-induced desensitisation helps to maintain high-frequency synaptic transmission (Constals *et al*., 2015). Transmembrane AMPAR regulatory proteins (TARPs) are a family of novel proteins which act as supporting subunits to modulate AMPAR trafficking and function. The trafficking of AMPARs plays a key role in various forms of synaptic plasticity, including long-term potentiation (LTP) and long-term depression (LTD) via

regulation of the number of receptors found at the synapse.

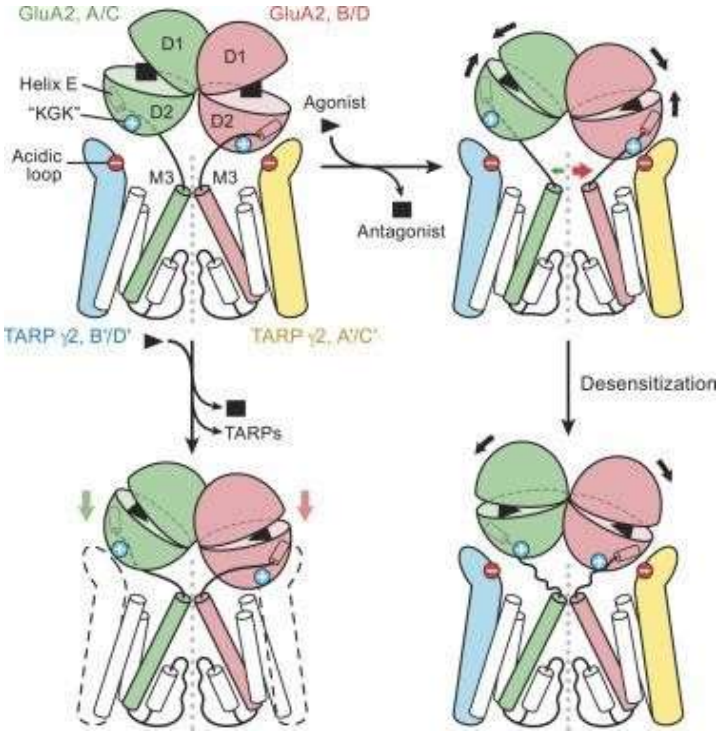

Figure 1.3: Mechanisms of AMPAr activation and desensitisation (Chen *et al.*, 2017).

Two GluA2-containing AMPArs along with two TARP subunits can be seen in the ligand-binding domain (LBD) layer. TARPs encircle agonist-bound LBDs, reducing the conformational changes upon desensitisation when compared to the isolated receptor. TARPs enable faster resensitisation of receptors by restricted the LBD layer from large-scale rearrangement during desensitisation.

1.1.1.3 KArs:

KArs are homo- or heteromeric structures comprised of subunits GluK1-5 (Traynelis *et al.*, 2010; Akgul & McBain, 2016). KARs are activated directly by glutamate but show greater decay kinetics and generate lower amplitude EPSPs than AMPArs (Cossart *et al.*, 2002). KARs found on postsynaptic dendrites work to integrate excitatory synapses and contribute to neuronal excitability, while presynaptically located KARs contribute to neurotransmitter release on both excitatory and inhibitory cells (Lerma & Marques, 2013). A common method of inducing gamma oscillations in acute brain slices

is the bath application of kainic acid (KA), Fisahn *et al*. found that KA application induces AMPAr-independent membrane depolarisation and increasing the firing of action potentials in pyramidal cells and interneurons which results in the generation of persistent gamma oscillations. However, excessive activation of KARs can result in the generation of epileptiform activity. This indicates that changes in the overall activity of KARs can affect the excitation-inhibition balance in neuronal networks and cause a switch from healthy gamma oscillations to seizure activity (Fisahn *et al*., 2004).

1.1.1.4 mGluRs:

mGluRs are GPCRs that activate biochemical cascades via activation of a G-protein when glutamate binds and can alter the levels of iGluR expression on the synaptic membrane. mGluRs can be divided into three groups: I (mGluR1, mGluR5), II (mGluR2, mGluR3) and III (mGluR4, mGluR6) (Nakanishi, 1994). Group I are expressed postsynaptically and mediate increased NMDAR activity via G_q activation. Stimulation of Group I mGluRs activates phospholipase C (PLC), producing inositol triphosphate (IP_3) and diacyl glycerol which causes Ca^{2+} release from intracellular stores and activation of protein kinase C (PKC). PKC phosphorylates target proteins facilitating an increase in iGluR trafficking to the synaptic membrane.

Group II & III are presynaptically expressed and decrease neuronal excitability through the activations of G_i/G_0 subunits. Activation of these receptors prevents cyclic AMP (cAMP) production, inhibiting protein kinase A (PKA), and preventing the phosphorylation of iGluR trafficking proteins. Group II/III can also regulate glucose release via autoreceptor activation, indicating they play a role in plasticity (Holscher *et al.*, 1999).

1.1.2 GABA:

Gamma-amino butyric acid (GABA) is the most abundant inhibitory neurotransmitter in the adult mammalian CNS. Most inhibitory neurons in the brain and spinal cord use either GABA (brain) or glycine (spinal cord) as a neurotransmitter. Exogenous GABA cannot penetrate the blood-brain barrier, so it is synthesised in the CNS via a glutamic acid decarboxylase (GAD) catalysed reaction between glutamate and cofactor pyridoxal phosphate which is an active form of vitamin B6 (Roberts & Frankel, 1950). There are two types of GABA receptor: $GABA_A$ receptors ($GABA_ARs$) and $GABA_B$ receptors ($GABA_BRs$). $GABA_ARs$ are fast acting ligand-gated Cl^- channels, while $GABA_BRs$ are slower acting GPCR-mediated metabotropic channels (Bormann, 2000).

During neonatal development GABA plays the role of an excitatory neurotransmitter due to an inverted Cl^- gradient. In the neonatal rat hippocampus, depolarisation caused by binding of GABA to $GABA_ARs$ activates voltage-gated Na^+ and Ca^{2+} channels and removes the Mg^{2+} blockade on NMDArs causing further depolarisation (Leinekugel *et al.*, 1999). This choride gradient is dependent on two co-transporters: K-Cl co-transporter 2 (KCC2; a chloride exporter) and Na-K-Cl co-transporter (NKCC1; a chloride importer), whose activity can decrease or increase the neuronal Cl^- concentration, respectively. During neonatal development the NKCC1 co-transporter is more prevalent, creating a higher intracellular Cl^- concentration which allows GABA to depolarise precursor and immature neurons, however, once the glutamatergic system is established the expression of the KCC2 co-transporter increases which leads to a more stable Cl^- gradient as intracellular Cl^- is reduced and the hyperpolarisation of mature neurons by GABA via Cl^- influx can take place (Watanabe & Fukuda, 2015). Altered expression/activity of either of these co-transporters has been associated with a wide variety of neurological disorders, including epilepsy and stroke (Schulte *et al.*, 2018; Sieghart & Savic, 2018).

In the adult brain, vesicular release of GABA into the synapse is likely to lead to inhibition rather than excitation (Mody *et al.*, 1994). GABA transmission in adults mediates inhibitory postsynaptic potentials (IPSPs) causing hyperpolarisation and consequently lower the probability that the neuron will fire an action potential. GABA binding most commonly causes increased membrane permeability to Cl^- and HCO^{3-} ions, an influx of negatively charged ions into the cell causes membrane hyperpolarisation (Staley *et al.*, 1995).

1.1.2.1 GABARs:

GABA interacts with GABA receptors (GABARs), of which there are two main types: $GABA_ARs$ &

$GABA_BRs$. $GABA_ARs$ are pentameric ligand-gated ion channels which are responsible for fast inhibitory synaptic transmission; they are characterised by a central pore which allows Cl^- and HCO^{3-} ion influx to pre- and post-synaptic neurons. $GABA_ARs$ are selectively permeable to Cl^- ions and to a lesser extent HCO^{3-}, depending on membrane potential and ionic concentration gradient this permeability changes to allow the flux of ions across the pore (Bormann *et al.*, 1987).

$GABA_ARs$ are derived from eight recognised subunit groups α (6 isoforms), β (3 isoforms), γ (3 isoforms) δ, ε, π, Θ and ρ (3 isoforms) (Olsen & Sieghart, 2008). The functional characteristics of a $GABA_AR$ are determined by its precise subunit composition with each $GABA_AR$ typically containing two GABA binding sites and one benzodiazepine binding site. The γ subunits have structural importance as they form part of the benzodiazepine binding site and can determine synaptic location. A_1 subunits are also important in the recognition of benzodiazepines, whereas the β subunits aid the recognition of GABA. The most common $GABA_AR$ subunit configuration in the mammalian brain is 2α, 2β, and either a γ or δ subunit, with the $GABA_A$ binding-site located on the α and β extracellular interfaces. The binding of GABA to $GABA_ARs$ induces a hyperpolarising effect on neurons that shunts excitatory inputs further from depolarisation, lowering neuronal excitability. Through $GABA_AR$ activation two types of inhibition can be produced, phasic inhibition which arises from a synchronised release of GABA into the synaptic cleft, activating postsynaptic $GABA_ARs$ or tonic inhibition which permits long-lasting neurotransmission via extra- or perisynaptic $GABA_AR$ activation (Farrant & Nusser, 2005). A subclass of $GABA_ARs$ known as $GABA_A$-Rho receptors (formerly known as $GABA_AC$ receptors), which are composed entirely of ρ subunits are insensitive to typical GABAR allosteric modulators such as benzodiazepines and barbiturates. As $GABA_A$-Rho do not contain any α or γ subunits they lack a benzodiazepine binding site, which is the reason they are insensitive to benzodiazepines and barbiturates (Morlock & Czajkowski, 2011). Stimulation of these receptors by GABA molecules has a slow initiation period, but the duration is more sustained when compared to the rapid onset and short duration of $GABA_AR$ activation. It has been reported that the effects of GABA are 10- to 100-fold more potent on $GABA_A$-Rho receptors than on typical $GABA_ARs$ (Naffaa *et al.*, 2017).

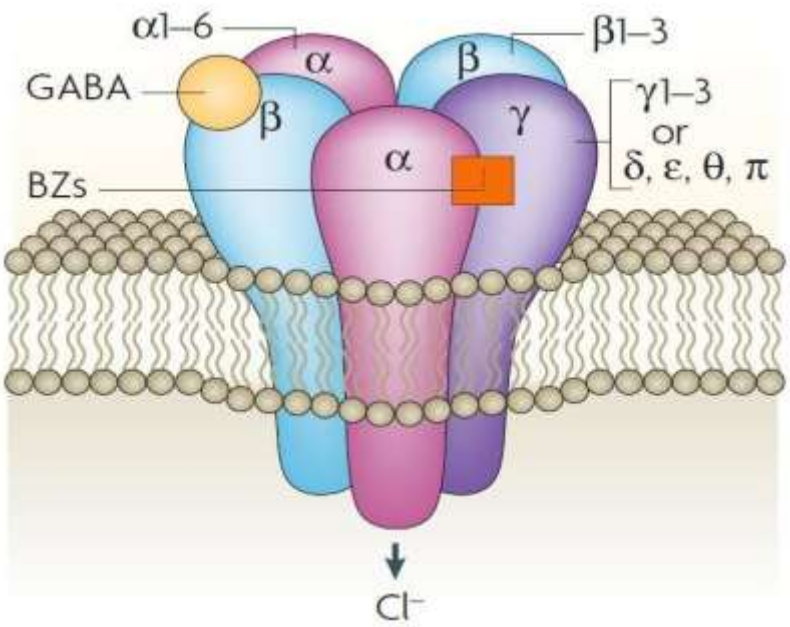

Figure 1.4: Schematic illustration of the GABAAR (Jacob et al., 2010).

Illustration demonstrates the pentameric structure of the receptor, showing the common subunit arrangement as well as the GABA and benzodiazepine binding sites.

$GABA_BRs$ are metabotropic transmembrane GPCRs which can be found both pre- and post- synaptically. These receptors are linked to G-protein coupled inwardly rectifying K^+ channels (GIRKs) and mediate inhibition through K^+ efflux, causing hyperpolarisation of the cell and inhibiting the production of cAMP and activation of PKA (Huang & Thathiah, 2015). GABA modulation of neural activity works on a slower time scale when $GABA_BRs$ are activated compared to $GABA_ARs$. Presynaptic $GABA_BRs$ act to limit the opening of voltage gated Ca^{2+} channels and prevent release of GABA into the extracellular space (Dutar & Nicoll, 1988a,b). Post-synaptic $GABA_BRs$ generate long-lasting hyperpolarising effects through activation of GIRKs (Luscher *et al.*, 1997; Kulik *et al*, 2006).

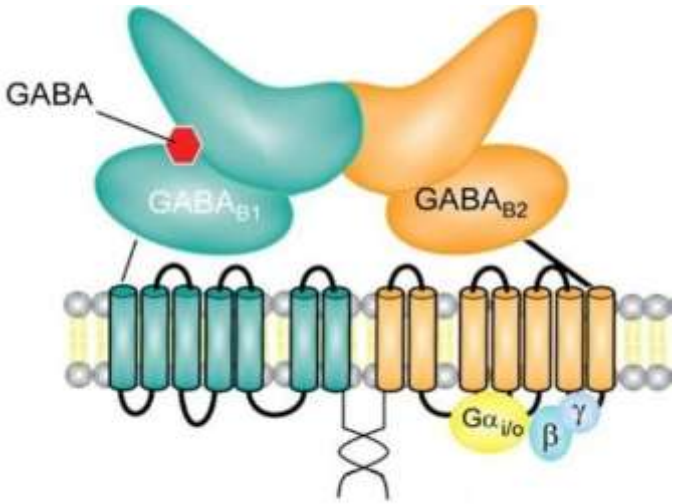

Figure 1.5: Structure of GABA$_B$Rs subunit composition (Benarroch, 2012).

Diagram depicting the structure of a GABA$_B$Rs subunit which exists a heterodimer of GABA$_{B1}$ and GABA$_{B2}$ both labelled above. The GABA binding site can be seen located on the GABA$_{B1}$ subunit.

1.2 Neural Oscillations:

Fluctuations in neuronal excitability summate and present as oscillations, also known as brain rhythms or brain waves in the popular consciousness, which can be observed as changes in voltage produced by intra- and extracellular mechanisms (Isomura *et al.*, 2006). Over the years, technological advancements have allowed individual neuronal populations to be identified, these populations act collaboratively to form synchronous neuronal networks that dictate brain function.

Neuronal oscillations are rhythmic or repetitive patterns of activity within the brain. They arise when synaptically-located ion channels are activated by neurotransmitter release, permitting the entry of cations into the intracellular space, producing an electrical imbalance. Oscillatory activity in the brain can be categorised based on frequency (Hz), neural oscillations can be broadly grouped into alpha (α), beta (β), delta (δ), gamma (ϒ) or theta (φ) waves (Roohi-Azizi, 2017). The range varies across different species depending on the region of origin, mechanisms that generate the oscillations, and the behavioural state of the brain.

Name	Frequency (Hz)	Functional Role
Delta (δ)	2-4 Hz	- Sleep & wakefulness - Encoding memory - Cognitive processing & integration
Theta (φ)	4-11 Hz	- Consolidation of memory - Non-REM Sleep - Locomotion
Alpha (α)	8-13 Hz	- REM Sleep
Beta (β)	10-30 Hz	- Working Memory - Decision Making
Gamma (ϒ)	30-100 Hz	- Voluntary Movement - Cognitive processing & integration - Encoding memory

Table 1.1: Table detailing the functions and the typical frequency range associated with each group (adapted from Abhang *et al*., 2016).

The first human brain oscillations were recorded by Hans Berger in 1929 using an electroencephalograph (EEG) following on from the pioneering work conducted by Richard Caton in the mammalian cortex in 1875 (Haas, 2003). Since then, there has been increasing evidence that neurons within the brain act collectively as groups of networks, which oscillate synchronously to facilitate network function. The discovery of EEG revolutionised neuroscience research and neurosurgical procedures, particularly for patients with epilepsy as they allow for non-invasive diagnosis of epilepsy as well as providing doctors the ability to localize seizure origins and regularly monitor how anti-seizure medication is working (Kiranyaz *et al*., 2013).

Oscillations can now be induced *in vitro* using a combination of pharmacological agents or electrical stimuli. The application of agents to induce oscillations in *in vitro* slice preparations is necessary as, while acute brain slices maintain their structural integrity, many neurons lose their normal afferent

connections from more distant brain areas which are not included within a given slice. Some neurons may also lose efferent connections, and synaptic innervations e.g. from the cortex or the midbrain. Studies using pharmacological or electrical stimuli to induce oscillations have been conducted in several brain areas including the hippocampus, entorhinal cortex, motor cortex, and somatosensory cortex (Fisahn *et al.*, 1998; Gillies *et al.*, 2002; Cunningham *et al.*, 2004; Yamawaki *et al.*, 2008; Johnson *et al.*, 2017). The *in vitro* study of oscillations is generally done via electrophysiological recordings of extracellular potentials (local field potentials; LFPs) and intracellular potentials (patch clamp recordings). These methods are used to examine the spiking patterns of neurons in response to different environmental stimuli, stress, or the activity of surrounding neurons.

Electrophysiological recordings for experimental and clinical use are made possible because of the electrical field potentials generated by current sinks and sources. The sink & source model is a theory which explains how extracellular field potentials arise through charge flow. Extracellular field potentials are generated via the summation of neuronal currents across a large area. Sinks and sources are necessary for maintaining a charge balance within the neuron, they act as a microcircuit that maintains ion influx and efflux in a neuron (Halnes *et al.*, 2016). Sinks arise when an influx of positive ions flow into dendrites following the activation of channels or receptors, creating an imbalance in the charge of the neuron, charge travelling from the extracellular to intracellular space. In order to maintain a balance, cations are released from the axon or perisomatically into the extracellular space (i.e. a source) working in opposition to this with a passive return travelling from intracellular to extracellular space forming a dipole which leads to current flow across the membrane.

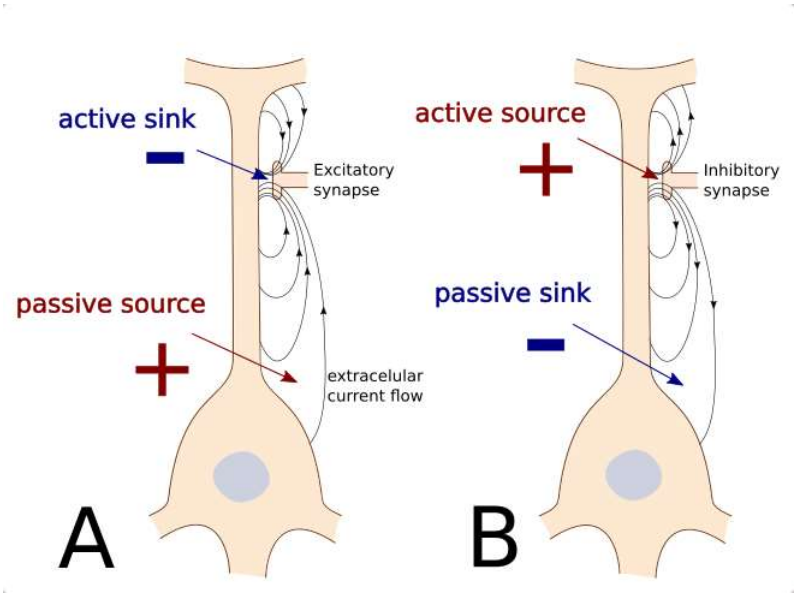

Figure 1.6: Schematic illustration of current flow patterns in the sink and source model (Maksymenko, 2019).

(A) Activation of an excitatory synapse results in membrane depolarisation, and a net flow of positive current towards inside the cell. This creates an active sink at the synapse site outside the cell and a passive source at the soma.

(B) Activation of an inhibitory synapse results in membrane hyperpolarisation and a net flow of positive current away from the cell. An active source is created at the synapse, and a passive sink at the soma.

1.2.1 Gamma:

Gamma oscillations (30-80 Hz) are fast network activity patterns which occur ubiquitously throughout the brain and are important for a number of cognitive functions, including memory, attention, and perception (Uhlhaas *et al.*, 2011). Gamma oscillations have been studied in various brain regions including the hippocampus, entorhinal cortex, somatosensory cortex, and primary motor cortex and are thought to occur due to the coordination of excitatory and inhibitory signals within the brain (Buzsaki *et al.*, 1984; Whittington *et al.*, 1995; Buhl *et al.*, 1998; Johnson *et al.*, 2017). These oscillations display similar key features across all areas of the brain, which has led to the identification of three fundamental requirements for the generation of gamma oscillations: a network of reciprocally projecting inhibitory interneurons connected via electrical gap junctions, a time constant mediated by $GABA_AR$s and an excitatory drive sufficient to elicit interneuronal firing (Whittington *et al.*, 1995; Traub *et al.*, 1996a,b).

Abnormal gamma activity, such as hypersynchronous, out-of-sync, or high frequency oscillations, has been described in a number of neurological conditions such as autism, epilepsy, and Alzheimer's disease (Uhlhaas & Singer, 2006). For this reason, it is necessary to carry out further studies into the mechanisms of pathological gamma oscillations and how they contribute to neurological disorders. Gamma oscillations can be induced in acute brain slices for *in vitro* experimentation via the depolarisation of excitatory inputs or pharmacological activation using muscarinic acetylcholine receptor (mAChR)/KAR agonists (Johnson *et al.*, 2017).

There are currently two hypotheses for gamma oscillation *in vitro*, which are the interneuron network gamma (ING) model and the pyramidal interneuron gamma (PING) model. Both models are centred around $GABA_A$-mediated inhibition (Buzsaki & Wang, 2012).

1.2.1.1 Interneuron Network Gamma (ING; the inhibitory-inhibitory model):

This model describes a reciprocally connected network of inhibitory cells and is demonstrated in Figure 1.7B. Following excitation, a group of interneurons will synchronize and discharge together to generate synchronous IPSPs in partner interneurons. Inhibited partner neurons will spike again following the decay of $GABA_A$-mediated hyperpolarisation, this cycle then repeats. IPSP duration is determined by the subunit composition of the $GABA_A$Rs and the frequency of the resulting gamma oscillation is determined by the kinetics of the IPSP and net excitation of neurons. Interneurons can propagate electrical activity generated by an action potential via gap junctions between neurons, causing neighbouring neurons to become depolarised (Whittington *et al.*, 1995). At any given time, inhibitory neurons within a network will fire out of phase with the population spike, this strongly inhibits non-firing neurons, therefore delaying their spike. With each cycle the delay moves the unsynchronised spike firing towards those already aligned, until the interneuron population discharges synchronously, generating synchronous IPSPs.

According to the ING model, gamma oscillations can arise either via a tonic or stochastic input. Tonic input causes neurons to fire with precision. Random inputs allow oscillations to emerge following activation of an entire network, interneurons will fire irregularly until the network is activated and groups of polarised neurons can randomly depolarise together, producing synchrony and allowing oscillations to emerge (Tiesinga & Sejnowski, 2009). *In vitro* studies have confirmed the ING mechanism of generating gamma oscillations through the use of various pharmacological agents to

increase the firing of connected interneurons, this mechanism is demonstrated in Figure 1.7 (Whittington *et al.*, 1995; Fisahn *et al.*, 1998, 2004; Hajos & Paulsen; 2009).

1.2.1.1 Pyramidal Interneuron Network Gamma (PING; excitatory-inhibitory model):

The PING model alternates between fast excitation and delayed feedback inhibition and is demonstrated in Figure 1.7A. Excitatory cells discharge activating their connecting inhibitory neurons and resulting in the perisomatic inhibition of excitatory cells. Once $GABA_A$-mediated hyperpolarisation has decayed excitatory cells can fire again, producing cyclic behaviour. The PING mechanism displays a network of reciprocally connected pyramidal and interneuronal cells which generate gamma oscillations. Synchronous firing is determined by phasic excitation and inhibition (Fisahn *et al.*, 1998; Roopun *et al.*, 2009).

Basket cells (BCs) impose IPSP rhythms onto pyramidal cells, creating a time-window inside of which neurons may fire. BCs are indirectly stimulated through low frequency, rhythmic EPSP discharges from pyramidal cells. Pyramidal cells discharge activating AMPArs on connecting inhibitory interneurons, leading to EPSP generation. Once EPSPs are generated $GABA_A$-induced inhibition of pyramidal cells is shunted via $GABA_A$-induced IPSPs. Once these $GABA_A$-mediated IPSPs decay pyramidal cells can fire once again creating synchronous, fast frequency firing between individual interneurons; in turn generating IPSP discharge in both the interneuron and pyramidal cell groups, mediated through $GABA_AR$ inhibition (Cobb *et al.*, 1995; Traub *et al.*, 1996). Oscillations generated by the PING mechanism were shown to be dependent on AMPAr activity, directly implicating the excitatory activity in oscillation generation (Fuchs *et*

al., 2007).

Both the ING and PING models have flaws; the ING model is influenced by excitatory input, so a varied input could result in a wide range of firing frequencies and decreased synchrony. The PING model was based on the theory that disconnection of inhibitory networks does not affect the power of gamma. However, gamma oscillations are apparent in brain areas which lack excitatory-inhibitory networks (e.g. basal ganglia). Buzsaki & Wang suggested that a hybrid model of the two could work to create gamma oscillations which are a closer representation of what happens *in vivo* (Buzsaki & Wang, 2012).

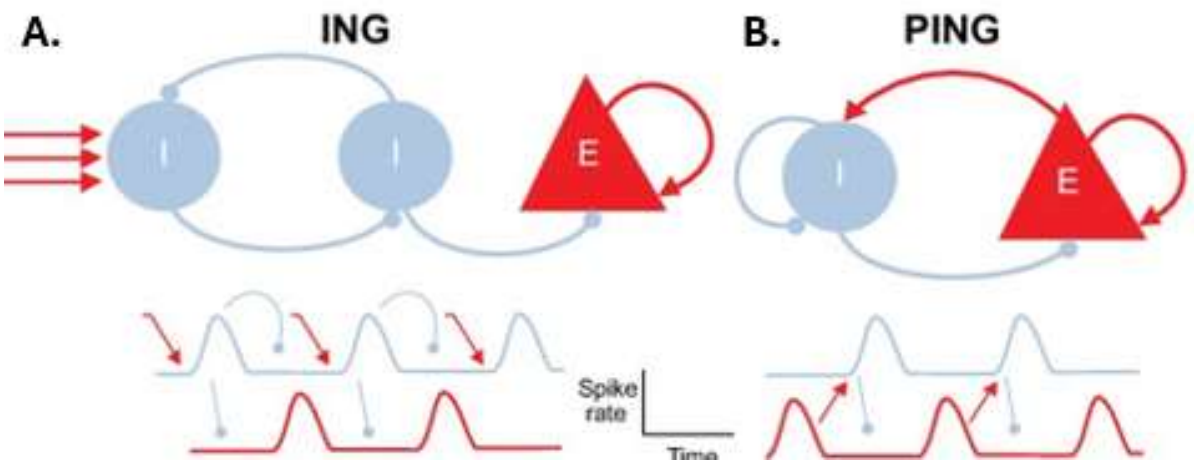

Figure 1.7: Illustration of gamma oscillation generation models (modified from Tiesinga & Sejnowski, 2009).

(A) The ING model - two inhibitory cells reciprocally connected, below the expected spike-rate relationships between the two neuronal populations (where blue = inhibitory signals, red = excitatory signals). **(B)** The PING model - shows an excitatory pyramidal neuron (E) and an inhibitory interneuron (I) with reciprocal connections, below the spike rate fluctuations between I and E cell populations can be seen.

1.2.1.2 The role of glutamate receptors in gamma oscillations:

In the PING model of gamma oscillation generation AMPArs drive fast excitatory neurotransmission from pyramidal cells to interneurons, this initiates the gamma oscillation and results in post-synaptic AMPAr activation. An EPSP is generated as Na^+ and K^+ ions flow into the cell. AMPAr antagonists, including NBQX, have been shown to abolish *in vitro* hippocampal gamma oscillations which indicates that AMPAr neurotransmission plays a critical role in the generation and elimination of gamma oscillations (Fisahn *et al*., 1998; Mann *et al*., 2005).

KArs are found ubiquitously throughout the hippocampus, and gamma oscillations are commonly induced *in vitro* via the application of KA, an analogue of glutamate. KA-induced hippocampal gamma oscillations were found to be initiated via AMPAr-independent membrane depolarisation which

increased the action potential firing of both interneurons and pyramidal cells. However, KA is a potent neurotoxin and excessive activation of KArs can be used to induce seizure activity in experimental models of epilepsy indicating that small changes in KAr activity can cause an imbalance between inhibitory and excitatory activity leading to epileptiform activity (Fisahn *et al*., 2004).

The role of NMDArs in gamma oscillations appears to be region-specific as some studies have suggested that application of NMDAr antagonist D-AP5 had no significant effect on induced gamma oscillations in the hippocampus (Mann *et al*., 2005). However, acute blocking of NMDArs using non-competitive antagonists such as ketamine or MK-801 resulted in increased gamma power in the hippocampus (Caixeta *et al*., 2013; Wang *et al*., 2020) and neocortex (McNally *et al*., 2011). An *in vivo* study of NMDAr knockout mice found that while no change in gamma oscillations occurred in the hippocampus, there was a significant reduction in power of gamma in the medial entorhinal cortex (Cunningham *et al*., 2006). It is proposed that the variation in results is due to fast-spiking parvalbumin positive (PV+) interneurons being more susceptible to depolarisation than regular spiking pyramidal neurons, causing the release of voltage-dependent Mg^{2+} blockade and allowing open-channels, non-competitive NMDAr antagonists to bind (Carlen *et al*., 2012).

1.2.1 Theta:

Theta oscillations (4-8 Hz) have been extensively studied within the hippocampus, prefrontal cortex, and visual cortex (Bland *et al.*, 2002; Cunningham *et al.*, 2003; Ishii *et al.*, 2013; Zold & Marshall, 2015), as they are involved in spatial navigation & learning, sleep, and movement (Hasselmo *et al.*, 2002; Cantero *et al.*, 2003). It has been suggested that theta provides a feedback loop between the cortex and hippocampus which enables networks to adapt to constant changes in sensory stimuli (Bland & Oddie, 2001).

Slow (≈25-50 Hz) and fast (>80 Hz) gamma oscillations are believed to occur in synchrony with high amplitude theta rhythms within the hippocampus. Theta oscillations in the hippocampus correlate with theta oscillations in many afferent/efferent hippocampal structures. Widespread synchrony between networks in the brain is possible due to theta's ability to tolerate long conductance delays. Hippocampal gamma oscillations exhibit their largest amplitude when nested in theta oscillations even though they are generated independently of each other. Gamma and theta oscillations have been shown to work in unison with each other for the encoding and retrieval of memory via a process known as cross-frequency coupling which allows spatial information to be represented in different

gamma subcycles nested in one theta cycle (Palva, 2005; Canolty, 2006; Lisman & Jensen 2016).

1.2.2 Phase Amplitude Coupling (PAC):

Although gamma oscillations typically arise locally as it is difficult for fast oscillations to synchronise over long distances, transient gamma bursts also exhibit long-range synchrony (known as coupling). This can occur via phase-phase, phase-amplitude, or amplitude-amplitude coupling. Phase-phase coupling involves two waveforms of identical frequency with identical phase angles; each cycle can emerge at multiple locations and are measured by phase coherence. For phase-amplitude coupling the phase of a slower frequency oscillation (e.g. theta) drives the power of the coupled higher frequency oscillation (e.g. gamma) resulting in synchronisation. Amplitude-amplitude coupling shows correlation between the signal amplitudes at two different frequencies.

Theta and gamma oscillations are generated simultaneously and exhibit PAC where the amplitude of theta oscillations synchronise with the phase of gamma oscillations, permitting theta oscillations to determine the amplitude of the gamma oscillations (Palva, 2005; Canolty, 2006). PAC enables the selective processing of network information by ignoring oscillations that are out of phase and preferentially accepting those that are in phase. Studies have shown that PAC between theta and gamma oscillations is critical for processing activity in the primary motor cortex, where the amplitude and frequency of network activity are modified when communicating with other spatially distinct cortical regions (Igarashi, 2013).

Most of the brain's cognitive functions are based on the coordinated interactions of large numbers of neurons distributed across and within specialised brain areas. The integration and segregation of neural activity must occur at specific spatial and temporal scales which are adjusted depending on the nature of the cognitive task they are encoding for (Uhlaas & Singer, 2006). Neural synchrony has been investigated in association with various neurological disorders including epilepsy, Parkinson's disease, autism, schizophrenia, and Alzheimer's disease (AD). These studies found that abnormalities in brain rhythms are usually associated with a lack of synchrony in firing discharges which leads to the development of these disorders (Bernier *et al.*, 2007; Roopun *et al.,* 2010).

1.3 The Hippocampus

The hippocampus is a major component of the brain in humans and other vertebrates, it is a conserved brain structure which can be found in species ranging from fish to birds to mammals (Kahn *et al*., 2009). Humans have a hippocampus in each hemisphere of the brain located in the medial temporal lobe of the cerebrum. The hippocampus is part of the limbic system with an integral role in the consolidation of information form short- to long-term memory, it is also involved in spatial memory which enables navigation and emotional processing, including anxious and avoidant behaviours (Terranova *et al*., 2019). Damage to the hippocampus can result in any of a various number of neurological disorders including Alzheimer's disease, schizophrenia, depression, and epilepsy with the hippocampus often being involved in seizure activity.

The hippocampus is made up of the hippocampal proper (cornu Ammonis, CA) which has 4 subfields CA1, CA2, CA3 and CA4, the subiculum and the dentate gyrus (DG). The flow of information in the hippocampus is managed via two circuits: the trisynaptic circuit and the monosynaptic circuit. In the trisynaptic circuit information inputs largely flow from the entorhinal cortex (EC) to the DG via the perforant path. The DG projects directly into CA3 via the mossy fibre pathway, where this information is processed, then this is projected from CA3 directly into CA1 through the Schaffer Collateral pathway. The circuit is completed by outbound projections to the subiculum and the EC (Brewer *et al*., 2021). CA3 also projects back onto other CA3 neurons and the DG creating a recurrent collateral pathway (Anand & Dhikav, 2012). The monosynaptic circuit is less well understood but it is believed to involve direct connections from the EC to CA1, bypassing the DG and CA3 and allowing a more direct flow of information within the hippocampus, however, the specific roles and functions of this circuit are still being researched. These circuits allow for complex processing and transfer of information within the hippocampus, contributing to its role in memory formation and spatial navigation.

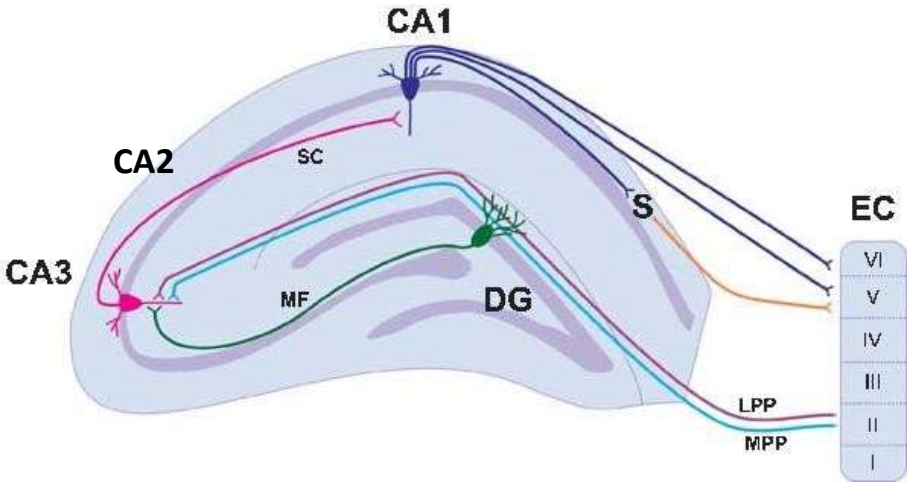

Figure 1.8: A simplified illustration of hippocampal circuitry demonstrating trisynaptic and monosynaptic circuits (Patten et al., 2015).

Layer II of the entorhinal cortex (EC) provides input to granule cells in the dentate gyrus (DG) via the medial and lateral perforant paths (blue and purple, respectively). DG cells project to pyramidal cells of CA3 via mossy fibre pathway (green). CA3 pyramidal neurons project to the CA1 via schaffer collaterals (pink). CA1 pyramidal cells project to both the subiculum and to layer V & VI of the entorhinal cortex. LPP = lateral perforant path; MPP = medial perforant path; S = subiculum.

CA2 is often considered to be a transitional area of the hippocampus as not much was known about its function, however, in recent years research has indicated that CA2 has its own distinct purpose as the response of CA2 to various neurodegenerative disorders differs from the response of the other hippocampal regions (Pang *et al*., 2019).

The EC provides major inputs to the hippocampus via two distinct pathways; the perforant pathways (LPP & MPP) which project from layer II of the medial EC (mEC) onto the DG and CA3 region, and the temporoammonic pathway which is a direct projection from layer III of the mEC to CA1 via the subiculum (Steward & Scoville, 1976; Witter *et al*., 2000). Feedback projections from CA1 are received in layers V & VI of the EC, with CA1 also projecting to the amygdala, prefrontal cortex, and the ventral striatum (Pang *et al*., 2016).

Due to the unique layering of the cell bodies in the hippocampus it is relatively easy to identify different hippocampal areas, CA1-CA3 can be identified by their dark cell body layers formed from 10-30 layers of excitatory pyramidal neurons. The pyramidal neurons found in CA1 and CA3 are the major

principal cell types of the hippocampus proper, with the majority of all hippocampal neurons (up to 90%) being excitatory pyramidal cells (Chauhan et al., 2021).

NMDArs also play an important role in synaptic plasticity, during synaptic maturation the subunit composition of these receptors changes in accordance with neuronal activity. Sanz-Clemente *et al.* (2013) demonstrated that NMDAr composition becomes predominantly GluN2A-containing during synaptic maturation and in response to stimuli during neonatal development. GluN2B-containing NMDArs are predominant in early development as they allow for longer EPSP duration, when GluN2A is then incorporated shorter EPSCs are produced due to faster decay kinetics (Liu *et al.*, 2004).

1.4 Epilepsy:

Epilepsy is a chronic neurological condition thataffects approximately 1% of the global population. Epilepsy occurs when a person is predisposed to seizures because of a chronic pathological state or genetic predisposition with approximately 75% of cases beginning in childhood. It is defined by the International League Against Epilepsy (ILAE) as "*at least two unprovoked (or reflex) seizures occurring more than 24 hours apart; one unprovoked (or reflex) seizure and a probability of further seizures similar to the general recurrence risk (at least 60%) after two unprovoked seizures, occurring over the next 10 years or diagnosis of an epilepsy syndrome*."

The aetiology of epilepsy is complex and can vary from person to person, it is caused by abnormal activity in the brain which can result from several different factors including familial genetics, head trauma, medical conditions affecting the brain such as stroke or tumour, infectious diseases of the brain such as meningitis, brain damage or injury caused during birth, or developmental brain disorders such as autism. Whatever the cause, epilepsy is a common final pathway for numerous pathophysiological processes (Sirven *et al*., 2015).

While the clinical classification of epilepsy is often changing, epilepsies tend to have two broad categories: focal and non-focal epilepsy (Korff *et al.*, 2013). Focal epilepsy is defined as a seizure originating within one cerebral hemisphere, whereas non-focal epilepsy is mostly a generalized epilepsy (GE). Non-focal epilepsy includes absence seizures characterized by a transitory alteration of consciousness, with or without other clinical signs, with each episode lasting between 3 and 30 seconds. All epilepsies can be treatment resistant, however, seizure-associated epileptic encephalopathies (e.g. FIRES or Dravet syndrome) are among the most resistant to treatment (Kramer

et al., 2011, Shmuely *et al.*, 2016).

Epilepsy has numerous manifestations and causes which each reflect underlying brain dysfunction (Shorvon *et al.* 2011), the most common manifestation of epilepsy is seizures, sudden uncontrolled electrical disturbances in the brain which disrupts its normal function, caused by an extreme, atypical, hypersynchronous firing of neurons (Stafstrom & Carmant, 2015).

1.4.1 Seizure Activity:

Seizure initiation is fundamentally caused by an imbalance in the inhibition and excitation of the neuronal network which causes sustained neuronal depolarisation resulting in the burst firing of action potentials, recruitment of surrounding groups of neurons leads to seizure propagation (Bromfield *et al*, 2006). This imbalance of inhibition/excitation can result from various changes to neuronal structure or function including neuronal loss, mossy fibre sprouting or loss of GAD enzymes via the loss of GABAergic interneurons (Buckmaster & Dudek, 1997; Wuarin & Dudek, 1996 & 2001; Shetty & Turner, 2001; Marx *et al*., 2013).

Epileptic seizures can be divided into three groups: generalised seizures, localised (focal) seizures, and epileptic spasms. Generalised seizures occur in bilateral neuronal networks and can be subdivided into tonic-clonic, absence, and myoclonic seizures. Localised seizures are localised to a specific hemisphere of the brain but can become generalised within that hemisphere. An epileptic spasm consists of brief (1-3 second) events which involve involuntary flexion or extension of the arms, legs, or head, they typically occur in clusters over a period of 5 to 10minutes.

Seizures are defined as a transient occurrence of symptoms (e.g. altered motor/autonomic function or sensation) due to abnormal neuronal activity which interrupts normal brain function. Seizures can be initiated in the cortex or subcortical regions; the initiation location will vary depending on the type of seizure with pathologies often being named after the region in which seizures begin (e.g., temporal lobe epilepsy originates within the temporal lobe) (Berg *et al*., 2010).

Seizures often have a clear onset and remission period, however when a patient experiences an abnormally long seizure (5 minutes or more) this is known as status epilepticus (SE). SE is one of the most severe manifestations of epilepsy. During this prolonged seizure activity patients are at risk of developing pharmacoresistance to antiepileptic drugs (AEDs) which could go on to result in SUDEP (sudden death). Despite a newer generation of AEDs being available management of epilepsy and SE

has not yet been resolved (Jones *et al.*, 2002; Shorvon *et al*., 2011; Ben-Menachem, 2014).

The use of EEG has played a crucial role in the identification, classification, and quantification of seizures and seizure-like events (SLE) (Blume *et al*., 1984). Seizures and SLE can display many different patterns and epileptiform discharges, each of these can be categorised by their electrophysiological profile; ictal discharges are prolonged epileptiform discharges lasting more than a few seconds, interictal discharges are single population bursts (approximately 100 ms in duration) and postictal discharges are single population bursts which follow postictal depression. Some late recurrent discharges (LRDs) which do not fit the profile of ictal, interictal or postictal discharges have been identified *in vitro* and been equated to SE in humans as they were found to be resistant to common AEDs such as valproic acid (Treiman *et al*., 1990; Zhang *et al*, 1995; Sokolova *et al*., 1998; Quilichini *et al*., 2002).

1.4.2 Receptors in Epilepsy:

As detailed above, $GABA_AR$s are selectively permeable to Cl^- ions and are modulated by multiple allosteric modulators (e.g. benzodiazepines or barbiturates). It is believed the functional properties of $GABA_AR$s are altered during SE as studies have shown prolonged seizures reduce $GABA_AR$ inhibition, which is correlated to the development of SE (Kapur & Lothman, 1989; Kapur, *et al.*, 1994). Reduced AED efficacy in late-stage SE suggests the functional properties of $GABA_AR$s are rapidly modified during SE. Goodkin *et al.* (2008) used an *in vitro* model of SE combined with electrophysiological and cellular imaging techniques to investigate how modification of $GABA_AR$s may contribute to SE in some cases. Their study postulated $GABA_AR$-mediated inhibition was reduced in the hippocampi of animals during SE and miniature IPSC (mIPSC) frequency was reduced due to the rapid internalisation of $GABA_AR$s associated with seizures. Results suggested there are both pre- and postsynaptic changes to $GABA_AR$s during SE, and the rate of $GABA_AR$ internalisation is mediated by neuronal activity. Studies in both the KA and pilocarpine-induced models of epilepsy have shown decreased surface membrane expression of γ2, β2/3, and α1 subunits, in the hippocampi of animals undergoing SE (Bouilleret *et al.*, 2000; Goodkin *et al.*, 2008; Terunuma *et al.*, 2008). Increased internalisation of $GABA_AR$ subunits γ2 and β2/3 is seen in conditions which simulate recurrent bursting in SE. Increased internalisation of the γ2 subunit during SE could contribute to the reduced benzodiazepine efficacy that is observed. It has also been established that the increased rate of intracellular accumulation of $GABA_AR$ during SE is

modulated by neuronal activity, increased by recurrent bursting, and reduced by activity blockade. A positive correlation was found between epileptic activity and the number of $GABA_A$Rs found at the intracellular level, indicating that seizure activity was responsible for the internalisation (Goodkin *et al.*, 2003, 2005, 2008). Benzodiazepine-insensitive $GABA_A$Rs (containing α4 and δ subunits) do not internalise with prolonged seizure activity, as these are localised extrasynaptically. This makes these subunits attractive targets for RSE therapy/treatment options (Goodkin *et al.*, 2008).

NMDArs are sensitive to multiple inputs (e.g. the presence of agonists, membrane voltage or changes in pH) and it is hypothesised that the functional properties of NMDArs are altered during SE – a hypothesis demonstrated in multiple animal studies (Nagy *et al.*, 2005; Kumar & Foster, 2019). Epileptic seizure activity has been shown to downregulate NMDAr subunits GluN1 and GluN2A/B – it has been suggested that this may be to prevent excitotoxicity related to glutamatergic overstimulation (Wyneken *et al.*, 2003). NMDAR-mediated miniature excitatory postsynaptic potentials (mEPSCs) recorded from dentate granule cells in hippocampal slices show an increased amplitude from animals undergoing SE compared to controls (Naylor *et al.*, 2013; Niquet *et al.*, 2016). Furthermore, recent studies have found that there are no significant changes in NMDAR subunits GluN1 or GluN2A/B during SE in the hippocampus, however, the GluN2A subunit density was decreased during the latent period of SRSE in both the hippocampus and temporal lobe (Needs *et al.*, 2019). NMDAr densities have been shown to be significantly reduced in the CA1 & CA4 regions of the hippocampus in mTLE specimens, when compared with non-mTLE specimens. NMDArs appear to play a key role in accelerating internalization of $GABA_A$Rs during SE. Activation of NMDArs during SE also appears to enhance AMPAR–mediated neurotransmission.

Dysfunction or dysregulation of AMPArs has been implicated in contributing to the pathology of epilepsy (Beneyto & Meador-Woodruff, 2004). It is suggested that seizures potentiate AMPAR-mediated neurotransmission via the removal of Ca^{2+}-impermeable AMPArs and subsequent insertion of Ca^{2+}-permeable AMPArs, enhancing neurotransmission and resulting in seizure propagation (Martin & Kapur, 2008, Prasad *et al.*, 2002). AMPAR-mediated mEPSC and spontaneous EPSCs recorded from hippocampal CA1 showed increased amplitude in pilocarpine-induced epilepsy relative to control animals. Increased surface expression of GluA1 was noted, despite a decline in intracellular expression (Joshi *et al.*, 2017a). These findings however are contradicted by those of Needs *et al.* (2019) who examined AMPAR expression in Reduced Intensity Status Epilepticus (RISE) rats – RISE provide an optimised model of chronic epilepsy with an extremely low mortality rate (Modebadze, *et al.*, 2016).

This study reported decreases in AMPAr subunits in the hippocampus, following insult and SE induction. During the latent period, all AMPAr subunits decreased dramatically when compared with age-matched control rats. These findings implicate AMPAr across all stages of epileptogenesis (Needs *et al.*, 2019). The difference in these results could be due to the time allowed for AMPAR phosphorylation following SE. Lopes *et al.*, (2013) details a time and structure dependent imbalance on AMPA transmission in response to pilocarpine-induced SE.

The 'Glu2A hypothesis' is a theory which suggests that neurological insult causes changes in AMPAr plasticity which in turn potentiates seizures. This may underlie the failure of current medications to terminate RSE (Joshi & Kapur, 2018). AMPAR-mediated currents recorded from CA1 pyramidal neurons became inwardly rectifying during RSE, characteristic of Ca^{2+}-permeable AMPArs. This was accompanied by alterations in AMPAr subunit expression, particularly overexpression of GluA1 and reduced expression of GluA2, supporting the theory that AMPAR-mediated excitatory neurotransmission is enhanced during SE (Rajasekaran *et al.*, 2012).

Pharmacologically, agonists of ionotropic glutamate receptors act as convulsants. Infusion of AMPA, kainate, and NMDA has been shown to elicit seizures in rodents (Kaminski *et al.*, 2004), this would indicate that both NMDA- and AMPArs are contributors to ictogenesis. Kainate (an agonist of the kainate receptor) also acts as an AMPAR agonist and has been used in the past to create animal models of both TLE and SE. (Levesque *et al.*, 2016, Yamada & Turetsky, 1996).

1.4.3 Epileptogenesis:

Epileptogenesis is a chronic pathological process through which the brain typically develops epilepsy and enters into spontaneous recurrent seizures (SRS). There are several progressive steps involved in this process which can develop over a period of weeks, months or even years. Animal models of epileptogenesis dictate that the phases of progression into epileptogenesis can be broken down into four phases: phase one is the initial period of no seizure activity known as the latent period, phase two involves a gradual increase in seizure frequency with highly variable intervals between seizure activity, during phase three there is an exponential increase in seizure frequency and when phase four is reached seizure frequency has stabilised at a maximal rate (Williams *et al.*, 2009; Wong, 2009). During this progression into epileptogenesis it is thought that there are continual changes in brain activity at a molecular, cellular and network level.

Studies in patients suffering from a brain injury have shown that interictal spikes are observed on EEGs prior to their first spontaneous seizure, there is an immediate loss of interneurons following traumatic brain injury (TBI) which leads to reduced synaptic inhibition and the development of interictal spikes. These spikes may cause increased synaptic strength and network excitability, altering the ion channel balance and ultimately leading to a progression into SRS (Angeleri *et al*., 1999; Staley & Dudek, 2006).

The latent period is of great interest in epilepsy research as it provides a promising target for therapeutic treatment of patients before they reach symptomatic epilepsy, however this is difficult to pinpoint in humans as the initial indictors are very subtle and can be considered typical human behaviours (French *et al*., 2013). For this reason, it is in the interest of researchers to create alternative methods of studying the process of epileptogenesis using *in vivo* and *in vitro* models of epilepsy.

1.4.4 Anti-epileptic Drugs (AEDs):

The primary therapeutic target in the treatment of epilepsy is the suppression of neuronal and network hyperexcitability. Several currently used AED therapies aim to reduce this hyperexcitability in order to suppress seizure generation, this is achieved by reducing neuronal excitation or increasing neuronal inhibition (Stafstrom & Carmant, 2015). Current pharmacological treatments cannot cure epilepsy; however, they do act to limit epileptic activity and prevent seizures. AEDs limit high-frequency repetitive firing in hyperexcitable networks via the direct or indirect modulation of ion channels, ligand-gated receptor activity and neurotransmitter release. Each individual AED acts on a distinct molecular target and possesses a unique pharmacological profile, but all fall under the same functional umbrella of reducing excitability or increasing inhibition of target neurones. Further investigation is required to identify the effects of AEDs on local and global network activity.

1.4.4.1 Mechanisms of action or AEDs:

The mechanisms of action of the first-generation of AEDs can be broadly categorised into three groups: Na^+ channel blockade, GABA potentiation and Ca^{2+} channel blockade. Na^+ channel blockade was the most common mechanism of action of early AEDs, such as phenytoin and lamotrigine, whereby the blockage of the voltage-gated Na^+ channel prevents repetitive firing of neurons, reducing neural conductance (Yaari *et al.*, 1986; McNamara *et al*, 2006). Agonism or positive modulation of GABARs is another common mechanism of action of AEDs, in particular benzodiazepines which bind

to the extracellular area of GABARs between the α and ϒ subunits, primarily α1 and ϒ2. Barbiturates are also positive GABAr modulators, however, they are targeted towards the binding site on the membrane (Uusi-Oukari & Korpi, 2010). Both benzodiazepines and barbiturates allow Cl^- influx to induce antiepileptic activity. The blockade of presynaptic Ca^{2+} channels also confers antiepileptic activity, with some evidence suggesting that phenytoin may have some activity in inhibiting Ca^{2+} channel activation presynaptically (Meldrum, 2007).

Many older AEDs are limited by severe adverse effects, complicated drug-drug interactions, and a narrow therapeutic index. Felbamate and phenytoin are two examples of AED which have been shown to have negative side effects (Perucca, 2006; Johannessen & Landmark, 2010).

More recently developed AEDs aim to provide more tolerable treatments that require less complicated drug-drug interactions and yield consistent and predictable bioavailability with low variability.

Newer AEDs such as Brivaracetam and selectracetam are potent inhibitors of the synaptic vesical 21 (SV2a) protein. The inhibition of this protein appears to cause broad-spectrum attenuation of excitatory activity by disrupting neurotransmitter exocytosis into the synaptic cleft (Landmark & Johannessen, 2008). Several new generation AEDs are targeted towards NMDArs, acting on postsynaptic Ca^{2+} channels to inhibit the actions of glutamate on NMDArs, including topiramate and zonisamide (Czapinski *et al.*, 2005). Retigabine is a drug which increases the level of newly synthesised GABA resulting in the activation and prolonged opening of neuronal KCNQ2 & KCNQ3 channels, resulting in antiepileptic activity (Rundfeldt & Netzer, 2000). Rufinamide is thought to suppress neuronal hyperexcitability by prolonging the inactive state of voltage gated Na^{2+} channels. Alterations in GABAergic inhibition of neurons can also be achieved by new methods aside from enhancing the endogenous activity of GABA. Vigabatrin inhibits GABA-transaminase, the enzyme responsible for GABA degradation in the synaptic cleft, causing an increase in GABA concentration (Czapinski *et al.*, 2005). Other new antiepileptic agents that work to inhibit or decrease AMPAR activity have the potential to reduce extreme excitatory responses (Meldrum& Rogawski, 2007).

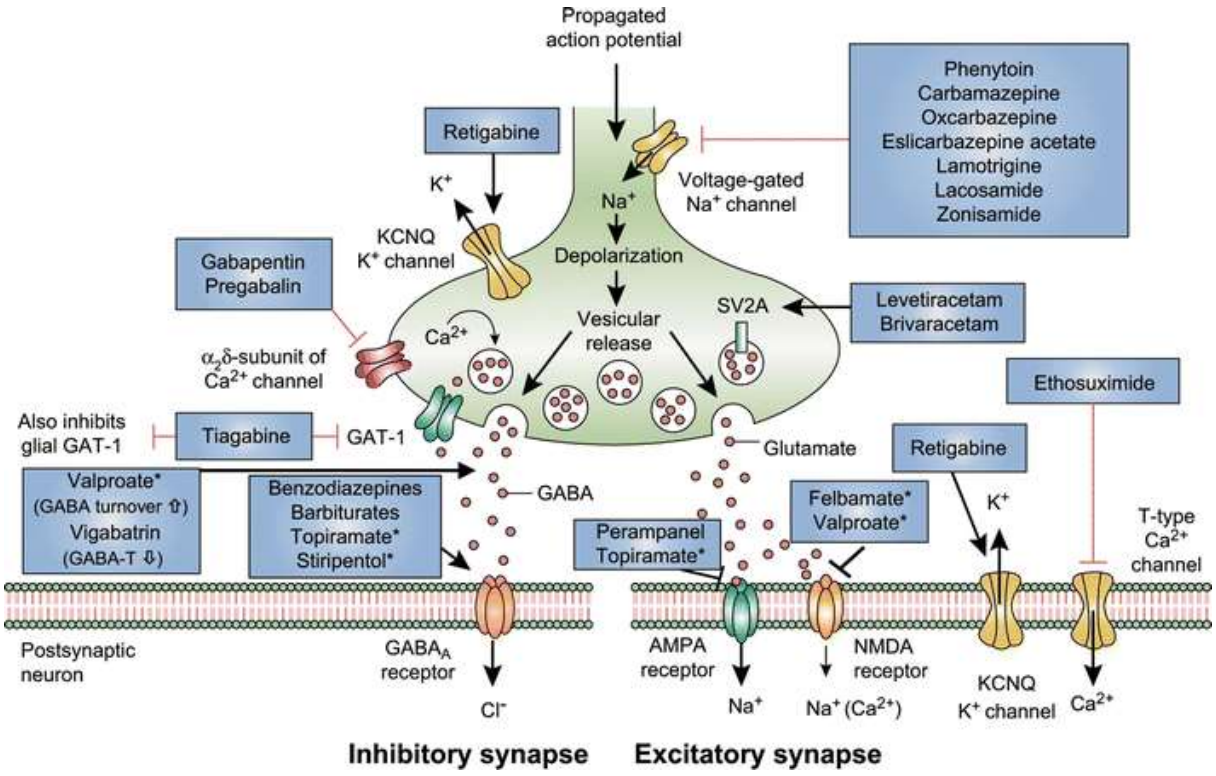

Figure 1.9: Mechanism of action of clinically approved anti-seizure medications (Loscher et al., 2016).

This diagram indicates the various different receptors and ion channels that are involved in epilepsy and the medications which target them. Drugs marked with *asterisks* indicate they act via multiple mechanisms (not all mechanisms shown here).

1.5 Models of Epilepsy:

Animal models of epilepsy have played a crucial role in understanding the disease and how it progresses, rodents are a popular choice for animal models of epilepsy and other neurological conditions given the similarity in structure and function of their brains with the human brain. Despite having a considerably different timeline, the sequence of events leading to maturation is comparable and there are distinct similarities in functionality (Semple *et al*., 2013). However, it is important to consider these age-dependent neurological differences when using rodent models of epilepsy.

Animal models of epilepsy currently used in research include the pilocarpine and KA models whereby epilepsy is induced via the injection of chemoconvulsants, the electro-shock and kindling models where electrical stimulation is applied to induce seizures, models which alter the pathology of the

brain including neonatal hypoxia and induced TBI and genetic models whereby knocking out certain genes induces genetic changes (Kandratavicius *et al*., 2014). While these models often lead to rodents displaying behavioural and electrographic epileptic activity comparable with those seen in human patients, they are often accompanied by a high mortality rate which draws the validity of these models into question (Turski *et al*., 1983; Curia *et al*., 2008).

A more recent model of TLE developed by researchers at Aston University uses a low-dose lithium-pilocarpine application coupled with a 'stop' drug cocktail to induce epilepsy and epileptogenesis in rodents. This model, known as the Reduced Intensity Status Epilepticus (RISE), boasts a high morbidity rate, with a mortality rate of only 1%. The RISE model also offers reduced seizure severity when compared with seizure induced in other models of TLE. The significant reduction in mortality rate and seizure severity means that this model fulfils two (refinement & reduction) or the 3Rs noted in the National Centre for Replacement, Refinement and Reduction (NC3Rs) guidelines (Modebadze *et al*., 2016).

Another model of epilepsy which had been used for drug screening of AEDs and meets the NC3R guidelines is to induce epileptogenesis *in vitro* in organotypic slice cultures over a period of time, this greatly reduces the number of rodents necessary to gain experimental data as cultured slices can be used over a period of weeks to months.

1.6 Tissue Slice Cultures:

Mammalian organs are difficult to study as they are fairly inaccessible to experimental manipulation and optical observation. In recent decades, organotypic cultures have been used to study tissue in a more accurate *in vivo* environment. Organotypic cultures allow the original tissue to remain intact, enabling structural organisation studies. When studying brain function there is evidently a need for a 3D structure in which a cell's natural architecture and connectivity is maintained. Organotypic tissue cultures have been an enormously useful technique in the *in vitro* study of cellular processes in the brain.

The first organotypic brain slices were cultured using the roller tube technique, with the procedure optimized following the discovery brain slices respond well to being cultured on semipermeable membrane (Gähwiler 1981, 1988; Braschler *et al.*, 1989; Stoppini *et al.*, 1991; Gähwiler *et al.*, 1997, 2001). In both physiological and disease-based neuroscience research organotypic brain tissue slices,

extracted from young rodents, are hugely advantageous over cell cultures as they allow cellular connectivity and local circuitry to remain intact. Several applications of *in vitro* organotypic brain slice cultures have been described, such as repeated multi-electrophysiological recordings and stimulations (Egert *et al.*, 1998; Jahnsen *et al.*, 1999; Karpiak & Plenz, 2002; Dong & Buonomano, 2005). Several areas of the brain have been cultured as organotypic brain slices, including; the cortex (Giesing *et al.*, 1975), the striatum (Ostergaard *et al.*, 1995), and the basal forebrain (Robertson *et al.*, 1997), as well as many others including the hypothalamus, thalamus and or olfactory system.

Whilst organotypic brain tissue slices maintain their connections within the slice, they lose important efferent connections with target areas via the slicing process. As a response to the traumatic injury caused by extraction and slicing deafferentation and axonal sprouting takes place within the slices, which causes connectivity between pyramidal cells to increase from 3% in acute slices (post-slicing) to 30% in organotypic cultures (Sakaguhci *et al.*, 1994; Gutierrez & Heinmann, 1999; Pavlidis & Madison 1999). This is one major disadvantage of the slice culture system as it causes neuronal death via axotomy, especially in embryonic and neonatal brains. In more mature brains axotomy may produce regenerative response without causing any severe neuronal damage, due to the production of growth factors. Some of the neurons in the slice will lose normal afferent connections with more distant areas and levels not included in the slice. Loss of afferent neuronal connections within the cultured slices, combined with the loss of efferent connectivity to normal target areas, leads to a reorganization of intrinsic axons in the slice (Humpel, 2015). It is important to note that this reorganisation of connectivity within the slice is likely to alter the functionality of neurons within the slice, this must be taken into consideration when studying organotypic slice cultures. Organotypic slice cultures are a pioneering tool in the *in vitro* study of complex neuronal networks as they allow for the study of several cell types. Slices can be cultured either as single regions or as whole-brain slices. Improving this method and creating new techniques may make it possible to study entire functional models of the brain with intrinsic connectivity preserved, which could provide a more accurate model for studying neurological and neurodegenerative disorders.

Hippocampal culture models are often used to study neuronal activity due to the importance of the hippocampus in learning and memory as well as a site of seizure generation (Bird & Burgess, 2008; Chatzikonstantinou, 2014). Observing spontaneous activity in organotypic slice preparations provides a more realistic view of the full spectrum of spontaneous epileptic activity and a better representation of how the brain will respond to different anticonvulsants, including the development of drug resistance (Berdichevsky *et al*., 2016; Liu *et al*., 2017).

An even more accurate representation of neuronal activity during epilepsy in humans could be provided using cultured human tissue from resective surgery. However, human tissue samples are difficult to obtain and even more difficult to successfully culture, because of this there is little experimental data from human organotypic cultures highlighting the need for an efficient and accessible method of culturing human tissue samples.

1.7 Aims and Objectives:

This project aims to refine the culture methods of organotypic slices cultures to create a fast, efficient, repeatable, and cost-effective model of epileptogenesis. Organotypic slice cultures will be used to study the process of epileptogenesis in *in vitro* slice cultures. The effectiveness of novel AEDs will be assessed in both spontaneous and induced epileptic activity. This project also aims to induce epilepsy in resected human tissue samples using the same methods that induce epileptogenesis in rodent organotypic slices.

Chapter 2: Materials and Methods

2.1 Ethical approval & animals:

All animal procedures were performed in accordance with the Animals Scientific Procedures Act (ASPA) 1986 UK (amended in 2012), European Communities Directive 1986 (86/609/EEC), HTA, NHS and local ethical review boards and the Aston University ethical review document.

2.2 Slice preparation:

Slices were prepared from both male and female Wistar rats, the experimental objectives determined the age of rat used for each experiment. Rodents between the ages of P3-P21 were used over the course of the experiments. 350µM slices were used for all experimental conditions to maintain uniformity in cultures as discussed in Chapter 3. Coronal slices were used throughout as these prove to be more resilient to the culture environment.

Prior to the extraction of the brain, rats were anaesthetised using 5% isoflurane in a mixture of O_2/NO_2. The depth of anaesthesia was determined, in accordance with the ASPA 1986, by testing for the absence of a normal pedal reflex via a pinch test. If no reflex was present, rats were immediately decapitated followed by rapid dissection and extraction of the brain. Brains were placed in ice-cold sucrose-based artificial cerebrospinal fluid (aCSF), containing (in mM): 180 sucrose, 2.5 KCl, 10 $MgSO_4$, 1.25 NaH_2PO_4, 25 $NaHCO_3$, 10 glucose, 0.5 $CaCl_2$ and 1 L-ascorbic acid, 2 N-acetyl-L-cysteine, 1 taurine and 20 ethyl pyruvate. Neuroprotectants were also added to aCSF for control conditions to minimize neuronal damage in slices, the neuroprotectants used were (in mM): 0.045 indomethacin, 0.2 aminoguanidine, 0.4 uric acid, and 0.2 Brilliant Blue G. Complete aCSF was saturated with 95% O_2/5% CO_2 (carbogen) prior to extraction to maintain a pH of 7.3, and osmolarity of 300 – 310 mOsm/L. Once placed into the sucrose-based aCSF solution, brains were transported back to the laboratory for slicing. Slices were cut while submerged in ice-cold aCSF using a 7000smz-2 model Vibrotome (Campden Instruments Ltd., UK). Slices were then transferred to an interface chamber to acclimatise at room temperature for 1 hour in a glucose- based aCSF solution containing (in mM): 126 NaCl, 3.5 KCl, 2 $CaCl_2$, 1.3 $MgCl_2$, 25 $NaHCO_3$, 1.2 NaH_2PO_4 and 11 D-glucose. Continual bubbling of carbogen through aCSF throughout helped to maintain pH
7.3 and osmolarity 300 – 310 mOsm/L.

2.2.1 Coronal Slices:

Initially, a range of slice orientations were explored in setting up the culture experiments. Coronal slices were used for culture experiments given that they held together better and maintain more connections when cultured long-term compared to sagittal and horizontal slices prepared during preliminary experiments.

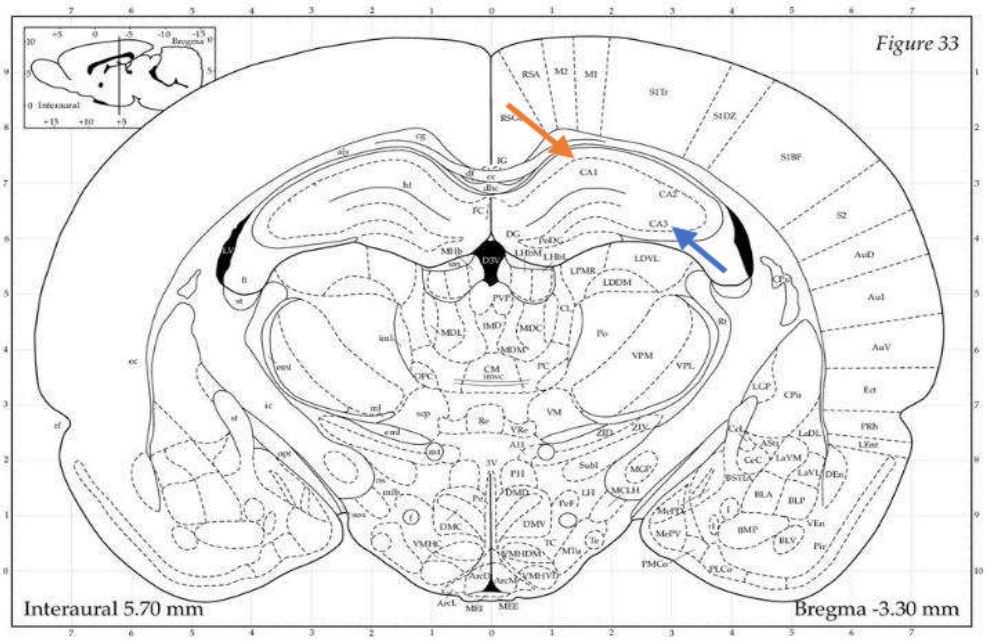

Figure 2.1: Coronal brain slice.

Image demonstrating where the CA1 (orange) and CA3 (blue) pyramidal cell layers can be found within coronal slices for placement of electrodes.

Image is taken from The Rat Brain in Stereotaxic Coordinates by Paxinos & Watson.

2.2.2 Human Tissue Slices:

Human tissue samples were obtained from a variety of brain regions, most commonly from the temporal lobe, with informed consent by GCP-trained staff from paediatric patients at Birmingham Children's Hospital who had to have resective surgery for epileptic seizures. For transport to the laboratory, samples were places in ice-cold, choline-based aCSF containing (in mM): 110 choline

chloride, 26 $NaHCO_3$, 10 D-glucose, 11.6 ascorbic acid, 7 $MgCl_2$, 3.1 sodium pyruvate,
2.5 KCl, 1.25 NaH_2PO_4, and 0.5 $CaCl_2$ with additional 0.04 indomethacin and 0.3 uric acid for neuroprotection. Choline-based aCSF was bubbled with carbogen continuously until samples reached the laboratory. Human tissue samples were then glued to agar stages to support the tissue and allow slicing all the way to the end of the tissue block and cut into 350µM slices using the same method as described above.

2.3 Organotypic Tissue Culture:

To maintain a sterile environment for slices and to avoid infection of cultures, all instruments used for both dissection and slicing were autoclaved beforehand and any equipment which could not be sterilised in the autoclave was sprayed down with 70% ethanol to kill any bacteria. Using a steriflip vacuum-driven sterile filter system (Merck Millipore, UK) solutions were filtered through 0.22µm pores to eliminate any contamination which may have occurred during the preparation of aCSF solutions.

Following the dissection, slicing and the acclimatisation period, the slices were transported to a cell culture lab in glucose-based aCSF and placed into a class 2 biological safety cabinet. Slices were then washed with culture media for 10 minutes, this was repeated once and then slices were placed onto hydrophilic PTFE, 0.4µM pore cell culture inserts (Merck, UK). Residual aCSF was aspirated off the inserts and the inserts were then placed into 6-well plates containing 1.5ml culture media. The culture media was prepared using Neurobasal-A media (Thermo Scientific, UK) supplemented with 0.5mM glutaMAX, 30mg/ml gentamicin and 1ml B27 (Thermo Scientific, UK). Slices were then incubated in a humidified incubator (Thermo Scientific, UK) at 37^{o}C, 5% CO_2, with a media change at least twice weekly. Slices were cultured for up to 14 days before performing experiments.

2.3.1 Chronic and Acute Dosing of Cultured Slices:

Chronically treated tissue slices were cultured with either Dexfenfluramine (AbCam, US) or Tianeptine (AbCam, US) at 1/10th of the standard dosage used for acute experiments. Drug compounds were added to culture media (recipe given above), applied to slices starting from DIV0 and reapplied with every media change. After 14 days in culture epileptic activity in slices was measured using LFP recordings, these data were compared with control slices which had been cultured for 14 days in the absence of the drugs being tested.

For acutely dosed slices, the slices were left untreated in culture from DIV0-DIV7 or DIV0-DIV14 – once removed from culture conditions slices had either dexfenfluramine or tianeptine bath applied to determine the drugs effect on epileptic activity. At the various time points throughout the culture process slices were transferred off the culture well inserts onto a piece of lens tissue and placed in the interface chamber of a local field potential (LFP) rig. While on the LFP rig, slices were continually perfused with glucose-based aCSF and bubbled with carbogen, if slices began to exhibit epileptiform activity drugs were applied at 10x the concentration used for chronic dosing.

2.3.2 Nomenclature:

Throughout this thesis a distinction is made between the age of animal from which the slices were taken and the number of 'days *in vitro*' the cultured slices have experienced. For example, a slice produced from a three-day old rat pup which had then been cultured for fourteen days would be referred to as P3 DIV14. Keeping a separate track of both animal age and culture length allows an approximation of the age-matched control tissue needed; although it is clear thatthe development of the brain will be different *in vitro* vs *in vivo,* neuronal maturation and network connectivity will continue to happen in the organotypic slices during their timein culture, so comparisons with naïve tissue from age matchedanimals can give an indication ofdifferences in cellular activity and network function between networks that have matured in culture vs the naturally occurring maturation of neuronal networks.

2.4 *In vitro* Electrophysiology:

2.4.1 Extracellular recordings:

Following a one-hour acclimatisation in the holding interface chamber (detailed in Figure 2.3), acute slices were transferred to an interface chamber on a local field potential (LFP) rig (Scientific Systems Design Inc, Canada). Cultured slices did not require the acclimatisation period and so were floated off culture well inserts, manoeuvred onto lens tissue using a small spatula and placed directly into the LFP interface chamber. Slices were continually perfused with glucose-based aCSF (bubbled with carbogen) at a flow rate of 3-5ml/min and temperature of 30–33^{o}C using a proportional temperature controller PTC03 (Scientific Systems Design Inc, Canada). Microelectrodes were pulled from borosilicate glass (1.2mm diameter, Warner Instruments,USA) at a resistance of 3-5MΩ using a PC-10 micropipette

puller (Narishige Ltd, Japan). Microelectrodes were filled with glucose-based aCSF and a chloride-coated silver wire was inserted into each microelectrode, microelectrodes were then fitted into one of four headstages.

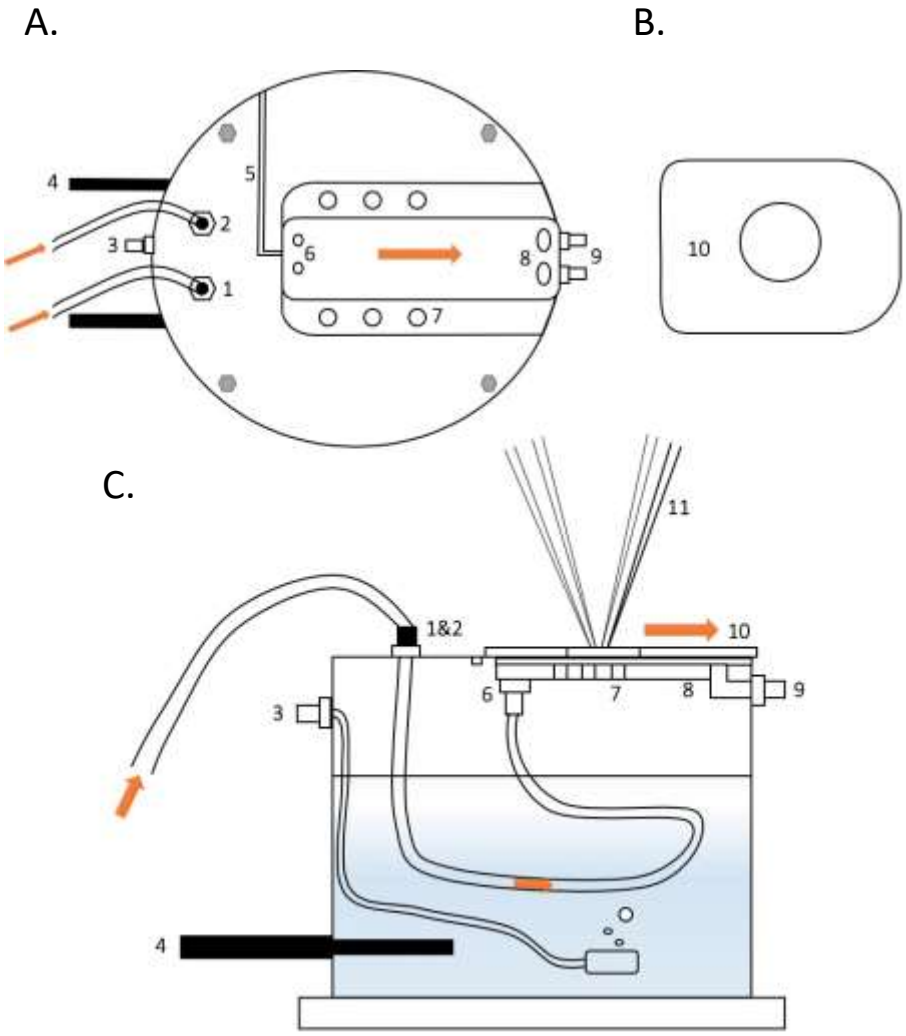

Figure 2.2: LFP interface recording chamber.

(A) Top view of the interface chamber. Tubes labelled 1 and 2 show the points through which aCSF enters the interface chamber, aCSF is then circulated through tubes on the inside of the interface chamber and exits at point 6, moving into the tray which will hold the brain slices. The tube labelled 3 demonstrates the point where gas is fed into the interface chamber. Interface heaters are shown by label 4 and help to maintain the temperature of water below the slices at 30 – 33°C. The area labelled 5 shows the guideline for insertion of the grounding wire. Port holes (7) allow rising humidified gas to leave the underneath area of the interface chamber. aCSF flows out of the

interface chamber at point labelled 8, which feeds into the drippers (9) and allows for recirculation of aCSF. (B) An Acrylic lid is placed over the slice(s), the hole in the centre allows for microelectrode access whilst maintaining high humidity. (C) Side view of the interface chamber. Water contained within the interface chamber is bubbled with carbogen via the gas feed (3). aCSF flows through tubes 1 & 2, through the water which warms up the aCSF. Microelectrodes (11) are inserted into the slice(s) via the hole in the acrylic lid (10).

Orange arrows indicate the direction of flow of aCSF.

Microelectrodes were manipulated using an MM-3 micromanipulator (Narishige Ltd, Japan) and an Olympus SZ51 (Olympus, UK) stereomicroscope was used for visualisation. Microelectrodes were inserted into layers CA1 or CA3 of the hippocampus. Depending on the experimental objectives, drugs such as dexfenfluramine, tianeptine, gabazine or CNQX were also added to aCSF to be bath applied to the slices and recirculated as required.

The receiving signals were amplified 100x using EX10-2F amplifiers (NPI Electronics GMBH, Germany) setting a high-pass filter of 0.1Hz and a low-pass filter of 1kHz. Electrical noise (50Hz) was filtered by passing the signal through Humbugs (Quest Scientific, Canada). The receiving signal was amplified a further 10x using LHBF-48X amplifiers (NPI Electronics GMBH, Germany) with a high-pass filter of 0.3Hz and a low-pass filter of 700Hz. Signals were digitised at a sampling rate of 5kHz using a CED Micro1401-3 analogue-to-digital converter (Cambridge Electronic Design, UK) and recorded using Spike2 software (Cambridge Electronic Design, UK).

The signal received is a summation of transient changes in extracellular ion concentrations. Local field potentials are generated by groups of neurons which produce sinks and sources (see Chapter 1), the currents arise as a result of synaptic activity (EPSPs and IPSPs) but is also influenced by other intrinsic events. LFP, therefore, provides an insight into the cooperative behaviour of neurons (Buzsaki et al., 2012). However, it is important to remember that the microelectrode tip at this impedence has a recording area of roughly 250µm (Katzner et al., 2009) providing a relatively small sampling area when compared to other field recording techniques, such as microelectrode arrays.

For acute dosing experiments, activity was recorded for up to 40 minutes before the application of any drug. Following drug application, a 20-minute period was given to allow drugs to act before analysing the effects on epileptiform activity.

2.4.3 Intracellular recordings:

Gap free whole-cell patch-clamp recordings were made using standard techniques (Woodhall et al., 2009). Whole-cell voltage-clamp involves holding cells at a set voltage or membrane potential (mV) to measure the flow of current (pA) passing through the cell via the ion channels. Activation of ion channels by neurotransmitters causes an influx of ions across the cell membrane, and because the membrane potential is clamped at a specific voltage, the current required to equate this flux acts as a proxy measurement for synaptic currents generated by receptor activation. Therefore, a current equal and opposite to the current through the channels will pass in order to ensure the maintenance of the clamped membrane potential, these currents are displayed as 'events'.

Electrodes for patch-clamp experiments were pulled from borosilicate glass (1.2mm diameter) at a tip resistance of 2.5-5MΩ using a P-1000 Flaming/Brown micropipette puller (Sutter Instruments, US). Electrodes were filled with an internal solution specific for recordings either spontaneous inhibitory post-synaptic currents (sIPSCs) or spontaneous excitatory post-synaptic currents (sEPSCs).

The internal solution for measuring sIPSCs contained (in mM): 100 CsCl, 40 HEPES, 1 Qx-314, 0.6 EGTA, 5 MgCl2, 10 TEA-Cl, 4 ATP-Na, 0.3 GTP-Na (titrated with CsOH to pH 7.3) at 290–295 mOsm. For measuring sEPSCs the internal solution contained (in mM): 100 Cs-gluconate, 40 HEPES, 1 Qx-314, 0.6 EGTA, 2 NaCl, 5 Mg-gluconate, 5 TEA-Cl, 10 Phospho-Creatinine, 4 ATP-Na, 0.3 GTP-Na (titrated with CsOH to pH 7.3) at 285-290 mOsm. Both internal solutions had a final pH of 7.3.

As in the LFP experiments, for the patch-clamp recordings, acute slices required a one-hour acclimatisation period before being transferred onto the patch rig for recording. The cultured slices did not require an acclimatisation period and were transferred onto the patch rig by floating them directly off the PTFE inserts from culture. Recordings were performed in a submerged chamber, slices were weighed down using platinum rods to ensure that they did not move during the recording. The temperature of the circulating aCSF was maintained and ~30^{o}C using a TC-324C single channel temperature controller (Warner Instruments, USA). Filled electrodes were fitted to a CV 203BU head stage (Molecular Devices, USA) which was manipulated using a PatchStar Micromanipulator (Scientifica, UK). A Basler Ace 2.3 MP PowerPack Microscopy camera (Basler, Germany) and Olympus BX51 microscope with Nomarski optics was used for locating and visualising target cells, once appropriate cells were located, the electrode was lowered to just above the cell wall. A seal was then formed between the membrane and the electrode tip, a resistance of at least 1GΩ was reached before attempting to break through the cell membrane. Once the cell membrane had been broken through,

a seal test (5mV pulse at 50Hz) was applied for 7-10minutes to allow adequate filling of the cell with the internal solution. An Axopatch 200B Microelectrode Amplifier (Molecular Devices, USA) was used to hold cells at a voltage of -70 mV. After filling the cell, at least 5 minutes of baseline was recorded before the bath application of drugs. A seal test was applied every 10 minutes to monitor any changes in the access resistance to the cell. Any recordings where the seal test altered >30% of the original access resistance, or where the holding current of the cell dropped below -500pA, were immediately discarded. Large changes in access resistance could alter the amplitude and kinetics of the events, therefore undermining the effect of any drugs, making the results invalid.

IPSCs and EPSCs were recorded at a holding potential of -70mV using an Axopatch 200B amplifier (Molecular Devices, US). Signals were filtered at 5kHz with an 8-pole Bessel filter and digitized at 10kHz using a Digidata 1440A digitizer and recorded using pClamp software (Molecular Devices, US). Data were analysed using Clampfit 10.7, GraphPad prism 8 and Microsoft Excel. The data were normalised and presented as mean with SEM.

2.4.4 Drugs & Reagents:

The drugs used were gabazine, valproate, lamotrigine, topiramate, dexfenfluramine and tianeptine (Tocris Bioscience, UK, Sigma-Aldrich, UK). Drugs were dissolved in either dH_2O or DMSO and diluted into stock solutions of 1-50mM and stored in aliquots at -20^{o}C. Prior to being added to brain slices, aliquots were defrosted and diluted down to their final concentration. Drugs were then bath applied to the slices by adding them directly into the perfusing aCSF and then were left to stabilise for at least 40 minutes or until slice had displayed epileptiform activity multiple times. Once slices had stabilised, subsequent drug application was recorded for 30 – 40 mins following the application of each drug for LFP recordings. For patch-clamp recordings drug application was recorded for 15-20 mins following application of the drug.

2.5 Data collection and Analysis:

2.5.1 LFP data analysis:

Data were recorded and visualised using Spike2 software (Cambridge Electronic Design, UK). Activity from slices was monitored for up to 120 minutes, starting from the time electrodes were placed. Epochs of 120 seconds were used for data analysis, were drugs were applied epochs were taken 45 minutes after the bath application of the drug. Data collected from Spike2 were then transferred into Microsoft Excel. Graphs were plotted and statistical analysis was performed using GraphPad Prism8. The data are presented as mean with SEM.

2.5.2 LFP Seizure Analysis & Definition:

Seizure-like activity was defined as a series of paroxysmal discharges which could be clearly distinguished from baseline activity and lasted for a duration of longer than 5 seconds, containing events with an interevent interval of less than 800ms. Where bursting events occurred, events that deviated from the baseline within 5 seconds of return were classed as the same seizure-like event.

Seizures were determined via manual analysis of raw LFP traces, using Spike2 software to access seizure duration and interevent intervals.

2.5.3 Patch-Clamp Analysis:

Patch-clamp data were analysed in ClampFit (version 10.4, Molecular Devices) and transferred to Microsoft Excel and GraphPad Prism (version 8.0.1) for further analysis. For event detection, an event template of ~20 events was created before carrying out a threshold search. For each condition, 200 events were extracted from gap free recordings. Peak amplitude (pA), decay tau (ms), and inter-event interval (IEI) (ms) were determined and used as the basis of event analysis. Data were transferred to GraphPad Prism for statistical analysis.

2.5.4 Immunohistochemical staining:

Brain slices were initially placed in 4% paraformaldehyde (PFA) in PBS for 3-7 days (depending on time spent in culture) to provide a moderate fix and then transferred into 30% sucrose in PBS for 24 hours. Slices were then re-sectioned into 80uM slices using a freezing-stage sledge microtome (Bright

Instruments, UK). Following this, slices were incubated at room temperature in PBS, supplemented with 10% normal goat serum (NGS) and 0.3% triton x-100 for 2 hours. Slices were then washed 3 times with PBS and following this, anti-NeuN and anti-GFAP primary antibodies (Cell Signalling Technologies & AbCam, US) were added at a 1:200 and 1:1000 dilution, respectively, and incubated at 8^{o}C on a shaking platform for 24 hours. Following this incubation period, slices were again washed 3 times with PBS, then the anti-NeuN and anti-GFAP secondary antibodies (Cell Signalling Technologies & AbCam, US) were added at a dilution of 1:500 and 1:2000, respectively, to stain for neuronal nuclei and identify any astrocytic activity. Slices were then incubated on a shaking platform at 8^{o}C overnight. Slices were given 3 final washes with PBS and mounted onto glass slides for imaging using VECTASHIELD antifade mounting medium (Thermo Scientific, UK).

Prior to mounting slices coverslips were coated in 1% Gelatin (Sigma-Aldrich, UK) to assist with adherence.

Samples were imaged using confocal SP8/Falcon microscope (Leica Microsystems, Germany).

2.5.5 Image Analysis:

All images were analysed using ImageJ software where a region of interest (within the hippocampus) was determined, the channel split function was used to split the merged images into separate red and green fluorescence images. Fluorescence analysis was then performed on each image separately, using the measure fluorescence function, to determine the mean fluorescence of each stain within the region of interest. Data were transferred to GraphPad Prism to plot graphs and determine statistical significance.

Chapter 3: Culture Optimisation

3.1 Introduction:

The analysis of animal models of neurological disorder has been instrumental in the study of neurodevelopment and diseases of the brain. Advances in neuroscience and cell culture techniques have made it possible to study cultured neurons as isolated cells or as groups of neurons which have formed connections with one another in culture, either spontaneously or via chemical induction. *In vitro* cell culture allows researchers to study large quantities of homogenous cells in isolation and gain an understanding of their cellular processes. Primary dissociated cell cultures can be used as a supplement for *in vivo* animal experimentation in some cases, however, these cultures do not reflect the nature of the organ as a whole due to a lack of contact with surrounding cells. Neuroscientists may use cultures of primary dissociated neurons, astrocytes, or oligodendrocytes to study the survival, morphology and function of cells while also greatly reducing the number of animals needed for experimentation (Potter & DeMarse, 2001). While this knowledge is helpful it cannot provide any information on the network function of the brain and how cells communicate with each other or with cells in other brain regions. Being able to study and assess how cells communicate with each other as a network is necessary for the study of brain function and diseases of the brain such as epilepsy. For this reason, organotypic slice cultures are an important middle ground between cell cultures and *in vivo* animal experiments as they simulate a more accurate *in vivo*-like environment. Organotypic cultures allow the basic structural and connective organisation of the original tissue to be preserved which enables researchers to carry out structural organisation studies, this is particularly important when studying the brain as organotypic cultures allow aspects of both the structural and synaptic organisation of the brain to be preserved.

While the study of acute slices also provides the ability to study certain network function and cellular communications organotypic slices cultures provide the advantage of enabling long term studies to be carried out on slices extracted from the same animal over weeks or months. This ability to sustain organotypic slices in culture for long periods of time provides an opportunity to carry out chronic dosing experiments, where slices can be subject to a low-dose of a drug over an extended period of time. This is particularly useful when studying diseases such as epilepsy where patients are typically treated with medication for the rest of their lives.

The term organotypic was first coined when researchers began culturing various organs taken from chick embryos (Loffredo & Sampaolo, 1956; Monesi, 1960; Reinbold, 1984). In 1970, organotypic

mouse cerebellum was cultured by M.K. Wolf (Wolf, 1970). Following on from these experiments in 1981, BH Gähwiler cultured organotypic brain slices using the roller tube technique where slices were embedded in a plasma clot, attached to coverslips by the addition of thrombin and cultured inside roller-tubes (Gähwiler, 1981). Since then the procedure has been optimised and slices are now often cultured on semi-permeable membranes (Gähwiler 1988; Braschler *et al.*, 1989; Stoppini *et al.*, 1991; Gähwiler *et al.*, 1997, 2001). This technique calls for slices to be placed onto a semi-permeable membrane with media underneath and placed in humidified incubators at 37^{o}C with 5% CO_2, slices cultured in this way only need to be handled when changing the media. Depending on the pore size of the membrane that is used the specific substrates that can pass through the membrane and diffuse into the slice can be controlled.

The age of the animal donor for cultured organotypic slices is an important consideration to take when creating hippocampal slice cultures as tissue/cells taken from embryonic donors generally survive better than that taken from older animals. Early postnatal donors are the most favourable for organotypic brain slice cultures due to their morphology, survival rate and stability (Hutter-Schmid *et al*., 2015). Tissue from late foetal (E21) to P7 rats have been cultured for up to 60 days using Gähwilers roller tube technique (Ostergaard *et al*., 1990). More recently, slices taken from P8 – P10 brains have been cultured and are reported to have survived well using the semi-permeable membrane technique for up to several months (Marksteiner & Humpel, 2008). In 2015, Mosa *et al*. used this technique to study postnatal neurogenesis in the hippocampus claiming the method allowed slices to maintain their characteristic topographical morphology whilst allowing pharmacological agents to be directly applied to the developing dentate gyrus of the hippocampi. Slice cultures were able to be maintained for up to 4 weeks, therefore allowing the maturation of new neurons to be studied as well (Mosa *et al*., 2015).

Few papers using intact slices from adult donors have been published, however, in 2002, healthy adult hippocampal slices were maintained for up to 6 days using an aCSF-like media (Wilhelmi *et al*., 2002). Other papers have reported that adult rodent slices were successfully cultured and used to follow the process of naturally occurring cell death over several weeks, looking specifically at the maturation and plasticity of the neuronal circuits (Lossi *et al*., 2009). A 2015 paper claims to have dissected slices from 9-month-old mice and culture them for a 2-week period to study amyloid plaques in Alzheimer's disease. The cultured slices showed amyloid beta plaques surrounded by reactive neurons and microglia, however more sensitive neurons did not survive the culture process (Humpel, 2015). While these results look promising and could provide a useful method for the study of transgenic animals

and resected human tissue there is still much more research required into the culturing of adult organotypic rodent slices, the process still needs optimisation.

Organotypic brain slice cultures offer possibilities of studying various brain cells *in vitro*, so far,they have been utilised in voltage-clamp, current-clamp and LFP recordings, long- term live imaging, immunohistochemistry, extraction of cells for cell-based assays and more (Jahnsen *et al*., 1999; Dong & Buonomano, 2005; Gogolla *et al*., 2006; Ullrich *et al*., 2011). Current neuroscience research will often use organotypic brain slice cultures where the brains are extracted from young rodents as they provide many advantages over neuronal cell cultures. However, whilst these cultures allow for some of the brains local circuitry to remain intact, many important afferent and efferent connections are still lost within the target areas via the slicing process as the slices are an axotomized system. The axotomy of cells is a major drawback to using organotypic slice cultures as it can induce neuronal cell death; embryonic/neonatal brains are particularly sensitive to this as they are still maturing and require neurotrophic factors to specific target areas and patterned activity (Noraberg *et al*., 1999).

The loss of both afferent and efferent connections within these cultured slices causes a reorganisation of neurons within the slices whereby axons within the slice will migrate to reach areas which have been axotomized to form new neural connections (Novak & Bolz, 1993). However, this axotomy does allow for the study of synaptogenesis and neuronal sprouting as cultured brain slices have been shown to form new functional synaptic connections and recover neuronal transmission following injury (Stoppini *et al*., 1993). It has been proposed that the sprouting reaction and synaptic regeneration are associated with the expression of a highly sialylated form of neuronal cell adhesion molecule (N-CAM) following axotomy. N-CAM mediates cell-cell interactions and has previously been implicated in axonal pathway formation, neurite outgrowth and synaptic remodelling. The mechanism by which N- CAM contributes to such events is presumed to be due to modifications which result in the polysialation of the molecule, as when the polysialaic acid portions of N-CAM are removed the sprouting reaction becomes significantly delayed (Muller *et al*., 1994).

Another disadvantage of using organotypic cultures is that the tissue is continuously changing while in culture with slices becoming thinner with increasing days in culture which can create problems when trying to characterise the functionality of the tissues in *in vitro* experiments (Mosa, *et al*., 2015).

All of these experiments indicate that, despite the above issues, long-term organotypic slices are a compelling model for the study of synaptogenesis, neural plasticity, and cellular atrophy (Bahr, 1995). Organotypic brain slices cultures offer several advantages for the study of epilepsy, as previously

mentioned they maintain much of the original brain structure which allows interactions between cells and networks to be studied in a more natural environment. As organotypic slice cultures allow for quick and precise application of drugs, they are an efficient model for drug testing and they can remin viable for long periods of time in culture making them a stable platform for long-term studies such as chronic dosing studies (Plug et al., 2024). They also enable the recording of electrical activity via electrophysiology and can be used to model various aspects of epilepsy including genetic mutations, environmental factors or potential therapeutic interventions, which is crucial for understanding the mechanisms of epilepsy and how they may be treated (Chong et al., 2023; Oblasov et al., 2023). However, while this *in vitro* model helps us to gain insights into the mechanisms of neuronal activity and bridge the gap between *in vitro* cell cultures and *in vivo* animal models, it is still unclear how similar these models are to *in vivo* animal models and therefore any research on organotypic slice cultures must still be translated to animal models for validation. Further improvement and new techniques still need to be researched to improve both healthy and disease models in organotypic slice cultures, but they are a promising model for the study of neurodegenerative and neurological diseases, including epilepsy, whilst helping to reduce the number of animal experiments required for this kind of research.

For the past 40 years, *in vitro* research has been done in acute brain slices to study the neurobiology of epilepsy in preclinical research. Using electrophysiology, optical imaging and cell/molecular biology techniques, researchers have been able to gain insight into the pathology of epilepsy via *in vitro* brain slice experimentation. While this research is translational and extremely important in the study of epilepsy, a better alternative would be to carry out the same research in live human brain tissue, e.g. from resective surgery. As mentioned previously, many epilepsies are refractory and resective brain surgery to remove the seizure focus is the only option for some patients to prevent seizures. When these resective surgeries take place, the resected tissue is often discarded. However, the live human brain tissue can be easily retrieved from these surgeries and used for experimental purposes in a laboratory. At present this technique is not so widely used as it requires a close working relationship – and often a close physical proximity – between hospitals and research institutions. The lab where the experiments are taking place must be relatively near the hospital to ensure tissue is still living when it returns to the lab for experiments. Due to the variability of the tissue received and the rarity of some conditions it can take a long time to accumulate satisfactory results from these experiments. There is also a lack of control tissue available as when doing resective surgery neurosurgeons want to remove as little healthy tissue as possible, so non-epileptic control samples are difficult to obtain, especially from paediatric patients. However, despite these considerations the use of living human

brain tissue can provide us with extremely relevant information about the pathology of epilepsy and can help to create a better, more accurate and translational animal model of epilepsy (Jones *et al*., 2016).

In this chapter we will look at the effects of both age of donor and culture media composition on the survival of organotypic brain slices cultures and spontaneous epileptic activity, touching on the feasibility of culturing live human brain tissue sections using the same method.

3.2 Materials & Methods:

3.2.1 Ethical approval:

All animal procedures were performed in accordance with the Animals Scientific Procedures Act (ASPA) 1986 UK (amended 2012), European Communities Council Directive 1986 (86/609/EEC), and the Aston University ethical review document.

3.2.2 Slice Preparation:

300 – 450µM sagittal or coronal slices were prepared from either P3, P7 or P21 (15-60g) Wistar rats of either sex. Prior to the extraction of the brain, rats were anaesthetised using 5% isoflurane in a mixture of O_2/NO_2 until no pedal reflex was detected. For rats aged P21, further anaesthetisation was required following isoflurane, so rats were then injected subcutaneously with pentobarbital (600mg/kg) and intramuscularly with xylazine (10mg/kg) to induce deep anaesthesia. Depth of anaesthesia was determined by testing for the absence of a normal pedal reflex via a pinch test. If no reflex was present, rats were then bathed in ice-cold water for approximately 45 seconds, pedal and corneal reflexes were then tested again before performing a transcardial perfusion. P21 rats were perfused with 30 – 40ml ice-cold sucrose-based artificial cerebrospinal fluid (aCSF) which contains (in mM): 180 sucrose, 2.5 KCl, 10 $MgSO_4$, 1.25 NaH_2PO_4, 25
$NaHCO_3$, 10 glucose, 0.5 $CaCl_2$ and 1 L-ascorbic acid, 2 N-acetyl-L-cysteine, 1 taurine and 20 ethyl pyruvate. Neuroprotectants were also added to aCSF to protect against neuronal damage and improve slice viability, neuroprotectants used were (in mM): 0.045 indomethacin, 0.2 aminoguanidine, 0.4 uric acid, and 0.2 brilliant blue G. Complete aCSF was saturated with 95% O_2/5% CO_2 (carbogen) prior to perfusion to maintain a pH of 7.3, and osmolarity of 300 – 310 mOsm/L. Following the perfusion, the

brain was quickly dissected, extracted from the skull, and placed in the remaining aCSF solution for transportation.

For rats aged P7 following anaesthetisation rats were immediately euthanised by decapitation using surgical scissors and the brain extracted from the skull as quickly as possible. Once extracted the brains were placed in a sucrose-based artificial cerebrospinal fluid (aCSF) solution which contains (in mM): 180 sucrose, 2.5 KCl, 10 $MgSO_4$, 1.25 NaH_2PO_4, 25 $NaHCO_3$, 10 glucose, 0.5 $CaCl_2$ and 1 L-ascorbic acid, 2 N-acetyl-L-cysteine, 1 taurine and 20 ethyl pyruvate. Complete aCSF had been saturated with 95% O_2/5% CO_2 (carbogen) prior to the extraction to maintain a pH of 7.3, and osmolarity of 300 – 310 mOsm/L. Brains were then transported back to the lab in the aCSF solution, once back in the lab slices were glued onto a stage and submerged in ice-cold aCSF to be sliced.

Slices were cut while submerged in ice-cold aCSF using a 7000smz-2 model Vibrotome (Campden Instruments Ltd., UK). Slices were then transferred to an interface chamber to acclimatise at room temperature for 1 hour in a glucose-based aCSF solution containing (in mM): 126 NaCl, 2.5 KCl, 1$MgCl_2$, 2.5 $CaCl_2$, 26 $NaHCO_3$, 2 NaH_2PO_4 and 10 D-glucose. Neuroprotectants were also added (in mM): 0.045 indomethacin and 0.4 uric acid. Continual bubbling of carbogen through aCSF throughout helped to maintain pH 7.3 and osmolarity 300 – 310 mOsm/L.

3.2.3 LFP Recording:

Following acclimatisation in the holding chamber, slices were transferred to an interface chamber on a local field potential (LFP) rig (Scientific Systems Design Inc, Canada). Slices were continually perfused with glucose-based aCSF (bubbled with carbogen) at a flow rate of 3 – 4ml/min and temperature of 30 – 33^{o}C using a proportional temperature controller PTC03 (Scientific Systems Design Inc, Canada).

Microelectrodes were pulled from borosilicate glass (1.5mm diameter) at a resistance of 3-5MΩ using a PC-10 micropipette puller (Narishige Ltd, Japan). Microelectrodes were filled with glucose-based aCSF, then a chloride-coated silver wire could be inserted into the microelectrode, and microelectrodes were placed into a head stage. Microelectrodes were manipulated using an MM-3 micromanipulator (Narishige Ltd, Japan) and an Olympus SZ51 (Olympus, UK) stereomicroscope was used for visualisation. Microelectrodes were inserted into layers CA1 or CA3 or the hippocampus. The receiving signals were amplified 100x using EX10-2F amplifiers (setting a low-pass filter of 0.1 Hz and a high-pass filter of 1k Hz) (NPI Electronics GMBH, Germany). Electrical noise (50Hz) was filtered by passing the signal through Humbugs (Quest Scientific, Canada). The receiving signal was amplified a

further 10x using LHBF-48X amplifiers (low-pass filter 0.3 Hz, high-pass filter of 700 Hz) (NPI Electronics GMBH, Germany). Signals were digitised at sampling rate of 5 kHz using a CED Micro1401-3 analogue-to-digital converter (Cambridge Electronic Design, UK) and recorded using Spike2 software (Cambridge Electronic Design, UK).

Data were visualised using Spike2 software (Cambridge Electronic Design, UK). Continuous recording monitored activity from slices for up to 120 minutes, starting from the time electrodes were placed. Epochs of 120 seconds were used for data analysis. Raw data were filtered using a Bessel filter (bandpass of 0.5 – 15Hz for theta oscillations and 20 – 80 Hz for gamma oscillations). Power spectrum analysis was preformed using Clampex10.3 and Clampfit to produce Fast-Fourier transforms (FFTs) with a bin size of 8192, from 120 second epochs of recorded activity. Data collected from Spike2 was then transferred into Microsoft Excel. Statistical analysis was performed using GraphPad Prism8. The data are presented as mean with SEM.

3.2.4 Tissue Culture:

To maintain a sterile environment for slices and avoid infection of cultures, all instruments used for both dissection and slicing were autoclaved beforehand. Any equipment which could not be sterilised in the autoclave was sprayed down with 70% ethanol to kill any bacteria.

Following the dissection and slicing, brain slices were bathed in an oxygenated glucose-based aCSF solution containing (in mM): 126 NaCl, 3.5 KCl, 1.3 $MgCl_2$, 1.2 NaH_2PO_4, 25 $NaHCO_3$, 2 $CaCl_2$ and 11 glucose for 1 hour before being transferred to a biosafety cabinet, washed in culture media for 10 minutes and placed onto hydrophilic PTFE, 0.4µM pore cell culture inserts (Merck, UK). Residual aCSF was then aspirated off and inserts were placed into 6-well plates containing 1.5ml culture media.

The medias used for these experiments was prepared using Advanced Dubecco's Modified Eagles-Medium (DMEM/F12) (ThermoFisher, UK), 1% penicillin/streptomycin (Sigma-Aldrich, UK) and 8µM L-glutamate (Sigma-Aldrich, UK) supplemented with 10% FBS (Sigma-Aldrich, UK) in some instances. The other culture media which was tested was prepared using Neurobasal-A media (NBA) (Thermo Scientific, UK) supplemented with 0.5mM glutaMAX, 30mg/ml gentamicin and 1ml B27 (Thermo Scientific, UK).

Brains used for tissue culture were dissected and extracted as described in Chapter 2. Following extraction brains were sliced inside a Class 2 biological cabinet using a manual slicer. Once slices were

cut, they were bathed in standard aCSF (components listed above) for 30-40 minutes at room temperature before being transferred onto a PTFE 0.4µM pore inserts (Merck, UK). Any residual aCSF remaining on the slices/inserts was then aspirated off and inserts were placed into the wells of a 6-well plate containing 1.5mL culture media. Slices were then incubated in a humidified incubator (Thermo Scientific, UK) at 37°C, 5% CO_2, with a media change twice weekly.

3.2.5 Drugs & Reagents:

Gabazine was used to determine slice viability on LFP recordings. Gabazine was dissolved into stock solutions of 2.5mM in DMSO and stored in aliquots at -20°C. Prior to being added to brain slices, aliquots were defrosted and diluted down to their final concentration. Drugs were then bath applied to slices by adding them directly into the perfusing aCSF and were left to stabilise for at least 45 minutes. 250nM – 500nM gabazine (GBZ) (Sigma-Aldrich, UK) was applied at the end of each experiment to see if activity could be induced in slices as an indication of surviving neurons.

3.2.6 Immunohistochemistry:

Slices which were to be immunolabelled were initially placed individually into wells of a 24-well plate containing 4% paraformaldehyde (PFA) in PBS overnight to provide a moderate fix and then transferred in 30% sucrose in PBS for 24 hours. Rodent slices were then resectioned into 80µM slices using a freezing stage sledge microtome (Bright Instruments, UK). Slices were incubated at room temperature in PBS supplemented with 10% normal goat serum (NGS) and 0.3% Triton x-100 for 2 hours. Slices were then washed 3 times with PBS and following this anti-NeuN and anti-GFAP primary antibodies (Cell Signalling Technologies & AbCam, US) were added at a 1:200 and 1:1000 dilution, respectively, to visualise the quantities of neuronal nuclei and glial fibrillary acidic protein present in slices and determine the expression of neurons and glia over time.Slices were thenincubated at 8°C on a shaking platform for 24 hours, following this incubation period slices were again washed 3 times with PBS then the anti-NeuN and anti-GFAP secondary antibodies (Cell Signalling Technologies & AbCam, US) were added at a dilution of 1:500 and 1:2000, respectively. Slices were then incubated on a shaking platform at 8°C overnight. Slices were given 3 final washes with PBS and mounted onto glass slides for imaging using VECTASHIELD antifade mounting medium (Thermo Scientific, UK). Prior to mounting slices coverslips were coated in 1% Gelatin (Sigma-Aldrich, UK) to assist with adherence. Slices were imaged using confocal SP8/Falcon microscope (Leica Microsystems, Germany).

3.2.7 PBS & PLA inserts:

A separate series of experiments was conducted to determine whether bespoke biomaterial mesh made from polybutylene succinate (PBS) or polylactic acid (PLA) created by the Chemistry group at Aston University would increase the health or viability of culture slices for epileptic slices cultures. Inserts were created using various combinations of ratios of PBS and PLA and placed into culture wells directly beneath slices taken from P7 rats. Inserts were formed using an electro-spin syringe pump, where the distance of the syringe needle from the collector determined the thickness of the mesh created (the closer the needle of the syringe was to the collector, the thicker the final mesh product). It was hypothesized that the use of biological materials could maintain healthy slices for a longer time in culture, while a thicker insert may improve gaseous diffusion and therefore further improve the health of slices. Whether or not a slice was healthy was determined using LFP recordings, slices which did not show any signs of epileptic activity were deemed healthy. Application of gabazine at the end of recordings was used to determine whether slices were alive but not epileptic or had died in culture.

3.3 Results:

3.3.1 Refinement of culturing slices:

Initial organotypic culture experiments used brain tissue extracted from P21 rats and sliced into sections of thickness 450µM. These slices were cultured on standard PTFE inserts with a 0.4µM pore with 2mL media in the wells of a 6-well plate. It was observed quite quickly that 2mL media was too much as it caused slices to float within the wells, so they were unable to form an attachment to the inserts. In subsequent experiments the volume of media per well was reduced to 1.5mL which was capable of covering the bottom of the well and insert without causing the slices to free float.

To begin with the media used was advanced DMEM media supplemented with L-glutamate in an attempt to create a serum and antibiotic free way to culture organotypic slices. However, 100% of all the cultures set up using this media developed an infection within the first 4 days in culture so 1% penicillin/streptomycin was added to the media to prevent infection. To improve the sterility of extraction and slicing of the brain, all surgical and experimental tools were prepared using a desktop autoclave (Prestige Medical, UK). Anything that could not be autoclaved was sterilised using 70%

ethanol. Following the addition of antibiotic and refined aseptic technique, slice viability increased from approximately 40% to 75% (data prior to aseptic refinements not shown) and infections rate decreased by up to 38%. Media changes per week were also reduced by 50% to minimise the number of times the slices cultures had to be handled. Whether the nutrients within the media had been exhausted or not was determined by colour change from pink/red to yellow/orange since media did not reach the yellow/orange stage when doing 4x media changes per week it was concluded that 2x a week media change was sufficient.

Once the method of extraction and dissection had been optimised, the effects of slice thickness on survival rate were examined. Slices of thickness 450µM, 400µM and 350µM were compared with 350µM slices producing noticeably healthier cultured slices after just 2-3DIV. It was determined that slicing at a thickness of 350µM produced the healthiest slices as thicker slices dried out on the upper surface and were more prone to infection. The health of slices was determined by checking cultures daily for signs of infection such as the colour and transparency of slices – slices which were not surving well in culture became dried out, spread across the inserts and turned a white-grey tone whilst healthy slices exhibited a small reduction in size and remained the standard pink-peach colour. Data for these experiments is not shown as 400-450 µM slices did not maintain structural integrity throughout the culture process and no electrophysiology or immunolabelling could be performed on these cultures.

P7 and P21 rodent tissue slices were then investigated as Berdichevsky *et al.* (2016) have previously described, using NBA supplemented with B27, L-glutamate and 1% pen/strep, to create epileptic hippocampal cultures (Berdichevsky *et al*., 2016). This media composition was compared with DMEM supplemented with L-glutamate, and DMEM supplemented with 10% FBS and L-glutamate to assess which media composition produced the most viable slices after 2 weeks in culture.

DMEM is a general-purpose culture media used widely for cell and tissue culture as it supports a wide range of cell types, it is commonly used in combination with supplements like N-2 and FBS to support the growth of astrocytes and glia. This media was tested against NBA, a media specifically designed to support the growth of neurons and suppress glial cell growth, in combination with a B-27 supplement which enhances neuronal survival and function. These medias were tested against each other to confirm whether NBA with B-27 would provide an optimal environment for the long-term culture of organotypic brain slices, as overexpression of glia and astrocytes can be an indicator of disease within the brain it is preferable to keep their growth while in culture to a minimum.

3.3.2 Culture Slice Infection rates:

Figure 3.1 shows the infection rate of slices cultured in each media composition, comparing antibiotic free media compositions with media to which 1% penicillin streptomycin (pen-strep) was added and media to which 30mg/ml gentamicin was added. Infected cultures displayed a distinct white/pale ink precipitate that formed on top of slices and spread over the culture well inserts. The degree of infection could be determined by how far this precipitate had spread across the cultures. Infections caused slices to become extremely fragile and disintegrate when being removed from the wells.

Pen-strep is a commonly used antibiotic combination in many cell culture protocols as it provides broad-spectrum coverage against gram-positive and gram-negative bacteria, but it has potential cytotoxic effects for brain slices cultures which may affect their viability (Bak et al., 2023). Gentamicin is also a broad-spectrum antibiotic; however, it is generally less cytotoxic to mammalian cells compared with other antibiotics making it more suitable for delicate cultures (Plug et al., 2024). These two conditions were compared against an antibiotic free control to determine which condition was most suitable for long-term slice cultures.

Data collected from both P7 and P21 cultures is pooled in these data as age did not appear to be a critical factor in determining the likelihood of a culture becoming infected.

Figure 3.1A demonstrates the infection rate for each individual culture condition against the others, unfortunately, due to low number of repeats (n=4 each condition) the data shown in Figure 3.1A does not indicate culture condition which significantly reduces the infection rate.

For this reason, the data have been pooled to determine the effectiveness of the antibiotic conditions alone and demonstrate conditions where n = 15 observations per group (shown in Figure 3.1B). An RM one-way ANOVA with a Tukey's multiple comparisons post hoc test determined that there was a significant difference between the non-antibiotic group and the group cultured with 30mg/ml gentamicin present (56.00% to 40.33% ± 5.65%, $p < 0.05$, n = 15, DF = 14).

From this data it was determined that the addition of antibiotics to media would be beneficial going forward given that the addition of 30mg/ml gentamicin significantly reduced the infection rates in the various media compositions. Antibiotic free media would be preferable as antibiotics may affect metabolism, proliferation, or differentiation of cells, and therefore have the possibility of skewing the results. However, in this instance, as it significantly reduces the infection rates it is worth using gentamicin going forward.

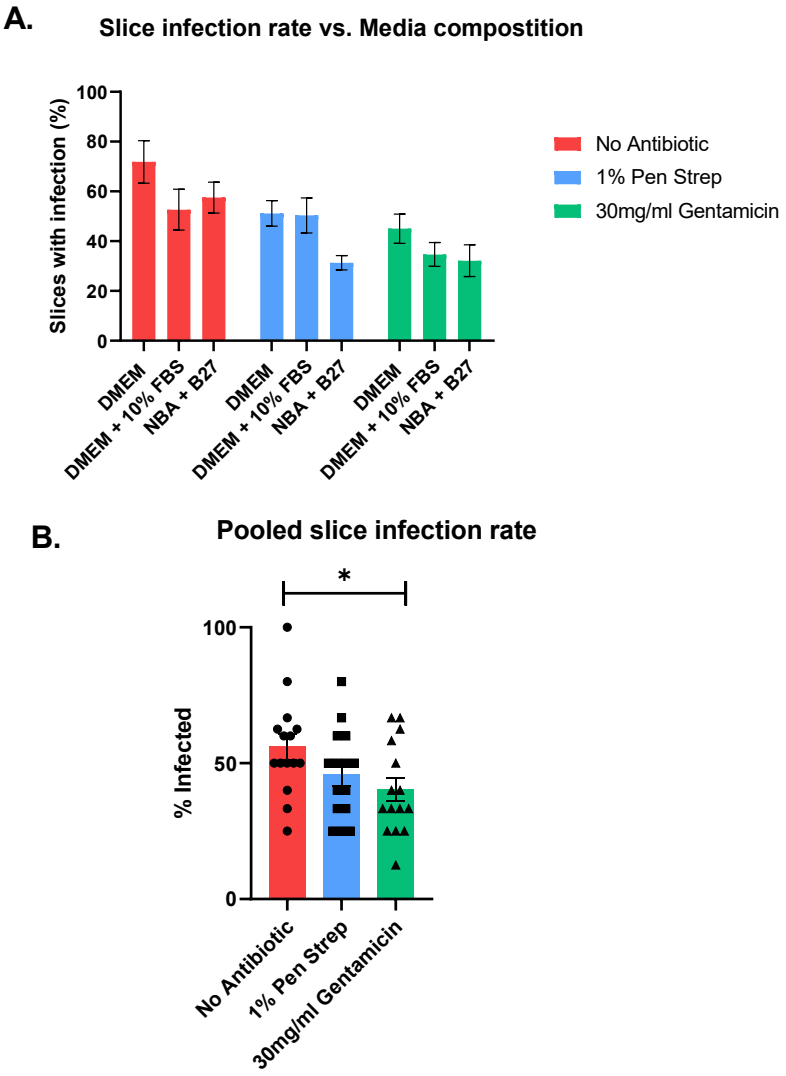

Figure 3.1: Comparison of various antibiotic conditions and their effect on infection of slices.

(A) Bar chart demonstrating the percentage infection rates of cultured slices from P21 and P7 rats when cultured in various different antibiotic conditions, where no antibiotic is shown in red, 1% pen/strep is shown in blue and 30mg/ml gentamicin is shown in green. Conditions are also split into groups according to the media which antibiotics were added to. **(B)** Shows pooled data from each individual antibiotic condition. Where RM one-way ANOVA with a Tukey's multiple comparisons post hoc test determined p = * (≤ 0.05) across conditions and * denotes significant differences between groups ($p \leq 0.05$, DF = 14). Error bars represent SEM and n = 15 in each case.

3.3.3 Effects of media composition on slice survival:

Figure 3.2 compares the survival rates of slices when cultured using different media compositions. In order to assess for the optimum experimental model with which to demonstrate the effects of each media composition, we initially split results into groups based on DIV. Figure 3.2A displays the pooled percentage slice viability of slices extracted from rats at P7 or P21 across 35 days *in vitro* where results are split into groups according to DIV. LFP recordings were taken from the CA1 and CA3 regions of slices once they had been removed from culture slices were moved onto an LFP rig for electrophysiology recorded to be carried out and gabazine was bath applied to slices to determine whether or not they were still viable, slices in which gabazine induced activity were viable and slices which had no activity were presumed dead. In some instances, for the later stages of the culture process slices had completely disintegrated and readings could not be taken – this is reflected in the lack of results at later DIV for DMEM cultured slices.

Unfortunately, in the data shown in Figure 3.2A there was no obvious timepoint at which any culture media composition had the greatest effect on slice viability. For this reason, the data from all DIV were pooled and statistically analysed using an RM one-way ANOVA with a Tukey's multiple comparisons post hoc test. As Figure 3.2B shows, under conditions where n=24 observations per group were analysed, there was a significant increase in the viability of control slices and those cultured in NBA supplemented with B27 (17.36% to 40.48% ± 6.689%, $p \leq 0.005$, DF = 23, n = 24 or n = 4 for each DIV).
A significant increase between slices cultured in DMEM with 10% FBS and those cultures in NBA supplemented with B27 was also noted (21.01% to 40.28% ± 5.628%, $p \leq 0.005$, DF = 23, n = 24 or n = 4 for each DIV).

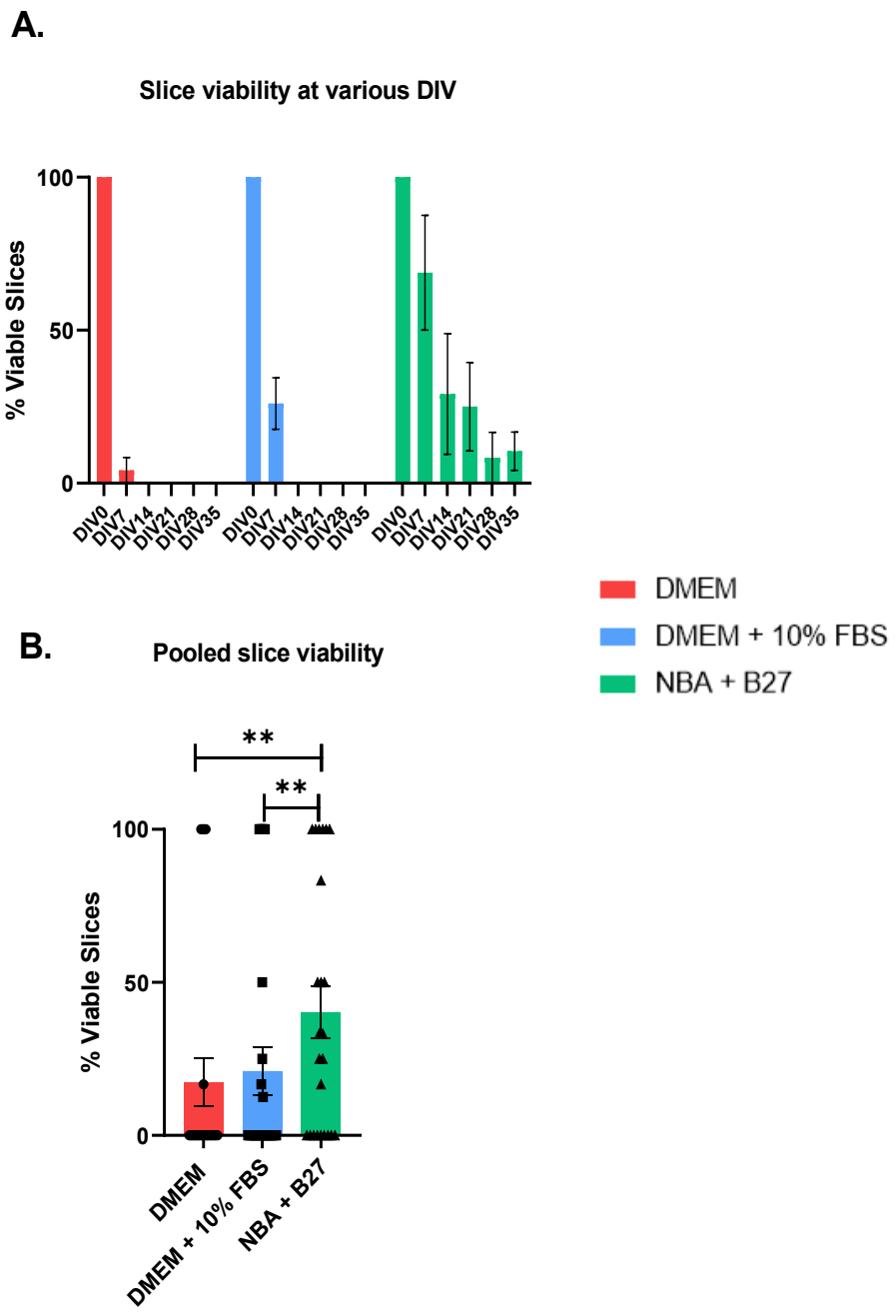

Figure 3.2: Effects of media compositions on slices viability.

(A) Bar chart demonstrating the survival rates of cultured slices from P21 and P7 donors when cultured using DMEM only (red) vs DMEM + 10% FBS (orange) vs NBA + B27 media (green) from DIV0 up to DIV35.

(B) Shows pooled data from each individual DIV. Where an RM one-way ANOVA with a Tukey's multiple comparisons post hoc test was used to determine significance and ** denotes $p \leq 0.005$. Error bars represent SEM and n = 24 in each case, n = 4 for each DIV tested.

3.3.4 Spontaneous activity of slices:

Data shown in Figure 3.3A shows LFP recordings taken from the CA1 and CA3 hippocampal area in cultured brain slices at various days *in vitro*. Cultured slices were exposed to different media conditions containing the antibiotic gentamicin (30mg/ml) as determined from previous experiments. Slices were extracted from two different aged rats to determine which condition provided the best environment for creating spontaneously epileptic slices. Results were initially split into groups based in DIV to assess the optimum experimental paradigm, however, these data did not provide any statistically significant results due to a lack of repeats, and variations in n number, for each individual group. So, no optimum condition could be determined from these data.

For this reason, the data for each DIV were pooled, to look closer at the effects of the age of rats and media composition on epileptic activity, determined using LFP recording, and statistical significance was determined using an RM one-way ANOVA with Tukey's post hoc multiple comparisons test. Figure 3.3C-D show that the condition which provided the highest percentage of spontaneously epileptic slices was slices taken from rats at age P7 and cultured in NBA media supplemented with B27 which produces a significantly higher percentage of spontaneously epileptic slices, where slices seized without any intervention, than in any other condition tested.

Where NBA supplemented with B27 produced a significant increase in spontaneous epileptic activity in both cultures taken from P21 (2.238% to 22.5% ± 5.283%, $p \leq 0.01$, DF = 15, n = 15) DIV and P7 rats (5.208% to 95.66% ± 3.137%, $p \leq 0.001$, DF = 23, n = 24) when compared with the DMEM only condition. A significant increase can also be seen between the DMEM only and DMEM + 10% FBS condition in P21 slices (3.238% to 13.33% ± 3.202%, $p \leq 0.05$, DF = 14, n=15) and between the DMEM + 10% FBS and the NBA + B27 condition for P 7 slices (14.72% to 95.66% ± 1.193%, $p \leq 0.001$, DF = 23, n=24).

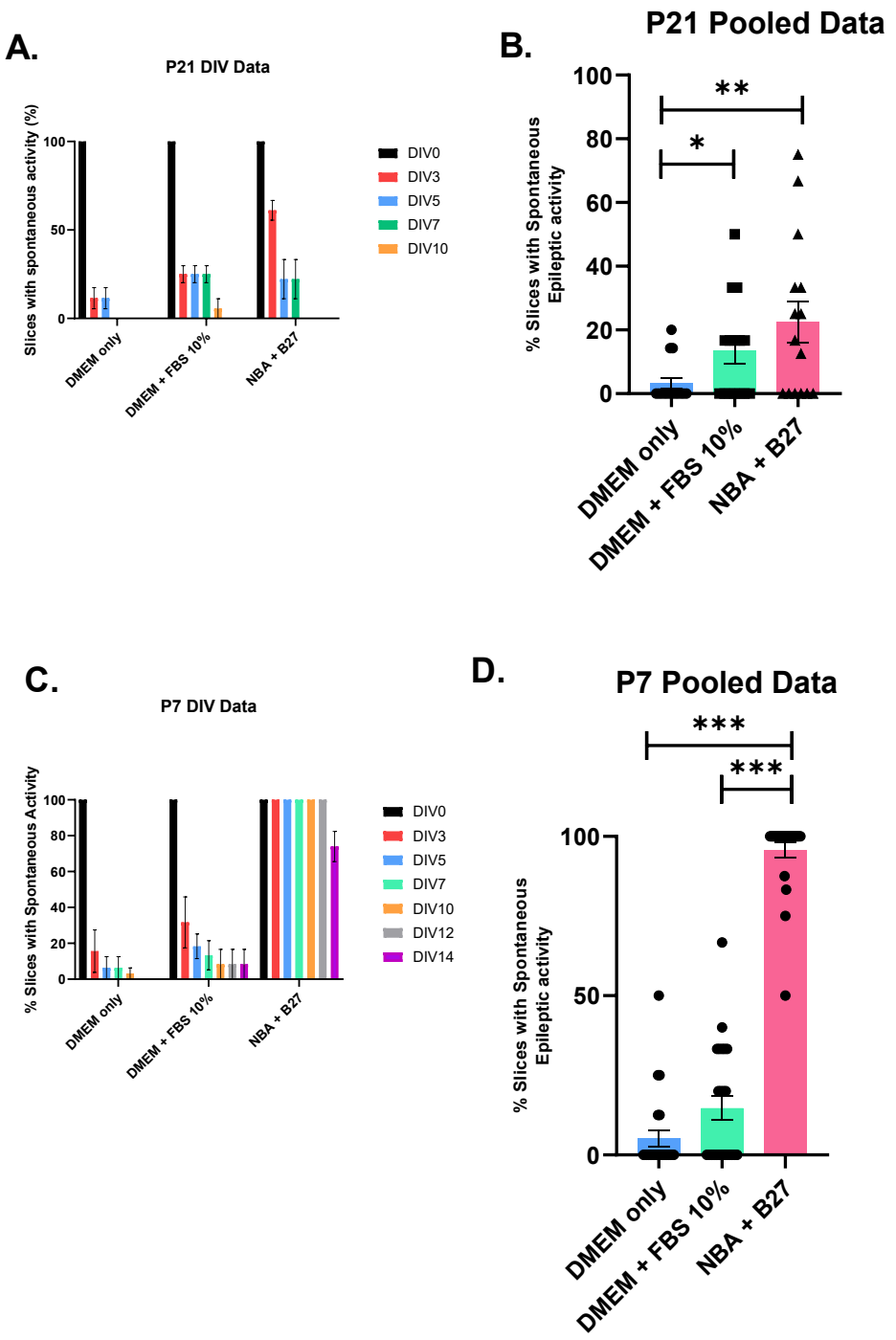

Figure 3.3: How age of rat and media composition affect spontaneous activity in slices over days in vitro.

(A) Bar chart demonstrating how different media compositions affect the percentage of slices from either P21 rats exhibiting spontaneous epileptic activity over a period 14 days *in vitro*. (DIV0 shown in black, DIV3 shown in red, DIV5 shown in blue, DIV7 shown in green, DIV10 shown in orange)

(B) Shows pooled DIV data for slices obtained from P21 rats demonstrating how media composition affects the percentage spontaneous epileptic activity. DMEM only conditions can be seen in grey, DMEM + FBS conditions shown in blue and NBA + B27 conditions shown in green. P values were determined using an RM one-way ANOVA with Tukey's multiple comparisons post hoc test, where ** denotes $p \leq 0.01$, and * denotes $p \leq 0.05$. Error bars represent SEM and n = 5 for each condition.

(C) Bar chart demonstrating how different media compositions affect the percentage of slices from either P7 rats exhibiting spontaneous epileptic activity over a period 14 days *in vitro*. (DIV0 shown in black, DIV3 shown in red, DIV5 shown in blue, DIV7 shown in green, DIV10 shown in orange, DIV12 shown in grey and DIV14 shown in purple).

(D) Shows pooled DIV data for slices obtained from P7 rats demonstrating how media composition affects the percentage spontaneous epileptic activity. DMEM only conditions can be seen in grey, DMEM + FBS conditions shown in blue and NBA + B27 conditions shown in green. An RM one-way ANOVA with Tukey's multiple comparisons post hoc test, where *** denotes $p \leq 0.005$. Error bars represent SEM and n = 8 for each condition.

3.3.5 Culture lifespan of slices:

Follow up experiments used slices taken from P3 rats to determine whether even younger donors would provide more resilient culture slices, the slices were cultured using NBA media supplemented with B27 as it had provided the most promising conditions in earlier experiments. The bar chart shown in Figure 3.4 demonstrates that the most successful cultures were those in which slices dissected from P7 donors were used as they survived longest in culture conditions. Slices from P21 donors had the least longevity, only lasting up to DIV10 in culture. Slices taken from P3 donors could last up to 2 weeks in culture, but slices taken from P7 donors remained living in culture for significantly longer with some cultures showing signs of life up to week 5 (DIV35) in culture. Statistical analysis determined that there was a significant difference in the longevity of slices taken from P7 rats and those taken from P3 rats ($p \leq 0.005$, n = 21, DF = 39.7) and those taken from P21 rats ($p \leq 0.005$, n = 21, DF = 39.85).

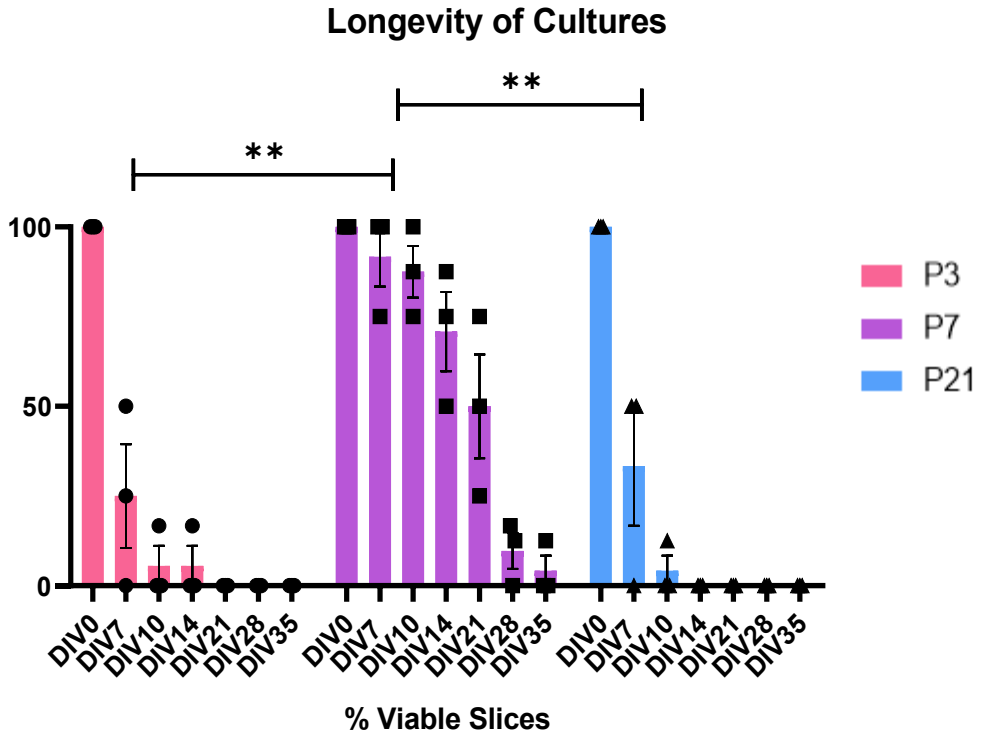

Figure 3.4: Effect of age of rat on slice longevity in culture

Bar chart demonstrating the longevity of slices in culture against the age of rat they were extracted from. Statisical significance was determined using a 2-way ANOVA with a Tukey's multiple comparisons post hoc test, where ** denotes $p \leq 0.005$. Error bars represent SEM and n = 21 for each age group.

3.3.6 Increased disease state over time in culture:

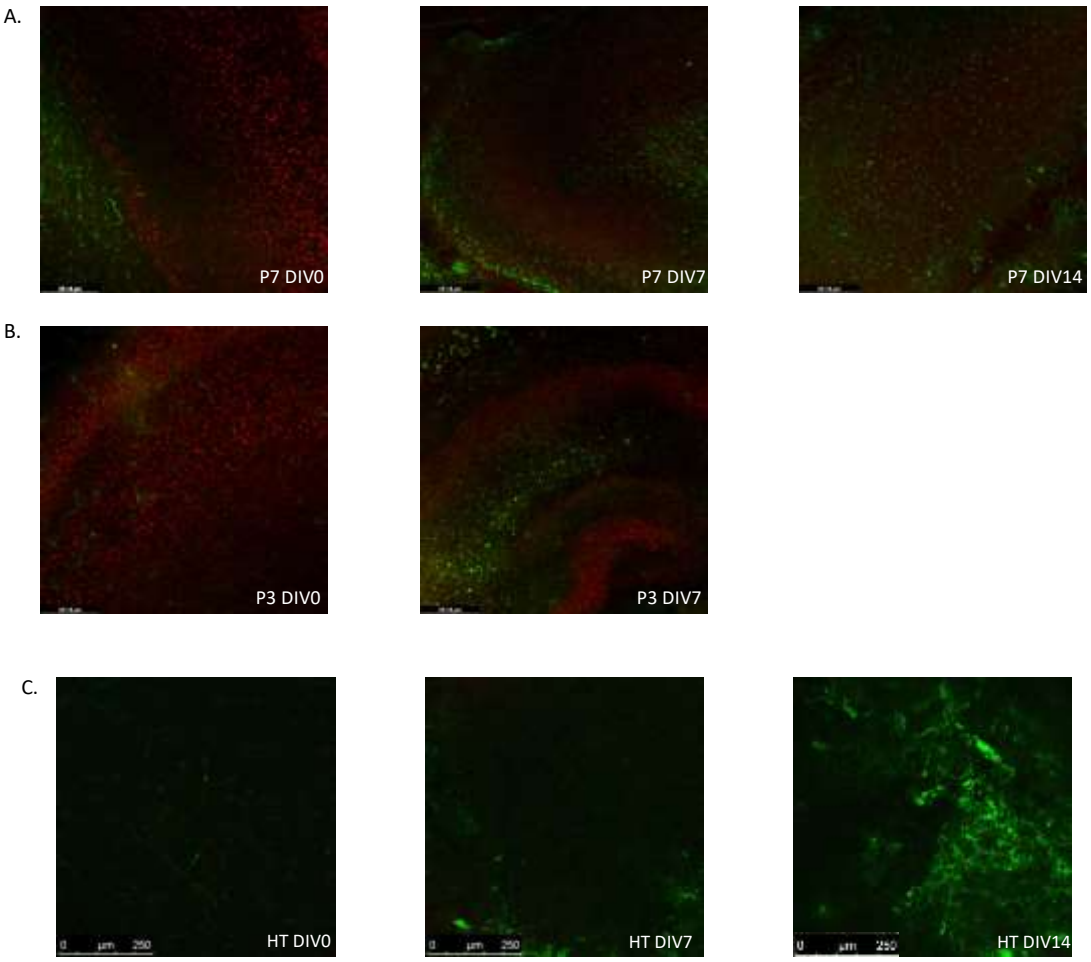

Figure 3.5: Immunohistochemical staining of NeuN and GFAP in cultured slices.

Confocal images of cultured slices stained for NeuN (red) and GFAP (green). **(A)** Shows slices taken from P7 donor at DIV0, DIV7 and DIV14 taken with 10x ocular, scale bar = 231.8µm. **(B)** Shows slices taken from P3 donor at DIV0 and DIV7 taken with 10x ocular, scale bar = 231.8µm. **(C)** Shows slices obtained from Human Tissue brain resection at DIV0, DIV7 and DIV14 taken with 20x ocular, scale bar = 250µm.

Confocal images taken of P3 and P7 rodent slices and resected human tissue at DIV0, DIV7 and DIV14 shown in Figure 3.5 give an indication of the survival of neurons throughout time in culture. NeuN which is shown in red, indicates the presence of healthy, postmitotic neurons whilst GFAP (shown in green) is largely expressed in astrocytes and is used as a marker of astrocytic injury. The NeuN staining suggests a decrease in healthy postmitotic neurons over time in both rodent and human tissue. GFAP

staining indicates a significant increase in the glial fibrillary acidic protein which has been associated with numerous neurological conditions. Taking into consideration the decrease in healthy neurons paired with the increase in markers of disease, it is reasonable to conclude that the disease state of slices increases over time in culture.

3.3.7 PBS & PLA inserts:

Culture well inserts were created by the Chemistry team at Aston University using a variety of combinations of polybutylene succinate (PBS) and poly lactic acid (PLA). PBS and PLA are both biodegradable polyesters, which decompose into carbon dioxide, water and lactic acid for PLA. PLA is widely used in medical devices, food packaging and 3D printing due to its biocompatibility and ease of processing. These biomaterials were tested in a preliminary study to determine whether they would provide a cheaper, more readily available and environmentally friendly alternative when compared with the standard Millipore cell culture inserts.

A variety of parameters used to create culture well inserts were tested to determine their effects on slice survival and activity in slices extracted from P7 rats. LFP recordings were taken from slices at DIV14 to determine activity.

Mesh inserts were initially tested at either 2µm or 3µm thickness and compared with the standard Millipore cell culture inserts (0.45 µm) used to determine whether the thickness of well inserts would affect slices viability. It was hypothesised that a thicker mesh would improve gaseous diffusion, resulting in increased slice health and viability. Figure 3.6A demonstrates that the thickness of the mesh insert did not have any significant effect on the survival of slices, which was determined using LFP recording and bath applying gabazine to slices to see if they had any response. However, when looking at Figure 3.6B it can be seen that the biomaterial used to create the mesh has a significant effect in the percentage of slices which exhibit spontaneous activity. The various combinations of mesh used were either made entirely of PBA, entirely of PLA or a mixture of both. The use of PBS10, PLA20 and PLA:PBS 3:1 all significantly reduce the percentage of slices exhibiting activity by DIV14 . But no significant differences were reported when comparing the PBS20, PBS25 and PBS:PLS 3:1 conditions to the Millipore cell culture inserts.

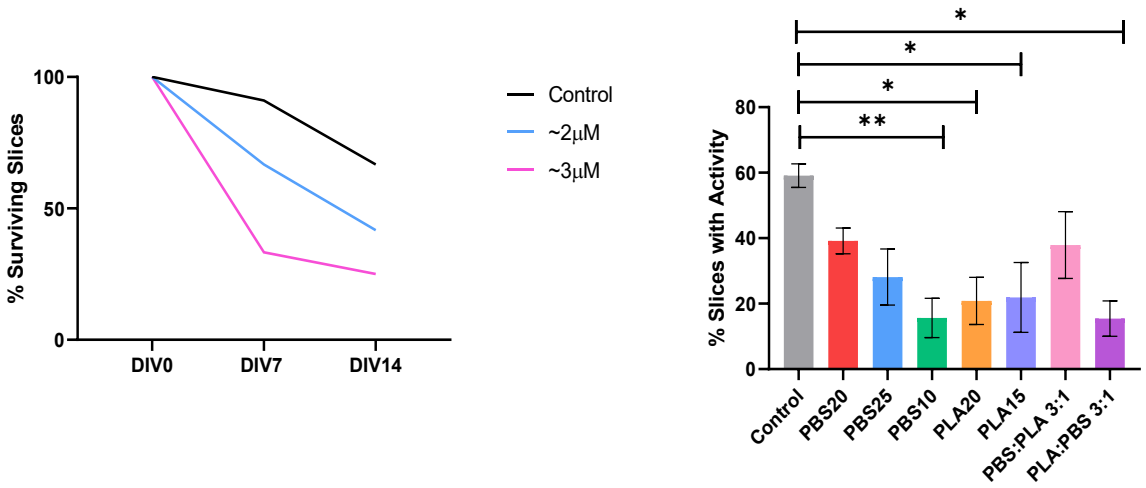

Figure 3.6: Slice survival on PBS/PLA inserts at DIV14.

(A) XY plot depicting the percentage survival of slices cultured on inserts of varying thicknesses (n = 3 for each group). **(B)** Bar chart shows the percentage of living slices after 14 days of culture on various different culture well inserts manufactured from PBS, PLA, or a combination of both.
Where the number following the material indicates the distance of the needle from the collector (in cm) when spinning the mesh. Where * denotes $p \leq 0.01$ and ** denotes $p \leq 0.05$. Error bars show SEM. N = 4 for all groups.

3.4 Discussion:

3.4.1 Optimising media volume:

One method of determining the health of a slice which has been cultured is to observe whether the slice has flattened and adhered to the culture inserts (Yifat *et al.*, 2011). During the initial culture attempt 2mL media was placed at the bottom of the well below the inserts to feed the slices, however this volume of media caused slices to become free floating within the wells and they could not adhere to the cell culture inserts. These slices disintegrated when removed from the wells and so a reduced volume of media was used on the next attempt. 1.5mL media was sufficient to feed the slices but not cause them to detach from the cell culture inserts, meaning 1.5mL was used consistently moving forward. Slices cultured with 1.5mL media in the bottom of the well could be visibly seen to flatten over their time *in vitro* which indicated adhesion if slices to the cell culture membrane and survival of the slices.

3.4.2 Optimal slice thickness and orientation:

Multiple organotypic tissue culture studies have reported varying slice thicknesses from 110µM to 450µM to be successful depending on a number of variables, including age of donor and brain area being cultured (Komal *et al*, 2009). Initially slices were cut at a thickness of 450µM, however, these slices were visibly drying out between media changes. This may be due not using a rocking platform in the incubator, as most organotypic brain cultures make use of a rocking platform to increase gaseous diffusion across slices and prevent drying of the slices – something which in turn provides compromises in mechanical stress, mechanoreceptor activation and infection risk. However, it is also possible that 450µM was too thick as it is the largest recorded slice thickness for carrying out organotypic cultures. To determine whether or not thinner slices were more appropriate for culture slices cut at 450µM, 400µM and 350µM were compared. 400µM slices still became drier on top but this didn't occur until DIV7-8. However, at 350µM slices remained moist throughout the culture process up to DIV35 in some of the preliminary experiments for longevity. It was decided that going forward 350µM would be an appropriate slice thickness for both culture and electrophysiology readings given that slices for patch-clamp electrophysiology are also cut at 350µM as a standard in our laboratory. Slice orientation was another factor which determined the success of the cultures. In the initial experiments slices were cut across a sagittal plane, however due to the connections that were severed during the slicing process many of the slices lost their hippocampi via disintegration within the culture wells. For this reason, cultures using slices cut along the coronal were compared with sagittal slices to determine whether this would reduce the number of hippocampi lost during slicing. Coronally cut slices kept their hippocampi intact throughout the culture process, increasing the number of slices which could be cultured at a given time and therefore this was the preferred method of slicing for future culture set ups.

3.4.3 Slice adherence:

Another important criterion for observing and evaluating whether or not a slice has been well-cultured is a shift in the colour and transparency of the slices. Well-cultured slices would become more transparent and change from a white-ish colour to a greyer tone over the first week in culture (Gähwiler *et al*., 1997). This criterion was very helpful in identifying cultures which were not going to adhere to the cell culture insert and survive long-term as it was visible within the first 7 days of culture whether they would be viable or not. Cultured slices which expanded or did not exhibit some change

in colour by DIV7 could be immediately discarded along with any cultures which had become infected and displayed obvious signs of infection such as pink precipitate in the culture well or on slices, within the first 7 days of culture. Infected or non-adherent cultures were determined to be dead tissue as they disintegrated on removal form culture media and therefore could not be used for further experiments.

3.4.4 Addition of antibiotics to the media:

Non-antibiotic media is preferable for both cell and tissue culture as antibiotics may affect metabolism, proliferation, or differentiation of cells, and therefore has the possibility of skewing the results that are obtained (Llobet *et al*., 2015). It is for this reason slice culture initially attempted using antibiotic free media, however the infection rates for slices that were placed in the incubator without antibiotics present in the media presented with unacceptable infection rates. While optimising the procedure for organotypic slice culture, the initial infections observed were a distinct white/pale ink precipitate could be seen forming on top of slices and spreading over the culture well inserts. Due to the lack of odour and the fact the precipitate had no yellow or black colour it was determined that the infection was bacterial and not fungal. This infection caused slices to become extremely fragile and disintegrate when manoeuvred from the inserts for analysis, therefore there is no electrophysiological or immunohistochemical data available for these experiments. Infections were apparent from 1-2 DIV and slices were dead and disintegrating by DIV3.

Penicillin and Streptomycin are often used together to prevent bacterial contamination of cell cultures due to their effective combined action against gram-positive and gram-negative bacteria. Penicillin is a beta-lactam antibiotic which inhibits the growth of gram-positive bacteria by disrupting the cell membrane of bacteria, while Streptomycin is an aminoglycoside antibiotic that is effective against most gram-negative bacteria (Miller *et al*., 1986). Gentamicin is another type of aminoglycoside, used to treat several different types of bacterial infections, which disrupts the ability of bacteria to make new proteins, thereby killing the bacteria (Ali *et al*., 2011).

Pen/Strep or gentamicin were added to various compositions of culture media and compared to determine whether this could reduce the infection rate and produce healthier slices. As can be seen in Figure 3.1 the addition of antibiotics reduced the rate of infection in all media conditions, in the DMEM only condition Pen/Strep was the most effective antibiotic. However, in both the DMEM + 10% FBS media and the NBA + B27 media the addition of gentamicin proved most effective at preventing infections.

For this reason, we chose to add 30mg/ml gentamicin to all culture media moving forward.

3.4.5 Media composition:

Three different compositions of media were tested to determine which would provide the best environment for the culture or organotypic brain slices. Figure 3.2 shows the combined data from P21 and P7 donors, it can be seen taht the most successful cultures were cultured in NBA + B27 media as slices were able to survive for up to 5 weeks when cultured in this media. All slices cultured using DMEM only media were dead or infection by DIV7 and slices cultured in DMEM + 10% FBS had died or become infected by DIV14.

DMEM is a well-established culture medium and is known to successfully culture glial cells, fibroblasts, human endothelial cells, and rat fibroblasts. However, there is not much evidence to suggest that it is regularly used when culturing organotypic slices. Here, we attempted to use DMEM without the addition of FBS initially as serum-free media offers the advantage of increased consistency and reduced risk of viral contaminants that may be present in serum. However, our experiments proved DMEM-only media to be an unsuccessful medium for the culture of organotypic brain slices. The addition of 10% FBS to the medium created a more effective culture medium increasing the survival and longevity of slices.

NBA medium is a culture media designed for the long-term maintenance and maturation of prenatal and foetal neuronal populations; it promotes the growth of neurons while suppressing glial growth. B27 is an optimised serum-free supplement which supports growth and viability of neurons. As both B27 and NBA are serum-free the resulting culture medium is also serum-free. From Figure 3.2 it is evident that NBA + B27 media created the most effective culture medium out of the three conditions tested as it maintained slices for up to 5 weeks *in vitro*. Figure 3.4 demonstrates that NBA + B27 with slices form P7 donors was successful in maintaining spontaneous activity in slices for up to DIV14.

3.4.6 Age of donor animal:

It is well established in the literature that slices taken from younger donors are more favourable for slice culture set ups as they have a greater capacity for regeneration and adaptation. This is reflected in our results as Figure 3.3B and 3.3C demonstrate that slices taken from P7 donors had a much greater survival rate than P21 donors, with slices showing activity each week up until DIV35, whereas slices

taken from P21 donors ceased to exhibit any electrophysiological signs of life after just 7 days *in vitro*. P3 donors were also cultured to see if a younger animal would provide a greater yield of a more successful, longer living culture slices, but pulling from the data shown in Figures 3.2, 3.3 and 3.4 it is evident that slices extracted from P7 donors had more longevity, when compared with P21 or P3 donors.

3.4.7 Human Tissue studies:

Following the optimisation of the culture procedure, the same procedure was used to attempt the culture of resected human tissue. Any parameter change had to be carried out in rodent slices prior to attempting to experiment with human tissue due to its limited availability and that it is a very valuable research tool.

Confocal images shown in Figure 3.5 depict progressive cell loss in P7, P3s and human tissue as they show a decrease in the number of neural nuclei with and an increase in GFAP which is a common marker of cell stress. The figure indicates that while slices from P3 and P7 donors still contained living neurons which were able to absorb the anti-NeuN antibodies up until DIV7 and DIV14 respectively and an increase in green fluorescence indicates a progressing disease state over days *in vitro*. For human tissue, NeuN staining is clearly apparent on DIV0 while GFAP staining increases at DIV7 and again at DIV14.

Human tissue samples provided challenges in the imaging process. Firstly, resectioning of the already fragile human tissue was very difficult given the variability of the tissue. For this reason, human tissue samples were not resectioned and staining was carried out on 350µM as opposed to 80µM for P3 and P7 slices, this has caused the images to have increased background fluorescence. Another issue with human tissue samples is difficulty in localising the exact cortical area or orientation, whereas as when P3 and P7 slices were imaged the hippocampus could be easily detected to get reproducible images from each repeat.

3.4.8 Culture well inserts:

Figures 3.6B demonstrate a significant decrease in the percentage of slices exhibiting spontaneous activity (ictal events or epileptiform activity) when PBS10, PLA20 and PLA:PBS 3:1 are placed under slices before being placed into culture. However, PBS20, PBS25 and PBS:PLS 3:1 did not cause any significant changes in slice activity when compared with the control condition. Slice activity was

determined via LFP recordings, gabazine was added to slices at the end of experiments as a reaction to gabazine confirmed slices were alive if no spontaneous activity was detected. It is possible that slices without any spontaneous activity are healthier slices, as inserts made of these biomaterials have been reported to improve gas barrier performance within cultures due to their oxygen permeability (Zhang *et al*., 2022). Taken together this data indicates that for the purposes of this thesis the use of Millipore cell culture inserts is the best option, but the use of PBS/PLA may be beneficial for culturing healthier organotypic slices cultures.

Further research is required for this study, however the data shown in Figure 3.6 shows promising preliminary data for the use of these culture inserts in creating non-disease state organotypic tissue.

Chapter 4: The process of epileptogenesis

4.1 Introduction:

Epilepsy is one of the most common neurological disorders in the world, affecting approximately 1% of the global population, affecting around 50 million people worldwide. It is characterized by unprovoked, recurrent seizures which can result from sudden bursts of abnormal electrical activity in the brain.

Epilepsy has numerous manifestations but one of the most common is seizure activity which is caused by a sudden uncontrolled electrical disturbance in the brain that disrupts normal brain function. Seizures are defined as a transient occurrence of symptoms caused by an extreme, hypersynchronous firing of neurons and can be characterised by sudden, involuntary muscle movements. Transient seizures often have a clear onset and remission period. However, some patients will experience unusually long seizures (anything over 5 minutes), this is known as status epilepticus (SE). SE is one of the most severe manifestations of epilepsy, but it can also occur in non-epileptic patients, with up to 54% of cases of SE being reported in non-epileptic individuals (Al-Mufti & Claassen, 2014). During these prolonged seizures there is a possibility that patients will develop pharmacoresistance to antiepileptic drugs (Jones *et al.*, 2002).

Epilepsy is considered to be resolved for individuals who had an age-dependent epilepsy syndrome but are now past the applicable age or those who have remained seizure free for 10 years and unmedicated for at least 5 years. However currently almost 1/3 of all epilepsy patients have seizures which are medically intractable so many of the anticonvulsant or antiepileptic medications which are available will not work in these individuals. Most anti-epileptic drugs which are currently on the market primarily target the suppression of neuronal hyperexcitability to treat seizures, this is either achieved through the reduction of neuronal excitation or an increase in neuronal inhibition (Stafstrom & Carmant, 2015).

Epilepsy can be genetic, however traumatic brain injury (TBI) can lead to acquired epilepsy and it has been hypothesised that neuronal death and axonal damage resulting from the initial trauma initiate the process of epileptogenesis (Pitkanen *et al.*, 2011). Consequences of neuron damage can include the loss of inhibition due to death of interneurons and axonal sprouting which leads to hyperexcitability and spontaneous seizures (Cossart *et al.*, 2001; Escalpez *et al.*, 1999; Jefferys, 2003; Kobayashi & Buckmaster, 2003; Okazaki *et al.*, 1995; Smith and Dudek, 2001;). When seizure activity

is prolonged, it can also lead to neuronal death, and it is widely accepted that when patients enter SE this results in neuronal necrosis (Meldrum, 2002). Previous studies have demonstrated via MRI analysis and analysis of resected brain tissue that even brief, spontaneous seizures cause neuronal death in patients with intractable epilepsy (Henshall *et al.*, 2004; Bernhardt *et al.*, 2009).

Current treatment of seizures in post-traumatic epilepsy include treatment with anticonvulsants such as phenytoin, although to date anticonvulsants have not demonstrated antiepileptogenic efficacy (Schierhout & Roberts 2001; Temkin, 2001 & 2009). Long-term monitoring studies indicate that epilepsy continues to worsen after the first seizure which further supports the hypothesis that seizures themselves contribute to epileptogenesis (Williams *et al.*, 2009). Organotypic brain or hippocampal only slices allow us to monitor the progression of epileptogenesis in slices following traumatic brain injuryand the effects that different drugs have on posttraumatic epileptogenesis at different timepoints in the progression. It has been reported that cultures become spontaneously epileptic after a latent period *in vitro* following extraction and slicing of the brain tissue. Spontaneous activity is usually reported from 14 days *in vitro* (DIV) (Dyhrfjeld-Johnsen *et al.*, 2010).

Electrographic potentials that are said to represent the activity within the epileptic brain have been quantified to aid the characterisation of epilepsy models. It is assumed that epileptiform discharges, which present as abnormal electrical activity patterns in LFPs, consisting of short duration spikes, sharp waves or a combination of both and last longer that 2-3s are considered to be ictal (D'Ambrosio & Miller, 2010). However, a more stringent criteria is necessary as there is still no general consensus on how to define a seizure. Seizure patterns comparable to those described in vivo (both in animals and focal epilepsy human patients) can be reproduced *in vitro* in slices of brain tissue maintained in culture without the use of pharmacological, mechanical or electrical intervention, providing an advantage over using acute slices in which seizure activity needs to be evoked.

The absence of any limbs means that classification of seizures in *in vitro* slices must be determined by the identification of ictal and epileptiform or seizure-like events using electrophysiological recordings alone. Epileptiform events are often characterized by fast activity at onset, followed by irregular spiking and terminating with periodic bursting discharges and can be induced using pharmacological agents for example the addition of 4AP (Gnatkovsky *et al.*, 2008; Uva & De Curtis, 2005).

According to several studies performed on slice preparations, prolonged epileptiform events are characterized by either repeated spike patterns or large paroxysmal depolarising events followed by a plateau potential where smaller discharges occur (De Curtis & Avanzini, 2001). However, these types

of discharge are often defined as "seizure-like" as they are not observed in spontaneous seizures in vivo.

Some recent findings have demonstrated that seizure-like events are initiated via the activation of inhibitory networks - analysis of seizure-like discharges in neocortical and hippocampal slices exposed to different pro-epileptic conditions demonstrate that GABAergic networks are active from the very start of a seizure (Derchansky *et al.*, 2008; Fujiwara-Tsukamoto *et al.*, 2004 & 2010; Lopanstev & Avoli &, 1998; Ziburkus *et al.*, 2006). This was confirmed *in vitro* in an isolated guinea-pig brain (Gnatkovsky *et al.*, 2008; De Curtis & Gnatkovsky, 2009)

Neuronal cell death has also been implicated as a key factor which causes the development or progression of epileptic disorders, and this may also contribute to the development of epilepsy in culture as we know that from the moment slices are extracted and sliced the cells begin to die, cell death within the slice continues in culture however some neurons will rearrange their dendrites to form new connections following axotomy (Dingledine *et al.*, 2014).

Over the years the development of anticonvulsant drugs for epilepsy has relied on experimental drug screening methods due to insufficient knowledge about the pathophysiology of epilepsy (Lillis *et al.*, 2015). In recent years many new anticonvulsant drugs have been created, however almost one-third of all epilepsies remain medically intractable - this is quite likely due to the current screening method for antiepileptic medication (French *et al.*, 2013; Wilcox *et al.*, 2013).

Most initial screening methods currently rely on the application of convulsant drugs/conditions to healthy brain tissue to produce patterns of epileptic activity in slices, however, these patterns differ significantly from actual spontaneous epileptic activity we see in chronically epileptic tissue (Löscher & Schmidt; 2011; Sabolek *et al.*, 2012). Current models of chronic epilepsy in animals tend to establish chronic epileptic conditions *in vivo,* extract brain tissue from the animals and use *in vitr*o experiments to determine the changes in neuronal networks that accompany chronic seizures. Unfortunately, when looking at chronic epilepsy *in vivo* the seizure activity is unpredictable and slow to develop following insult or injury, and once seizures do begin there is often a high mortality & morbidity rate as the frequency of seizures necessary for anticonvulsant drug screening purposes is also dangerous for the animals. Another drawback of this model is that individual animals must be sacrificed at arbitrary timepoints making for a high degree of variability in the data, therefore, a much more efficient way of screening anticonvulsant/antiepileptic drugs would be to use chronically epileptic

slices as an initial screening method for acutely evaluating these drugs. An *in vitro* model of chronic epilepsy could be developed using organotypic slice cultures as brain tissue can be obtained from normal rats and maintained in long term organotypic cultures. This method would allow for longitudinal testing monitoring of changes in network activity and since slices are prepared from a single animal both treated and untreated slices could be tested in parallel to determine the effects of anti-epileptic treatments.

Organotypic tissue cultures can be used to create an *in vitro* model of spontaneous seizures as the circuitry within the hippocampus can be preserved quite well (De Simoni *et al.*, 2003). This model for creating epileptic brain slices *in vitro* involves massive axotomy to the brain at the cut surfaces, which can be considered a model of severe traumatic brain injury. As a response to this traumatic injury deafferentation and axonal sprouting takes place within the slices, which causes connectivity between pyramidal cells to increase from 3% in acute slices (post-slicing) to 30% in organotypic cultures (Sakaguhci *et al.*, 1994; Gutierrez & Heinmann, 1999; Pavlidis & Madison 1999).

Acute *in vitro* preparations provide a quick, flexible, and straightforward approach to issues which have been long-standing in the study of epilepsy and epileptic conditions - including ictogenesis, epileptogenesis, and drug resistant epilepsies. Acute slices have reduced network connectivity that has typically been compensated for through the application of acute convulsant drugs. This approach does however have some limitations as epileptic activity in patients develops spontaneously and not via pharmaceutical intervention. Looking at spontaneous activity in organotypic slice preparations provides a more realistic view of the full spectrum of spontaneous epileptic activity and a better representation of how the brain will respond to different anticonvulsants, including the development of drug resistance (Berdichevsky *et al.*, 2016; Liu *et al.*, 2017). They may also provide a more accessible model of chronic epilepsy as organotypic slices have been reported to be maintained for up to 5 months in culture and can begin to exhibit epileptic activity after just 14 days (Croft et al., 2019).

While both organotypic slice cultures and acute slices retain the cellular architecture and connectivity found in an intact brain acute slices only remain viable for hours to days, organotypic slices provide a platform that allows for long-term studies. The fact these cultures can last weeks to months in culture provides the ability to carry out chronic dosing studies which is hugely advantageous when studying epilepsy and other neurological disorders. They also allow for longitudinal studies to be done over time as slices obtained from a single animal can be tested at various timepoints throughout the culture process and compared.

Using the organotypic model of epilepsy fulfils two (refinement and reduction) of the 3Rs in line with the National Centre for Replacement, Refinement and Reduction (NC3Rs) guidelines (Modebadze *et al.*, 2016) as the number of animals necessary for experiments is greatly reduced and the morbidity rate is zero given that epileptic activity is induced post-mortem.

This chapter will follow the process of epileptogenesis in cultured organotypic brain slices at different time points from DIV0-DIV14.

4.2 Methods:

4.2.1 Animals and Ethical approval:

All animal procedures were performed in accordance with the Animals Scientific Procedures Act (ASPA) 1986 UK (amended in 2012), European Communities Directive 1986 (86/609/EEC), and the Aston University ethical review document.

4.2.2 Slice preparation:

350µM coronal slices were prepared from postnatal day 3-7 (10-20g) Wistar rat pups of either sex. Prior to the brain extraction, rats were anaesthetised by inhalation of 5% isoflurane in a mixture of O_2/NO_2 until no pedal or corneal reflex was detected – depth of anaesthesia was determined, in accordance with the ASPA 1986, by testing for the absence of normal reflexes via a pinch test. Following anaesthetisation rats were euthanised by decapitation using surgical scissors and the brain immediately extracted from the skull. Once extracted the brains were placed in a sucrose-based artificial cerebrospinal fluid (aCSF) solution which contains (in mM): 180 sucrose, 2.5 KCl, 10 $MgSO_4$, 1.25 NaH_2PO_4, 25 $NaHCO_3$, 10 glucose, 0.5 $CaCl_2$ and 1 L-ascorbic acid, 2 N-acetyl-L-cysteine, 1 taurine and 20 ethyl pyruvate. Complete aCSF had been saturated with 95% O_2/5% CO_2 (carbogen) prior to the extraction to maintain a pH of 7.3, and osmolarity of 300 – 310 mOsm/L. Brains were then transported back to the lab in the aCSF solution, once back in the lab slices were glued onto a stage and submerged in ice-cold aCSF to be sliced into 350µM slices using a 7000smz-2 model Vibrotome (Campden Instruments Ltd., UK).

4.2.3 Organotypic Tissue Cultures:

To maintain a sterile environment for slices and avoid infection of cultures as much as possible all

instruments used for both dissection and slicing were autoclaved beforehand, any equipment which could not be sterilised in the autoclave was sprayed down with 70% ethanol to kill any bacteria.

Following the dissection, once slices were cut, they were bathed in an oxygenated glucose-based aCSF solution containing (in mM): 126 NaCl, 3.5 KCl, 1.3 $MgCl_2$, 1.2 NaH_2PO_4, 25 $NaHCO_3$, 2 $CaCl_2$ and 11 glucose for 1 hour before being transferred to a biosafety cabinet, washed in culture media for 10 minutes and placed onto hydrophilic PTFE, 0.4µM pore cell culture inserts (Merck, UK). Residual aCSF was then aspirated off and inserts were placed into 6-well plates containing 1.5ml culture media. The culture media was prepared using Neurobasal-A media (Thermo Scientific, UK) supplements with 0.5mM glutaMAX, 30mg/ml gentamicin and 1ml B27 (Thermo Scientific, UK). Slices were then incubated in a humidified incubator (Thermo Scientific, UK) at 37°C, 5% CO_2, with a media change twice weekly.

4.2.4 Drugs & Reagents:

Gabazine (Sigma-Aldrich, UK) was diluted into a stock solution of 2.5mM and stored in aliquots at -20°C. Prior to being added to brain slices, aliquots were defrosted and diluted down to their final concentration. Drugs were then bath applied to slices by adding them directly into the perfusing aCSF and were left to stabilise for at least 40 minutes or until slice had seized multiple times. Once slices had stabilised, subsequent drug application was recorded for 30 – 40 mins following the application of each drug for LFP recordings. For patch-clamp recordings drug application was recorded for 15-20 mins following application of the drug.

4.2.5 Electrophysiology:

4.2.5.1 Extracellular recordings:

Extracellular LFP recordings were taken from cultured slices on DIV0, DIV3, DIV7, DIV10 and DIV14 to study the progression of epileptogenesis. After being removed from the incubator slices were transferred onto lens tissue and placed in an interface chamber on a local field potential (LFP) rig (Scientific Systems Design Inc, Canada). Slices were continually perfused with glucose-based aCSF (bubbled with carbogen) at a flow rate of 3-5ml/min and temperature of 30–34°C using a proportional temperature controller PTC03 (Scientific Systems Design Inc, Canada). Microelectrodes were pulled from borosilicate glass (1.5mm diameter) at a resistance of 3-5MΩ using a PC-10 micropipette puller

(Narishige Ltd, Japan). Microelectrodes were filled with glucose-based aCSF, then a chloride-coated silver wire could be inserted into the microelectrode, and microelectrodes were placed into a head stage. Microelectrodes were manipulated using an MM-3 micromanipulator 22 (Narishige Ltd, Japan) and an Olympus SZ51 (Olympus, UK) stereomicroscope was used for visualisation. Microelectrodes were inserted into pyramidal cell layers of areas CA1 and CA3 of the hippocampus in slices. The receiving signals were amplified 100x using EX10-2F amplifiers (setting a low-pass filter of 0.1 Hz and a high-pass filter of 1k Hz) (NPI Electronics GMBH, Germany). Electrical noise (50Hz) was filtered by passing the signal through Humbugs (Quest Scientific, Canada). The receiving signal was amplified a further 10x using LHBF-48X amplifiers (low-pass filter 0.3 Hz, high-pass filter of 700 Hz) (NPI Electronics GMBH, Germany). Signals were digitised at sampling rate of 5 kHz using a CED Micro1401-3 analogue-to-digital converter (Cambridge Electronic Design, UK) and recorded using Spike2 software (Cambridge Electronic Design, UK).

4.2.6 Patch-clamp recordings:

Gap free whole-cell patch-clamp recordings were made using standard techniques (Woodhall *et al.*, 2009). 350uM slices were placed onto the patch rig where they were submerged in aCSF and weighed down using platinum rods. Electrodes were pulled from borosilicate glass (1.5mm diameter) at a resistance of 3.5-5MΩ using a P-1000 flaming/brown micropipette puller (Sutter Instruments, US). Electrodes were filled with an internal solution containing (in mM): 100 CsCl, 40 HEPES, 1 Qx-314, 0.6 EGTA, 5 MgCl2, 10 TEA-Cl, 4 ATP-Na, 0.3 GTP-Na (titrated with CsOH to pH 7.25) at 290–295 mOsm for IPSCs, or 100 Cs-gluconate, 40 HEPES, 1 Qx-314, 0.6 EGTA, 2 NaCl, 5 Mg-gluconate, 5 TEA-Cl, 10 Phospho- Creatinine, 4 ATP-Na, 0.3 GTP-Na (titrated with CsOH to pH 7.3) at 285-290 mOsm for EPSCs.

4.2.7 Data Collection and Analysis:

LFP data were visualised using Spike2 software (Cambridge Electronic Design, UK). Raw data were filtered using a Bessel filter with a high-pass of 0.5Hz and low-pass of 50Hz. 120 second epochs of recorded activity was extracted from continuous raw traces at specific timepoints (pre- and post-compound application) and analysed for epileptiform activity from initial placement of the electrodes until the addition of any drugs onto the slice. Data were normalised and are presented as mean median values and error bars represent SEM. Statistical analysis was performed using GraphPad Prism8.

4.2.8 Event Detection:

sIPSCs and sEPSCs were recorded at holding voltage of -70mV using an Axopatch 200B amplifier (Molecular Devices, US). Signals were low-pass filtered at 5kHz with an 8-pole Bessel filter and digitized at 10kHz using a Digidata 1440A digitizer and recorded using pClamp software (Molecular Devices, US). Data were analysed using Axograph and Prism8 software. The data were normalised and presented as mean with SEM.

4.2.9 Seizure definition:

Seizure activity was defined as a series of paroxysmal discharges which could be clearly distinguished from baseline activity, lasting for a duration of longer than 5 seconds and contained events with an interevent interval of less than 800ms. Where bursting events occurred, events that deviated from the baseline within 5 seconds of return were classed as the same seizure-like event.

Seizures were determined according to the definition outlined above and selected from raw LFP traces, using Spike2 software. Seizure activity was determined by eye and cursors were placed to calculate seizure duration and interevent intervals.

4.3 Results:

4.3.1 Epileptogenesis in cultured neuronal networks:

Coronal slices were prepared using brains extracted from P3 or P7 rats and extracellular field recordings were taken across various days in vitro (DIV0, DIV3, DIV7, DIV10 and DIV14). Seizure frequency and duration were analysed to assess the differences in spontaneous epileptic activity over time in culture.

Recordings were taken from the CA1 and CA3 areas of the hippocampus simultaneously using the standard LFP method (as outlined in Chapter 2.4.1) and any spontaneous epileptic activity which was observed was plotted to determine the time course of epileptogenesis in juvenile cultured slices.

Figure 4.1A and 4.1B demonstrate seizure frequency and duration, respectively, recorded from slices obtained from P3 rats. Data from slices obtained from P3 rats could only be recorded up to DIV7 due to slices not lasting as long in culture conditions as those obtained from P7 rats, and a much smaller number of slices being able to be cut from one brain due to the size. As can been seen from Figure 4.1A and 4.1B no ictal activity was recorded from any slices at DIV0, however, both hippocampal areas

exhibited a significant increase in both seizure duration and seizure frequency following a 7-day period *in vitro*. Figure 4.1A shows an increase from 0 to 9.75 (± 2.509sph, n=6, $p \leq 0.01$) seizures per hour observed in both hippocampal areas from DIV0 to DIV7 recordings. Figure 4.2A shows that there was also a significant increase in seizure duration with the mean median seizure duration CA1 at DIV7 was on average 76.454 ± 14.426s (n = 6, p = ≤ 0.01, using 2-way ANOVA with Sidak's post hoc test), while in CA3 a mean median seizure duration of 76.526 ± 14.432s (n = 6, $p \leq 0.01$, using 2-way ANOVA with Sidak's post hoc test is shown. This suggests that there is a large reconfiguration of network activity during culture in slices from P3 animals. As results later in this chapter suggest, there is little evidence of change in inhibitory or excitatory activity in P3-based cultures at a cellular level. Whether the observed changes are due to changes in intrinsic membrane excitability, network effects such as gap-junction or glial activity or a more radical reconfiguration of the network due to structural changes requires further study.

In contrast, Figure 4.2A and 4.2B show the seizure frequency and duration recorded from P7 cultured slices at DIV0 (n=2), DIV3 (n=30), DIV7 (n=8), DIV10 (n=7) and DIV14 (n=6), respectively. Figure 4.1Ci-Cv and Di-Dv demonstrates 30s and 200ms (respectively) epochs of raw LFP traces recorded at each timepoint.

As can be seen in Figure 4.1A seizure activity in both CA1 and CA3 does not differ significantly from that seen on DIV0, and although the trend appears to be an increase in seizure frequency over time (2 sph at DIV0 up to 6.2 sph at DIV14 ± 3.124 sph, n=2 for DIV0 and n = 6 for DIV14, p = ns, DF = 1) there was no significant difference seen between any of the days *in vitro* or between CA1 and CA3, statistical significance was determined using the mixed-effect model with a Tukey's multiple comparisons post hoc test . It could therefore be suggested that using P7 tissue as the basis of organotypic culture work represents a stable network state with no significant progression in the rate or duration of seizure-like activity.

In both cases (for P3 and P7 slices) results for CA1 and CA3 are very similar, this suggests that seizure activity in CA3 drives seizure activity in CA1 and is in keeping with other studies where researchers observed synchronous discharges between CA1 and CA3. However, it was discovered when the connection between CA3 and CA1 was severed epileptiform discharges from CA1 disappeared (Zapukhliak et al., 2021).

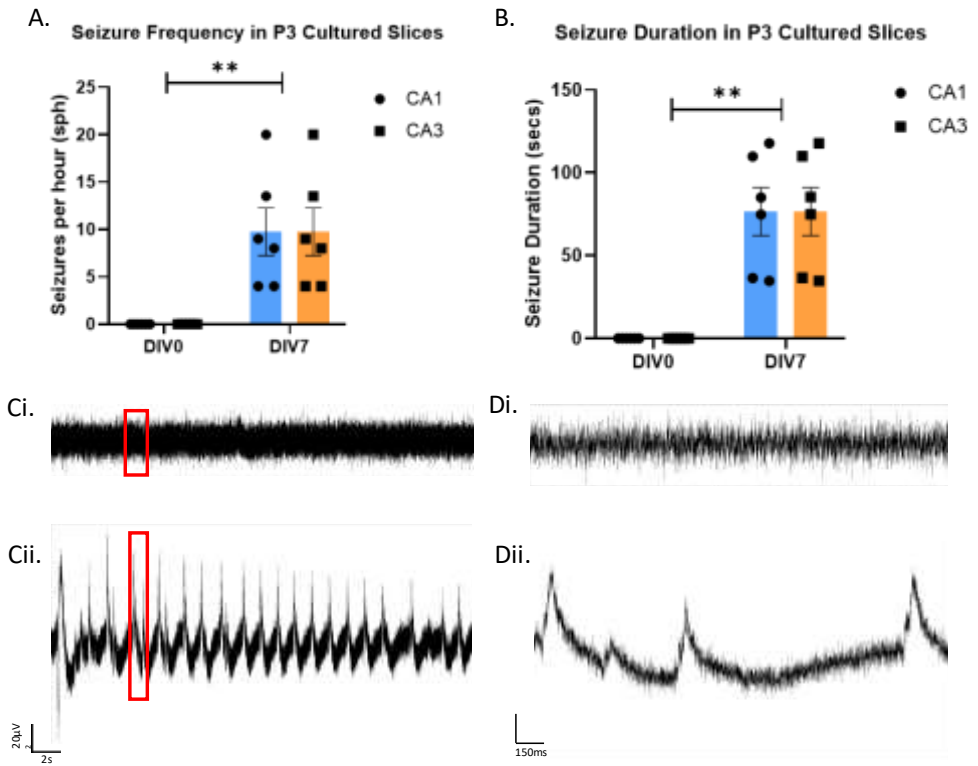

Figure 4.1 Seizure frequency and duration in P3 slices

Bar graphs 4.1A & 4.1B demonstrate mean median spontaneous seizure activity and seizure duration (respectively) in CA1 (shown in blue) and CA3 (shown in orange) at DIV0 and DIV7. n = 5 in each case. Statistical significance was determined using a 2-way ANOVA with a Sidak's multiple comparisons post hoc test, where ** denotes $p \leq 0.005$. Error bars show SEM.

Traces from raw LFP data shown in Figure 4.1 Ci & 4.1 Cii show 30 second epochs of spontaneous epileptiform activity in DIV0 & DIV7 slices respectively, while traces show in Di & Dii display 2 second epochs of the same traces. The areas which have been highlighted in red in 4.1C are the areas that are zoomed in on in 4.1D.

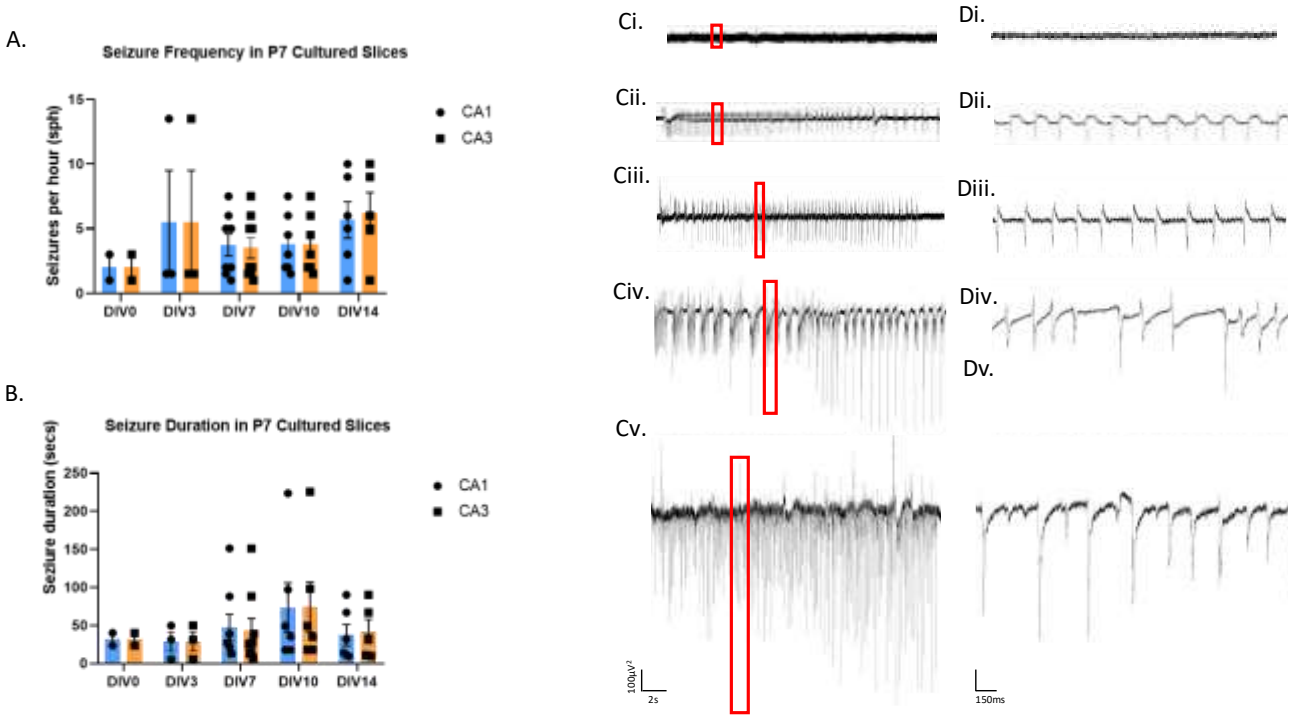

Figure 4.2 Seizure frequency and duration in P7 slices

Bar graphs 4.2A & 4.2B demonstrate mean median spontaneous seizure activity and seizure duration (respectively) in CA1 (shown in blue) and CA3 (shown in orange). Medians for mean median seizure frequency & duration were taken for each slice meaning sample size varies for each DIV (n = 2 for DIV0, n=3 for DIV3, n = 8 for DIV7 CA3, n= 7 for DIV7 CA1 & DIV10, n = 5 for DIV14). Statistical significance was determined using mixed-effects analysis with a Tukey's multiple comparisons post hoc test. Error bars show SEM. Traces from raw LFP data shown in Figure 4.2Ci-Cv show 30 second epochs of spontaneous epileptiform activity in DIV0-DIV14 slices respectively, while traces show in Di-Dv display 2 second epochs of the same traces. The areas which have been highlighted in red in 4.2C are the areas that are zoomed in on in 4.2D.

4.3.2 Single cell recordings from cultured slices:

Whole-cell voltage-clamp recordings were conducted to investigate the effects of varying days *in vitro* on sIPSC activity of hippocampal pyramidal cells from cultured slices taken acutely from rats at either P3 or P7. Recordings were taken from CA1 and CA3 at DIV0 (n=8 for P7, n=5 for P3), DIV3 (n =6 for P7), DIV7 (n=3 for P7, n=5 for P3), DIV10 (n=5 for P7) and DIV14 (n=3 for P7), however, due to the loss of cells via slicing and the culture process it was difficult to maintain consistent repeats from each specific area over time in culture so for the purposes of these experiments data from both areas have been pooled together. The standard patch-clamp technique (as outlined in Chapter 2) was used to obtain recordings from hippocampal neurons at timepoints which correlate to those used for LFP experiments previously described in Figures 4.1 and 4.2. Whole-cell patch recordings were also obtained acutely from age matched rats (P7 (n=8), P10 (n=2 for P7 comparison and n=3 for P3 comparison), P14 (n=2), P17 (n=3) and P21 (n=5)) to compare to each *in vitro* timepoint.

The parameters assessed here are the mean median peak amplitude (pA), interevent interval (IEI, ms), decay time constant (tau, ms) and the events detected per minute. The median peak amplitude was used here to gain a better measure of the overall activity in recordings as some amplitudes recorded were extremely high,

Figure 4.3 demonstrates sIPSC recordings for cultured slices extracted from P7 rats vs their age matched counterparts, where Figure 4.3A shows peak amplitude (pA), 4.3B shows decay tau (ms), 4.3C shows IEI (ms) and 4.4D shows events recorded per minute. Statisical analysis between conditions was performed using an unpaired t-test. Looking at Figure 4.3A the only significant difference which is denoted can be seen at DIV10 (n = 5) where peak amplitude shows a decrease of 3.1027 ± 1.545 pA ($p \leq 0.05$, DF = 6) compared with P17 (n = 3) age match control. A significant difference can also be seen in Figure 4.3D when comparing DIV10 (n = 4) to that of the P17 (n = 3) age match control (1408 to 258.3 events per minute, $p \leq 0.01$, DF = 5). No significant differences are reported for IEI (Figure 4.3B) ordecay tau (Figure 4.3C) between cultured slices and their equivalent age matched control can be seen (p = ns for both). A mixed-effect analysis with Tukey's multiple comparisons post hoc test was also used to determine significant differences between DIV, Figure 4.3D shows a significant increase in events per minute from DIV0 to DIV10 (205.4 to 1132 ± 169.8, $p \leq 0.005$, DF = 21) and from DIV3 to DIV10 (206.7 to 1132 ± 179.6, $p \leq 0.005$, DF = 21). The same statistical analysis indicated no significant differences between DIVs for median peak amplitude (Figure 4.3A), decay tau (Figure 4.3B), or IEI (Figure 4.3C), it also determined no significant differences between age matched control for any measure taken.

The lack of significant differences found between the cultured slices and the correlating age matched slices indicate that the culturing of slices does not have an impact the inhibitory activity which occurs naturally over the same time period, at least in a slice preparation where the loss of interneurons in the extraction and slicing process must be considered – lack of difference in these data indicate that any loss between acute slices and organotypic preparations is consistent.

While the amplitude, IEI and decay remained largely unchanged over time in culture the increase in the frequency of events per minute from DIV0 to DIV14 is significant and reflects the trend shown in Figure 4.2A. This increase in activity suggests that inhibitory synapses are firing more often which could shift the balance between excitation and inhibition, thereby contributing to the network seizure activity which can be seen in LFP recordings.

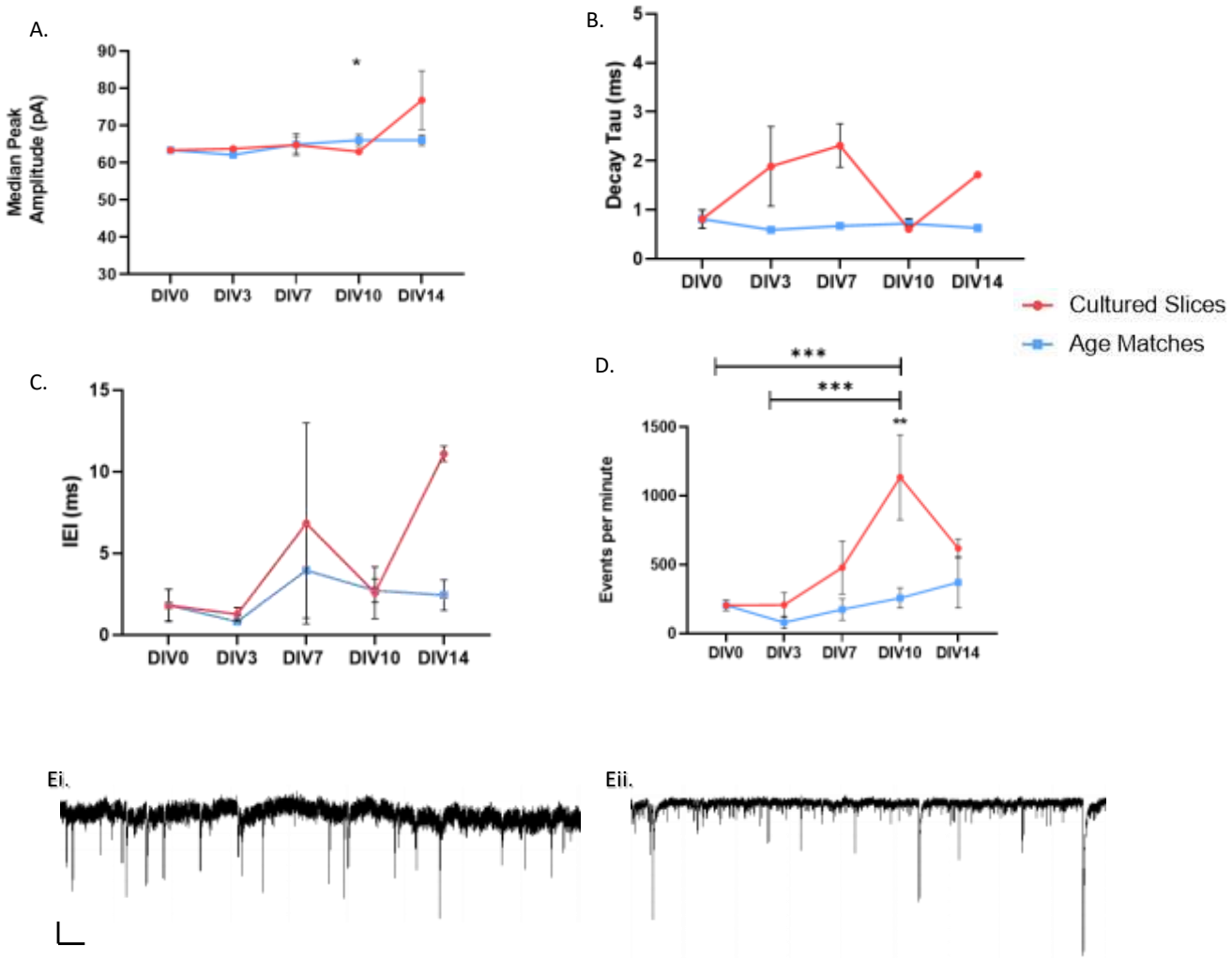

Figure 4.3 Changes in sIPSC activity in P7 cultured slices vs age matched controls.

Connected column graphs depict mean median peak amplitude (A), IEI (B), decay tau (C) and events per minute (D) at various timepoints in vitro (DIV0 (n=8), DIV3 (n=6), DIV7 (n=3), DIV10 (n=5) & DIV14 (n=3)) (shown in red) vs the age match control for each timepoint (P7, P10, P14, P17 & P21) (shown in blue) for sIPSC data. Error bars indicate SEM. Statistical analysis were performed using unpaired t-tests to compare each culture condition against their age match control, where * denotes $p \leq 0.05$ and ** denotes $p \leq 0.01$. A mixed-effect analysis with Tukey's multiple comparisons post hoc test was also used to determine significant differences between DIV, where *** denotes $p \leq 0.005$ for cultured slices and no significant differences were observed in control slices.

Figure 4.3Ei & Eii show example traces of sIPSC at DIV0 (Ei) and DIV14 (Eii), recorded from CA1 of P7 cultured slices. Scale bars represent 20pA on the y axis and 1s on the x axis.

Figure 4.4 shows whole-cell EPSC recordings taken from pyramidal hippocampal neurons of cultured slices extracted from P7 rats at DIV0 (n=7), DIV3 (n=1), DIV7(n=7), DIV10 (n=10) and DIV14 (n=6). Figure 4.4A shows peak amplitude (pA), 4.4B shows decay tau (ms), 4.4C shows IEI (ms) and 4.4D shows events recorded per minute. A one-way ANOVA was used to determine statistical significance, where no statistical significance was determined across days *in vitro* indicating that the excitatory activity of a cell is unchanged during the culture process.

The overall data from Figures 4.3 and 4.4, when looked at as whole, suggests that the kinetics of sIPSCs and sEPSCs at any timepoint remain unaffected by the culture process.

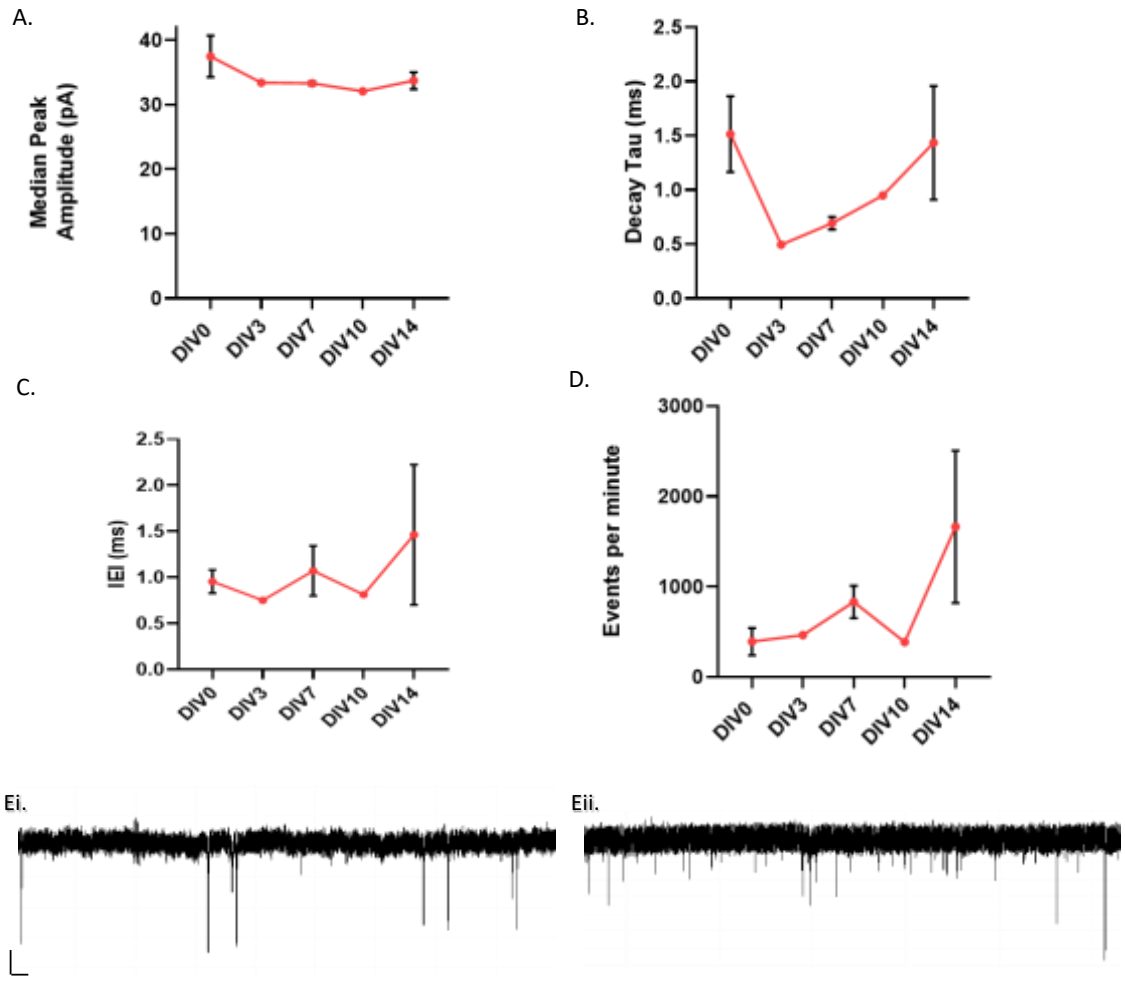

Figure 4.4 Changes in sEPSC activity in P7 cultured slices.

Connected column graphs depict mean median peak amplitude (A), IEI (B), decay tau (C) and events per minute (D) at various timepoints in vitro (DIV0, DIV3, DIV7, DIV10 & DIV14) for sEPSC data. Error bars indicate SEM. A one-way ANOVA determined p=ns between DIV for all measure tested (n numbers vary for each group where n=7 for DIV0 & DIV7, n=5 for DIV14 and n=1 for DIV3 &, DIV10).

Figure 4.5 shows whole-cell sIPSC recordings from cultured slices taken from P3 rats at DIV0 and DIV7 (n=5 for both) and their corresponding age matched acute slices (P3 (n=5) & P10 (n=3)), where Figure 4.5A shows peak amplitude (pA), 4.5B shows decay tau (ms), 4.5C shows IEI (ms) and 4.4D shows events recorded per minute. Unpaired t-tests were used to determine statistical significance between sIPSC between cultured slices and their equivalent age matched control, one significant

difference was noted in event per minute (Figure 4.5D0 between DIV7 slices and their corresponding age matched control (1558 to 258.3 events per minute ± 410.1, $p \leq 0.05$, DF = 5). For median peak amplitude, IEI, and decay tau (Figure 4.5A-C) no significant differences were found between the cultured slices and the correlating age matched slices indicating that, similarly to data shown above in Figure 4.4, the culturing of slices did not have a significant impact the amplitude of inhibitory events in maturing neurons after being extracted from P3 rats and placed into culture. This suggests that the activity of individual neurons remains largely unchanged even though epileptic activity increases (as seen in Figure 4.2).

However, an increase in the frequency of inhibitory events per minute from DIV0 to DIV7 is in keeping with the data shown in Figure 4.3D and the trend indicated in Figure 4.2A. Furthering the idea this increased firing of inhibitory synapses is causing an imbalance between excitation and inhibition and contributing to seizure activity.

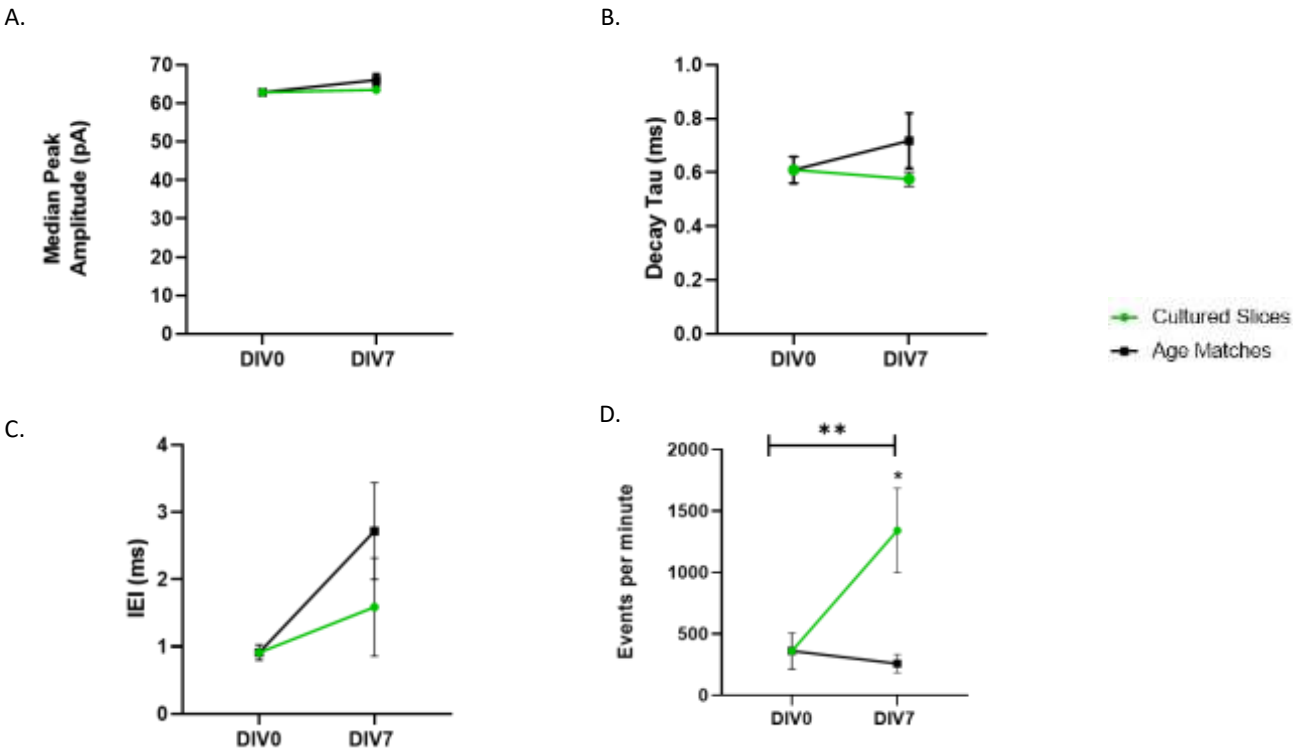

Figure 4.5 sIPSC activity in P3 cultured slices vs age matched controls.

Connected column graphs depict mean median peak amplitude (A), IEI (B), decay tau (C) and events per minute (D) at DIV0 and DIV7 (shown in green) vs the age match control for each timepoint (P3 & P10) (shown in black) for sIPSC data. Error bars indicate SEM. (n=5 for DIV0, DIV7 & P3, n=3 for P10). Statistical analyses were performed using unpaired t-tests to compare each culture condition against their age match control, where * denotes $p \leq 0.05$. A mixed-effect analysis with Tukey's multiple comparisons post hoc test was also used to determine significant differences between DIV, where ** denotes $p \leq 0.01$ for cultured slices and no significant differences were observed in control slices.

Figure 4.6 shows whole-cell EPSC recordings taken from pyramidal hippocampal neurons of cultured slices extracted from P7 rats at DIV0 (n=1) & DIV7 (n=6). Figure 4.6A demonstrates changes in peak amplitude (pA), 4.6B shows decay tau (ms), 4.6C shows IEI (ms) and 4.6D shows events recorded per minute. A test was performed to determine statistical significance between any DIV0 and DIV7 measurements, however no statistical significance was determined across days *in vitro* due to a lack of repeat conditions for DIV0. These data indicate that the excitatory activity of a cell is unchanged

during the culture process, however much more research is required to confidently determine the differences in activity between DIV0 and DIV7 in culture.

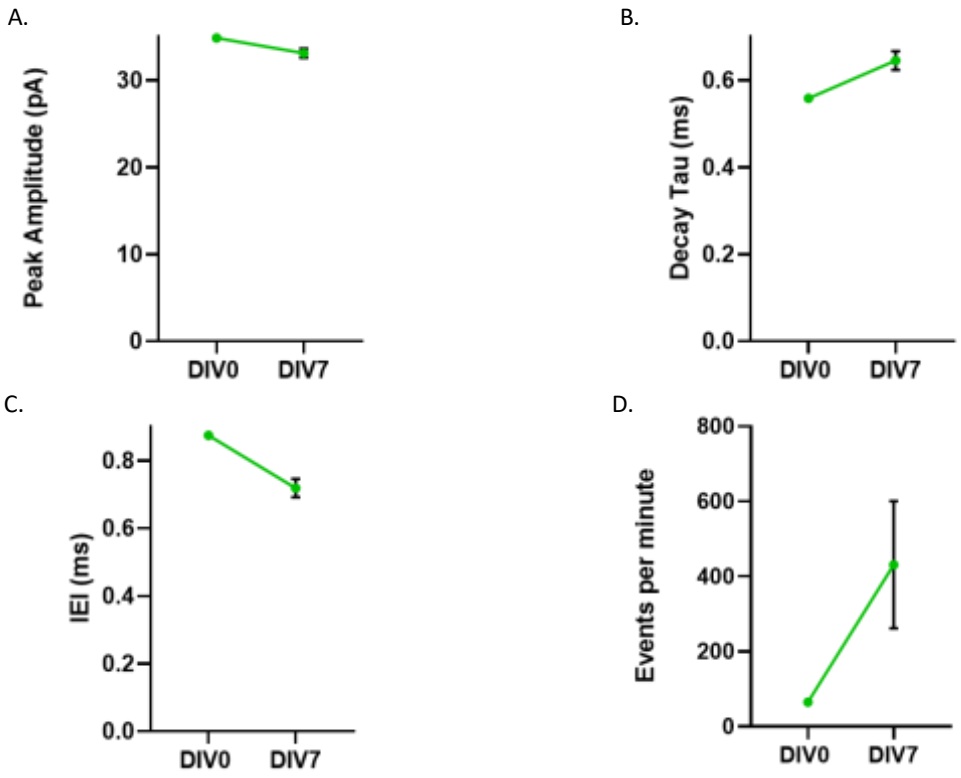

Figure 4.6 Changes in sEPSC activity in P3 cultured slices vs age matched controls.

Connected column graphs depict mean median peak amplitude (A), IEI (B), decay tau (C) and events per minute (D) at DIV0 (n=1) and DIV7 (n=6). An unpaired t-test was used to determine significance, p= ns for each measurement. Error bars indicate SEM.

Cumulative frequency curves were used to assess the overall distribution of data for the peak amplitudes of sIPSCs & sEPSCs recorded from P7 culture slices and the corresponding age match controls (Figure 4.7) were also produced for each timepoint. These cumulative frequency curves indicate that the relative frequency of sIPSC peak amplitude for P7 cultured slices at DIV0, DIV3, DIV7, DIV10 and DIV14 (Figure 4.7A), sIPSCs of their age matched controls at P7, P10, P14, P17 and P21 (Figure 4.7B) and the sEPSCs recorded from P7 cultured slices at DIV0, DIV3, DIV7, DIV10 and DIV14 (Figure 4.7C).

For sIPSC data (Figure 4.7A & 4.7B) in each case the relative percentage of peak amplitudes of events remains consistent throughout increasing days *in vitro*. This reflects the mean median data which was obtained and is presented below.

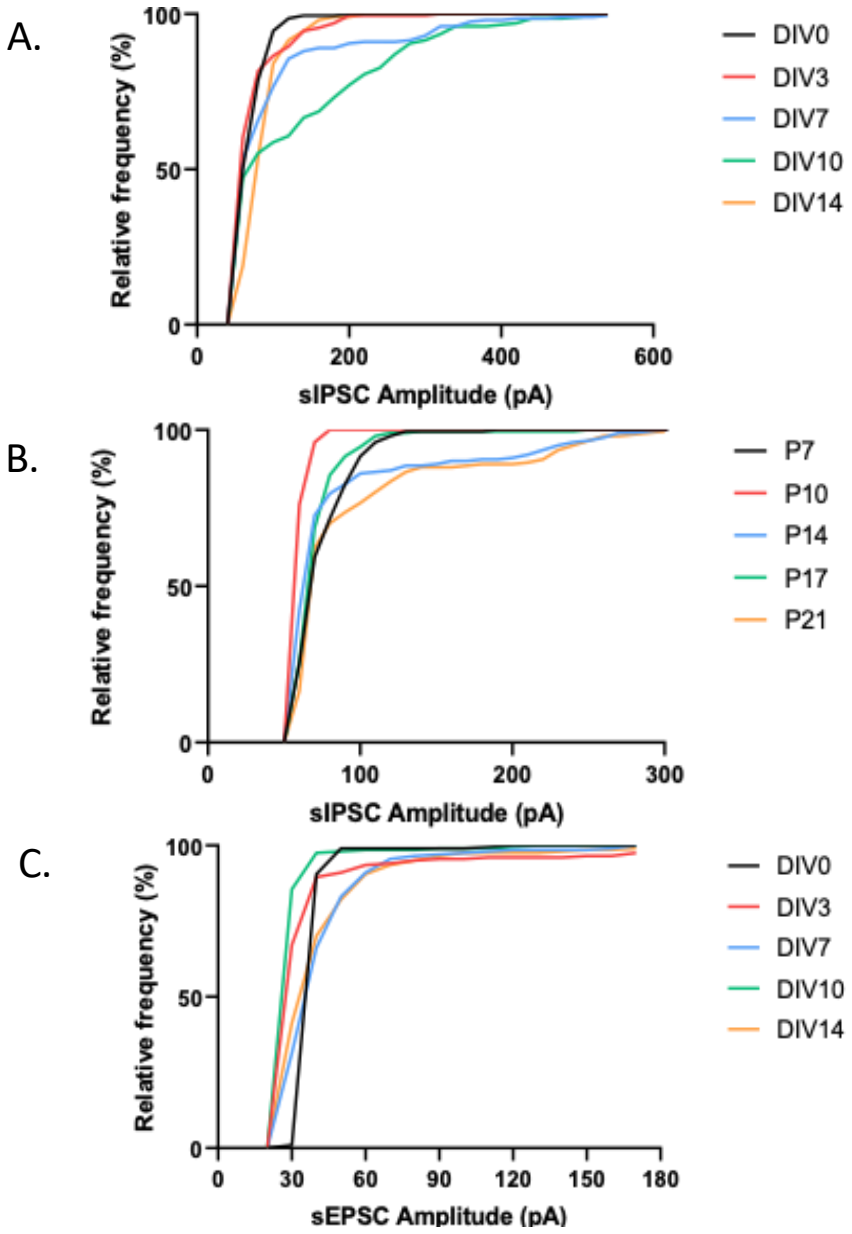

Figure 4.7 Cumulative frequency curves peak amplitude in cultured P7 slices & age match controls.

Cumulative frequency curves of sIPSC peak amplitude amplitude in cultured P7 slices (A) and their age matched controls (B). Cumulative frequency curves of sEPSC peak amplitude amplitude in cultured P7 slices (C). Black = DIV0, red = DIV3, blue = DIV7, green = DIV10 and orange = DIV14 (n=200 for each group, KS test determined p = ns sIPSC and sEPSC in culture slices while p ≤ 0,05 for sIPSC of control slices).

Cumulative frequency curves for the peak amplitudes of sEPSCs recorded from P7 culture slices for each timepoint are shown in Figure 4.7C. These cumulative frequency curves indicate that the amplitude remains consistent throughout increasing days *in vitro*.

Figure 4.8 shows the cumulative frequency curves for the amplitudes of sIPSCs & sEPSCs recorded from P3 culture slices at both the beginning (DIV0) and end of their culture process (DIV7). These cumulative frequency curves for both SIPSCs and sEPSC (Figure 4.8A and 4.8B, respectively) indicate that the distribution of sEPSC and sIPSC amplitudes ($p \leq 0.001$, KS test) changes between day 0 and day 7 *in vitro*. In contrast to the mean median data which was obtained and is presented above in Figure 4.5 & Figure 4.6 where no statistical significance was found between timepoints on a cellular level, this may go some way to explain any network-level changes in the P3 cultures via synapse-specific changes that may not be reflected in cellular-level averages.

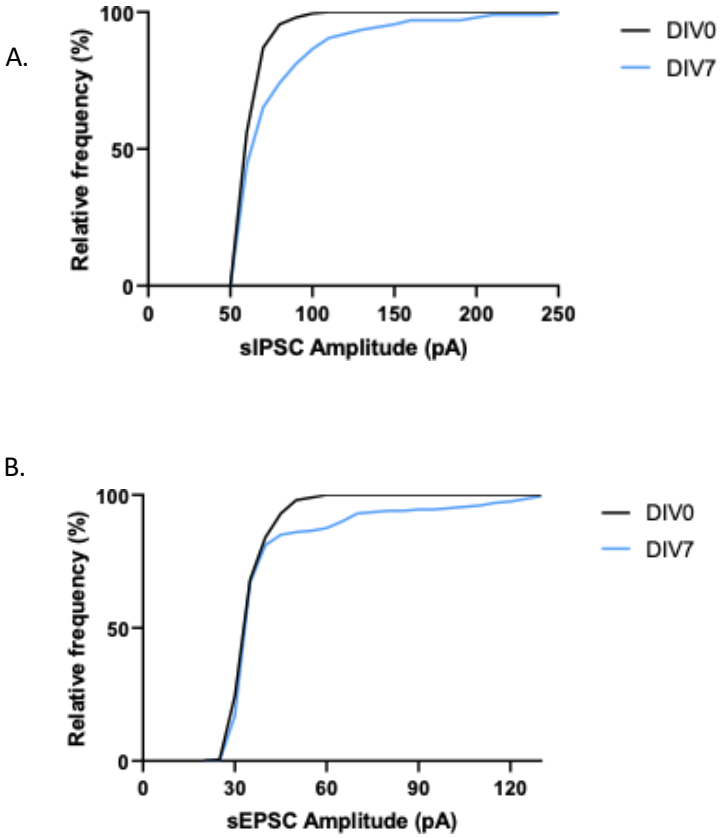

Figure 4.8 Cumulative frequency curves of sIPSC activity in cultured P3 slices.

Cumulative frequency curves of sIPSC peak amplitude amplitude (A), and sEPSC peak amplitude (B) represent whole-cell recordings obtained for P3 cultured slices at DIV0 and DIV7.Where black = DIV0 and blue = DIV7. KS tests determine $p \leq 0{,}001$ for both sIPSC and sEPSC, n=200 per group).

4.4 Discussion:

4.4.1 The process of epileptogenesis in cultured slices:

The data presented in this chapter indicate that epileptic activity in cultured slices increasing over time in culture, while patch-clamp recording suggest that the kinetics of sIPSCs and sEPSCs are not significantly impacted by the culture process there is a clear increase in the number of sIPSC events that occur when slices from both P3 and P7 rats have been cultured. This increase in inhibitory synaotic activity may be causing an imbalance of excitation and inhibition within networks in slices, leading to the increases in seizure activity that can be seen on a network level in LFP recordings.

The model that has been used here to induce epilepsy in *in vitro* slices involves significant axotomy to the cells at the sliced surface. As a response to this traumatic injury deafferentation and axonal sprouting takes place within the slices, which causes connectivity between pyramidal cells to increase while in culture (Sakaguhci *et al.*, 1994; Gutierrez & Heinmann, 1999; Pavlidis & Madison 1999). These new connections which are formed during time in culture may well contribute to the increase in epileptiform activity seen in the P3 preparations, as the new connections will disrupt the balance of inhibition and excitation. In the human epileptic hippocampus, the dentate gyrus undergoes changes consisting of the loss of dentate hilus interneurons, appearance of newly formed ectopic granule cells, and sprouting of mossy fibres which suggests that a high remodelling of the dentate-hippocampal circuits has a correlation to epileptogenesis (Pitkanen & Sutula, 2002). It is possible that this loss of interneurons is mimicked during the process of slicing prior to placing slices in culture, as slices must undergo axotomy resulting in the loss of normal afferent connections and important efferent connections. The combined loss of afferent neuronal connections with distant brain areas and efferent connectivity to typical target areas results in a reorganisation of intrinsic axons within the slice (Humpel, 2015). This loss of important efferent and afferent connections can also result in neuronal death, which is implicated another key factor in the development/progression of epileptic disorders, which may also contribute to the development of epilepsy in culture as we know that from the moment slices are extracted and sliced the cells begin to die, cell death within the slice continues in culture however some neurons will rearrange their dendrites to form new connections following axotomy (Dingledine *et al.*, 2014).

Figures 4.1 and 4.2 indicate that the process of culturing slices following acute extraction induces a differential epileptogenic effect dependent upon the age of the initial tissue, causing an increase in the frequency and duration of spontaneous seizures in P3 tissue whilst remaining at a relatively stable level of activity in P7. While the data recorded from slices from P7 rats did not show any significant

differences between days *in vitro*, there was a trend of increasing epileptic activity. The data recorded from P3 rats showed significant increases in both seizure duration and seizure frequency from DIV0 to DIV7, with no seizure activity at all detected in DIV0 recordings.

Less data is available for P3 slice culture in these results as P3 cultures did not survive well in culture past DIV7, so no data was obtained past this point. P7 cultures were more robust and lasted longer in culture allowing for more experimental timepoints.

Data shown across Figures 4.3 to 4.8 display a number of analyses on sIPSCs and sEPSCs recorded using whole-cell patch clamp in slices extracted for P3 or P7 rats, and acute slices from corresponding age match controls. The parameters for sIPSC and sEPSC recordings differ as EPSCs are generally smaller than IPSCs due to differences in receptor types and ion channels on inhibitory and excitatory neurons, this is reflected in the data shown as most sEPSCs detected were less than 40pA while most sIPSCs were 50pA or above (detected using a threshold search in Clampfit software). This data exhibits very little statistical significance between sIPSCs for culture slices and sIPSCs for their age matched controls (Figure 4.3, 4.5, 4.7 & 4.8), and no statistical significance is seen at all at different timepoints for central measures of either sEPSCs. However, the number of events per minute in both P3 and P7 cultures increased significantly over time in culture which indicates that the frequency of inhibitory synaptic activity is increasing over time in cultured slices. There also appear to be changes in the distribution of amplitudes in both inhibitory and excitatory events between DIV0 and DIV7 cells from P3 cultures, which may go some way to explaining some of the network-level effects observed.

The lack of significant changes in much of the patch-clamp data would indicate that while the kinetics of neurons are not altered on an individual level the loss of neurons in the hippocampus over time in culture could be affecting the ability of cells to communicate with one another as a network. The significant increase in inhibitory events seen in patch-clamp recording could be due to the loss particular neuronal types (e.g interneurons which are the first to die in culture as they are more sensitive than other neuronal types), as there is no significant effect of culture on excitatory synaptic activity in either P3 or P7 cultures it is likely that culturing these slices is causing an imbalance of inhibition and excitation within the hippocampal network. This imbalance of inhibition/excitation is likely to eventually cause the hippocampal network to be pushed towards seizure generation.

4.4.2 Limitations of the study:

This study had some limitations due to the challenging of obtaining whole-cell patch-clamp recordings

from cultured hippocampal neurons due to the fragility of slices when they are removed from culture wells. Hippocampal cultured neurons also lost mass over days *in vitro* leading to difficulties in recording with adequate access resistance. Smaller tipped electrodes with a higher impedance are used in some laboratories, however, these naturally reduce access to the cell and can exacerbate series resistance.

4.4.3 Using cultured slices as a model of epileptogenesis:

Overall, the data presented in this chapter provides promising results for the use of these epileptic slice cultures in epilepsy research. Here a more widely accessible model has been optimised in which the need for a shaking platform inside the incubator is negated and cultures can be performed on static inserts within standard 6-well plates. The process of cultured slices from P3 or P7 rats provides a repeatable and reliable method by which epileptic activity and epileptogenesis can be modelled.

There is a marked difference between P3 and P7 slices in terms of epileptiform activity across the recorded days *in vitro*. P7 slices appear to already be susceptible to epileptiform discharges at the beginning of the culture period but show no significant changes in activity between DIV0 and DIV14 whereas P3 slices start without seizure activity and develop spontaneous recurrent discharges by DIV7. While the culture process appears to induce a higher frequency of inhibitory synaptic events for both P3 and P& cultures very little difference is seen in the other central measurements of cellular-level activity in either age of animal throughout the culturing process. However, a clear difference in cumulative distribution of sIPSC and sEPSC amplitude is seen between DIV0 and DIV7 in the P3 slices, suggesting that although on a cellular level the central measurements do not significantly change, synapse-specific changes in amplitude may be driving the network towards a different activity state. If, for example, these synaptic weighting changes are on those close to the somata of the cells, fast oscillatory activity (as suggested by the PING model discussed in Chapter 1) may be significantly affected. Preliminary results from the RISE model of *in vivo* epilepsy suggest similar changes in amplitude distribution and marked differences between the latent period of epileptogenesis and cells in animals exhibiting spontaneous recurrent seizures (Marley, unpublished thesis data).

Both P3 and P7 tissue will be used in experiments going forward but due to P7 tissue representing a more stable network state with slower epileptic progression, it will be used as the basis of organotypic culture work throughout the rest of this thesis.

Chapter 5: Common Frontline AEDs

Epilepsy is the most common neurological condition, for decades different kinds of medication have been used in the treatment of epilepsy. Up to 70% of patients with epilepsy can become seizure free when given the optimum antiepileptic drug (AED) therapy, many seizures can be controlled with the use of one AED. The number of commercially available antiepileptic drugs has increased steadily in recent years, and this increases the options now available for epilepsy patients and makes the individualisation of treatments more effective, however there remains a cohort of patients who are non-responsive even to polytherapy.

The electrophysiological and behavioural aspects of seizures vary from patient to patient and can be caused by a number of different underlying aetiologies including tumour, epilepsy, and infection. An imbalance between glutamate and GABA systems in the brain can lead to neuronal hyperexcitability. A combination of enhanced excitatory transmission and failure on inhibitory transmissions result in repetitive firing of neuronal discharges (Duncan et al., 2006).

Treatment for epilepsy is determined by how the epilepsy has been classified. Classification depends on a patient's history, age, and seizure type. An appropriate diagnosis paired with the correct utilisation of AEDs is necessary for successful management of seizures. The primary therapeutic target in the treatment of epilepsy is the suppression of neuronal hyperexcitability or hypersynchrony. Several currently used AED therapies aim to reduce this hyperexcitability in order to suppress seizure generation, this can be achieved either by reducing neuronal excitation, increasing neuronal inhibition, or both (Stafstrom & Carmant, 2015). Current pharmacological treatments cannot cure epilepsy; however, they do act to limit epileptic activity and prevent seizures. AEDs limit high-frequency repetitive firing in hyperexcitable networks via the direct or indirect modulation of ion channels, ligand-gated receptor activity and neurotransmitter release. There are many types of AEDs, each individual AED acts on distinct molecular targets and possesses a unique pharmacological profile, but most fall under the same functional umbrella of reducing excitability or increasing inhibition of target neurons. Further investigation is required to identify the effects of AEDs on local and global network activity as many have been discovered empirically rather than by targeted design.

The mechanisms of action of the first-generation of AEDs can be broadly categorised into three groups: Na^+ channel blockade, GABA potentiation and Ca^{2+} channel blockade. Na^+ channel blockade was the most common MOA of early AEDs, such as phenytoin and lamotrigine, whereby the blockage of the voltage-gated Na^+ channel prevents repetitive firing of neurons, slowing neural conductance (Yaari *et al.*, 1986; McNamara, 2006). Positive allosteric modulation of GABARs is another common mechanism of action of AEDs, in particular benzodiazepines which bind to the extracellular area of

GABARs between the α and ϒ subunits, primarily α1 and ϒ2. Barbiturates are also positive allosteric modulators of GABArs however, they are targeted towards the binding site on the membrane (Uusi-OuKAri & Korpi, 2010). Both benzodiazepines and barbiturates allow Cl^- influx to induce antiepileptic activity. The blockade of presynaptic Ca^{2+} channels also confer antiepileptic activity by reducing postsynaptic excitabilility, with some evidence suggesting that phenytoin may have some activity in inhibiting Ca^{2+} channel activation presynaptically (Meldrum, 2007).

Many older AEDs are limited by severe adverse effects, complicated drug-drug interactions caused by patients requiring a combination of AEDs to suppress seizure acivity, and a narrow therapeutic index. Felbamate and phenytoin are two examples of AED which have been shown to have negative side effects (Perucca, 2006; Johannessen & Landmark, 2010).

Valproate is a broad-spectrum anticonvulsant drug which is primarily used for the treatment of seizures but can also be used to treat bipolar disorder and occasionally used to prevent migraines (Losher et al., 2002). The exact mechanism of action is not completely understood but it is thought to work by increasing the levels of GABA in the brain to reduce activity of hyperexcitable neurons and prevent seizures. It has also been shown to alter the activity of 5-hydroxytryptamine (5-HT) and dopamine which may contribute to the mood-stabilising effects of the drug. Valproate has been shown to act on several different ion channels in the brain, including voltage-gated sodium & calcium channels, and potassium channels – another method by which valproate can reduce neuronal excitability and prevent the rapid firing of action potential leading to seizure activity. Valproate can also enhance the activity of certain potassium channels to help stabilise neuronal activity, preventing seizure. It has also been shown to alter the activity of proteins in the brain including enzymes involved in the synthesis and breakdown of neurotransmitters which may also contribute to the MOA (Walden et al., 1993; Collins et al., 1999).

Lamotrigine is also primarily an anticonvulsant but can also be used to treat bipolar disorder. It works by blocking voltage gated sodium channels to reduce neuronal excitability to stabilise electrical activity and prevent seizure activity. Several studies have shown that lamotrigine is effective in reducing both the frequency and the severity of seizure in both children and adults with epilepsy (Goa et al., 1993; Guerrini et al., 1998; Culy & Goa, 2000). It can be used as a maintenance treatment to prevent seizure recurrence. Lamotrigine works by modulating the activity of voltage-gated sodium channels and is thought to inhibit the release of excitatory neurotransmitters, such as glutamate, and reduce the release of calcium ions which helps stabilise electrical activity (Grunze et al, 1998; Choi & Morrell, 2003). It is also known to have some effects on the GABAergic system, but these are not yet fully

understood. Lamotrigine is a complex medication with multiple MOAs which are still being investigated.

Topiramate is a drug which is used for epilepsy and migraines, it has been proven to be effective in reducing both the frequency and severity of seizures in adults and children against a broad range of seizures and can also be used for seizure maintenance. Topiramate enhances the activity of GABA to reduce neuronal excitability, it is also thought to block the activity of voltage-gated sodium channels to reduce abnormal activity which leads to seizures (Steve et al., 1997; Petroff et al., 1999 & 2001; White, 2005). Topiramate is also known to block the activity of certain glutamate receptors including AMPARs and KARs, by blocking AMPAR & KAR activity excitatory signalling in the brain is reduced and this helps prevent the development of seizures – studies have suggested that topiramate binds to specific sites on the receptors to alter their activity via the modulation of ion channels or other signalling pathways, but the mechanism is still not fully understood (Kaminski et al., 2004; Delorenzo et al., 2005)

Recently developed AEDs include a variety of new pharmacological targets, with increased binding specificity. New AEDs aim to provide more tolerable treatments that require less complicated drug-drug interactions and yield consistent and predictable bioavailability with low variability.

These newer AEDs such as Brivaracetam (inhibitor of fast inactivation of voltage-gated Na^+ channels) and selectracetam are potent inhibitors of the synaptic vesical 21 (SV2a) protein. The inhibition of this protein appears to cause broad-spectrum attenuation of excitatory activity by disrupting neurotransmitter exocytosis into the synaptic cleft (Landmark & Johannessen, 2008). Several new generation AEDs are NMDAR agonists which act on postsynaptic Ca^{2+} channels to inhibit the actions of glutamate on NMDARs, including topiramate and zonisamide (Czapinski *et al.*, 2005). Retigabine is a drug which increases the level of newly synthesised GABA resulting in the activation and prolonged opening of neuronal KCNQ2 & KCNQ3 channels, resulting in antiepileptic activity (Rundfeldt & Netzer, 2000). Rufinamide (a Na^{2+} channel blockade) is thought to suppress neuronal hyperexcitability by prolonging the inactive state of voltage gated Na^{2+} channels. This treatment was found to be effective in the treatment of Lennox-Gastraut syndrome patients (Perucca *et al.*, 2008). Alterations in GABAergic inhibition of neurons can also be achieved by new methods aside from enhancing the endogenous activity of GABA. Vigabatrin inhibits GABA-transaminase, the enzyme responsible for GABA degradation in the synaptic cleft, causing an increase in GABA concentration (Czapinski *et al.*, 2005). Other new antiepileptic agents that work to inhibit or decrease AMPAR activity have the potential to reduce extreme excitatory responses (Meldrum& Rogawski, 2007).

This chapter will look at some preliminary data testing the effects of some well-established AEDs on spontaneous epileptic activity in cultured brain slices to ensure that slices have not become drug-resistant while in culture as some of the literature suggests. These experiments will investigate whether this model is appropriate for the screening of new candidate AEDs.

5.2 Methods:

5.2.1 Ethics & animals:

All animal procedures were performed in accordance with the Animals Scientific Procedures Act (ASPA) 1986 UK (amended in 2012), European Communities Directive 1986 (86/609/EEC), and the Aston University ethical review document.

5.2.2 Slice Preparation:

350µM coronal slices were prepared from postnatal day 7(20-25g) Wistar rat pups of either sex. Prior to the brain extraction, rats were anaesthetised by inhalation of 5% isoflurane in a mixture of O_2/NO_2 until no pedal or corneal reflex was detected – depth of anaesthesia was determined by testing for the absence of normal reflexes via a pinch test. Following anaesthesia rats were euthanised by decapitation using surgical scissors and the brain immediately extracted from the skull. Once extracted the brains were placed in a sucrose-based artificial cerebrospinal fluid (aCSF) solution which contains (in mM): 180 sucrose, 2.5 KCl, 10 $MgSO_4$, 1.25 NaH_2PO_4, 25 $NaHCO_3$, 10 glucose, 0.5 $CaCl_2$ and 1 L-ascorbic acid, 2 N-acetyl-L-cysteine, 1 taurine and 20 ethyl pyruvate. Complete aCSF had been saturated with 95% O_2/5% CO_2 (carbogen) prior to the extraction to maintain a pH of 7.3, and osmolarity of 300 – 310 mOsm/L. Brains were then transported back to the lab in the aCSF solution, once back in the lab slices were glued onto a stage and submerged in ice-cold aCSF to be sliced into 350µM slices using a 7000smz-2 model Vibrotome (Campden Instruments Ltd., UK). Slices were then transferred to an interface chamber to acclimatise at room temperature for 1 hour in a glucose-based aCSF solution containing (in mM): 126 NaCl, 3.5 KCl, 2 $CaCl_2$, 1.3 $MgCl_2$, 25 $NaHCO_3$, 1.2 NaH_2PO_4 and 11 D-glucose. Continual bubbling of carbogen through aCSF throughout helped to maintain pH 7.3 and osmolarity 300 – 310 mOsm/L.

5.2.3 Organotypic Tissue Culture:

To maintain a sterile environment for slices and avoid infection of cultures as much as possible all instruments used for both dissection and slicing were autoclaved beforehand, any equipment which could not be sterilised in the autoclave was sprayed down with 70% ethanol to kill any bacteria.

Following the dissection, once slices were cut, they were bathed in an oxygenated glucose-based aCSF solution containing (in mM): 126 NaCl, 3.5 KCl, 1.3 $MgCl_2$, 1.2 NaH_2PO_4, 25 $NaHCO_3$, 2 $CaCl_2$ and 11 glucose for 1 hour before being transferred to a biosafety cabinet, washed in culture media for 10 minutes and placed onto hydrophilic PTFE, 0.4µM pore cell culture inserts (Merck, UK). Residual aCSF was then aspirated off and inserts were placed into 6-well plates containing 1.5ml culture media. The culture media was prepared using Neurobasal-A media (Thermo Scientific, UK) supplements with 0.5mM glutaMAX, 30mg/ml gentamicin and 1ml B27 (Thermo Scientific, UK). Slices were then incubated in a humidified incubator (Thermo Scientific, UK) at 37^oC, 5% CO_2, with a media change twice weekly.

5.2.4 Extracellular recordings:

LFPs were recorded to determine network seizure activity within slices. Slices were manoeuvred onto lens tissue and then placed directly into LFP interface chamber. Microelectrodes were filled with glucose-based aCSF and inserted into layers CA1 or CA3 of the hippocampus. The receiving signals were amplified 100x (setting a low-pass filter of 0.1 Hz and a high-pass filter of 1k Hz). Electrical noise (50Hz) was filtered out using Humbugs (Quest Scientific, Canada). The receiving signal was amplified a further 10x (low-pass filter 0.3 Hz, high-pass filter of 700 Hz). Signals were digitised at a sampling rate of 5 kHz and recorded using Spike2 software (Cambridge Electronic Design, UK).
120 second epochs of recorded activity were extracted from continuous raw LFP traces at specific timepoints (pre- and post-compound application) and analysed for epileptiform activity from initial placement of the electrodes until the addition of any drugs onto the slice, post-drug application epochs were taken 40 minutes after bath applying drugs to slices.

Seizure activity was determined by eye in line with the definition stated in chapter 2.4.2. Median values were determined using Microsoft Excel and then transferred to GraphPad Prism for graph plotting and statistical analysis.

5.2.5 Drugs & Reagents:

The drugs used were valproate, and topiramate (Tocris Bioscience, UK, Sigma-Aldrich, UK), these specific drugs were selected as they had been successfully used by other researchers in this lab to significantly reduce seizure hyperactivity in acute slices. Topiramate and valproate were diluted into stock solutions of 1-50mM and stored in aliquots at -20^oC. Prior to being added to brain slices, aliquots

were defrosted and diluted down to their final concentration. Drugs were then bath applied to slices by adding them directly into the perfusing aCSF and were left to stabilise for at least 40 minutes or until slice had seized multiple times. Once slices had stabilised, subsequent drug application was recorded for 30 – 40 mins following the application of each drug for LFP recordings.

5.3 Results:

5.3.1 Acute dosing of epileptic organotypic cultures with Valproate and Topiramate:

The effects of well-established AEDs valproate and topiramate on cultured organotypic slices taken from P7 donors at DIV14 were investigated. It was important to carry out these preliminary experiments before testing novel AEDs on organotypic slices cultures to ensure slices had not become drug-resistant as some studies have reported the development of drug-resistant epilepsy in culture slices (Albus et al., 2008; Wahab et al., 2010). Figure 4.1A-C indicates that culture slices with spontaneous epileptic activity appeared to respond to application of AEDs although repeat numbers are too low to confidently apply statistical analysis (n=2 for each group).

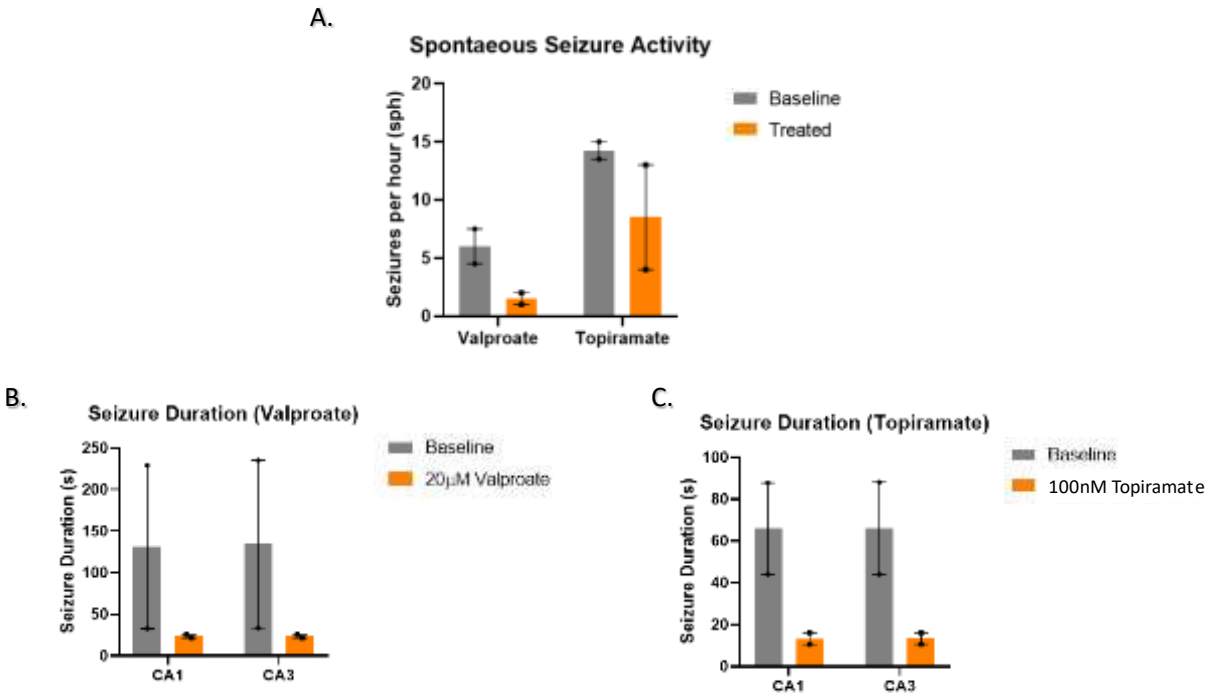

Figure 5.1: Antiepileptic effects of well-established AEDs on epileptic activity in cultured slices.

The bar graph shown in 5.1A demonstrates the average number of spontaneous seizures per hour occurring in P7 DIV14 organotypic cultured slices. Grey bars depict the baseline seizure activity, while orange bars depict seizure activity following the bath application of valproate (left) and topiramate (right).

5.1B demonstrates the mean median duration of spontaneous seizures in CA1 and CA3 before and after the bath application of 20µM valproate. Pink bars are for baseline activity, while purple bars show activity following the bath application of valproate. 5.1C demonstrates the mean median duration of spontaneous seizures in CA1 and CA3 before and after the bath application of 100nM topiramate. Grey bars are for baseline activity, while orange show activity following the bath application of topiramate. Each before and after measurement are from recordings taken from the same slice. (n=2 for each group, stats could not be performed).

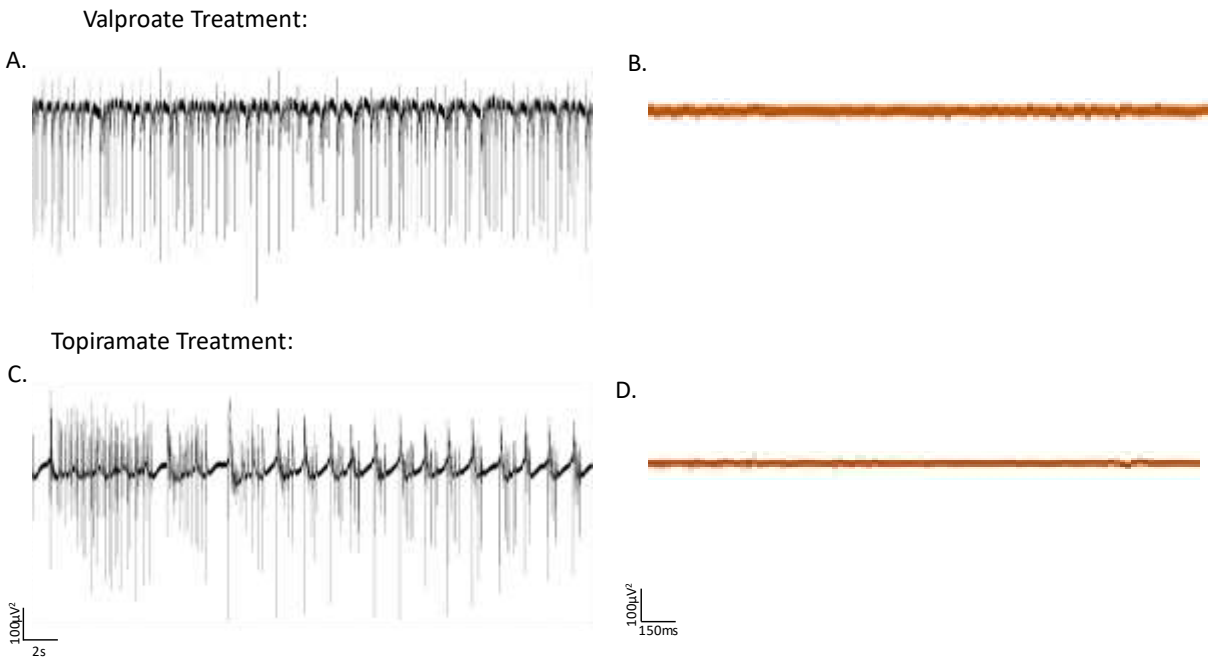

Figure 5.2: Example traces from slices treated with common AEDs.

Panels A&B show before (A) and after (B) a 40-minute treatment with 20µM valproate. Panels C&D show before (C) and after (D) a 40-minute treatment with 100nM topiramate. Scale bars represent 100µV^2 on the x-axis and 2 seconds or 150 milliseconds on the y axis.

5.4 Discussion:

5.4.1 Common frontline AEDs effectively reduced seizure activity in cultured slices:

The data shown in Figure 5.1A-C suggest that slices have not developed drug-resistance after 14 days *in vitro*. However, this is when considering central measurements of seizure activity, whereas there appears to be a clear change in LFP activity after treatment in Figure 5.2. Some earlier studies have suggested that epileptiform activity in rat organotypic hippocampal slice cultures can develop pharmacoresistance to the majority of AEDs (Albus et al., 2008; Wahab et al., 2010), so it was important that before moving forward with the screening of novel antiepileptic drugs to prove that epileptiform activity in the slices was responsive to AEDs which were already established to be effective in treating epilepsy in both human patients and other animal models of seizure. It is for this reason we tested two well-known AED on slice cultures before moving forward with novel AED experiments.

While neither drug had a statistically significant effect on seizure activity in slices and the number of repeats obtained was small, the results shown indicated that slices had not become drug-resistant while in culture and so the testing of novel antiepileptic drugs dexfenfluramine and tianeptine using this organotypic slice culture model of epileptiform activity could proceed.

5.4.2 Limitations of epileptic organotypic slice cultures:

Organotypic slices cultures do have certain limitations however, it is difficult to obtain repeat experiments as spontaneous epileptic activity varies from slice to slice. Some slices exhibit seizure at DIV14 while other slices may only exhibit brief ictal-like events but never enter a full-blown seizure, P7 slices have been used in this instance however the same limitations arise when using P3 slices. Another issue is that slices may die throughout the culture process as longitudinal recordings are not possible without further compromising slice health.

5.4.3 Chronic dosing of cultures with valproate and topiramate:

Chronic dosing of culture with valproate and topiramate was attempted to determine whether low chronic dosing with these drugs would provide an effective treatment of epileptiform activity in culture slices, however, in contrast to other AEDS in Chapters 6 and 7 all slices subjected to these conditions were either dead or infected by the experiment end point of DIV14. This would indicate that these drugs may have had a neurotoxic effect on slices when given in a lower, constant dosage

considering that slices which did not receive the drug were viable.

The effects of dexfenfluramine and tianeptine will still be investigated both acutely and chronically in the following chapters.

Chapter 6: Effects of Tianeptine on spontaneous epileptic activity

6.1 Introduction:

Tianeptine is an atypical tricyclic antidepressant which was used to treat mild to moderate depressive disorders, discovered in France in the 1960s. It is a drug which interacts with various neurotransmitter systems including 5-HT, glutamate, GABA and dopamine. It can also influence synaptic activity including LTP and promotes plasticity by protecting neurons from damage (McEwen & Olie, 2005). It has been suggested that tianeptine may reduce hyperexcitability in the hippocampus and has anxiolytic properties which are thought to be a result of serotonergic modulation. Tianeptine is used for the treatment of major depressive and anxiety disorders. Unlike typical antidepressants such as SSRIs and SNRIs tianeptine is an agonist of μ-opioid receptor and works by increasing the uptake of 5-HT in the brain. μ-opioid receptors are currently being studied as effective targets for antidepressant therapies – it is believed to be the modulation of these receptors that induces the clinical effects that are seen in studies (McHugh & Kelly, 2018). Earlier studies have also shown tianeptine to affect a range of serotonergic receptors, dopamine receptors and glutamate receptors (Dziedzicka-Wasylewska *et al.*, 2001; Kole *et al.*, 2002; Brink *et al*., 2006; Wlaź *et al.*, 2011).

Studies from the last 10 years have evidenced that tianeptine can be prescribed safely to patients with epilepsy without concerns of exacerbating seizure frequency (Moon et al., 2014). Tianeptine has now been identified as having potential therapeutic uses in the treatment of epilepsy but as tianeptine is a newer antidepressant the mechanisms of action of tianeptine on seizure activity are still largely unknown and limited to a few animal studies, making it an interesting drug to test on the spontaneously epileptic culture slice model.

Multiple studies found that the chronic administration of tianeptine causes an increase in phosphorylation of the AMPAR subunit GluA1 in both the hippocampus and the frontal cortex, with a more pronounced effect in CA3 than CA1 (Magariños *et al.*, 1999; Kole *et al.*, 2002; Svenningsson *et al.*, 2007). Phosphorylation at the Ser831 and Ser845 sites on the GluA1 subunit is thought to affect the functional properties of AMPARs. Phosphorylation of the Ser831 residue on GluA1 results in an increase in channel conductance while phosphorylation of the Ser845 residue on the same subunit causes alterations in AMPAR trafficking by increasing GluA1-containing AMPAR localisation on the post-synaptic membrane therefore increasing AMPAR synaptic function (Derkach *et al.*, 1999; Lee *et al.*, 2000; Man *et al.*, 2007; Liu *et al.*; 2009; Jenkins &Traynelis, 2012).

Tianeptine does not bind with adrenergic, dopaminergic or serotonergic receptors/transporters like

SSRIs, it is thought to activate calcium/calmodulin-dependent protein kinase (CaMKII) and protein kinase C (PKC) indirectly through its interactions with various neurotransmitter systems assoicated with the modulation of synaptic plasticity and neuronal excitability which leads to the potentiation of AMPARs. It is also reported that tianeptine leads to decreased surface diffusion of AMPARs as the activation of CaMKII leads to phosphorylation of stargazin - an AMPAR auxillary subunit. Stargazin is involved with the transportation of AMPARs to the synaptic membrane and their receptor rate constant via interactions with on the extra cellular domains of AMPARs (Doris *et al.*, 2005). Stargazin serves multiple roles in trafficking and stabalisation of AMPARs, and the phosphorylation of this subunit leads to immobilisation and anchoring of AMPARs in the post-synaptic membrane (Szegedi *et al.*, 2011; Zhang *et al.*, 2013).

6.1.1 Depression in epilepsy:

Depression is the most frequent comorbid psychiatric disorder in epilepsy with a 30% higher prevalence in patients with epilepsy than in the general population (Kanner, 2003; Mensah *et al.*, 2006; Kanner *et al.*, 2012), however it is largely untreated due to concerns about seizure exacerbation by use of antidepressants. It is thought that depression in epilepsy could be iatrogenically induced following resective surgery or via the use of various antidepressant drugs. Antidepressants have been shown to lower seizure threshold, however, this may be an issue related to the dosage being prescribed for treatment, where higher doses of certain antidepressants may increase the likelihood of a seizure, rather than the drugs themselves (Pisani *et al.*, 2002; Montgomery, 2005). Due to concerns that antidepressant treatments may increase the frequency/severity of seizures depression can often go untreated in epileptic patients. However, more recent studies have found that alternative marketed antidepressants such as selective serotonin reuptake inhibitors (SSRIs) and serotonin and norepinephrine reuptake inhibitors (SNRIs) rarely cause the exacerbation of seizures in epileptic patients (Kanner, 2016; Ribot *et al.*, 2017). Tianeptine is an example of one of these drugs as a retrospective 2014 study found that tianeptine prescribed to patients with epilepsy for the treatment of depression had no effect on seizure frequency (Moon et al., 2014).

6.1.2 Tianeptine in epilepsy:

A 2014 study by Moon *et al.* reviewed retrospective medical records of patients with epilepsy who received tianeptine found that tianeptine can be safely prescribed to epilepsy patients to treat depression without increasing seizure frequency, regardless of the baseline severity of epilepsy

(Moon *et al.*, 2014). Tianeptine has also been found to stimulate the uptake of 5-HT & 5-HIAA (the main metabolite of 5- HT) in brain tissue (Wilde & Benfield, 1995) and reduce stress-induced atrophy of neuronal dendrites, does not appear to be associated with adverse cognitive, psychomotor, sleep, cardiovascular or bodyweight effects & has a low propensity for abuse (Wagstaff *et al.*, 2001).

Tianeptine has a more favourable pharmacokinetic profile than other antidepressants as it has a high bioavalibity, limited distribution throughout the body and is rapidly eliminated – this offers advantages over tricyclic antidepressants as it allows more flexibilty with treatment changes and reduces potential interactions with other medication (Whitton *et al.*, 1991). However, the rapid elimination of tianeptine means it requires a strict adherence to dosage schedules.

Tianeptine has recently (Reeta *et al.,* 2016; Sharma *et al.,* 2016) been identified as a drug which has potential therapeutic uses in the treatment of epilepsy with the potential to slow the progression of epileptogenesis into clinical seizure activity. Reeta and colleagues evaluated the effects of tianeptine against pentylenetetrazole (PTZ)-induced seizures in rats, cognitive impairment and oxidative stress in rats. Three doses of tianeptine (20, 40 and 80 mg/kg) were administered in three doses 30 min before intraperitoneal injection of 60mg/kg PTZ. MK801, an NMDAr antagonist, and naloxone, an opioid receptor antagonist, were administered with tianeptine to evaluate whether there was any involvement of NMDA and opioid receptors, respectively. Tianeptine showed dose-dependent protection against PTZ-induced seizure activity, while coadministration of tianeptine with MK801 increased the anticonvulsant effects of tianeptine the administration of naloxone with tianeptine reduced its protective effects. It was also found that tianeptine attenuated seizure induced oxidative stress and improved learning and memory (determined by behavioral tests). This study determined that tianeptine has a significant anticonvulsant effect, which was enhanced when used in conjunction with MK801. Hence, tianeptine could be a useful drug in epileptic patients with depression as it works both as an anticonvulsant and an antidepressant Reeta *et al.,* 2016).

Sharma et al., investigated the anticonvulsant activity of tianeptine and its interaction with conventional AEDs - valproate, phenobarbitone and phenytoin in mice. Tianeptine was administered to mice orally and the electroconvulsive threshold method was used to determine the outcome. The effects of tianeptine on the median effective dose (ED_{50}) of valproate, phenobarbitone and phenytoin was also studied using a maximal electroshock seizure test after administering tianeptine with AEDs in various combinations. The study found that tianeptine increased electroconvulsive threshold in dose dependent manner, but this effect was significant only at doses of 20 and 40 mg/kg. They also found that tianeptine exhibited a dose dependent reduction in ED_{50} of all the studied AEDs, however,

with significant reductions in ED_{50} stated for both valproate and phenobarbitone when tianeptine was administered at 40 mg/kg, while significant reductions in ED_{50} of phenytoin were observed when tianeptine was administered at doses of both 20 and 40 mg/kg. It was concluded that tianeptine exhibits anticonvulsant action alone, while also exhibiting synergistic anticonvulsant activity when paired with valproate, phenobarbitone and phenytoin. These results suggest that tianeptine could be a safe treatment option for epilepsy patients who also have depression (Sharma *et al.,* 2016).

This chapter will look at the effects of tianeptine on the *in vitro* organotypic culture model of epileptogenesis described in Chapter 4. This study will look at the effects of both acute and low-dose chronic dosing of cultures from P3 and P7 rats using tianeptine.

6.2 Methods:

6.2.1 Tissue Slices:

Brains were extracted from postnatal day 3-7(10-25g) Wistar rat pups and cut into 350µM slices of either coronal or horizontal orientation. Prior to the brain extraction, rats were anaesthetised by inhalation of 5% isoflurane in a mixture of O_2/NO_2 until no pedal or corneal reflex was detected – depth of anaesthesia was determined, in accordance with the ASPA 1986, by testing for the absence of normal reflexes via a pinch test. Following anaesthetisation rats were euthanised by decapitation using surgical scissors and the brain immediately extracted from the skull. Once extracted the brains were placed in a sucrose-based artificial cerebrospinal fluid (aCSF) solution. Complete aCSF had been saturated with 95% O_2/5% CO_2 (carbogen) prior to the extraction to maintain a pH of 7.3, and osmolarity of 300 – 310 mOsm/L. Brains were then transported back to the lab in the aCSF solution, once back in the lab slices were glued onto a stage and submerged in ice-cold aCSF to be sliced into 350µM slices using a 7000smz-2 model Vibrotome (Campden Instruments Ltd., UK). Slices were then transferred to an interface chamber to acclimatise at room temperature for 1 hour in a glucose-based aCSF solution. Continual bubbling of carbogen through aCSF throughout helped to maintain pH 7.3 and osmolarity 300 – 310 mOsm/L.

Once brain slices were cut, they were bathed in an oxygenated glucose-based aCSF solution for 1 hour before being transferred to a biosafety cabinet, washed in culture media for 10 minutes and placed onto hydrophilic PTFE, 0.4µM pore cell culture inserts (Merck, UK). Residual aCSF was then aspirated off and inserts were placed into 6-well plates containing 1.5ml culture media. Slices were then incubated in a humidified incubator (Thermo Scientific, UK) at 37^{o}C, 5% CO_2, with a media change twice weekly.

6.2.2 Electrophysiological Recordings:

Slices activity was recorded using both LFP and patch-clamp electrophysiology.

LFP slices were manoeuvred onto lens tissue and placed directly into LFP interface chamber. Microelectrodes were filled with glucose-based aCSF and inserted into layers CA1 or CA3 of the hippocampus. The receiving signals were amplified 100x (setting a low-pass filter of 0.1 Hz and a high-pass filter of 1k Hz). Electrical noise (50Hz) was filtered out using Humbugs (Quest Scientific, Canada). The receiving signal was amplified a further 10x (low-pass filter 0.3 Hz, high-pass filter of 700 Hz).

Signals were digitised at sampling rate of 5 kHz and recorded using Spike2 software (Cambridge

Electronic Design, UK). 120 second epochs of recorded activity was extracted from continuous raw traces at specific timepoints (pre- and post-compound application) and analysed for epileptiform activity from initial placement of the electrodes for up to one hour, tianeptine was then bath applied to slices for a period of 40 minutes to determine its effects on seizure activity for acute dosing experiments with 10µM tianeptine. For chronic dosing experiments 1µM tianeptine was added to NBA media from DIV0 and reapplied with every media change. After 14 days in culture epileptic activity in slices was measured using LFP recordings, these data were compared with control slices which had been cultured for 14 days in the absence of the drugs tianeptine treatment. Gap free whole-cell patch-clamp recordings for acute dosing of slices were made using standard techniques (Woodhall *et al.*, 2009). 350µM slices were placed onto the patch rig where they were submerged in aCSF and weighed down using platinum rods. Electrodes were filled with internal solution and events were recorded at an inward current of -70mV, signal were filtered at 5kHz, digitized at 10kHz and recorded using pClamp software (Molecular Devices, US). Baseline activity in slices was recorded for 15-20 minutes before bath applying 10µM tianeptine for a period of at least 20 minutes.

6.2.3 Drugs & Reagents:

Tianeptine sodium salt powder (Tocris Biosciences, UK) was diluted into a stock solution of 10mM in DMSO and stored in 100uL aliquots at -20^{o}C. Prior to being added to brain slices, aliquots were defrosted and diluted down to their final concentration. Slices were left to stabilise for at least 40 minutes or until slices had seized multiple times. Once slices had stabilised, tianeptine was then bath applied to slices by adding it directly into the perfusing aCSF following drug application activity was recorded for 30 – 40 mins for LFP recordings. For patch-clamp recordings drug application was recorded for 15-20 mins following application of the drug.

6.3 Results:

6.3.1 Effects of tianeptine on spontaneous network activity:

The effects of tianeptine on spontaneous epileptic network activity was investigated using LFP recordings taken from the CA1 and CA3 hippocampal areas of cultured slices which had been extracted from either P3 or P7 rats. Recordings were taken across various days *in vitro* (DIV-DIV14), due to the shortage of repeats at some timepoints, data were pooled together to obtain an overall insight into tianeptines effects on epileptic network activity in slices cultures from P7 rats.

Figure 6.1 demonstrates results recorded from each hippocampal area and is split according to age of rat on the day of extraction. The most significant result which can be seen here is that the bath application of 10µM tianeptine significantly *increased* the seizure frequency in both CA1 and CA3 of slices obtained from P3 rats (Figure 6.1A and 6.1A, respectively). An increase in seizure frequency from 1.6667 ± 0.9156 seizures per hour to 9.583 ± 3.734 seizure per hour in both cases ($p \leq 0.05$, $n = 12$). All other conditions indicate that tianeptine had no statistically significant effect on epileptic network activity, however the trend appears to be that tianeptine increases epileptic activity when applied acutely to spontaneously epileptic slices. More repeats are required to determine statistical significance of these results as not enough data were gathered due to time constraints and slices which did not exhibit any epileptic activity reduced the number of useable traces for analysis.

Looking at Figure 6.2, it appears that tianeptine provides greater seizure suppression when applied to slices chronically at a lower dosage as opposed to the results seen when applying a higher dosage acutely. A 2-way ANOVA with a Sidak's multiple comparisons post hoc test determined a significant decrease in both seizure duration (87.81s to 0s ± 16.59s) and frequency (6..67 sph to 0 sph ± 1.33 sph) ($p \leq 0.01$, $n=3$, $DF = 8$ for both), however the number of repeats are low, and more experiments are required to determine statistical significance more accurately. These data are promising preliminary data for the application of tianeptine as a chronic treatment of epilepsy.

Raw LFP traces obtained from the CA1 of a P7 rat at DIV10 are shown in Figure 6.3, demonstrating epileptic activity before and after the acute application of 10µM tianeptine. While Figure 6.4 shows the results of chronic dosing of P3 slices for 7 days *in vitro*, corresponding to the data shown in Figure 6.2.

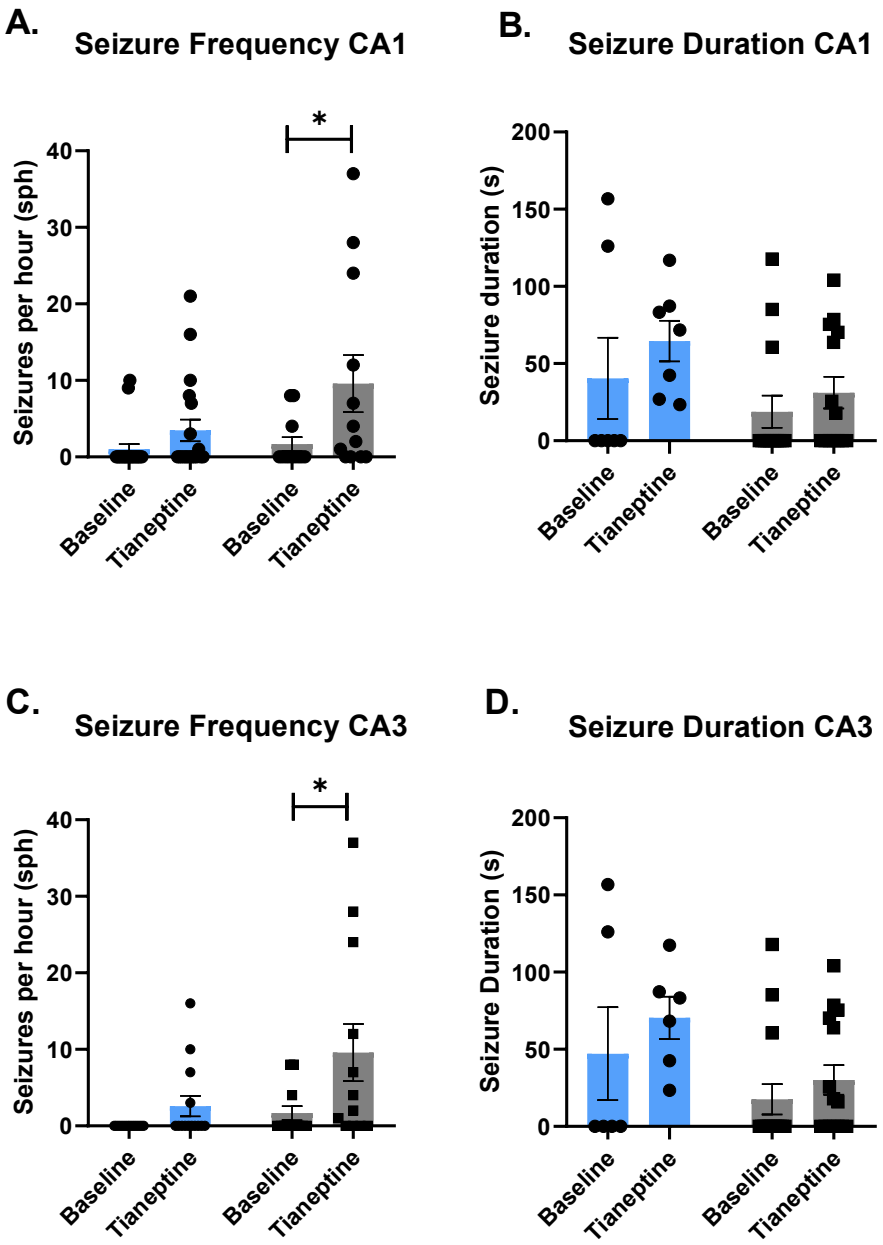

Figure 6.1: Effects of acute tianeptine application to spontaneously epileptic network activity in cultured slices.

Bar graphs demonstrating the mean median spontaneous frequency (A & C) and duration (B & D) in slices extracted from P7 rats (shown in blue, n=7) or P3 rats (shown in grey, n=14) before and after the bath application of 10μM tianeptine. Recordings were taken from slices at various stages throughout days *in vitro* (DIV0-DIV14 for P7 culture and DIV0-DIV7 for P3 cultures). Statistical significance was determined using a 2-way ANOVA with a Sidak's multiple comparisons test, where * denotes $p \leq 0.05$. Error bars represent SEM.

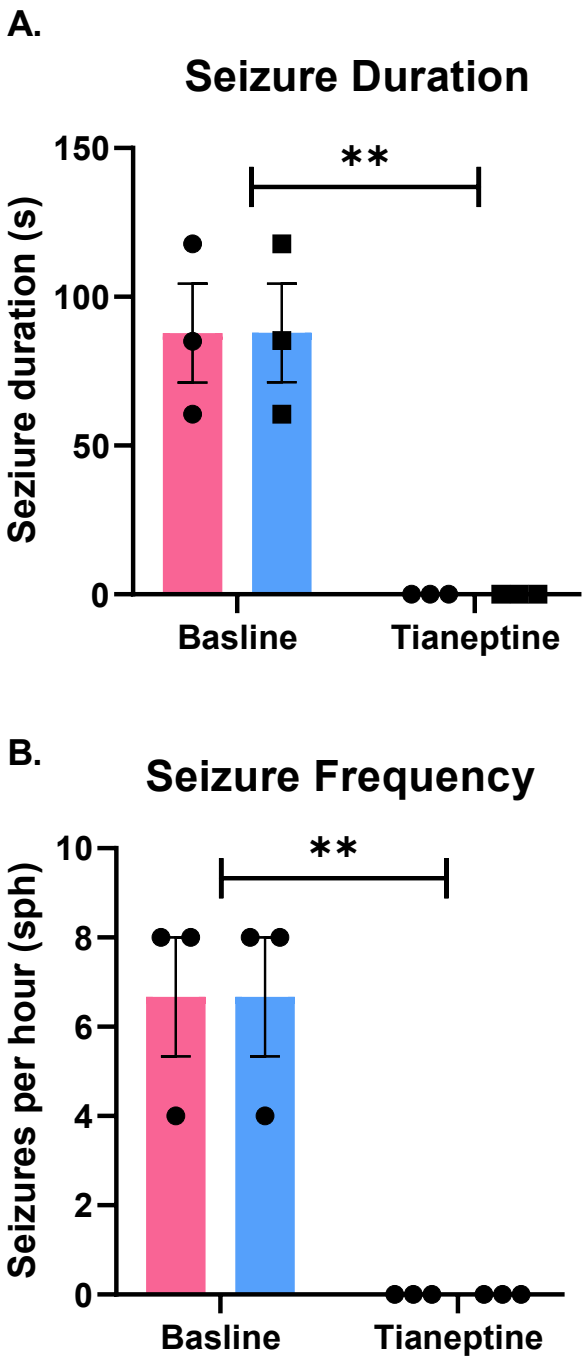

Figure 6.1: Effects of chronic tianeptine dosing of P3 cultured slices.

Bar graphs demonstrating the mean median spontaneous duration (A) and frequency (B) in slices extracted from P3 rats, where CA1 is shown in pink and CA3 is shown in blue, in control slice vs slices treat chronically with 1µ tianeptine for a period of 7 days *in vitro.* Statistical significance was determined using a 2-way ANOVA with a Sidak's multiple comparisons test, where ** denotes $p \leq 0.01$. Error bars represent SEM.

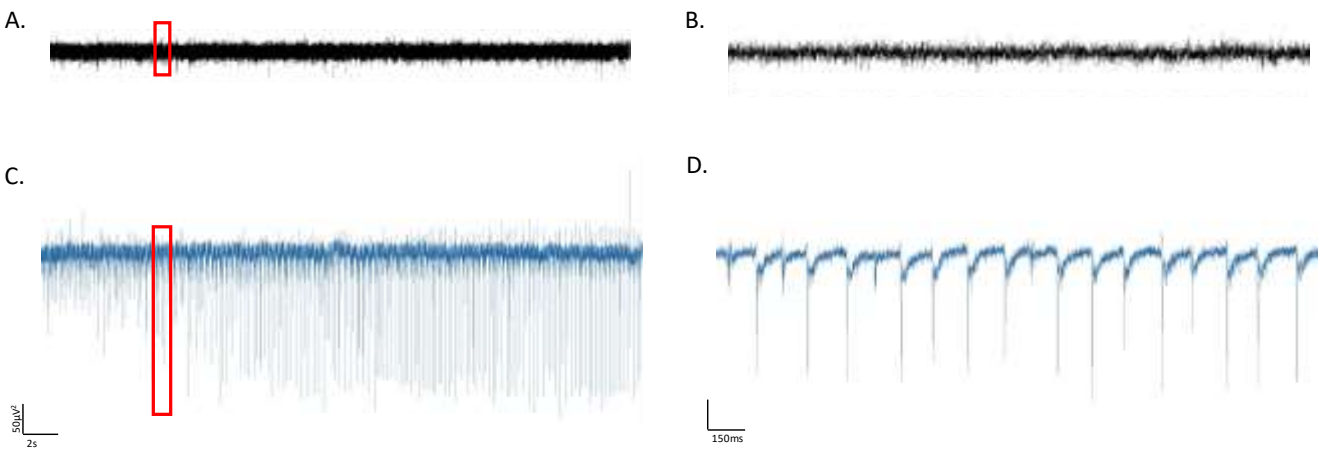

Figure 6.3 Effects of acute dosing with tianeptine on spontaneously epileptic cultures.

Traces from raw LFP data shown in Figure 6.3A & 6.3C depict 30 second epochs of spontaneous epileptiform activity in CA1 of P7 slices respectively, while traces 6.3B & 6.3D show 2 second epochs of the same traces. Black traces (A & B) show the baseline epileptic activity, while blues traces show epileptic activity following the application of tianeptine. Scale bars are 50µV on the y axis and 2s in A&C or 150ms in B&D on the x axis. The areas highlighted in red in A & C reflect the areas that are expanded in B & D.

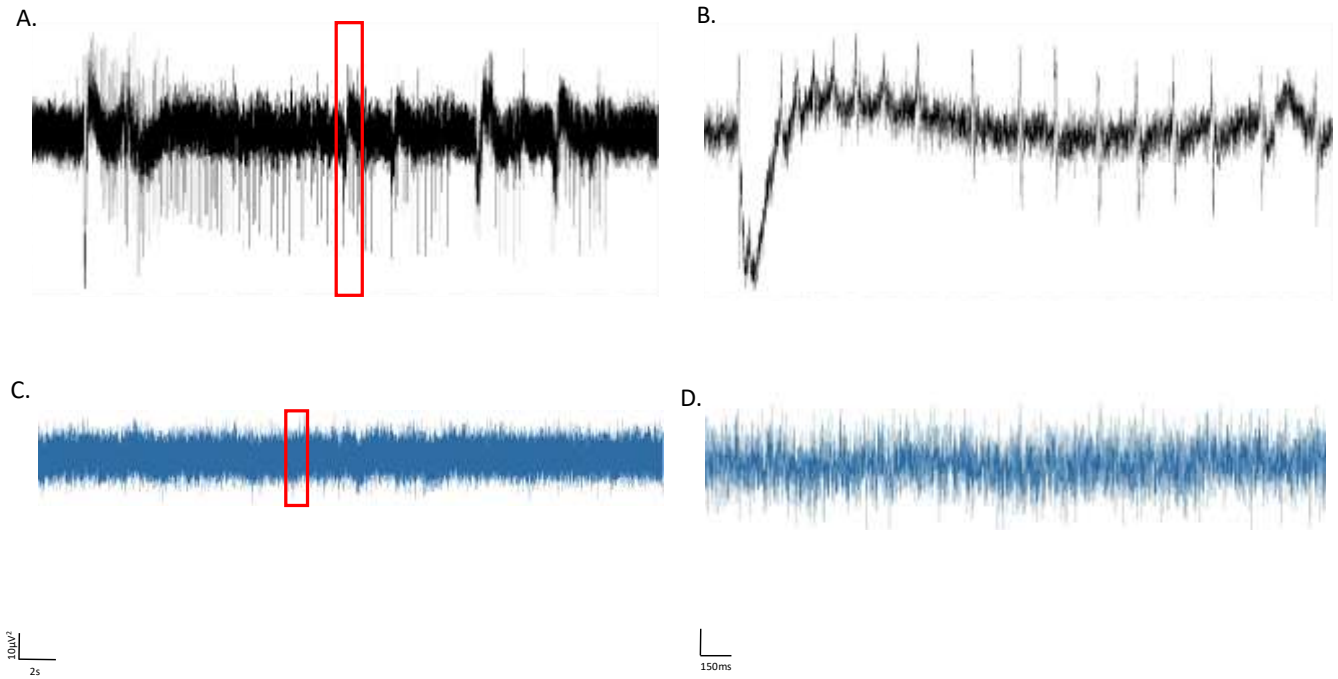

Figure 6.4 Effects of chronic dosing with tianeptine on P3 slice cultures.

Traces from raw LFP data shown in Figure 6.4A & 6.4C depict 30 second epochs of spontaneous activity in CA1 of P3 slices respectively, while traces 6.4B & 6.4D show the corresponding 2 second epochs. Black traces (A & B) show the spontaneous epileptic activity in control slices (no drug), while blues traces show activity following 7 days chronic dosing with tianeptine. Scale bars are 50µV on the y axis and 2s in A&C or 150ms in B&D on the x axis. The areas highlighted in red in A & C reflect the areas that are expanded in B & D.

6.3.2 Whole-cell effects of tianeptine on cultured slices:

Whole-cell patch clamp recordings taken from cultured P7 slices indicate the presence of two separate types of IPSC events occurring within neurons, which is uncommon and seems to be unique to this preparation. Looking at the median amplitude underestimates the differences in current amplitude, this is also true when using the mean current amplitude, therefore in the following analysis data has been separated based on the amplitude of the events to take this into consideration. Type 1 events are classified as events with an amplitude greater the -80pA, while Type 2 events have an amplitude less than -80pA.

Figure 6.5A demonstrates how the two types of events appear in a raw path clamp recording from a P7 slice at DIV0, while Figure 6.5B, 6.5C & 6.5D show the amplitude (pA), decay tau (ms) and IEI (ms), respectively, of Type 1 vs Type 2 events. A significant increase in both peak amplitude and IEI can be seen in figures 6.5B and 6.5D, respectively, while there is a significant decrease in the decay tau ($p \leq 0{,}005$, n=33 matched pairs of events, data was collected across n=2 rats for all data shown).

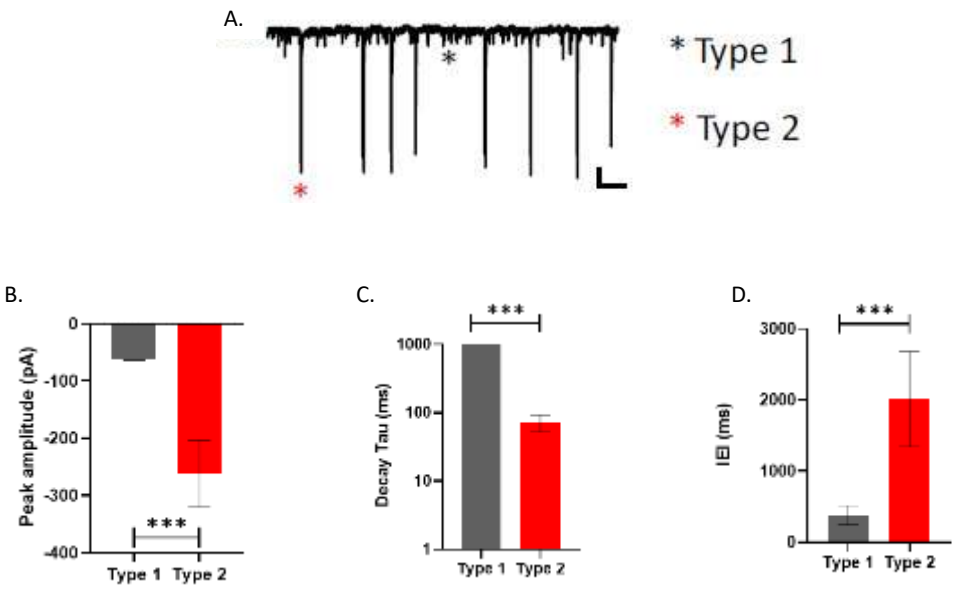

Figure 6.5 Whole-cell recordings of IPSC activity taken from CA1 of a P7 DIV0 cultured slice.

Figure 6.5A shows a 1-minute epoch of a whole cell recording from a P7 DIV0 pyramidal cell. Two types of events can be seen, these are denoted by * (Type 1) and * (Type 2). Scale bars indicate 50pA on the y axis and 10s on the x axis. Figures 6.5B, 6.5C & 6.5D depict bar charts showing differences in amplitude **(B),** decay tau **(C)** and IEI **(D)** of type 1 vs type 2 events. Grey bars represent type 1 events, while red bars represent type 2 events in each case. Statistical significance was determined using the Wilcoxon matched-pairs test, where *** denotes $p \leq 0.005$ (n=33 matched pairs of events, data was collected across n=2 rats). Error bars represent SEM.

Figure 6.6A depicts Type 1 and Type 2 events recorded from a P7 slice at DIV10. Figures 6.5B, 6.5C & 6.6D depicts the amplitude (pA), decay tau (ms) and IEI (ms), respectively, of Type 1 vs Type 2 events. A significant increase in both peak amplitude, decay tau and IEI can be seen in figures 6.5B-D ($p \leq 0{,}005$, n=47 matched pairs of events, data was collected across n=3 rats for all data shown).

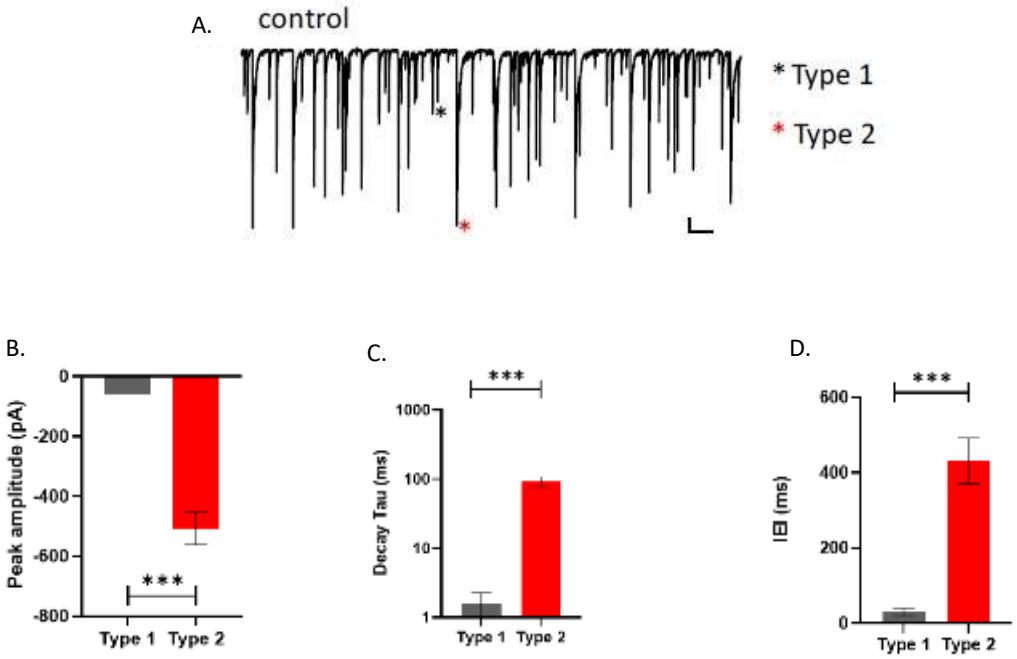

Figure 6.6 Whole-cell recordings of IPSC activity taken from CA1 of a P7 DIV10 cultured slice.

Figure 6.6A show a 1-minute epoch of a whole cell recording from a P7 DIV10 CA1 pyramidal cell. Two types of events can be seen, these are denoted by * (Type 1) and * (Type 2). Scale bars indicate 50pA on the y axis and 10s on the x axis. Figures 6.6B, 6.6C & 6.6D show differences in amplitude **(B),** decay tau **(C)** and IEI **(D)** of type 1 vs type 2 events. Grey bars represent type 1 events, while red bars represent type 2 events in each case. Statistical significance was determined using the Wilcoxon matched-pairs test, where *** denotes $p \leq 0.005$ (n=47 matched-pairs, data was collected across n=3 rats). Error bars represent SEM. Error bars demonstrate SEM.

Figure 6.7A depicts Type 1 and Type 2 events recorded from a P7 slice at DIV10 before and after the acute application of 10µM tianeptine. Figures 6.7B-D show the effects of the application of tianeptine on Type 1 events, while Figures 6.6E-G show the amplitude, decay tau and IEI (respectively) of Type 2 events before and after tianeptine was applied to slices. No significant differences were determined using a Wilcoxon matched pairs test (n=200 matched-pairs, data was collected across n=3 rats for type 1 events and n=50 matched pairs collected from n=2 rats for type 2 events), in either case as a larger number of experimental repeats is required.

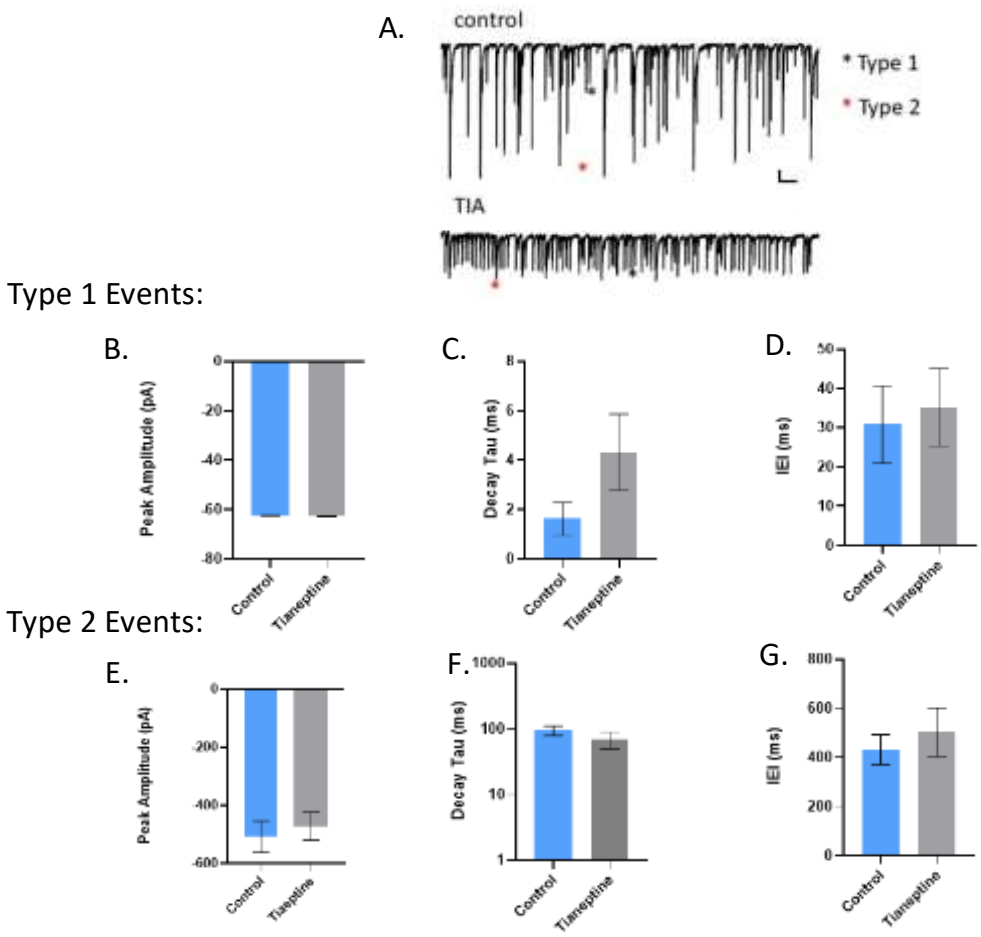

Figure 6.7 Effects of tianeptine on type 1 and type 2 IPSC activity.

Figure 6.7A shows a 1-minute epoch of a whole cell recording from a P7 DIV10 pyramidal cell before and after the application of 10µM tianeptine. Two types of events are denoted by * (Type 1) and * (Type 2). Scale bars indicate 50pA on the y axis and 10s on the x axis.

Figures 6.7B, 6.7C & 6.7D depict differences in amplitude **(B),** decay tau **(C)** and IEI **(D)** of Type 1 events before and after the application of 10µM tianeptine, while Figure 6.7E, 6.7F & 6.7G depict differences in amplitude **(E),** decay tau **(F)** and IEI **(F)** for Type 2 events. No statistical differences were determined using a Wilcoxon matched pairs test (n=200 matched-pairs, data was collected across n=3 rats for type 1 events and n=50 matched pairs collected from n=2 rats for type 2 events Error bars demonstrate SEM.

6.3 Discussion:

6.3.1 Network activity effects of tianeptine:

The main result that can be seen from Figures 6.1A-D is that tianeptine significantly increases apparent seizure frequency in both CA1 and CA3 in slices extracted from P3 & P7 rats. It is possible that this reflects the anticonvulsant effects of tianeptine turning full seizure activity into interictal discharges – in other words a longer run of 'less severe' activity compared to bursts of much more emphatic seizure-like events, however more data are needed to determine whether or not this is the case as significant changes in seizure duration also need to be determined. A significant increase in seizure frequency, alongside a significant decrease in seizure duration would confirm whether or not tianeptine transforms seizure activity to interictal discharges. The data currently being discussed does not contain enough experimental repeats of the spontaneously epileptic condition to perform accurate statistical analysis. This observed increase in seizure activity is contrary to what was expected based on the literature referenced in 6.1.2, however, it was reported that the effects of tianeptine were dose-dependent so this may have affected the outcome. Figure 6.2 indicates that while tianeptine has some significant effects on epileptic activity in the hippocampus of P3 cultured slices, greater seizure suppression is seen when slices receive a chronic low dosage of the drug. A significant decrease in both seizure duration (87.81s to 0s ± 16.59s. $p \leq 0.01$, n=3, DF = 8) and frequency (6.67 sph to 0 sph ± 1.33 sph, $p \leq 0.01$, n=3, DF = 8) can be seen when compared control slices to slices that had been cultured with 1µM tianeptine. While the data set presented here is small, these experiments provide promising preliminary data for chronic dosing of epileptic culture slices with tianeptine. The need for chronic treatment in epilepsy patients is not uncommon with many pathologies of the disease requiring life-long treatment. The ability to test how the chronic application of certain drugs can affect network and whole cell activity demonstrates how valuable the use of cultured epileptic slices can be in the approach to drug discovery.

6.3.2 Whole cell effects of tianeptine:

When looking at the data from patch clamp recordings shown in Figures 6.5 & 6.6, the identification of two different types of events is interesting. The events that can be seen are quite consistent Type 1 (small) and Type 2 (large) events, which were separated according to their amplitude for analysis (Type 1 = peak amplitude > -80pA, Type 2 = peak amplitude ≤ -80pA). The existence of these two separate events indicates the presence of two distinct neuronal populations, and it is likely that the smaller Type 1 events represent the normal neuronal activity while the larger Type 2 events could be

due to large synaptic events synchronised across the network, perhaps by gap junctions.

Due to limited data the effects of tianeptine could not be determined on DIV0 cells, however, analysis was performed before and after the acute application of 10µM tianeptine to DIV10 slices. These data are shown in Figure 6.7. The traces shown in Figure 6.7A indicate that the application of tianeptine reduces the amplitude of larger events within the cell, however, when statistical analysis was performed no significant difference in amplitude, IEI or decay was found for Type 1 or Type 2 events (Figure 6.7B-6.7D and 6.7E-6.7G, respectively).

6.3.3 Future improvement of whole-cell voltage clamp experiments:

Due to the fragility of cultured slices and the shrinking of neurons throughout the culture process it was difficult to obtain a high number of repeats for patch clamp experiments in the time frame that was given and no clear trend for the effects of tianeptine on whole cell IPSC activity could be determined. Future work should look to explore the effects of tianeptine further with larger data sets, improving the statistical power of the results.

Future work may also look to study the acute effects of tianeptine on EPSCs of cultured pyramidal cells as some studies have found the application of tianeptine to result in a two-fold increase in peak amplitude and an increase in decay time (Kole et al., 2002, Pillai et al., 2012).

Overall, the data shown in this chapter is inconclusive as it stands but provides some promising preliminary data for the use of tianeptine as a chronic treatment for epilepsy. Further work is required.

Chapter 7: Effects of Dexfenfluramine on spontaneous epileptic activity

7.1 Introduction:

Fenfluramine is an amphetamine derivative that promotes the release of neuronal serotonin whist also blocks it reuptake. Fenfluramine was first introduced in the 1970s as an appetite suppressant which had less side effects that other amphetamines, the anorectic effect if fenfluramine was thought to be mediated by its modulation of serotonergic systems (Rothman & Baumann, 2002). The drug was approved as a shirt-term treatment for obesity until safety concerns arose and it was subsequently taken off the market due to accumulating evidence of damage to heart valves (Mast et al., 2001, Sachdev et al., 2002). The use of fenfluramine was associated with the occurrence of pulmonary hypertension and valvular heart disease, with some individuals being given up to 222mg per day (Adenhaim et al., 1996; Connolly et al, 1997). It is now thought that damage caused to the heart was a dose dependent response and fenfluramine has since been approved by the US Food and Drugs Administration for the treatment of both Dravet syndrome and Lennox-Gastaut syndrome. The drug has been repurposed as an anti-seizure medication, prescribed at a fraction of the dosage that was correlated with heart problems, as it acts as a 5-HT2 receptor agonist and has been found effective in treating seizures associated with conditions like Dravet syndrome and Lennox-Gastaut syndrome. The potential anti- seizure effects of fenfluramine were first identified in photosensitive epilepsy in the 1980s but the drug has not been thoroughly explored as a treatment for epilepsy until recent years (Sullivan & Simmons, 2021).

Early antiseizure medications mainly helped to prevent seizures via the modulation of voltage-gated sodium channels or increasing GABAergic neurotransmission, however the antiseizure medications which are now coming to the forefront of epilepsy research aim to correct the inhibition-excitation balance by modulating other neurotransmitter systems such as the serotonergic system. Increased 5-HT levels have been known to inhibit seizure activity in rats since the original studies of Bonnycastle and colleagues in 1957 (Bonnycastle et al., 1957).

Fenfluramine is a drug of the phenethylamine family, which is structurally similar to 5-HT, it acts to reduce seizure activity by modulating the serotonergic system. Fenfluramine increases levels of extracellular 5-HT in the brain via its ability to modulate presynaptic 5-HT receptors, increasing synaptic release of 5-HT whilst inhibiting reuptake (Fuller et al., 1988).

5-HT is a neurotransmitter which plays an important role in the regulation of mood, sleep, and appetite and by increasing 5-HT fenfluramine can regulate electrical activity in the brain leading to the prevention of seizure activity. Therefore, despite being withdrawn from the market as a treatment for obesity fenfluramine has remained of interest in the study of treatment of epilepsy.

5-HT acts on several different subtypes of receptor found throughout the hippocampus and the neocortex, the majority of these are GPCRs which activate an intracellular second messenger cascade (Hannon & Hoyer, 2008). The 5-HT2C receptor is of particular interest in the study of epilepsy as it is found on GABA interneurons in the brain and plays a role in control of inhibitory tone. 5-HT2C receptors exert their function via the activation of phospholipase C, when 5-HT2C is activated by serotonin phospholipase C starts to metabolise phosphatidylinositol 4,5-biphosphate (PIP_2) into inositol 1,4,5-triphosphate (IP_3) and diacylglycerol (Shen & Andrade, 1998). IP_3 can then bind to IP_3 receptors, triggering the release of Ca^{2+} thereby increasing membrane excitability. Hence, activation of the 5-HT2C receptors causes GABA to be released which can prevent seizures via the suppression of neuronal activity (Giorgetti & Tecott, 2004).

Studies conducted in animal models of epilepsy have found that low doses of fenfluramine can reduce both the frequency and the duration of seizures, however these results vary from study to study. One 2000 study found that fenfluramine was able to block low-Mg^{2+} induced epileptic activity in the rat entorhinal cortex (Gentsch et al., 2000). In a maximal electroshock model of seizure activity fenfluramine was successful in preventing seizures in rats but not in mice, and in the same study researchers could not identify any reliable antiseizure effect of fenfluramine in standard acute seizure tests or in a kindling model of epilepsy (Silenieks et al., 2019). Similarly, fenfluramine was reported not to protect against chemical or electrical stimulation-induced clonic seizures in rats, mice or zebrafish. However, in the same study fenfluramine was reported to reduce seizure incidence, severity, and seizure-induced respiratory arrest in a DBA/1 mouse model of Sudden Unexpected Death in Epilepsy (SUDEP) (Faingold & Tupal, 2019).

In zebrafish models of epilepsy fenfluramine suppressed epileptiform discharges by acting as a 5-HT agonist, and blocked seizure-like activity with epileptiform discharges in a model of Dravet Syndrome (Dinday & Baraban, 2015, Zhang et al., 2015).

In addition to its serotonergic function, fenfluramine also interacts with sigma-1 receptors, initially classed as a type of opioid receptor (but increasingly suggested to have much wider-ranging effects) that modulate ion channels and neurotransmitters via the mobilisation of intracellular Ca^{2+}. The interaction of fenfluramine with the sigma-1 receptor can reduce seizure activity by decreasing excitability of glutamatergic neurons (Rodriquez-Munoz et al., 2018, Vavers et al., 2019).

Various studies in human patients have shown efficacy of repurposed fenfluramine for the treatment of seizures associated with Lennox-Gastaut Syndrome (LGS) and Dravet Syndrome (DS).

7.1.1 Dravet Syndrome (DS):

Dravet Syndrome (DS) is a rare and severe form of epilepsy which usually is onset from the first year of life. Up to 30% of patients with DS will enter status epilepticus (SE) which can degenerate to become acute encephalopathy. A retrospective study involving 12 patients who presented with the typical Dravet Syndrome phenotype who had been receiving a daily low-dose of fenfluramine as an add-on treatment for DS over 1-19 years found that 7 of the 10 patients who were still taking fenfluramine at their follow up appointment (≈11.5 years after initial dose) had been seizure free for at least one year prior to that visit (Ceulemans et al., 2012).

In a randomised control trial of DS patients with intractable seizures 119 patients were treated with high-dose fenfluramine, low-dose fenfluramine or a placebo for 14 weeks. The trial found that patients receiving the high dose (0.7 mg/kg/day) showed a 62.3% reduction in seizures while the low dose (0.2 mg/kg/day) showed a 32.4% reduction in monthly seizures when compared with the monthly seizure frequency of placebo patients. 8% of patients receiving either high- or low-dose fenfluramine became completely seizure free when compared to 0% of patients in the control group (Lagae et al., 2019).

A 2020 randomised clinical trial reported very similar results, 142 patients with DS showed a statistically significant reduction in seizures when being treated with either high or low dose fenfluramine. Patients receiving either high or low dose fenfluramine treatment exhibited a considerably greater reduction in monthly seizures compared with placebo group. Patients in both fenfluramine treatment groups also had significantly longer seizure-free periods than the placebo group. Additionally, this trial found that the high dose (0.7 mg/kg/day) treatment was more efficient at treating and preventing seizures than the low dose (0.2 mg/kg/day) treatment which indicates a dose-dependent relationship (Sullivan et al., 2020).

7.1.2 Lennox-Gastaut Syndrome (LGS):

LGS is another severe form of epilepsy which develops in childhood and is characterised by multiple types of seizure which are often resistant to traditional forms of anti-seizure medication. In 1987 Gastaut and Zifkin treated 33 children with intractable epilepsy with fenfluramine, 46% of these patients saw a 50% reduction in seizures (Gastaut & Zifkin, 1987). A later study published in 1996 used fenfluramine as an add-on treatment for 11 children with intractable epilepsy, of the patients 7 were reported to achieve complete seizure freedom while the remaining 4 saw >75% reduction in seizure

activity. Patients were treated with fenfluramine over an average of 5 years with no major adverse effects reported (Boel & Casaer, 1996). A larger cohort study published by the same group stated that of 22 patients using fenfluramine 10 patients showed a >90% seizure reduction and 6 patients become completely seizure free (Boel & Casaer, 2002). Several more recent studies have been conducted to determine the efficiency of fenfluramine as a treatment for patients with LGS, fenfluramine has been found to significantly reduced the frequency of drop seizures in LGS patients in one study while another study found fenfluramine to reduce the frequency of multiple seizure phenotypes including atonic, tonic, and tonic-clonic seizures (Ferrie & Patel, 2009; Verotti et al., 2018; Brigo et al., 2021).

Following these studies, in 2020 the FDA and the EU approved fenfluramine for use in seizures associated with DS in patients over 2, and in March 2022 the FDA also approved it for treating LGS associated seizures (Specchio et al., 2020; Simon et al., 2022). Dexfenfluramine is the d-isomer of fenfluramine, it exhibits the same effects on serotonin levels in the brain but with the stimulating psychological effects associated with amphetamines, making it a promising, lower risk alternative for the treatment of epilepsy.

7.1.3 Mechanisms of anticonvulsant actions of fenfluramine

Dexfenfluramine is the active stereoisomer of the drug fenfluramine and is a selective serotonin reuptake inhibitor (SSRI) which works by stimulating 5-HT (serotonin) release whilst inhibiting the presynaptic reuptake of 5-HT (Grosso et al., 2001). Dexfenfluramine not only had the ability to modulate the serotonergic system, but it may also inhibit potassium channels via mechanisms involving 5-HT which could be an advantage in the treatment of epilepsy (Archer et al., 1996). It is also thought to induce positive allosteric modulation of sigma-1 receptors, to reduce excitability in glutamatergic circuits (Cattaneo et al., 2021, Martin et al., 2022).

The multiple mechanisms of dexfenfluramine may underlie its ability to prevent seizures in the most difficult to treat epilepsies. In 2001, a study of the effects of dexfenfluramine on a patient whose seizures were resistant to treatments including phenobarbital, valproic acid, benzodiazepines, and many more known AEDs reported that low doses of dexfenfluramine alleviated all seizure activity, however, when dexfenfluramine was withdrawn the seizures returned (Grosso et al., 2001).

A later study in a zebrafish model of DS reported that seizure-like activity was reduced by 80-84% following dexfenfluramine administration (Li et al., 2018).

Despite there currently being over 30 different antiseizure medications on the market the proportion of these patient who are refractory to antiseizure medication has not changed. Refractory seizures are reported in almost every patient who develops an epileptic encephalopathy, these patients are unlikely candidates for resective surgery and so there is a need for newer, safer, and more efficient antiseizure medications.

Currently there has been a significant amount of research carried out to study the effects of fenfluramine in epilepsy which has found the fenfluramine reduces both the severity and frequency of seizures in various animal models of epilepsy (Schoonjas et al., 2016; Rodriguez-Munoz et al., 2018; Dvir et al., 2019; Tupal & Faingold, 2019; Sullivan et al., 2020), however there is not much research available on the effects of dexfenfluramine.

In this chapter we will look into the effects of both acute and chronic dosing of dexfenfluramine on spontaneous and induced seizure activity in an organotypic model of epilepsy.

7.2 Methods:

7.2.1 Rodent Slice Preparation:

350µM coronal slices were prepared from postnatal day 3-7(10-25g) Wistar rat pups. Prior to the brain extraction, rats were anaesthetised by inhalation of 5% isoflurane in a mixture of O_2/NO_2 until no pedal or corneal reflex was detected – depth of anaesthesia was determined in accordance with the ASPA 1986 by testing for the absence of normal reflexes via a pinch test. Following anaesthetisation rats were euthanised by decapitation using surgical scissors and the brain immediately extracted from the skull. Once extracted the brains were placed in a sucrose-based artificial cerebrospinal fluid (aCSF) solution. Complete aCSF had been saturated with 95% O_2/5% CO_2 (carbogen) prior to the extraction to maintain a pH of 7.3, and osmolarity of 300 – 310 mOsm/L. Brains were then transported back to the lab in the aCSF solution, once back in the lab slices were glued onto a stage and submerged in ice-cold aCSF to be sliced into 350µM slices using a 7000smz-2 model Vibrotome (Campden Instruments Ltd., UK). Slices were then transferred to an interface chamber to acclimatise at room temperature for 1 hour in a glucose-based aCSF solution. Continual bubbling of carbogen through aCSF throughout helped to maintain pH 7.3 and osmolarity 300 – 310 mOsm/L.

Following the dissection, once slices were cut, they were bathed in an oxygenated glucose-based aCSF solution for 1 hour before being transferred to a biosafety cabinet, washed in culture media for 10 minutes and placed onto hydrophilic PTFE, 0.4µM pore cell culture inserts (Merck, UK). Residual aCSF was then aspirated off and inserts were placed into 6-well plates containing 1.5ml culture media. Slices were then incubated in a humidified incubator (Thermo Scientific, UK) at 37°C, 5% CO_2, with a media change twice weekly.

7.2.2 Electrophysiological Recordings:

Activity in slices was recorded using both LFP and patch-clamp electrophysiology.

LFP slices were manoeuvred onto lens tissue and the placed directly into LFP interface chamber. Microelectrodes were filled with glucose-based aCSF and inserted into layers CA1 or CA3 of the hippocampus. Voltage signals were amplified 100x (setting a low-pass filter of 0.1 Hz and a high-pass filter of 1k Hz). Electrical noise (50Hz) was filtered out using Humbugs (Quest Scientific, Canada). The filtered signal was amplified a further 10x (low-pass filter 0.3 Hz, high-pass filter of 700 Hz) and digitised at sampling rate of 5 kHz and recorded using Spike2 software (Cambridge Electronic Design, UK). Seizure activity was determined by eye in line with the definition stated in chapter 2.4.2. Median

values were determined using Microsoft Excel and then transferred to GraphPad Prism8 for graph plotting and statistical analysis. 120 second epochs of recorded activity was extracted from continuous raw traces at specific timepoints (pre- and post-compound application) and analysed for epileptiform activity from initial placement of the electrodes for up to one hour, tianeptine was then bath applied to slices for a period of 40 minutes to determine its effects on seizure activity for acute dosing experiments with 500nM dexfenfluramine. For chronic dosing experiments 50nM dexfenfluramine was added to NBA media from DIV0 and reapplied with every media change. After 14 days in culture epileptic activity in slices was measured using LFP recordings, these data were compared with control slices which had been cultured for 14 days in the absence of the drugs tianeptine treatment.

Gap free whole-cell patch-clamp recordings were made using standard techniques (Woodhall et al., 2009). 350uM slices were placed onto the patch rig where they were submerged in glucose-based aCSF and weighed down using platinum rods. Electrodes were filled with internal solution and events were recorded at an inward current of -70mV, signal were filtered at 5kHz, digitized at 10kHz and recorded using pClamp software (Molecular Devices, US). Baseline activity in slices was recorded for 15-20 minutes before bath applying 500nM dexfenfluramine for a period of at least 20 minutes.

7.2.3 Drugs & Reagents:

Dexfenfluramine (Tocris Biosciences, UK) was diluted to a stock solution of 10mM in DMSO and stored in 100uL aliquots at -20^{o}C. Prior to being added to brain slices, aliquots were defrosted and diluted down to their final concentration. Slices were left to stabilise for at least 40 minutes or until slices had seized multiple times. Once slices had stabilised, dexfenfluramine was then bath applied to slices by adding it directly into the perfusing aCSF following drug application activity was recorded for 30 – 40 mins for LFP recordings. For patch-clamp recordings drug application was recorded for 15-20 mins following application of the drug.

7.3 Results:

7.3.1 Effects of acute dosing with dexfenfluramine on spontaneously epileptic cultures:

Extracellular field recordings were recorded from the CA1 and CA3 areas of the hippocampus simultaneously in organotypic brain slice cultures taken from either P7 at various days in vitro (DIV), or P3 rats at DIV7. If spontaneous seizure-like activity was detected within the first 40 minutes of recording, 500nM of dexfenfluramine was then bath applied to slices to investigate the effects of acute application of the drug on epileptic activity. Pre-clinical studies in humans have determined that treatment of patients with DS ad LGS using 0.2-0.7mg/kg/day fenfluramine provides promising antiepileptic effects with a favourable overall safety profile (Balagura et al., 2020, Sullivan et al., 2020). Pharmacokinetic analysis (Gammaitoni et al., (2018) of single doses of fenfluramine hydrochloride at 0.8 mg/kg revealed an average maximum plasma concentration (Cmax) of 59 ng/l, which translates to a concentration of 200 nM. It is for this reason it was decided 500nM dexfenfluramine would be an appropriately robust and reliable concentration for acute dosing of slices.

In order to assess for the optimum experimental paradigm with which to demonstrate the effects of dexfenfluramine, groups were initially split results based on DIV. Unfortunately, there was no obvious timepoint at which dexfenfluramine showed greatest efficacy. Hence, as can be seen from Figure 7.1, acute bath application of dexfenfluramine onto spontaneous epileptic slice cultures did not have a significant effect on epileptic activity at any DIV (determined by mixed-effect analysis with Sidak's multiple comparisons post hoc test). While no statistical significance was determined, likely due to a small number of repeats (n=2 at DIV7 & DIV14, n=3 at DIV3 & DIV10) a decrease in both activity and duration can be seen at DIV14 for this reason, the data from all DIV were pooled and further statistical analysis undertaken. Figure 7.3 shows the pooled data from all DIV in P7 slices under conditions where n=10 observations per group.

Slice viability was confirmed by a reaction to the bath application of gabazine, or if slices remained epileptic/ictal when the experiment was ended.

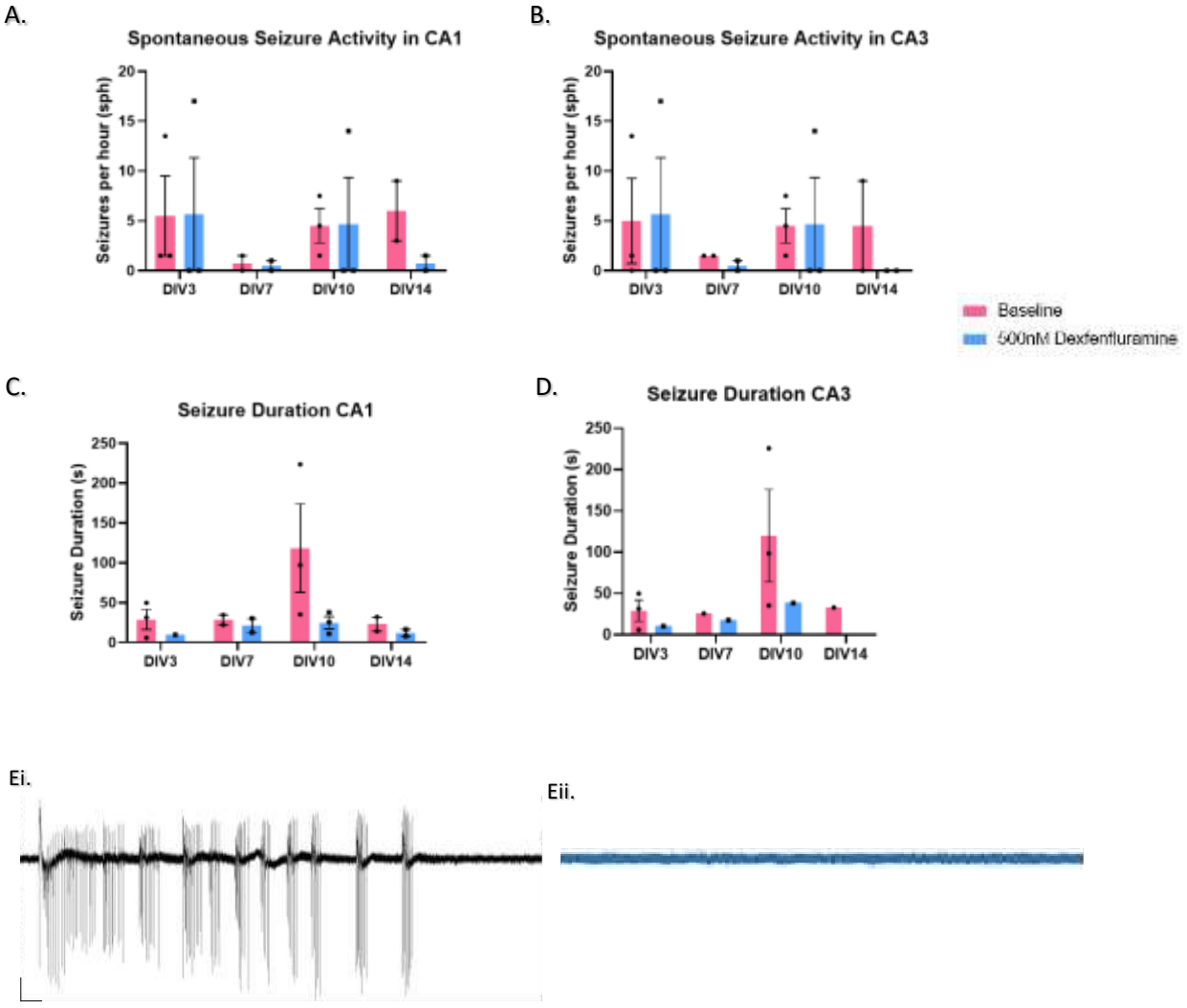

Figure 7.1: Effects of dexfenfluramine on spontaneously epileptic network activity in cultured P7 slices at various days *in vitro*.

Bar graphs demonstrating mean median spontaneous seizure activity and seizure duration in CA1 (A and C, respectively) and CA3 (B and D, respectively). Pink bars indicate baseline activity, while blue bars demonstrate activity following the bath application of 500nM dexfenfluramine. Recordings were taken from slices at DIV3 (n=3), DIV7 (n=2), DIV10 (n=3) and DIV14 (n=2). Statistical significance was determined using a mixed-effect analysis with Sidak's multiple comparisons post hoc test, no statistical significance was determined between control and treated slices, Error bars represent SEM.

Panels Ei and Eii show example LFPs before and after the acute application of 500nM dexfenfluramine (scale bar demonstrates 50µV on the y axis and 2s on the x axis). Recording was taken from the CA3 hippocampal area of a DIV14 cultured slice.

Figure 7.2 demonstrates the effects of acute dexfenfluramine application to P3 slices, no statistical significance was determined between groups due to a lack of repeats for these experiments (n=2 for each group, 2-way ANOVA determined p=ns). However, the trend that appears to be emerging is that the application of 500nM dexfenfluramine to slices reduces seizure frequency and duration (Figure 7.2A & 7.2B, respectively) in both CA1 and CA3.

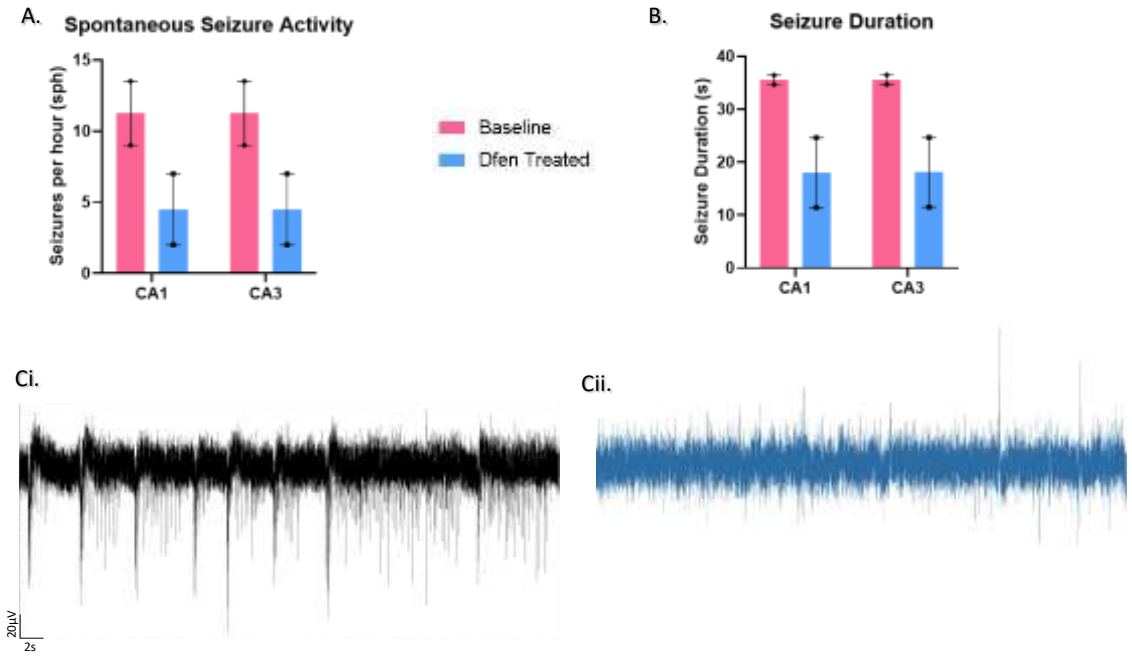

Figure 7.2: Effects of dexfenfluramine on spontaneously epileptic network activity in cultured P3 slices at DIV7.

Bar graphs demonstrating spontaneous seizure activity (A) and seizure duration (B) in CA1 and CA3. Pink bars indicate baseline activity, while blue bars demonstrate activity following the bath application of 500nM dexfenfluramine.Statistical significance was determined using a 2-way ANOVA using Sidak's multiple comparisons post hoc test, p = ns, n=2 for all groups. Error bars represent SEM.

Panels Ci and Cii show example LFPs before and after the acute application of 500nM dexfenfluramine (scale bar demonstrates 20µV on the y axis and 2s on the x axis). Recording were taken from the CA1 hippocampal area of a DIV7 cultured slice.

Figure 7.3 depicts the data that was pooled from all DIV showing the overall effects of dexfenfluramine in epileptic activity in slices. Figure 7.3Ai& 7.3B demonstrate a significant decrease, determined using a Wilcoxon matched pairs test, in seizure frequency following the application of dexfenfluramine to spontaneously epileptic culture slices in both CA1 (3.56 ± 1.13 sph to 0.31 ± 0.21 sph) and CA3 (2.44 ± 1.06 soh to 0 ± 0.13 sph) , respectively ($p \leq 0.05$, $n = 10$). Figure 7.3C & 7.3D demonstrate the application of dexfenfluramine also results in a significant decrease in the duration of seizures (56.87 ± 22.6s to 7.561± 4.13s in CA1, $p \leq 0.01$ and 42.14 ± 18.64s to 5.524 ± 3.395s in CA3, $p \leq 0.05$, $n= 10$, statistical analysis preformed was a Wilcoxon matched-pairs test).

For slices which did exhibit spontaneous epileptic activity, GBZ was added to induce epileptic activity in slices. In Figure 7.3E and 7.3F a Friedman test was carried out to assess statistical significance of the data, it was determined that there was a significant increase in seizure activity in slices following the application of GBZ ($p \leq 0.01$ for CA1 and $p \leq 0.001$ for CA3, $n = 15$). When dexfenfluramine was then bath applied to slices following the application of GBZ no significant decreases in epileptic activity can be seen for either CA1 or CA3 (Figure 7.3E& 7.3F, respectively). Figure 7.3E & &.3F also demonstrate that was effects of GBZ addition resulted in a more significant increase in seizure activity in CA3 than in CA1.

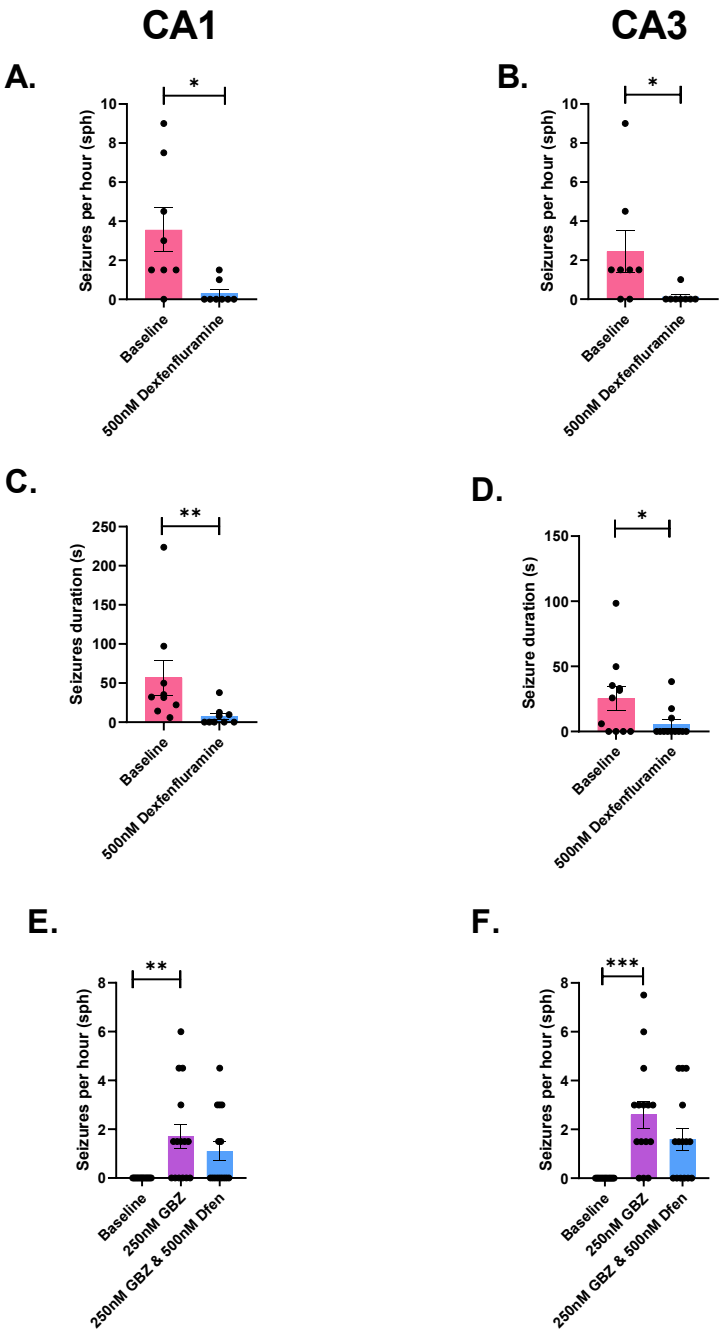

Figure 7.3 Pooled DIV0-14 data showing effects of dexfenfluramine in CA1 and CA3 of P7 cultured slices:

Bar graphs of pooled data across all days *in vitro* depicting seizures per hour in slices with spontaneous activity CA1 and CA3 (7.3A & 7.3B, respectively), spontaneous seizure duration in CA1 and CA3 (7.3c & 7.3D, respectively), and seizures per hour in slices with induced seizure activity in CA1 and CA3 (7.3E & 7.3F, respectively). *** denotes $p \leq 0.01$, ** denotes $p \leq 0.05$ and * denotes $p \leq 0.01$. For figure 7.3A-D a Wilcoxon matched pairs tested was used to analyses statistics (n=10), while for figure 7.3E-F a Friedman test was used to determine statistical significance (n=15).

7.3.2 Effects of acute dexfenfluramine administration on inhibitory synaptic activity in the hippocampus:

Whole-cell voltage-clamp recordings were conducted to investigate the effects of 500nM dexfenfluramine on sIPSCs of hippocampal pyramidal cells from cultured P7 donor slices at various timepoints throughout the culture process. Recordings were taken from CA1 or CA3, however, due to the loss of cells via slicing and the culture process it was difficult to maintain consistent repeats from each specific area over time in culture so for the purposes of these experiments data from both areas has been pooled together. The standard patch-clamp technique (as outlined in chapter 2.3.1) was used to obtain recordings from hippocampal neurons at timepoints which correlate to those used for P7 culture LFP experiments shown in Figure 7.1.

The parameters which were assessed here are median peak amplitude (pA), interevent interval (IEI, ms), decay time constant (tau, ms) and the events detected per minute. Looking at Figure 7.4 it can be seen that dexfenfluramine application to slices had no significant effects on sIPSC amplitude (7.4A), IEI (7.4B), or decay tau (7.4C) at any time point. The only significant result is seen as in increase in events per minute in DIV7 culture shown in Figure 7.4D, when compared with the control slices ($p \leq 0.05$, $n = 4$), significance here was determined using a Mann-Whitney test.

The overall data from Figure 7.4A-D when looked at as whole, the data are quite variable and further experiments would be required to determine the effects of dexfenfluramine on the kinetics if sIPSCs.

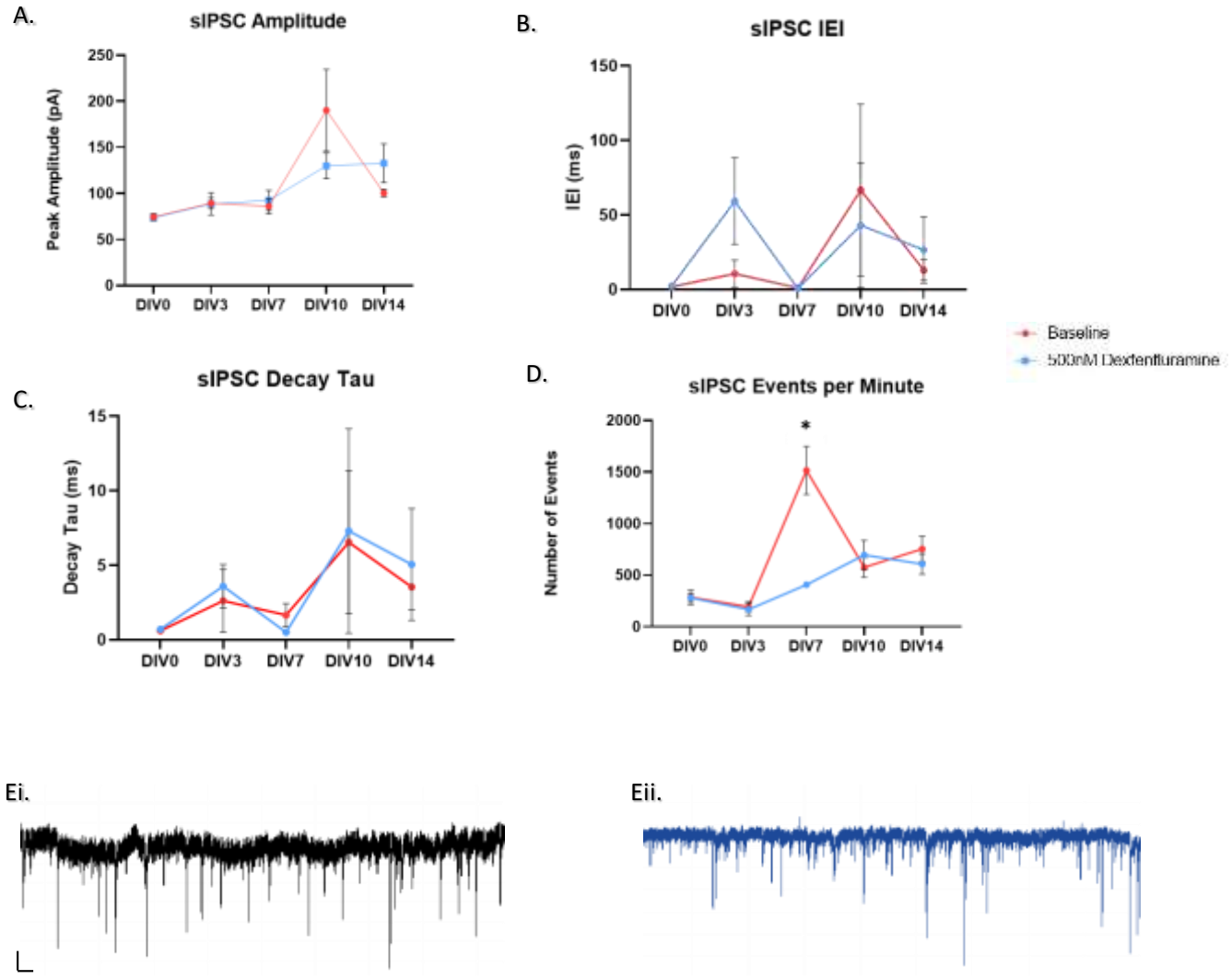

Figure 7.4: Effects of dexfenfluramine on inhibitory synaptic activity in cultured P7 slices.

Connected scatter plots depict the mean median peak sIPSC amplitude (A), IEI (B), decay tau (C) and events per minute (D) for baseline activity (shown in blue) and activity following the application of 500nM dexfenfluramine (shown in red) for cultured slices at various culture timepoints (DIV0, DIV3, DIV7, DIV10 & DIV14) at various days in vitro. Blue lines indicate baseline values, red lines indicate values post dexfenfluramine application. * = p value < 0.05, significance was determined using a Mann-Whitney test,n=4 for all groups. Error bars show SEM.

Figure 7.4Ei & Eii show example traces of sIPSC activity before (Ei) and after the application of 500nM dexfenfluramine (Eii, shown in blue). Scale bars represent 20pA on the y axis and 1s on the x axis.

Cumulative frequency curves for the peak amplitudes of sIPSCs were also produced for baseline and post dexfenfluramine conditions at each timepoint and are shown in figure 7.5A-E. A Kolmogorov-Smirnov test determined p = ns for all timepoints indicating that the application of dexfenfluramine did not have an effect on the frequency distribution of sIPSCs in cultured slices.

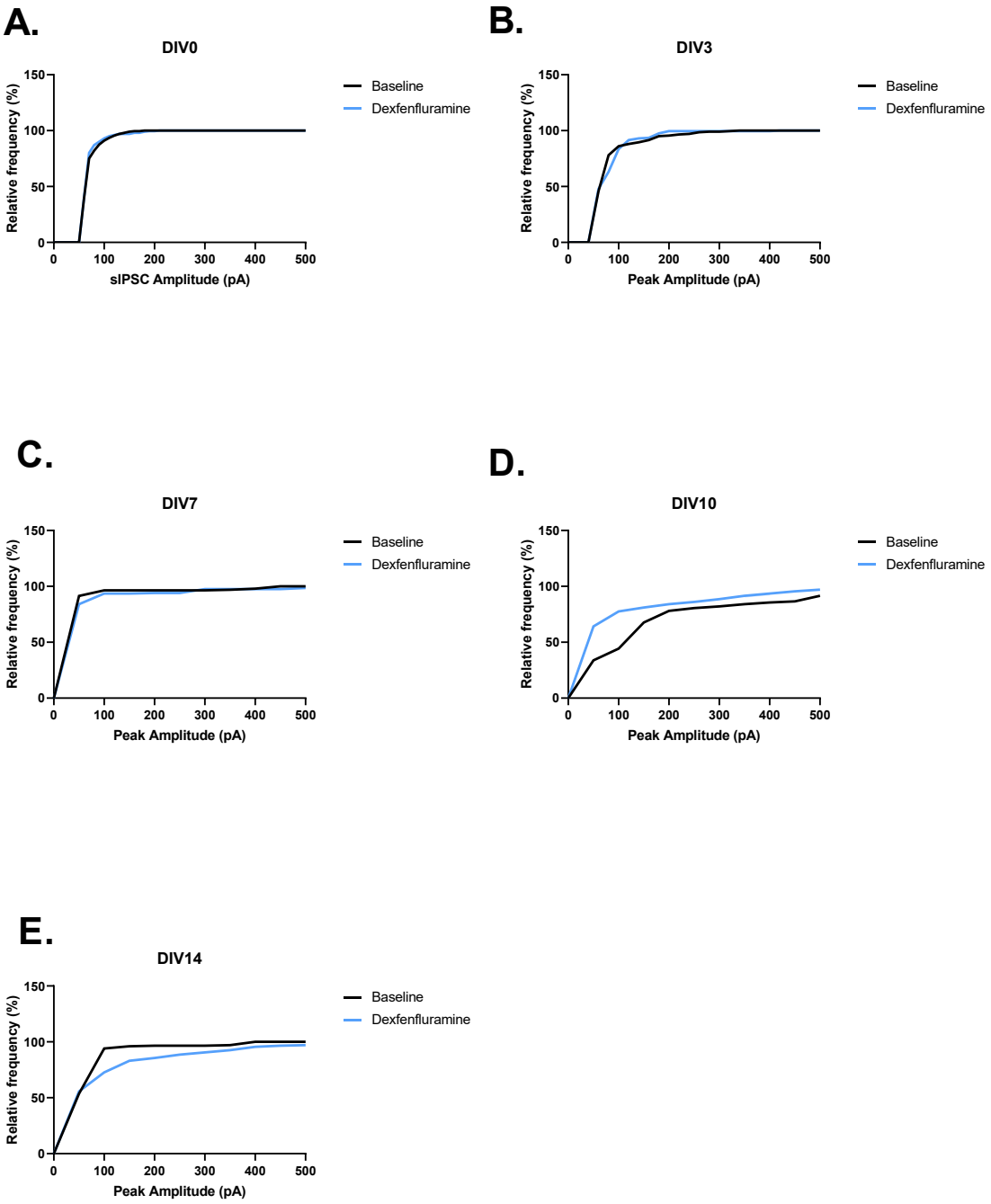

Figure 7.5: Cumulative frequency curves of sIPSC activity in cultured P7 slices across each DIV tested.

Cumulative frequency curves of sIPSC amplitude at DIV0 (A), DIV3 (B), DIV7 (C), DIV10 (D) and DIV14 (E) before (shown in black) and after (shown in blue) the bath application of 500nM dexfenfluramine.KS test determined p = ns in any DIV.

7.3.3 Effects of acute dexfenfluramine administration on excitatory synaptic activity in the hippocampus:

Further whole-cell voltage-clamp recordings were conducted to investigate the effects of 500nM dexfenfluramine on sEPSCs of hippocampal pyramidal cells from cultured P7 donor slices at various timepoints throughout the culture process. The same method as before was used and as mentioned above (Chapter 7.3.2) obtaining repeat recordings from specific hippocampal areas was difficult so data from both areas has been pooled together.

The parameters remained the same as with sIPSC experiments. Looking at Figure 7.6 it can be seen that dexfenfluramine application to slices had no significant effects on sEPSC amplitude (7.6A), IEI (7.6B), or decay tau (7.6C) at any time point. No significant differences in sEPSC kinetics were recorded for any parameter in Figure 7.6A-D, a 2-way ANOVA followed by Sidaks multiple comparisons test concluded p = ns across conditions (n=2 for each condition).

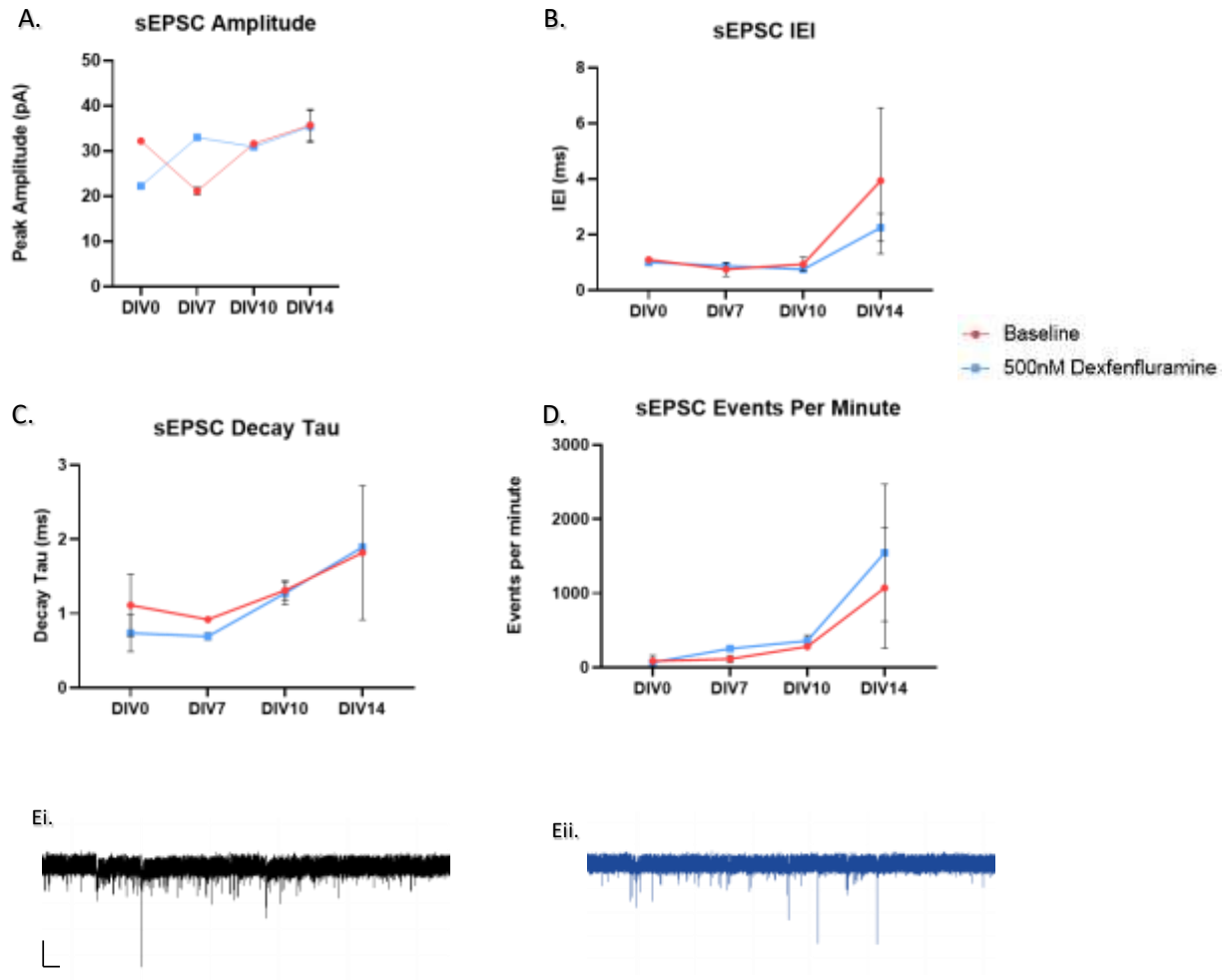

Figure 7.6: Effects of dexfenfluramine on excitatory synaptic activity in cultured P7 slices.

Connected scatter plots depict the mean median peak sEPSC amplitude (A), IEI (B), decay tau (C) and events per minute (D) for baseline activity (shown in blue) and activity following the application of 500nM dexfenfluramine (shown in red) for cultured slices (DIV0, DIV3, DIV7, DIV10 & DIV14) at various days in vitro. Blue lines indicate baseline values, red lines indicate values post dexfenfluramine application. A 2-way ANOVA followed by Sidaks multiple comparisons test concluded p = ns across conditions, n=2 for each group. Error bars show SEM.

Figure 7.6Ei & Eii show example traces of sIPSC activity before (Ei) and after the application of 500nM dexfenfluramine (Eii, shown in blue). Scale bars represent 20pA on the y axis and 1s on the x axis.

Similar to sIPSCs, cumulative frequency curves were also produced to demonstrate the cumulative peak amplitudes of sEPSCs recorded from slices at various DIV for baseline recordings and recordings following dexfenfluramine application (Figure 7.7A-D). Kolmogorov-Smirnov tests determined no significant differences in frequency distribution following the application of dexfenfluramine at any timepoint, indicating that dexfenfluramine had no significant effects on sEPSC frequency in cultured slices.

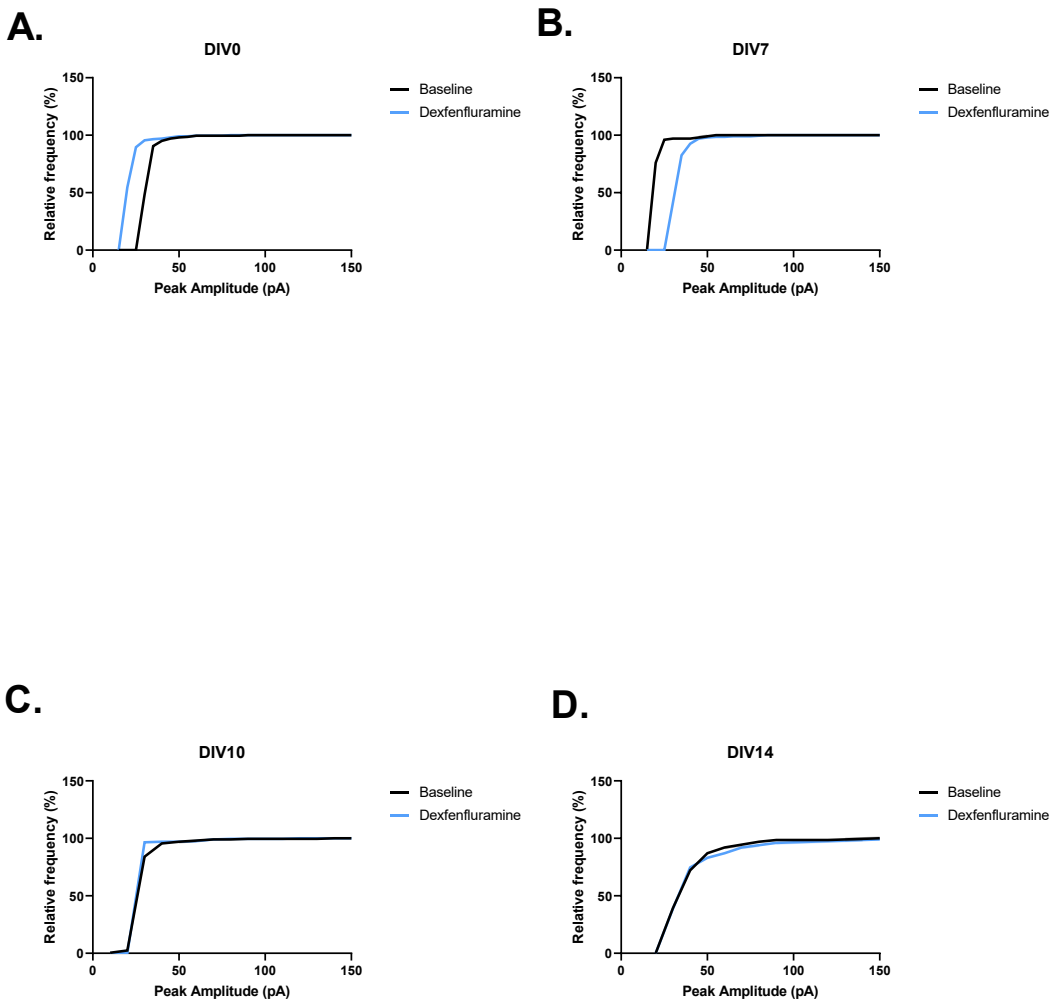

Figure 7.7: Cumulative frequency curves of sEPSC activity in cultured P7 slices across each DIV tested.

Cumulative frequency curves of sEPSC amplitude at DIV0 (A), DIV7 (B), DIV10 (C) and DIV14 (D) before (shown in black) and after (shown in blue) the bath application of 500nM dexfenfluramine. KS test determined p = ns in any DIV.

7.3.4 Effects of chronic low dose dexfenfluramine on P3 and P7 cultures:

To investigate the effects of chronic treatment with dexfenfluramine a dosage of 50nM was added into the culture media on DIV0 and used to feed cultures up until DIV7 for P3 cultures and DIV14 for P7 cultures. 10% of the acute dose was used as slices would be exposed to the drug for a significant period of time. Treated media was replaced for treated slices bi-weekly at the same time as control slices were having their media replenished. Figure 7.8A shows the results of 14 days dosing P7 organotypic slice cultures with 50nM dexfenfluramine, a 2-way ANOVA with Sidak's multiple comparisons post hoc test determined that dexfenfluramine significantly reduced seizure activity in CA3 ($p \leq 0.05$, n=3, DF=8) but not in CA1 (p=ns, n=3, DF=8). Figure 7.8B shows the effects of the same chronic dose applied to P3 slices for 7 day *in vitro,* a significant decrease in seizure activity can be seen in both CA1 and CA3 of P3 cultured slices ($p \leq 0.05$, n=2, DF=4, determined ny 2-way ANOVA and Sidak's multiple comparisons post hoc test). This is promising preliminary data as no seizure activity was recorded in either group following chronic dosing. Slice viability was confirmed via the application of gabazine to slices after a minimum of 40 minutes recording, if slices had no response to 250-500nM GBZ they were considered to have died in culture and were excluded from these data sets (data no shown).

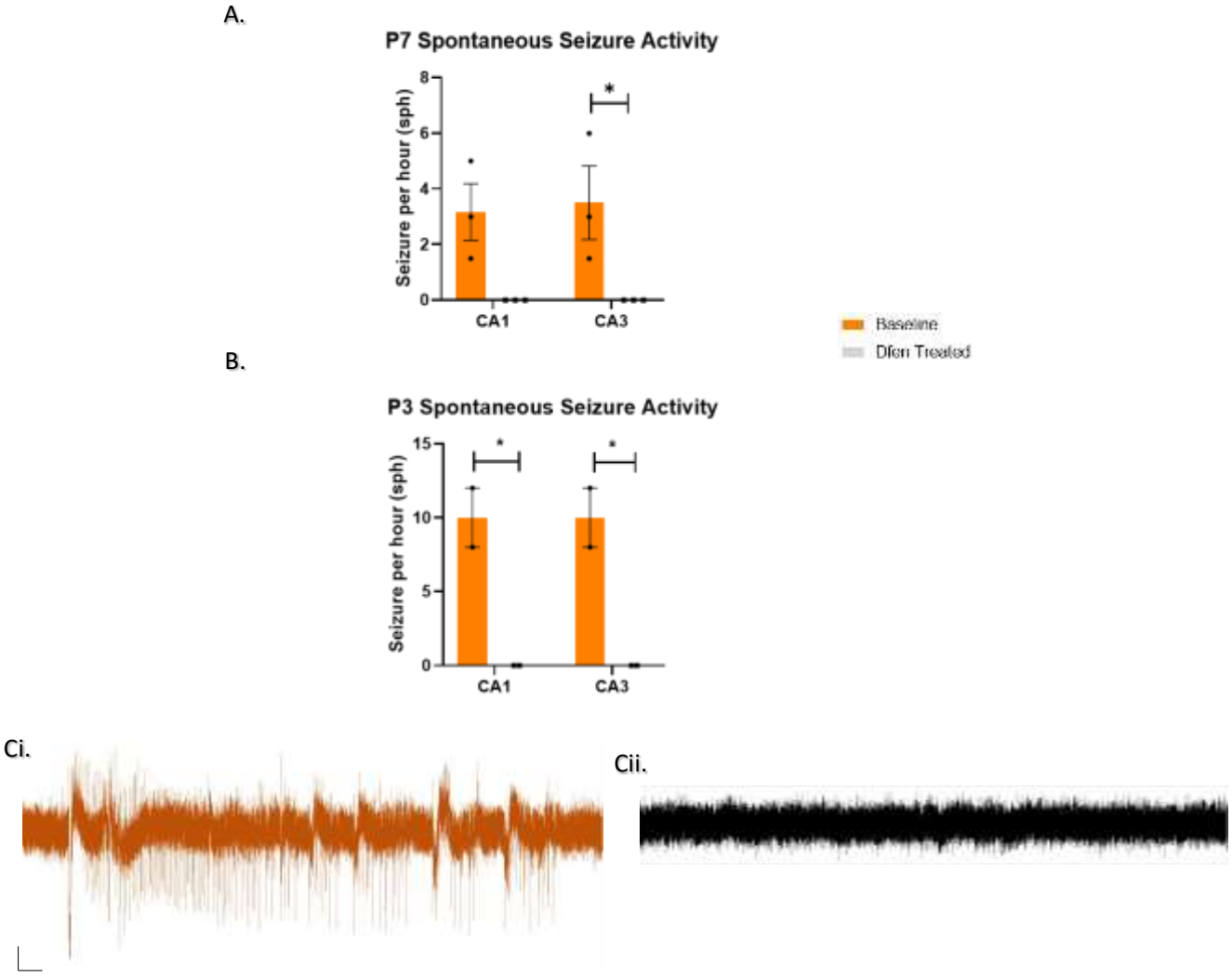

Figure 7.8: Effects of low, chronic dose of dexfenfluramine on cultured slices.

Bar graphs showing the effects of chronic dosing with 50nM dexfenfluramine after 14 days for P7 slices **(A)** and 7 days for P3 slices **(B)**. Individual values are depicted by black dots (control) or black squares (treated). Statisical analysis was performed for each condition using a 2-way ANOVA with Sidak's multiple comparisons post hoc test, where * denotes $p \leq 0.05$ (n=3 for P7 group, n=2 for P3 group). Error bars represent SEM.

Figure 7.8Ci & Cii show representative traces of seizure activity in CA1 of P3 DIV7 slices. Figure 7.8Ci demonstrates the seizure activity recorded from a control slice (DIV7, no dexfenfluramine), while figure 7.8Cii depicts the lack of seizure activity in a treated slice (DIV7, treated with 50nM dexfenfluramine). Scale bars represent 20pA on the y axis and 1s on the x axis.

7.4 Discussion:

7.4.1 Acute dosing of culture slices with dexfenfluramine reduces seizure frequency and duration in cultured organotypic slices:

Looking at the effects of dexfenfluramine on both spontaneously epileptic slices obtained from P7 and P3 donors, shown in Figures 7.1 and 7.2 indicate an overall trend of dexfenfluramine causing reduction in both seizure duration and frequency, however, no statistical significance was determined in either age group.

Activation of 5-HT2C receptors stimulates GABA release and can therefore result in the suppression of neuronal activity, preventing seizures (Giorgetti & Tecott, 2004). The antiepileptic effects of dexfenfluramine on these cultures could be a result of serotonergic modulation of GABAergic transmission which has been reported in earlier studies (Grosso et al., 2001). The increased release of GABA via activation of 5-HT2C receptors could be responsible for the inhibition of epileptic activity seen in this chapter as it may counteract a deficiency in GABA-mediated inhibition, leading more balanced interactions between inhibitory and excitatory signals within the brain,

Another possible mechanism by which dexfenfluramine could suppress seizure activity is via the inhibition of potassium channels, reported in 1996 by Archer et al. (Archer et al., 1996). A 2016 study found that when extracellular potassium levels reached concentrations of over 9mM seizure like events were blocked and neurons entered a depolarisation-blocked state (Wang et al., 2016).

More recent studies have suggested that dexfenfluramine may induce positive allosteric modulation of sigma-1 receptors, which causes a reduction in glutamatergic excitability in neurons (Cattaneo et al., 2021; Martin et al., 2022). This reduction in neuronal excitability would aid in slices in restoring the inhibition-excitation balance thereby causing the suppression of epileptic activity. Studies using fenfluramine reported that the interaction of fenfluramine with sigma-1 receptor reduced seizure activity via this exact mechanism and since dexfenfluramine is a stereoisomer of fenfluramine it is entirely possible that this is the mechanism of action causing the reduction in seizure duration and frequency seen in Figure 7.3.

The results reported in these studies are in keeping with studies carried out in human patients and animal models of seizure activity (Grosso et al., 2001; Li et al., 2018), reiterating the potential of

dexfenfluramine as a promising antiepileptic treatment. However, as previously mentioned there are not many studies which use dexfenfluramine and so further research is required. For these experiments specifically further study is needed to increase the number of repeat experiments, thereby increasing the reliability and significance of the data.

7.4.2 Dexfenfluramine induces seizure activity in non-epileptic slices:

It is worth noting that in experiments carried out on non-epileptic culture slices dexfenfluramine appeared to induce seizure activity indicating that the use of dexfenfluramine by non-epileptic patients could result in the development of seizure activity. *Data not shown*.

Further study into the effects of dexfenfluramine on healthy hippocampal neurons would need to be carried out to determine whether or not this effect was due to slices being in culture and being more susceptible to seizure or whether it was a direct effect of dexfenfluramine.

7.4.3 Dexfenfluramine effects on inhibitory and excitatory synaptic activity:

Whole-cell voltage-clamp experiments shown in Figures 7.4-7.7 demonstrate that the only significant difference caused by the application of dexfenfluramine was an increase in sIPSC events per minute. All other parameters tested showed dexfenfluramine to have no significant effects on the kinetics and frequency of sIPSCs or sEPSCs, however further exploration may reveal more and highlight a clear trend in these results. Further experiments would allow for significance to be determined and increase the reliability of the data.

At the time of writing no studies into the effects of dexfenfluramine on sIPSCs or sEPSCs were available to make comparisons.

7.4.4 Chronic dosing with dexfenfluramine abolishes seizure activity in P3 and P7 cultures:

Data shown in figure 7.8 indicates that chronic treatment with low dose (50nM) dexfenfluramine abolished seizure activity in both P3 and P7 cultured slices by the endpoint of time in culture. The viability of these slices was confirmed by the bath application of 250-500nM gabazine, if activity was induced in slices by the addition of gabazine slices were considered to be viable. This highlights the usefulness of chronic dosing with AEDs in organotypic slice cultures and provides further evidence for dexfenfluramine as a promising antiepileptic treatment in paediatric epilepsy.

As mentioned previously, further repeats of these experiments will be necessary to highlight the effectiveness of dexfenfluramine and increase reliability of the data.

Chapter 8: Discussio

8.1 Overarching conclusions

Although organotypic cultures of brain slices has been employed as a technique for many years, it is clear that more work needs to be done to increase the physiological and translational relevance of the preparations used. Despite the push towards serum- and antibiotic-free media, practical considerations need to balance the health of the tissue against the composition of the supportive medium used in experiments. This is particularly pressing when considering the use of human tissue, which is understandably more scarce and more variable than slices obtained from rodent donors. In this thesis we have attempted to strike a compromise between the maintenance of a maximally physiological environment and the length of culture possible with the available tissue. This includes the use of rockers or roller tubes in the maintenance of organotypic culture preparations; ideally there would be as little physical disturbance as possible, and the use of rhythmic mechanical 'washing' of slices risks the imposition of extrinsic stimulus via the activation of mechanoreceptors on neurons or glial cells that may not be present *in vivo*. When the focus of the lab is on oscillations and the generation of epileptiform activity, any 'extra' oscillations added from mechanical means is something which needs to be avoided.

So, in the experiments performed within this thesis we have tried to maintain an accessible, repeatable and physiological environment for the tissue used throughout. There are still many hurdles to overcome despite the relative maturity of organotypic culture, for example the limitations of recording electrophysiological data from cells and networks without increasing the risk cell death or infection posed by transporting cultures from the incubator to electrophysiology rigs. It may well be possible to remove cultures from the incubator and make single recordings with conventional electrophysiology setups used for *in vitro* work on acute slices, but each removal of the culture plate puts the tissue that is being placed back into the incubator in an environment that is likely to cause further cell death, temperature or osmotic shock and hugely increases the chances of an infection being brought back into the culture environment. Other labs have used multi-electrode arrays to grow or maintain cultures on, but this comes with its own drawbacks in terms of how much gas or nutrient transfer is available to the cells in the culture preparations. To that end we have chosen in this body of work to make electrophysiological recordings as an endpoint in the experiments. The initial work we are carrying out with electrospun plastic inserts

for the maintenance of cultured tissue may lead to further work incorporating electrodes and other supportive structures in the culture environment, but this work is at a very preliminary stage.

We've shown that we can maintain organotypic cultures of rodent tissue at various ages and have characterised the differences between the age of rats used vs the progression of cell death and epileptiform activity. Using a neuroprotectant-free preparation seems to lead to the reliable, repeatable creation of slices exhibiting repeated seizure-like activity, which in many cases seems to respond to established and putative anti-epileptic drugs both chronically and acutely. In some experiments, we have shown that the mechanisms of action of these possible future drugs depends upon the activity of $GABA_A$ receptors since the use of gabazine to provoke acute or exacerbated seizure-like activity can have different outcomes than using antiepileptic drugs on 'natural' seizure activity generated by the tissue itself.

8.2 Impact of COVID

Initially this thesis set out to provide a direct comparison of culturing rodent and human tissue, which is a goal of our laboratory group in order to provide a more translational model of epilepsy *in vitro* to complement the RISE model of *in vivo* epilepsy widely used at Aston. However, the supply of human tissue was limited by the suspension of elective surgeries (which epilepsy resections fall under) during the COVID period of 2020-2022. To compound this, the patients who were initially eligible for surgery after the resumption of procedures were too old to be included in our ethics agreement as the oldest patients were prioritised by the Birmingham Children's Hospital until the backlog was cleared. Thus, there was far less opportunity to access human tissue than we had hoped. Similarly, the ability to perform longitudinal culture experiments in rodents was limited by our suspension from the laboratory during the lockdown periods, which interrupted some experiments and led to low n-numbers in certain chapters. However, the availability of human tissue is now increasing from the BCH and the preliminary work carried out in this thesis will hopefully pave the way to more and better organotypic human tissue cultures in the future. Similarly, the work done in creating reliably epileptic rodent cultures will help to speed up the identification and development of novel anti-epileptic drugs in the future, as the use of cultures provides an opportunity to perform medium-throughput screening in a reliable model, faster than having to use *in vivo*-based epilepsy models or even cohort studies on rodent tissue *in vitro* since the compounds can be dosed on the cultures longitudinally, which better reflects how they would be used in the clinic. It would seem that both tianeptine and dexfenfluramine

are promising anti-epileptic drugs in certain cases, and this work will add to the efforts of epilepsy research labs across the world in identifying compounds that will target the hardest-to-treat forms of epilepsy. Although many people's seizures are well-controlled, there is still a large group of people with epilepsy who do not respond to currently available drug treatments.

8.3 Future Work

Future work in this area should focus on the careful distinction between epileptiform activity which has developed as the result of network and synaptic changes via normal plasticity mechanisms, and those which have arisen through the bulk death of interneurons or other less-relevant pathological processes. To some extent, the single-cell electrophysiology data shows promising indications that (for example looking at the amplitude distribution of IPSCs shown in figure 7.5A) there is a synapse-specific change in connectivity or synaptic weight which may be driving some of the activity seen in these preparations. This is even more encouraging when looking at the data from possible new anti-epileptic drugs such as tianeptine, where preliminary data suggests a specific change in the distribution of event amplitudes is being induced.

More needs to be done (and work is ongoing in the laboratory) on when and how tianeptine and dexfenfluramine could be useful in the treatment of epilepsy. The available data in the field are often sporadic case reports or do not go into a great deal of mechanistic detail. Hopefully the techniques developed in this thesis will go some way to increasing the body of knowledge surrounding these drugs and allow the development of similarly effective drug repurpose studies in the near future.

8.4 Materials Development

The materials used for supporting organotypic culture have not significantly changed over the past few decades. It is clear that, although microporous culture inserts provide a good substrate for nutrient transfer and in some cases culture adhesion, more can be done to explore novel ways of physically and physiologically supporting brain slice cultures to further increase the health and translational relevance of cultured tissue preparations. This is becoming more pressing with the increasing use of organoids and other 3D culture preparations in a range of physiology, toxicology and pharmacology studies; without being certain that these 'bottom up' culture approaches mimic the

activity of ‘real’ cells and tissue, wrong avenues of investigation may be taken. So, it’s important to provide the best possible way to support tissue taken from living organisms, whether from rodent models of disease or from human patients. The bespoke materials under development, and initially tested within this thesis, may provide ways to ensure better mechanical support, the inclusion of nanomaterials to enable drug delivery or electrophysiological recording, or to increase the sustainability of culture experiments via print-on-demand and/or biodegradable culture materials.

8.5 Conclusion

To conclude, although this thesis contains much preliminary work which requires careful follow-on experiments, we have developed and deployed an organotypic culture preparation which appears to show the development of reliable, treatable epileptiform activity which may lead to the more rapid and translational development of novel anti-epileptic drugs in future, and the more intensive use of human tissue from paediatric epilepsy patients.

References:

[1] Network Model of the Modulation of γ Oscillations by NMDA Receptors in Cerebral Cortex Eduarda Susin, Alain Destexhe eNeuro 8 November 2023, 10 (11) ENEURO.0157-23.2023; DOI: 10.1523/ENEURO.0157-23.2023

A. (2002) A model of atropine-resistant theta oscillations in rat hippocampal area CA1. *J Physiol*, 543(Pt 3), 779-93.

A. (2004) Coexistence of gamma and high-frequency oscillations in rat medial entorhinal cortex in vitro. *J Physiol*, 559(Pt 2), 347-53.

[2] Abenhaim L, Moride Y, Brenot F, et al. Appetite-suppressant drugs and the risk of primary pulmonary hypertension. International Primary Pulmonary Hypertension Study Group. N *Engl J Med.* 1996;335:609–16.

[3] Abhang, P. A., Gawali, B. W., & Mehrotra, S. C. (2016). Introduction to EEG- and Speech-Based Emotion Recognition. In *Introduction to EEG- and Speech-Based Emotion Recognition*.

[4] Akgül, G. & McBain, C. J. (2016) Diverse roles for ionotropic glutamate receptors on inhibitory interneurons in developing and adult brain. *J Physiol*, 594(19), 5471-90.

[5] Albertson, A. J., Yang, J. & Hablitz, J. J. (2011) Decreased hyperpolarization-activated currents in layer 5 pyramidal neurons enhances excitability in focal cortical dysplasia. *J Neurophysiol*, 106(5), 2189-200.

[6] Al-Mufti, F. and Claassen, J., 2014. Neurocritical Care. *Critical Care Clinics*, 30(4), pp.751-764.
alters oscillatory coupling in the hippocampus. *Scientific Reports*, *3*(1), 2348. https://doi.org/10.1038/srep02348

[7] Anand, K., & Dhikav, V. (2012). Hippocampus in health and disease: An overview. *Annals of Indian Academy of Neurology*, *15*(4), 239. https://doi.org/10.4103/0972-2327.104323

[8] Angeleri, F., Majkowski, J., Cacchio, G., Sobieszek, A., D'Acunto, S., Gesuita, R., Bachleda, A., Polonara, G., Krolicki, L., Signorino, M., & Salvolini, U. (1999). Posttraumatic Epilepsy Risk Factors: One-Year Prospective Study After Head Injury. *Epilepsia*, *40*(9), 1222–1230. https://doi.org/10.1111/j.1528-1157.1999.tb00850.x

associated protein kinase C activity underlie compromised synaptic inhibition during status epilepticus. *J Neurosci*, 28(2), 376-84.

[9] Attwell, D. & Gibb, A. (2005) Neuroenergetics and the kinetic design of excitatory synapses. *Nat Rev Neurosci*, 6(11), 841-9.

[10] Aur, D. The Physical Mechanism in Epilepsy - Understanding the Transition to Seizure. *Nat*

Prec (2010). https://doi.org/10.1038/npre.2010.5398.1

[11] Baldassari, S., Ribierre, T., Marsan, E., Adle-Biassette, H., Ferrand-Sorbets, S., Bulteau, C., Dorison, N., Fohlen, M., Polivka, M., Weckhuysen, S., Dorfmüller, G., Chipaux, M. & Baulac, S. (2019) Dissecting the genetic basis of focal cortical dysplasia: a large cohort study. *Acta Neuropathol*, 138(6), 885-900.

[12] Barkovich, A. J., Guerrini, R., Kuzniecky, R. I., Jackson, G. D. & Dobyns, W. B. (2012) A developmental and genetic classification for malformations of cortical development: update 2012. *Brain*, 135(Pt 5), 1348-69.

[13] Bellone, C., & Nicoll, R. A. (2007). Rapid Bidirectional Switching of Synaptic NMDA Receptors.

[14] Benarroch, E. E. (2012). GABAB receptors: Structure, functions, and clinical implications.

[15] Beneyto, M. & Meador-Woodruff, J. H. (2004) Expression of transcripts encoding AMPA receptor subunits and associated postsynaptic proteins in the macaque brain. *J Comp Neurol*, 468(4), 530-54.

[16] Ben-Menachem, E. & Krauss, G. L. (2014) Epilepsy: responsive neurostimulation-modulating the epileptic brain. *Nat Rev Neurol*, 10(5), 247-8.

[17] Berdichevsky, Y., Dzhala, V., Mail, M. and Staley, K., 2012. Interictal spikes, seizures and ictal cell death are not necessary for post-traumatic epileptogenesis in vitro. *Neurobiology of Disease*, 45(2), pp.774-785.

[18] Berdichevsky, Y., Saponjian, Y., Park, K., Roach, B., Pouliot, W., Lu, K., Swiercz, W., Dudek, F. and Staley, K., 2016. Staged anticonvulsant screening for chronic epilepsy. *Annals of Clinical and Translational Neurology*, 3(12), pp.908-923.

[19] Berger, T., Larkum, M. E. & Lüscher, H. R. (2001) High I(h) channel density in the distal apical dendrite of layer V pyramidal cells increases bidirectional attenuation of EPSPs. *J Neurophysiol*, 85(2), 855-68.

[20] Berger, T., Senn, W. & Lüscher, H. R. (2003) Hyperpolarization-activated current Ih disconnects somatic and dendritic spike initiation zones in layer V pyramidal neurons. *J Neurophysiol*, 90(4), 2428-37.

[21] Bernhardt, B., Worsley, K., Kim, H., Evans, A., Bernasconi, A. and Bernasconi, N., 2009. Longitudinal and cross-sectional analysis of atrophy in pharmacoresistant temporal lobe epilepsy. *Neurology*, 72(20), pp.1747-1754.

[22] Bernier, R., Dawson, G., Webb, S. & Murias, M. (2007) EEG mu rhythm and imitation impairments in individuals with autism spectrum disorder. *Brain Cogn*, 64(3), 228-37.

[23] Bingaman, W. E. (2004) Surgery for focal cortical dysplasia. *Neurology*, 62(6 Suppl 3), S30-4.

[24] Bird, C. M., & Burgess, N. (2008). The hippocampus and memory: Insights from spatial processing. *Nature Reviews Neuroscience*, *9*(3), 182–194. https://doi.org/10.1038/nrn2335

[25] Bland, B. H. & Oddie, S. D. (2001) Theta band oscillation and synchrony in the hippocampal formation and associated structures: the case for its role in sensorimotor integration. *Behav Brain Res*, 127(1-2), 119-36.

[26] Bland, B. H., Konopacki, J. & Dyck, R. H. (2002) Relationship between membrane potential oscillations and rhythmic discharges in identified hippocampal theta-related cells. *J Neurophysiol*, 88(6), 3046-66.

[27] Blume, W. T., Young, G. B., & Lemieux, J. F. (1984). EEG morphology of partial epileptic seizures. *Electroencephalography and Clinical Neurophysiology*, *57*(4), 295–302. https://doi.org/10.1016/0013-4694(84)90151-2

[28] Bormann, J. (2000) The 'ABC' of GABA receptors. *Trends Pharmacol Sci*, 21(1), 16-9.

[29] Bormann, J., Hamill, O. P., & Sakmann, B. (1987). Mechanism of anion permeation through channels gated by glycine and gamma-aminobutyric acid in mouse cultured spinal neurones.

[30] Bouilleret, V., Loup, F., Kiener, T., Marescaux, C. & Fritschy, J. M. (2000) Early loss of interneurons and delayed subunit-specific changes in GABA(A)-receptor expression in a mouse model of mesial temporal lobe epilepsy. *Hippocampus*, 10(3), 305-24.

[31] Braschler, U. F., Iannone, A., Spenger, C., Streit, J. & Lüscher, H. R. (1989) A modified roller tube technique for organotypic cocultures of embryonic rat spinal cord, sensory ganglia and skeletal muscle. *J Neurosci Methods*, 29(2), 121-9.

[32] Brink, C., Harvey, B., & Brand, L. (2006). Tianeptine: A Novel Atypical Antidepressant that May Provide New Insights into the Biomolecular Basis of Depression. *Recent Patents on CNS Drug Discovery*, *1*(1), 29–41. https://doi.org/10.2174/157488906775245327

[33] Brophy, G. M., Bell, R., Claassen, J., Alldredge, B., Bleck, T. P., Glauser, T., Laroche, S. M., Riviello, J. J., Shutter, L., Sperling, M. R., Treiman, D. M., Vespa, P. M. & Committee, N. C. S. S.

[34] Buckmaster, P. S., & Dudek, F. E. (1998). Neuron loss, granule cell axon reorganization, and functional changes in the dentate gyrus of epileptic kainate-treated rats. *Journal of Comparative Neurology*, *385*(3), 385–404.

[35] Buhl, E. H., Tamás, G. & Fisahn, A. (1998) Cholinergic activation and tonic excitation induce persistent gamma oscillations in mouse somatosensory cortex in vitro. *J Physiol*, 513 (Pt 1), 117-26.

[36] Buzsáki, G. & Silva, F. L. (2012) High frequency oscillations in the intact brain. *Prog Neurobiol*,

98(3), 241-9.

[37] Buzsáki, G. & Wang, X. J. (2012) Mechanisms of gamma oscillations. *Annu Rev Neurosci*, 35, 203-25.

[38] Buzsáki, G. & Watson, B. O. (2012) Brain rhythms and neural syntax: implications for efficient coding of cognitive content and neuropsychiatric disease. *Dialogues Clin Neurosci*, 14(4), 345-67.

[39] Buzsáki, G. (1984) Long-term changes of hippocampal sharp-waves following high frequency afferent activation. *Brain Res*, 300(1), 179-82.

[40] Buzsáki, G., Anastassiou, C. A. & Koch, C. (2012) The origin of extracellular fields and currents-

[41] Caixeta, F. V., Cornélio, A. M., Scheffer-Teixeira, R., Ribeiro, S., & Tort, A. B. L. (2013). Ketamine

[42] Calcagnotto, M. E., Paredes, M. F., Tihan, T., Barbaro, N. M. & Baraban, S. C. (2005) Dysfunction of synaptic inhibition in epilepsy associated with focal cortical dysplasia. *J Neurosci*, 25(42), 9649-57.

[43] Canolty, R. T., Edwards, E., Dalal, S. S., Soltani, M., Nagarajan, S. S., Kirsch, H. E., Berger, M. S., Barbaro, N. M. & Knight, R. T. (2006) High gamma power is phase-locked to theta oscillations in human neocortex. *Science*, 313(5793), 1626-8.

[44] Cantero, J. L., Atienza, M., Stickgold, R., Kahana, M. J., Madsen, J. R. & Kocsis, B. (2003) Sleep-dependent theta oscillations in the human hippocampus and neocortex. *J Neurosci*, 23(34), 10897-903.

[45] Carlén, M., Meletis, K., Siegle, J. H., Cardin, J. A., Futai, K., Vierling-Claassen, D., Rühlmann, C., Jones, S. R., Deisseroth, K., Sheng, M., Moore, C. I., & Tsai, L.-H. (2012). A critical role for NMDA receptors in parvalbumin interneurons for gamma rhythm induction and behavior. *Molecular Psychiatry*, *17*(5), 537–548. https://doi.org/10.1038/mp.2011.31

cellular alterations associated with the development of spontaneous seizures after status epilepticus (pp. 53–65). https://doi.org/10.1016/S0079-6123(02)35007-6

[46] Cepeda, C., André, V. M., Levine, M. S., Salamon, N., Miyata, H., Vinters, H. V. & Mathern, G.

[47] Chatzikonstantinou, A. (2014). *Epilepsy and the Hippocampus* (pp. 121–142). https://doi.org/10.1159/000356435

[48] Chauhan, P., Jethwa, K., Rathawa, A., Chauhan, G., & Mehra, S. (2021). The Anatomy of the Hippocampus. In *Cerebral Ischemia* (pp. 17–30). Exon Publications. https://doi.org/10.36255/exonpublications.cerebralischemia.2021.hippocampus

[49] Chen T-S, Huang T-H, Lai M-C, Huang C-W. The Role of Glutamate Receptors in Epilepsy. *Biomedicines*. 2023; 11(3):783. https://doi.org/10.3390/biomedicines11030783

[50] Chen, N., Luo, T., & Raymond, L. A. (1999). Subtype-Dependence of NMDA Receptor Channel Open Probability. *The Journal of Neuroscience*, *19*(16), 6844–6854. https://doi.org/10.1523/JNEUROSCI.19-16-06844.1999

[51] Chen, S., Zhao, Y., Wang, Y., Shekhar, M., Tajkhorshid, E., & Gouaux, E. (2017). Activation and Desensitization Mechanism of AMPA Receptor-TARP Complex by Cryo-EM. *Cell*, *170*(6), 1234-1246.e14. https://doi.org/10.1016/j.cell.2017.07.045

[52] Chong HK, Ma Z, Wong KKC, Morokoff A, French C. An In Vitro Brain Tumour Model in Organotypic Slice Cultures Displaying Epileptiform Activity. *Brain Sciences*. 2023; 13(10):1451. https://doi.org/10.3390/brainsci13101451

[53] Chu, Z., Galarreta, M. & Hestrin, S. (2003) Synaptic interactions of late-spiking neocortical neurons in layer 1. *J Neurosci*, 23(1), 96-102.

[54] Chuang, S. H. & Reddy, D. S. (2018) Genetic and Molecular Regulation of Extrasynaptic GABA-A Receptors in the Brain: Therapeutic Insights for Epilepsy. *J Pharmacol Exp Ther*, 364(2), 180-197.

[55] Cobb, S. R., Buhl, E. H., Halasy, K., Paulsen, O. & Somogyi, P. (1995) Synchronization of neuronal activity in hippocampus by individual GABAergic interneurons. *Nature*, 378(6552), 75-8.

[56] Connolly HM, Crary JL, McGoon MD, Hensrud DD, Edwards BS, Edwards WD, Schaff HV. Valvular heart disease associated with fenfluramine-phentermine. *N Engl J Med.* 1997;337:581–8.

[57] Constals, A., Penn, A. C., Compans, B., Toulmé, E., Phillipat, A., Marais, S., Retailleau, N., Hafner, A.-S., Coussen, F., Hosy, E., & Choquet, D. (2015). Glutamate-Induced AMPA Receptor Desensitization Increases Their Mobility and Modulates Short-Term Plasticity through Unbinding from Stargazin. *Neuron*, *85*(4), 787–803. https://doi.org/10.1016/j.neuron.2015.01.012

[58] Cossart, R., Dinocourt, C., Hirsch, J., Merchan-Perez, A., De Felipe, J., Ben-Ari, Y., Esclapez, M. and Bernard, C., 2001. Dendritic but not somatic GABAergic inhibition is decreased in experimental epilepsy. *Nature Neuroscience*, 4(1), pp.52-62.

[59] Cossart, R., Epsztein, J., Tyzio, R., Becq, H., Hirsch, J., Ben-Ari, Y. & Crépel, V. (2002) Quantal release of glutamate generates pure kainate and mixed AMPA/kainate EPSCs in hippocampal neurons. *Neuron*, 35(1), 147-59.

[60] Cotter, D. R., Honavar, M. & Everall, I. (1999) Focal cortical dysplasia: a neuropathological and

developmental perspective. *Epilepsy Res*, 36(2-3), 155-64.

[61] Croft, C.L., Futch, H.S., Moore, B.D. *et al.* Organotypic brain slice cultures to model neurodegenerative proteinopathies. *Mol Neurodegeneration* **14**, 45 (2019). https://doi.org/10.1186/s13024-019-0346-0

[62] Cunningham, M. O., Davies, C. H., Buhl, E. H., Kopell, N. & Whittington, M. A. (2003) Gamma oscillations induced by kainate receptor activation in the entorhinal cortex in vitro. *J Neurosci*, 23(30), 9761-9.

[63] Cunningham, M. O., Halliday, D. M., Davies, C. H., Traub, R. D., Buhl, E. H. & Whittington, M.

[64] Cunningham, M. O., Hunt, J., Middleton, S., LeBeau, F. E. N., Gillies, M. G., Davies, C. H., Maycox, P. R., Whittington, M. A., & Racca, C. (2006). Region-Specific Reduction in Entorhinal Gamma Oscillations and Parvalbumin-Immunoreactive Neurons in Animal Models of Psychiatric Illness. *The Journal of Neuroscience*, *26*(10), 2767–2776. https://doi.org/10.1523/JNEUROSCI.5054-05.2006

[65] Curia, G., Longo, D., Biagini, G., Jones, R. S. G., & Avoli, M. (2008). The pilocarpine model of temporal lobe epilepsy. *Journal of Neuroscience Methods*, *172*(2), 143–157. https://doi.org/10.1016/j.jneumeth.2008.04.019

[66] Curtis, D. R. & Watkins, J. C. (1960) The excitation and depression of spinal neurones by structurally related amino acids. *J Neurochem*, 6, 117-41.

[67] Czapiński, P., Blaszczyk, B. & Czuczwar, S. J. (2005) Mechanisms of action of antiepileptic drugs. *Curr Top Med Chem*, 5(1), 3-14.

D. A. & Moss, S. J. (2008) Deficits in phosphorylation of GABA(A) receptors by intimately D. R. (2001) A role for mitogen-activated protein kinases in the etiology of diabetic neuropathy. *FASEB J*, 15(13), 2508-14.

[68] D'Ambrosio, R. and Miller, J., 2010. What is an Epileptic Seizure? Unifying Definitions in Clinical Practice and Animal Research to Develop Novel Treatments. *Epilepsy Currents*, 10(3), pp.61-66.

[69] de Curtis, M. and Avanzini, G., 2001. Interictal spikes in focal epileptogenesis. *Progress in Neurobiology*, 63(5), pp.541-567.

[70] de Curtis, M. and Gnatkovsky, V., 2009. Reevaluating the mechanisms of focal ictogenesis: The role of low-voltage fast activity. *Epilepsia*, 50(12), pp.2514-2525.

[71] Derchansky, M., Jahromi, S., Mamani, M., Shin, D., Sik, A. and Carlen, P., 2008. Transition to

seizures in the isolated immature mouse hippocampus: a switch from dominant phasic inhibition to dominant phasic excitation. *The Journal of Physiology*, 586(2), pp.477-494.

[72] Derkach, V., Barria, A., & Soderling, T. R. (1999). Ca2+ /calmodulin-kinase II enhances channel conductance of α-amino-3-hydroxy-5-methyl-4-isoxazolepropionate type glutamate receptors. *Proceedings of the National Academy of Sciences*, *96*(6), 3269–3274. https://doi.org/10.1073/pnas.96.6.3269

[73] Dibué-Adjei, M., Kamp, M. A., Alpdogan, S., Tevoufouet, E. E., Neiss, W. F., Hescheler, J. & Schneider, T. (2017) Cav2.3 (R-Type) Calcium Channels are Critical for Mediating Anticonvulsive and Neuroprotective Properties of Lamotrigine In Vivo. *Cell Physiol Biochem*, 44(3), 935-947.

[74] Dingledine, R., Boland, L. M., Chamberlin, N. L., Kawasaki, K., Kleckner, N. W., Traynelis, S. F. & Verdoorn, T. A. (1988) Amino acid receptors and uptake systems in the mammalian central nervous system. *Crit Rev Neurobiol*, 4(1), 1-96.

[75] Dingledine, R., Borges, K., Bowie, D. & Traynelis, S. F. (1999) The glutamate receptor ion channels. *Pharmacol Rev*, 51(1), 7-61.

[76] Dingledine, R., Varvel, N. and Dudek, F., 2014. When and How Do Seizures Kill Neurons, and Is Cell Death Relevant to Epileptogenesis? *Issues in Clinical Epileptology: A View from the Bench*, pp.109-122.

[77] Dong, H. W. & Buonomano, D. V. (2005) A technique for repeated recordings in cortical organotypic slices. *J Neurosci Methods*, 146(1), 69-75.

[78] Donoghue, J. P. & Wise, S. P. (1982) The motor cortex of the rat: cytoarchitecture and microstimulation mapping. *J Comp Neurol*, 212(1), 76-88.

[79] Dudek, F. E., Hellier, J. L., Williams, P. A., Ferraro, D. J., & Staley, K. J. (2002). *The course of*

[80] Dutar, P. & Nicoll, R. A. (1988a) A physiological role for GABAB receptors in the central nervous system. *Nature*, 332(6160), 156-8.

[81] Dutar, P. & Nicoll, R. A. (1988b) Pre- and postsynaptic GABAB receptors in the hippocampus have different pharmacological properties. *Neuron*, 1(7), 585-91.

[82] Dyhrfjeld-Johnsen, J., Berdichevsky, Y., Swiercz, W., Sabolek, H. and Staley, K., 2010. Interictal Spikes Precede Ictal Discharges in an Organotypic Hippocampal Slice Culture Model of Epileptogenesis. *Journal of Clinical Neurophysiology*, 27(6), pp.418-424.

E. G. W. (2012) Guidelines for the evaluation and management of status epilepticus. *Neurocrit Care*, 17(1), 3-23.

[83] Eccles, J. C. (1981) The modular operation of the cerebral neocortex considered as the material basis of mental events. *Neuroscience*, 6(10), 1839-56.

[84] Eccles, J. C., & McGeer, P. L. (1979). Ionotropic and metabotropic neurotransmission. Trends Neurosci. 2, 39–40. *Trends in Neuroscience*, *2*, 39–40. https://doi.org/10.3389/fncel.2012.00054

-EEG, ECoG, LFP and spikes. *Nat Rev Neurosci*, 13(6), 407-20.

[85] Egert, U., Schlosshauer, B., Fennrich, S., Nisch, W., Fejtl, M., Knott, T., Müller, T. & Hämmerle,

[86] Engin, E., Benham, R. S. & Rudolph, U. (2018) An Emerging Circuit Pharmacology of GABA. *Trends Pharmacol Sci*, 39(8), 710-732.

[87] Esclapez, M., Hirsch, J., Ben-Ari, Y. and Bernard, C., 1999. Newly formed excitatory pathways provide a substrate for hyperexcitability in experimental temporal lobe epilepsy. *The Journal of Comparative Neurology*, 408(4), pp.449-460.

European Journal of Neuroscience, *30*(10), 1900–1908. https://doi.org/10.1111/j.1460-
Experimental Brain Research, *82*(3). https://doi.org/10.1007/BF00228796

F. (2003) Epilepsy-induced changes in signaling systems of human and rat postsynaptic densities. *Epilepsia*, 44(2), 243-6.

F. M., da Cunha, R. M., Walz, R. & Leal, R. B. (2013) Time-dependent modulation of AMPA receptor phosphorylation and mRNA expression of NMDA receptors and glial glutamate transporters in the rat hippocampus and cerebral cortex in a pilocarpine model of epilepsy. *Exp Brain Res*, 226(2), 153-63.

[88] Fan, B., Sun, Y. J., Liu, S. Y., Che, L. & Li, G. Y. (2017) Neuroprotective Strategy in Retinal Degeneration: Suppressing ER Stress-Induced Cell Death via Inhibition of the mTOR Signal. *Int J Mol Sci*, 18(1).

[89] Farrant, M. & Nusser, Z. (2005) Variations on an inhibitory theme: phasic and tonic activation of GABA(A) receptors. *Nat Rev Neurosci*, 6(3), 215-29.

[90] Fauser, S. & Schulze-Bonhage, A. (2006) Epileptogenicity of cortical dysplasia in temporal lobe dual pathology: an electrophysiological study with invasive recordings. *Brain*, 129(Pt 1), 82-95.

[91] Fauser, S., Schulze-Bonhage, A., Honegger, J., Carmona, H., Huppertz, H. J., Pantazis, G., Rona, S., Bast, T., Strobl, K., Steinhoff, B. J., Korinthenberg, R., Rating, D., Volk, B. & Zentner, J. (2004)

[92] Fauser, S., Sisodiya, S. M., Martinian, L., Thom, M., Gumbinger, C., Huppertz, H. J., Hader, C., Strobl, K., Steinhoff, B. J., Prinz, M., Zentner, J. & Schulze-Bonhage, A. (2009) Multi-focal occurrence of cortical dysplasia in epilepsy patients. *Brain*, 132(Pt 8), 2079-90.

[93] Fisahn, A., Contractor, A., Traub, R. D., Buhl, E. H., Heinemann, S. F., & McBain, C. J. (2004). Distinct Roles for the Kainate Receptor Subunits GluR5 and GluR6 in Kainate-Induced Hippocampal Gamma Oscillations. *The Journal of Neuroscience*, *24*(43), 9658–9668. https://doi.org/10.1523/JNEUROSCI.2973-04.2004

[94] Fisahn, A., Pike, F. G., Buhl, E. H. & Paulsen, O. (1998) Cholinergic induction of network oscillations at 40 Hz in the hippocampus in vitro. *Nature*, 394(6689), 186-9.

Focal cortical dysplasias: surgical outcome in 67 patients in relation to histological subtypes and dual pathology. *Brain*, 127(Pt 11), 2406-18.

[95] Fragale, J. E. C., Khariv, V., Gregor, D. M., Smith, I. M., Jiao, X., Elkabes, S., Servatius, R. J., Pang,
[96] French, J., White, H., Klitgaard, H., Holmes, G., Privitera, M., Cole, A., Quay, E., Wiebe, S., Schmidt, D., Porter, R., Arzimanoglou, A., Trinka, E. and Perucca, E., 2013. Development of new treatment approaches for epilepsy: Unmet needs and opportunities. *Epilepsia*, 54, pp.3-12.

Frontiers in Molecular Neuroscience, *12*. https://doi.org/10.3389/fnmol.2019.00179

[97] Fuchs, E. C., Zivkovic, A. R., Cunningham, M. O., Middleton, S., Lebeau, F. E., Bannerman, D. M., Rozov, A., Whittington, M. A., Traub, R. D., Rawlins, J. N. & Monyer, H. (2007) Recruitment of parvalbumin-positive interneurons determines hippocampal function and associated behavior. *Neuron*, 53(4), 591-604.

[98] Fujiwara-Tsukamoto, Y., Isomura, Y., Imanishi, M., Ninomiya, T., Tsukada, M., Yanagawa, Y., Fukai, T. and Takada, M., 2010. Prototypic Seizure Activity Driven by Mature Hippocampal Fast-Spiking Interneurons. *Journal of Neuroscience*, 30(41), pp.13679-13689.

[99] Fujiwara-Tsukamoto, Y., Isomura, Y., Kaneda, K. and Takada, M., 2004. Synaptic interactions between pyramidal cells and interneurone subtypes during seizure-like activity in the rat hippocampus. *The Journal of Physiology*, 557(3), pp.961-979.

[100] Gähwiler, B. (1997). Organotypic slice cultures: A technique has come of age. *Trends in Neurosciences*, *20*(10), 471–477. https://doi.org/10.1016/S0166-2236(97)01122-3

[101] Gähwiler, B. H. (1981). Organotypic monolayer cultures of nervous tissue. *Journal of*

[102] Gähwiler, B. H. (1988). Organotypic cultures of neural tissue. *Trends in Neurosciences*, *11*(11), 484–489. https://doi.org/10.1016/0166-2236(88)90007-0

[103] Gähwiler, B. H., Capogna, M., Debanne, D., McKinney, R. A. & Thompson, S. M. (1997) Organotypic slice cultures: a technique has come of age. *Trends Neurosci*, 20(10), 471-7.

[104] Gähwiler, B. H., Thompson, S. M., & Muller, D. (1999). Preparation and Maintenance of

Organotypic Slice Cultures of CNS Tissue. *Current Protocols in Neuroscience*, *9*(1). https://doi.org/10.1002/0471142301.ns0611s09

[105] Gansel KS. Neural synchrony in cortical networks: mechanisms and implications for neural information processing and coding. *Front Integr Neurosci.* 2022 Oct 3;16:900715. doi: 10.3389/fnint.2022.900715. PMID: 36262373; PMCID: PMC9574343.

[106] García-Cabezas, M. & Barbas, H. (2014) Area 4 has layer IV in adult primates. *Eur J Neurosci*, 39(11), 1824-34.

[107] Geiger, J. R. P., Melcher, T., Koh, D.-S., Sakmann, B., Seeburg, P. H., Jonas, P., & Monyer, H. (1995). Relative abundance of subunit mRNAs determines gating and Ca2+ permeability of AMPA receptors in principal neurons and interneurons in rat CNS. *Neuron*, *15*(1), 193–204. https://doi.org/10.1016/0896-6273(95)90076-4

[108] Ghosal, S., Hare, B. & Duman, R. S. (2017) Prefrontal Cortex GABAergic Deficits and Circuit Dysfunction in the Pathophysiology and Treatment of Chronic Stress and Depression. *Curr Opin Behav Sci*, 14, 1-8.

[109] Giese, K. P., Fedorov, N. B., Filipkowski, R. K. & Silva, A. J. (1998) Autophosphorylation at Thr286 of the alpha calcium-calmodulin kinase II in LTP and learning. *Science*, 279(5352), 870-3.

[110] Giesing, M., Neumann, G., Egge, H. & Zilliken, F. (1975) Lipid metabolism of developing central nervous tissues in organotypic cultures. I. Lipid distribution and fatty acid profiles of the medium for rat brain cortex in vitro. *Nutr Metab*, 19(5-6), 242-50.

[111] Gillies, M. J., Traub, R. D., LeBeau, F. E., Davies, C. H., Gloveli, T., Buhl, E. H. & Whittington, M.

[112] Gleichmann, M., Chow, V. W. & Mattson, M. P. (2011) Homeostatic disinhibition in the aging brain and Alzheimer's disease. *J Alzheimers Dis*, 24(1), 15-24.

[113] Gnatkovsky, V., Librizzi, L., Trombin, F. and de Curtis, M., 2008. Fast activity at seizure onset is mediated by inhibitory circuits in the entorhinal cortex in vitro. *Annals of Neurology*, 64(6), pp.674-686.

[114] Goodkin, H. P. & Kapur, J. (2003) Responsiveness of Status Epilepticus to Treatment with Diazepan Decreases Rapidly as Seizure Duration Increases. *Epilepsy Curr*, 3(1), 11-12.

[115] Goodkin, H. P., Joshi, S., Mtchedlishvili, Z., Brar, J. & Kapur, J. (2008) Subunit-specific trafficking of GABA(A) receptors during status epilepticus. *J Neurosci*, 28(10), 2527-38.

[116] Goodkin, H. P., Yeh, J. L. & Kapur, J. (2005) Status epilepticus increases the intracellular accumulation of GABAA receptors. *J Neurosci*, 25(23), 5511-20.

[117] Greenhill, S. D., Ranson, A. & Fox, K. (2015) Hebbian and Homeostatic Plasticity Mechanisms in Regular Spiking and Intrinsic Bursting Cells of Cortical Layer 5. *Neuron*, 88(3), 539-52.

[118] Griffith C. L. Regulation of Calcium/Calmodulin-Dependent Protein Kinase II Activation by Intramolecular and Intermolecular Interactions *Journal of Neuroscience* 29 September 2004, 24 (39) 8394-8398; **DOI:** 10.1523/JNEUROSCI.3604-04.2004

[119] Gross L (2006) Membrane Oscillations Keep Neurons on the Right Track. PLoS Biol 4(6): e191. https://doi.org/10.1371/journal.pbio.0040191

[120] Gutiérrez, R. and Heinemann, U., 1999. Synaptic reorganization in explanted cultures of rat hippocampus. *Brain Research*, 815(2), pp.304-316.

H. (1998) A novel organotypic long-term culture of the rat hippocampus on substrate-integrated multielectrode arrays. *Brain Res Brain Res Protoc*, 2(4), 229-42.

[121] Haas, L. F. (2003). Hans Berger (1873-1941), Richard Caton (1842-1926), and electroencephalography. *Journal of Neurology, Neurosurgery & Psychiatry*, *74*(1), 9–9. https://doi.org/10.1136/jnnp.74.1.9

[122] Hájos, N. & Paulsen, O. (2009) Network mechanisms of gamma oscillations in the CA3 region of the hippocampus. *Neural Netw*, 22(8), 1113-9.

[123] Halnes, G., Mäki-Marttunen, T., Keller, D., Pettersen, K. H., Andreassen, O. A. & Einevoll, G. T. (2016) Effect of Ionic Diffusion on Extracellular Potentials in Neural Tissue. *PLoS Comput Biol*, 12(11), e1005193.

[124] Hasselmo, M. E., Bodelón, C. & Wyble, B. P. (2002) A proposed function for hippocampal theta rhythm: separate phases of encoding and retrieval enhance reversal of prior learning. *Neural Comput*, 14(4), 793-817.

[125] Henley, J. M. & Wilkinson, K. A. (2013) AMPA receptor trafficking and the mechanisms underlying synaptic plasticity and cognitive aging. *Dialogues Clin Neurosci*, 15(1), 11-27.

[126] Henley, J. M. & Wilkinson, K. A. (2016) Synaptic AMPA receptor composition in development, plasticity and disease. *Nat Rev Neurosci*, 17(6), 337-50.

[127] Henshall, D., Schindler, C., So, N., Lan, J., Meller, R. and Simon, R., 2004. Death-associated protein kinase expression in human temporal lobe epilepsy. *Annals of Neurology*, 55(4), pp.485-494.

[128] Hildebrandt, M., Pieper, T., Winkler, P., Kolodziejczyk, D., Holthausen, H. & Blümcke, I. (2005) Neuropathological spectrum of cortical dysplasia in children with severe focal epilepsies. *Acta*

Neuropathol, 110(1), 1-11.

Hill, K. J., Collazo, A., Funari, V., Russ, C., Gabriel, S. B., Mathern, G. W. & Gleeson, J. G. (2012) De novo somatic mutations in components of the PI3K-AKT3-mTOR pathway cause hemimegalencephaly. *Nat Genet*, 44(8), 941-5.

[129] Hölscher, C. (1999) Synaptic plasticity and learning and memory: LTP and beyond. *J Neurosci Res*, 58(1), 62-75.

[130] Holtkamp, M., Othman, J., Buchheim, K., Masuhr, F., Schielke, E. & Meierkord, H. (2005) A "malignant" variant of status epilepticus. *Arch Neurol*, 62(9), 1428-31.

https://doi.org/10.1016/j.yebeh.2014.03.021
https://doi.org/10.1073/pnas.0611698104
https://doi.org/10.3389/fnhum.2014.00406

[131] Huang, Y. & Thathiah, A. (2015) Regulation of neuronal communication by G protein-coupled receptors. *FEBS Lett*, 589(14), 1607-19.

[132] Humpel, C. (2015) Organotypic brain slice cultures: A review. *Neuroscience*, 305, 86-98.

[133] Hunt, D. L. & Castillo, P. E. (2012) Synaptic plasticity of NMDA receptors: mechanisms and functional implications. *Curr Opin Neurobiol*, 22(3), 496-508.

[134] Hutter-Schmid, B., Kniewallner, K. M., & Humpel, C. (2015). Organotypic brain slice cultures as a model to study angiogenesis of brain vessels. *Frontiers in Cell and Developmental Biology*,

[135] Igarashi, J., Isomura, Y., Arai, K., Harukuni, R. & Fukai, T. (2013) A θ-γ oscillation code for neuronal coordination during motor behavior. *J Neurosci*, 33(47), 18515-30.

[136] Igarashi, J., Isomura, Y., Arai, K., Harukuni, R., & Fukai, T. (2013). A θ–γ Oscillation Code for Neuronal Coordination during Motor Behavior. *The Journal of Neuroscience*, *33*(47), 18515–18530. https://doi.org/10.1523/JNEUROSCI.2126-13.2013

Intelligent Signal Processing Conference 2013 (ISP 2013), 7.06-7.06. https://doi.org/10.1049/cp.2013.2060

International Journal of Basic and Clinical Pharmacology, 850–854. https://doi.org/10.18203/2319-2003.ijbcp20161533

[137] Ishii, R., Canuet, L., Ishihara, T., Aoki, Y., Ikeda, S., Hata, M., Katsimichas, T., Gunji, A., Takahashi, H., Nakahachi, T., Iwase, M., & Takeda, M. (2014). Frontal midline theta rhythm and gamma power changes during focused attention on mental calculation: An MEG beamformer analysis. *Frontiers in Human Neuroscience*, *8*.

[138] Isomura, Y., Sirota, A., Ozen, S., Montgomery, S., Mizuseki, K., Henze, D. A. & Buzsáki, G. (2006) Integration and segregation of activity in entorhinal-hippocampal subregions by neocortical

slow oscillations. *Neuron*, 52(5), 871-82.

J. J. & van Baalen, A. (2011) Febrile infection-related epilepsy syndrome (FIRES): pathogenesis, treatment, and outcome: a multicenter study on 77 children. *Epilepsia*, 52(11), 1956-65.

[139] Jacob, T. C. (2019). Neurobiology and Therapeutic Potential of α5-GABA Type A Receptors.

[140] Jahnsen, H., Kristensen, B. W., Thiébaud, P., Noraberg, J., Jakobsen, B., Bove, M., Martinoia, S., Koudelka-Hep, M., Grattarola, M. & Zimmer, J. (1999) Coupling of organotypic brain slice cultures to silicon-based arrays of electrodes. *Methods*, 18(2), 160-72.

[141] Jefferys, J., 2003. Models and Mechanisms of Experimental Epilepsies. *Epilepsia*, 44(s12), pp.44-50.

[142] Jenkins, M. A., & Traynelis, S. F. (2012). PKC phosphorylates GluA1-Ser831 to enhance AMPA receptor conductance. *Channels*, *6*(1), 60–64. https://doi.org/10.4161/chan.18648

[143] Jensen, O., Spaak, E., & Park, H. (2016). Discriminating Valid from Spurious Indices of Phase-Amplitude Coupling. *Eneuro*, *3*(6), ENEURO.0334-16.2016. https://doi.org/10.1523/ENEURO.0334-16.2016

[144] Jermakowicz WJ, Casagrande VA. Neural networks a century after Cajal. *Brain Res Rev.* 2007 Oct;55(2):264-84. doi: 10.1016/j.brainresrev.2007.06.003. Epub 2007 Jul 13. PMID: 17692925; PMCID: PMC2101763.

[145] Jeun, S. H., Cho, H. S., Kim, K. J., Li, Q. Z. & Sung, K. W. (2009) Electrophysiological Characterization of AMPA and NMDA Receptors in Rat Dorsal Striatum. *Korean J Physiol Pharmacol*, 13(3), 209-14.

[146] Johannessen, S. I. & Landmark, C. J. (2010) Antiepileptic drug interactions - principles and clinical implications. *Curr Neuropharmacol*, 8(3), 254-67.

[147] Johnson, N. W., Özkan, M., Burgess, A. P., Prokic, E. J., Wafford, K. A., O'Neill, M. J., Greenhill,

[148] Johnson, N. W., Özkan, M., Burgess, A. P., Prokic, E. J., Wafford, K. A., O'Neill, M. J., Greenhill,

[149] Jones, D. M., Esmaeil, N., Maren, S. & Macdonald, R. L. (2002) Characterization of pharmacoresistance to benzodiazepines in the rat Li-pilocarpine model of status epilepticus. *Epilepsy Res*, 50(3), 301-12.

[150] Jones, D., Esmaeil, N., Maren, S. and Macdonald, R., 2002. Characterization of pharmacoresistance to benzodiazepines in the rat Li-pilocarpine model of status epilepticus. *Epilepsy Research*, 50(3), pp.301-312.

[151] Joshi, S., Rajasekaran, K., Sun, H., Williamson, J. & Kapur, J. (2017a) Enhanced AMPA receptor-mediated neurotransmission on CA1 pyramidal neurons during status epilepticus. *Neurobiol Dis*, 103, 45-53.

[152] Joshi, S., Rajasekaran, K., Williamson, J. & Kapur, J. (2017b) Neurosteroid-sensitive δ-GABA. *Epilepsia*, 58(3), 494-504.

[153] Joshi, S., Sun, H., Rajasekaran, K., Williamson, J., Perez-Reyes, E. & Kapur, J. (2018a) A novel therapeutic approach for treatment of catamenial epilepsy. *Neurobiol Dis*, 111, 127-137.

[154] Ju, P., Ding, W., Chen, J., Cheng, Y., Yang, B., Huang, L., Zhou, Q., Zhu, C., Li, X., Wang, M., & Chen, J. (2020). The protective effects of Mogroside V and its metabolite 11-oxo-mogrol of intestinal microbiota against MK801-induced neuronal damages. *Psychopharmacology*, *237*(4), 1011–1026. https://doi.org/10.1007/s00213-019-05431-9

K. B., Yuan, H., Myers, S. J. & Dingledine, R. (2010) Glutamate receptor ion channels: structure, regulation, and function. *Pharmacol Rev*, 62(3), 405-96.

K. C. H., & Beck, K. D. (2016). Dysfunction in amygdala–prefrontal plasticity and extinction-resistant avoidance: A model for anxiety disorder vulnerability. *Experimental Neurology*, *275*, 59–68. https://doi.org/10.1016/j.expneurol.2015.11.002

[155] K. Ostergaard, Schou, J. P., & Zimmer, J. (1990). Rat ventral mesencephalon grown as organotypic slice cultures and co-cultured with striatum, hippocampus, and cerebellum.

[156] Kahn, M. C., & Bingman, V. P. (2009). Avian hippocampal role in space and content memory.

[157] Kaminski, R. M., Livingood, M. R. & Rogawski, M. A. (2004a) Allopregnanolone analogs that positively modulate GABA receptors protect against partial seizures induced by 6-Hz electrical stimulation in mice. *Epilepsia*, 45(7), 864-7.

[158] Kaminski, R. M., Tochman, A. M., Dekundy, A., Turski, W. A. & Czuczwar, S. J. (2004b) Ethosuximide and valproate display high efficacy against lindane-induced seizures in mice. *Toxicol Lett*, 154(1-2), 55-60.

[159] Kampa, B. M., Clements, J., Jonas, P. & Stuart, G. J. (2004) Kinetics of Mg2+ unblock of NMDA receptors: implications for spike-timing dependent synaptic plasticity. *J Physiol*, 556(Pt 2), 337-45.

[160] Kandratavicius, L., Balista, P., Lopes-Aguiar, C., Ruggiero, R., Umeoka, E., Garcia-Cairasco, N., Bueno-Junior, L., & Leite, J. (2014). Animal models of epilepsy: Use and limitations.

[161] Kanner, A. M. (2003). Depression in epilepsy: Prevalence, clinical semiology, pathogenic mechanisms, and treatment. *Biological Psychiatry*, *54*(3), 388–398. https://doi.org/10.1016/S0006-3223(03)00469-4

[162] Kanner, A. M. (2012). Depressive Disorders in Epilepsy. In *Depression in Neurologic Disorders: Diagnosis and Management* (pp. 126–144).

Wiley. https://doi.org/10.1002/9781118348093.ch11

[163] Kanner, A. M. (2016). Management of psychiatric and neurological comorbidities in epilepsy.

[164] Kapur, J. & Lothman, E. W. (1989) Loss of inhibition precedes delayed spontaneous seizures in the hippocampus after tetanic electrical stimulation. *J Neurophysiol*, 61(2), 427-34.

[165] Kapur, J. & Macdonald, R. L. (1997) Rapid seizure-induced reduction of benzodiazepine and Zn2+ sensitivity of hippocampal dentate granule cell GABAA receptors. *J Neurosci*, 17(19), 7532-40.

[166] Kapur, J., Lothman, E. W. & DeLorenzo, R. J. (1994) Loss of GABAA receptors during partial status epilepticus. *Neurology*, 44(12), 2407-8.

[167] Kapur, J., Stringer, J. L. & Lothman, E. W. (1989) Evidence that repetitive seizures in the hippocampus cause a lasting reduction of GABAergic inhibition. *J Neurophysiol*, 61(2), 417-26.

[168] Karpiak, V. C. & Plenz, D. (2002) Preparation and maintenance of organotypic cultures for multi-electrode array recordings. *Curr Protoc Neurosci*, Chapter 6, Unit 6.15.

[169] Kiranyaz, S., Ince, T., Zabihi, M., & Gabbouj, M. (2013). Patient-specific epileptic seizure detection in long-term EEG recording in paediatric patients with intractable seizures. *IET*

[170] Kobayashi, M. and Buckmaster, P., 2003. Reduced Inhibition of Dentate Granule Cells in a Model of Temporal Lobe Epilepsy. *The Journal of Neuroscience*, 23(6), pp.2440-2452.

[171] Kobow, K., Auvin, S., Jensen, F., Löscher, W., Mody, I., Potschka, H., Prince, D., Sierra, A., Simonato, M., Pitkänen, A., Nehlig, A. and Rho, J., 2012. Finding a better drug for epilepsy: Antiepileptogenesis targets. *Epilepsia*, 53(11), pp.1868-1876.

[172] Koh, D. S., Burnashev, N., & Jonas, P. (1995). Block of native Ca(2+)-permeable AMPA receptors in rat brain by intracellular polyamines generates double rectification. *The Journal of Physiology*, *486*(2), 305–312. https://doi.org/10.1113/jphysiol.1995.sp020813

[173] Kole, M. H. P., Swan, L., & Fuchs, E. (2002). The antidepressant tianeptine persistently modulates glutamate receptor currents of the hippocampal CA3 commissural associational synapse in chronically stressed rats. *European Journal of Neuroscience*, *16*(5), 807–816. https://doi.org/10.1046/j.1460-9568.2002.02136.x

[174] Kopell, N. & Ermentrout, B. (2004) Chemical and electrical synapses perform complementary roles in the synchronization of interneuronal networks. *Proc Natl Acad Sci U S A*, 101(43), 15482-7.

[175] Korff, C. M. & Scheffer, I. E. (2013) Epilepsy classification: a cycle of evolution and revolution. *Curr Opin Neurol*, 26(2), 163-7.

[176] Kramer, U., Chi, C. S., Lin, K. L., Specchio, N., Sahin, M., Olson, H., Nabbout, R., Kluger, G., Lin,
[177] Krsek, P., Maton, B., Jayakar, P., Dean, P., Korman, B., Rey, G., Dunoyer, C., Pacheco-Jacome, E., Morrison, G., Ragheb, J., Vinters, H. V., Resnick, T. & Duchowny, M. (2009) Incomplete resection of focal cortical dysplasia is the main predictor of poor postsurgical outcome. *Neurology*, 72(3), 217-23.

[178] Kulik, A., Vida, I., Fukazawa, Y., Guetg, N., Kasugai, Y., Marker, C. L., Rigato, F., Bettler, B., Wickman, K., Frotscher, M. & Shigemoto, R. (2006) Compartment-dependent colocalization of Kir3.2-containing K+ channels and GABAB receptors in hippocampal pyramidal cells. *J Neurosci*, 26(16), 4289-97.

[179] Kumar, A. & Foster, T. C. (2019) Alteration in NMDA Receptor Mediated Glutamatergic Neurotransmission in the Hippocampus During Senescence. *Neurochem Res*, 44(1), 38-48.

[180] Landmark, C. J. & Johannessen, S. I. (2008) Modifications of antiepileptic drugs for improved tolerability and efficacy. *Perspect Medicin Chem*, 2, 21-39.

[181] Lee, A., Scheuer, T. & Catterall, W. A. (2000a) Ca2+/calmodulin-dependent facilitation and inactivation of P/Q-type Ca2+ channels. *J Neurosci*, 20(18), 6830-8.

[182] Lee, H. K., Barbarosie, M., Kameyama, K., Bear, M. F. & Huganir, R. L. (2000b) Regulation of distinct AMPA receptor phosphorylation sites during bidirectional synaptic plasticity. *Nature*, 405(6789), 955-9.

[183] Lee, H.-K., Barbarosie, M., Kameyama, K., Bear, M. F., & Huganir, R. L. (2000). Regulation of distinct AMPA receptor phosphorylation sites during bidirectional synaptic plasticity. *Nature*, *405*(6789), 955–959. https://doi.org/10.1038/35016089

[184] Lee, J. H., Huynh, M., Silhavy, J. L., Kim, S., Dixon-Salazar, T., Heiberg, A., Scott, E., Bafna, V.,
[185] Leinekugel, X., Khalilov, I., McLean, H., Caillard, O., Gaiarsa, J. L., Ben-Ari, Y. & Khazipov, R. (1999) GABA is the principal fast-acting excitatory transmitter in the neonatal brain. *Adv Neurol*, 79, 189-201.

[186] Lerma, J. & Marques, J. M. (2013) Kainate receptors in health and disease. *Neuron*, 80(2), 292-311.

[187] Lévesque, M., Avoli, M. & Bernard, C. (2016) Animal models of temporal lobe epilepsy following systemic chemoconvulsant administration. *J Neurosci Methods*, 260, 45-52.

[188] Lillis, K., Wang, Z., Mail, M., Zhao, G., Berdichevsky, Y., Bacskai, B. and Staley, K., 2015. Evolution of Network Synchronization during Early Epileptogenesis Parallels Synaptic Circuit Alterations. *Journal of Neuroscience*, 35(27), pp.9920-9934.

[189] Lipton, J. O. & Sahin, M. (2014) The neurology of mTOR. *Neuron*, 84(2), 275-91.

[190] Lisman, J. (1989) A mechanism for the Hebb and the anti-Hebb processes underlying learning and memory. *Proc Natl Acad Sci U S A*, 86(23), 9574-8.

[191] Liu, J., Saponjian, Y., Mahoney, M., Staley, K. and Berdichevsky, Y., 2017. Epileptogenesis in organotypic hippocampal cultures has limited dependence on culture medium composition. *PLOS ONE*, 12(2), p.e0172677.

[192] Liu, X. B., Murray, K. D. & Jones, E. G. (2004) Switching of NMDA receptor 2A and 2B subunits at thalamic and cortical synapses during early postnatal development. *J Neurosci*, 24(40), 8885-95.

[193] Lopantsev, V. and Avoli, M., 1998. Laminar organization of epileptiform discharges in the rat entorhinal cortexin vitro. *The Journal of Physiology*, 509(3), pp.785-796.

[194] Lopes, M. W., Soares, F. M., de Mello, N., Nunes, J. C., Cajado, A. G., de Brito, D., de Cordova,
[195] Löscher, W. (2021). Single-Target Versus Multi-Target Drugs Versus Combinations of Drugs With Multiple Targets: Preclinical and Clinical Evidence for the Treatment or Prevention of Epilepsy. *Frontiers in Pharmacology*, *12*. https://doi.org/10.3389/fphar.2021.730257

[196] Löscher, W. and Schmidt, D., 2011. Modern antiepileptic drug development has failed to deliver: Ways out of the current dilemma. *Epilepsia*, 52(4), pp.657-678.

[197] Löscher, W., Gillard, M., Sands, Z. A., Kaminski, R. M. & Klitgaard, H. (2016) Synaptic Vesicle Glycoprotein 2A Ligands in the Treatment of Epilepsy and Beyond. *CNS Drugs*, 30(11), 1055-1077.

[198] Lüscher, C., Jan, L. Y., Stoffel, M., Malenka, R. C. & Nicoll, R. A. (1997) G protein-coupled inwardly rectifying K+ channels (GIRKs) mediate postsynaptic but not presynaptic transmitter actions in hippocampal neurons. *Neuron*, 19(3), 687-95.

[199] Magariños, A. M., Deslandes, A., & McEwen, B. S. (1999). Effects of antidepressants and benzodiazepine treatments on the dendritic structure of CA3 pyramidal neurons after chronic stress. *European Journal of Pharmacology*, *371*(2–3), 113–122. https://doi.org/10.1016/S0014-2999(99)00163-6

[200] Magee, J. C. (2000) Dendritic integration of excitatory synaptic input. *Nat Rev Neurosci*, 1(3), 181-90.

[201] Maksymenko, K. (2019). *Novel algorithmic approaches for the forward and inverse M/EEG problems*.

[202] Man, H.-Y., Sekine-Aizawa, Y., & Huganir, R. L. (2007). Regulation of α-amino-3-hydroxy-5-methyl-4-isoxazolepropionic acid receptor trafficking through PKA phosphorylation of the Glu

receptor 1 subunit. *Proceedings of the National Academy of Sciences*, *104*(9), 3579–3584.

[203] Mann, E. O., Radcliffe, C. A., & Paulsen, O. (2005). Hippocampal gamma-frequency oscillations: From interneurones to pyramidal cells, and back. *The Journal of Physiology*, *562*(1), 55–63. https://doi.org/10.1113/jphysiol.2004.078758

[204] Mao, T., Kusefoglu, D., Hooks, B. M., Huber, D., Petreanu, L. & Svoboda, K. (2011) Long-range neuronal circuits underlying the interaction between sensory and motor cortex. *Neuron*, 72(1), 111-23.

[205] Marksteiner, J., & Humpel, C. (2008). Beta-amyloid expression, release and extracellular deposition in aged rat brain slices. *Molecular Psychiatry*, *13*(10), 939–952. https://doi.org/10.1038/sj.mp.4002072

[206] Martin, B. S. & Kapur, J. (2008) A combination of ketamine and diazepam synergistically controls refractory status epilepticus induced by cholinergic stimulation. *Epilepsia*, 49(2), 248-55.

[207] Marx, M., Haas, C. A., & Häussler, U. (2013). Differential vulnerability of interneurons in the epileptic hippocampus. *Frontiers in Cellular Neuroscience*, *7*. https://doi.org/10.3389/fncel.2013.00167

[208] Matsuda, K., Kamiya, Y., Matsuda, S. & Yuzaki, M. (2002) Cloning and characterization of a novel NMDA receptor subunit NR3B: a dominant subunit that reduces calcium permeability. *Brain Res Mol Brain Res*, 100(1-2), 43-52.

[209] Mattia, D., Olivier, A. and Avoli, M., 1995. Seizure-like discharges recorded in human dysplastic neocortex maintained in vitro. *Neurology*, 45(7), pp.1391-1395.

[210] McBain, C., Boden, P. and Hill, R., 1989. Rat hippocampal slices 'in vitro' display spontaneous epileptiform activity following long-term organotypic culture. *Journal of Neuroscience Methods*, 27(1), pp.35-49.

[211] McCormick, D. A. & Pape, H. C. (1990) Properties of a hyperpolarization-activated cation current and its role in rhythmic oscillation in thalamic relay neurones. *J Physiol*, 431, 291-318.

[212] McEwen, B. S., & Olié, J. P. (2005). Neurobiology of mood, anxiety, and emotions as revealed by studies of a unique antidepressant: Tianeptine. *Molecular Psychiatry*, *10*(6), 525–537. https://doi.org/10.1038/sj.mp.4001648

[213] McHugh, K. L., & Kelly, J. P. (2018). *Modulation of the central opioid system as an antidepressant target in rodent models* (pp. 49–

87). https://doi.org/10.1016/bs.pbr.2018.07.003

[214] McNally, J. M., McCarley, R. W., McKenna, J. T., Yanagawa, Y., & Brown, R. E. (2011). Complex receptor mediation of acute ketamine application on in vitro gamma oscillations in mouse prefrontal cortex: Modeling gamma band oscillation abnormalities in schizophrenia.

[215] McNamara, J. O., Huang, Y. Z. & Leonard, A. S. (2006) Molecular signaling mechanisms underlying epileptogenesis. *Sci STKE*, 2006(356), re12.

[216] Meldrum, B. S. & Rogawski, M. A. (2007a) Molecular targets for antiepileptic drug development. *Neurotherapeutics*, 4(1), 18-61.

[217] Meldrum, B. S. & Rogawski, M. A. (2007b) Molecular targets for antiepileptic drug development. *Neurotherapeutics*, 4(1), 18-61.

[218] Meldrum, B., 2002. Concept of activity-induced cell death in epilepsy: historical and contemporary perspectives. *Progress in Brain Research*, pp.3-11.

[219] Meldrum, B., Vigouroux, R., Rage, P. and Brierley, J., 1973. Hippocampal lesions produced by prolonged seizures in paralyzed artificially ventilated baboons. *Experientia*, 29(5), pp.561-563.

[220] Mensah, S. A., Beavis, J. M., Thapar, A. K., & Kerr, M. (2006). The presence and clinical implications of depression in a community population of adults with epilepsy. *Epilepsy & Behavior*, *8*(1), 213–219. https://doi.org/10.1016/j.yebeh.2005.09.014

[221] Modebadze, T., Morgan, N. H., Pérès, I. A., Hadid, R. D., Amada, N., Hill, C., Williams, C., Stanford, I. M., Morris, C. M., Jones, R. S., Whalley, B. J. & Woodhall, G. L. (2016) A Low Mortality, High Morbidity Reduced Intensity Status Epilepticus (RISE) Model of Epilepsy and Epileptogenesis in the Rat. *PLoS One*, 11(2), e0147265.

[222] Mody, I., De Koninck, Y., Otis, T. S. & Soltesz, I. (1994) Bridging the cleft at GABA synapses in the brain. *Trends Neurosci*, 17(12), 517-25.

Molecular Brain, *13*(1), 23. https://doi.org/10.1186/s13041-020-0563-z

[223] MONESI, V. (1960). Differentiation of argyrophil and argentaffin cells in organotypic cultures of embryonic chick intestine. *Journal of Embryology and Experimental Morphology*, *8*, 302–313.

[224] Montenegro, M. A., Guerreiro, M. M., Lopes-Cendes, I., Guerreiro, C. A., Li, L. M. & Cendes, F. (2002) Association of family history of epilepsy with earlier age at seizure onset in patients with focal cortical dysplasia. *Mayo Clin Proc*, 77(12), 1291-4.

[225] Montgomery, S. A. (2005). Antidepressants and seizures: Emphasis on newer agents and clinical implications. *International Journal of Clinical Practice*, *59*(12), 1435–1440. https://doi.org/10.1111/j.1368-5031.2005.00731.x

[226] Moon, J., Jung, K.-H., Shin, J., Lim, J.-A., Byun, J.-I., Lee, S.-T., Chu, K., & Lee, S. K. (2014). Safety

[227] Morlock, E. V., & Czajkowski, C. (2011). Different Residues in the GABAA Receptor Benzodiazepine Binding Pocket Mediate Benzodiazepine Efficacy and Binding. *Molecular Pharmacology*, *80*(1), 14–22. https://doi.org/10.1124/mol.110.069542

[228] Mosa, A. J., Wang, S., Tan, Y. F., & Wojtowicz, J. M. (2015). Organotypic Slice Cultures for Studies of Postnatal Neurogenesis. *Journal of Visualized Experiments*, *97*. https://doi.org/10.3791/52353

[229] Murthy, V. N. & Fetz, E. E. (1996) Oscillatory activity in sensorimotor cortex of awake monkeys: synchronization of local field potentials and relation to behavior. *J Neurophysiol*, 76(6), 3949-67.

[230] Naffaa, M. M., Hung, S., Chebib, M., Johnston, G. A. R., & Hanrahan, J. R. (2017). GABA-ρ receptors: Distinctive functions and molecular pharmacology. *British Journal of Pharmacology*, *174*(13), 1881–1894. https://doi.org/10.1111/bph.13768

[231] Nagy, J., Kolok, S., Boros, A. & Dezso, P. (2005) Role of altered structure and function of NMDA receptors in development of alcohol dependence. *Curr Neuropharmacol*, 3(4), 281-97.

[232] Nakanishi, S. (1994) Metabotropic glutamate receptors: synaptic transmission, modulation, and plasticity. *Neuron*, 13(5), 1031-7.

Nature Reviews Neurology, *12*(2), 106–116. https://doi.org/10.1038/nrneurol.2015.243

[233] Naylor, D. E., Liu, H., Niquet, J. & Wasterlain, C. G. (2013) Rapid surface accumulation of NMDA receptors increases glutamatergic excitation during status epilepticus. *Neurobiol Dis*, 54, 225-38.

[234] Naylor, D. E., Liu, H., Niquet, J., & Wasterlain, C. G. (2013). Rapid surface accumulation of NMDA receptors increases glutamatergic excitation during status epilepticus. *Neurobiology of Disease*, *54*, 225–238. https://doi.org/10.1016/j.nbd.2012.12.015

[235] Needs, H. I., Henley, B. S., Cavallo, D., Gurung, S., Modebadze, T., Woodhall, G. & Henley, J. M. (2019) Changes in excitatory and inhibitory receptor expression and network activity during induction and establishment of epilepsy in the rat Reduced Intensity Status Epilepticus (RISE) model. *Neuropharmacology*, 158, 107728.

Neurology, *78*(8), 578–584. https://doi.org/10.1212/WNL.0b013e318247cd03

Neuron, *55*(5), 779–785. https://doi.org/10.1016/j.neuron.2007.07.035

Neuropharmacology, *41*(3), 360–368. https://doi.org/10.1016/S0028-3908(01)00079-X

Neuropsychiatric Disease and Treatment, 1693. https://doi.org/10.2147/NDT.S50371

Neuroscience Methods, *4*(4), 329–342. https://doi.org/10.1016/0165-0270(81)90003-0

Neuroscience, *199*, 51–63. https://doi.org/10.1016/j.neuroscience.2011.10.015

[236] Nguyen, Q.-T., & Kleinfeld, D. (2005). Positive Feedback in a Brainstem Tactile Sensorimotor Loop. *Neuron*, *45*(3), 447–457. https://doi.org/10.1016/j.neuron.2004.12.042

[237] Niquet, J., Baldwin, R., Suchomelova, L., Lumley, L., Naylor, D., Eavey, R. & Wasterlain, C. G. (2016) Benzodiazepine-refractory status epilepticus: pathophysiology and principles of treatment. *Ann N Y Acad Sci*, 1378(1), 166-173.

[238] Nudo, R. J., Jenkins, W. M., Merzenich, M. M., Prejean, T. & Grenda, R. (1992) Neurophysiological correlates of hand preference in primary motor cortex of adult squirrel monkeys. *J Neurosci*, 12(8), 2918-47.

[239] Oblasov I, Idzhilova O, Balaban P, Nikitin E. Cell culture models for epilepsy research and treatment. Explor Med. 2024;5:65–75. https://doi.org/10.37349/emed.2024.00206

of tianeptine use in patients with epilepsy. *Epilepsy & Behavior*, *34*, 116–119.

[240] Okazaki, M., Evenson, D. and Victor Nadler, J., 1995. Hippocampal mossy fiber sprouting and synapse formation after status epilepticus in rats: Visualization after retrograde transport of biocytin. *The Journal of Comparative Neurology*, 352(4), pp.515-534.

[241] Olsen, R. W., & Sieghart, W. (2009). GABAA receptors: Subtypes provide diversity of function and pharmacology. *Neuropharmacology*, *56*(1), 141–148. https://doi.org/10.1016/j.neuropharm.2008.07.045

Organization of the Parahippocampal-Hippocampal Network. *Annals of the New York Academy of Sciences*, *911*(1), 1–24. https://doi.org/10.1111/j.1749-6632.2000.tb06716.x

[242] Orlova, K. A. & Crino, P. B. (2010) The tuberous sclerosis complex. *Ann N Y Acad Sci*, 1184, 87-105.

[243] Ostergaard, K., Finsen, B. & Zimmer, J. (1995) Organotypic slice cultures of the rat striatum: an immunocytochemical, histochemical and in situ hybridization study of somatostatin, neuropeptide Y, nicotinamide adenine dinucleotide phosphate-diaphorase, and enkephalin. *Exp Brain Res*, 103(1), 70-84.

[244] Palmini, A., Najm, I., Avanzini, G., Babb, T., Guerrini, R., Foldvary-Schaefer, N., Jackson, G., Lüders, H. O., Prayson, R., Spreafico, R. & Vinters, H. V. (2004) Terminology and classification of the cortical dysplasias. *Neurology*, 62(6 Suppl 3), S2-8.

[245] Palva, J. M., Palva, S. & Kaila, K. (2005) Phase synchrony among neuronal oscillations in the human cortex. *J Neurosci*, 25(15), 3962-72.

[246] Pang, C. C.-C., Kiecker, C., O'Brien, J. T., Noble, W., & Chang, R. C.-C. (2019). Ammon's Horn 2 (CA2) of the Hippocampus: A Long-Known Region with a New Potential Role in

Neurodegeneration. *The Neuroscientist*, *25*(2), 167–180. https://doi.org/10.1177/1073858418778747

[247] Patsalos, P. N., Fröscher, W., Pisani, F., & Rijn, C. M. V. (2002). The Importance of Drug Interactions in Epilepsy Therapy. *Epilepsia*, *43*(4), 365–385. https://doi.org/10.1046/j.1528-1157.2002.13001.x

[248] Patten, A. R., Yau, S. Y., Fontaine, C. J., Meconi, A., Wortman, R. C., & Christie, B. R. (2015). The Benefits of Exercise on Structural and Functional Plasticity in the Rodent Hippocampus of Different Disease Models. *Brain Plasticity*, *1*(1), 97–127. https://doi.org/10.3233/BPL-150016

[249] Pavlidis, P. and Madison, D., 1999. Synaptic Transmission in Pair Recordings From CA3 Pyramidal Cells in Organotypic Culture. *Journal of Neurophysiology*, 81(6), pp.2787-2797.

[250] Perucca, E. (2006) Clinically relevant drug interactions with antiepileptic drugs. *Br J Clin Pharmacol*, 61(3), 246-55.

[251] Perucca, E., Cloyd, J., Critchley, D. & Fuseau, E. (2008) Rufinamide: clinical pharmacokinetics and concentration-response relationships in patients with epilepsy. *Epilepsia*, 49(7), 1123-41.

[252] Pitkänen, A., Bolkvadze, T. and Immonen, R., 2011. Anti-epileptogenesis in rodent post-traumatic epilepsy models. *Neuroscience Letters*, 497(3), pp.163-171.

[253] Pitkänen, A., Lukasiuk, K., Dudek, F. and Staley, K., 2015. Epileptogenesis. *Cold Spring Harbor Perspectives in Medicine*, 5(10), p.a022822.

[254] Plug, B.C., Revers, I.M., Breur, M. *et al.* Human post-mortem organotypic brain slice cultures: a tool to study pathomechanisms and test therapies. *acta neuropathol commun* **12**, 83 (2024). https://doi.org/10.1186/s40478-024-01784-1

[255] Poolos, N. P., Migliore, M. & Johnston, D. (2002) Pharmacological upregulation of h-channels reduces the excitability of pyramidal neuron dendrites. *Nat Neurosci*, 5(8), 767-74.

[256] Potter, S. M., & DeMarse, T. B. (2001). A new approach to neural cell culture for long-term studies. *Journal of Neuroscience Methods*, *110*(1–2), 17–24. https://doi.org/10.1016/S0165-0270(01)00412-5

[257] Prasad, A., Williamson, J. M. & Bertram, E. H. (2002) Phenobarbital and MK-801, but not phenytoin, improve the long-term outcome of status epilepticus. *Ann Neurol*, 51(2), 175-81.

[258] Purves, T., Middlemas, A., Agthong, S., Jude, E. B., Boulton, A. J., Fernyhough, P. & Tomlinson,

[259] Quilichini, P. P., Diabira, D., Chiron, C., Milh, M., Ben-Ari, Y., & Gozlan, H. (2003). Effects of Antiepileptic Drugs on Refractory Seizures in the Intact Immature Corticohippocampal Formation In Vitro. *Epilepsia*, *44*(11), 1365–1374. https://doi.org/10.1046/j.1528-

1157.2003.19503.x

[260] Rajani, V., Sengar, A. S., & Salter, M. W. (2020). Tripartite signalling by NMDA receptors.

[261] Rajasekaran, K., Todorovic, M. & Kapur, J. (2012) Calcium-permeable AMPA receptors are expressed in a rodent model of status epilepticus. *Ann Neurol*, 72(1), 91-102.

[262] Rawal, B.; Rancic, V.; Ballanyi, K. NMDA Enhances and Glutamate Attenuates Synchrony of Spontaneous Phase-Locked Locus Coeruleus Network Rhythm in Newborn Rat Brain Slices. *Brain Sci.* **2022**, *12*, 651. https://doi.org/10.3390/brainsci12050651

[263] Reeta, K., Prabhakar, P., & Gupta, Y. K. (2016). Anticonvulsant activity of the antidepressant drug, tianeptine, against pentylenetetrazole-induced seizures mitigates cognitive impairment in rats. *Behavioural Pharmacology*, *27*(7), 623–632. https://doi.org/10.1097/FBP.0000000000000257

repeated treatment with tianeptine and fluoxetine on the central α1-adrenergic system.

[264] Ribot, R., Ouyang, B., & Kanner, A. M. (2017). The impact of antidepressants on seizure frequency and depressive and anxiety disorders of patients with epilepsy: Is it worth investigating? *Epilepsy & Behavior*, *70*, 5–9. https://doi.org/10.1016/j.yebeh.2017.02.032

[265] Rioult-Pedotti, M. S., Friedman, D., Hess, G. & Donoghue, J. P. (1998) Strengthening of horizontal cortical connections following skill learning. *Nat Neurosci*, 1(3), 230-4.

[266] Rivara, C. B., Sherwood, C. C., Bouras, C. & Hof, P. R. (2003) Stereologic characterization and spatial distribution patterns of Betz cells in the human primary motor cortex. *Anat Rec A Discov Mol Cell Evol Biol*, 270(2), 137-51.

[267] Rivera, C., Voipio, J., & Kaila, K. (2005). Two developmental switches in GABAergic signalling: The K^+-Cl^- cotransporter KCC2 and carbonic anhydrase CAVII. *The Journal of Physiology*, *562*(1), 27–36. https://doi.org/10.1113/jphysiol.2004.077495

[268] Roberts, E. & Frankel, S. (1950) gamma-Aminobutyric acid in brain: its formation from glutamic acid. *J Biol Chem*, 187(1), 55-63.

[269] Robertson, R. T., Baratta, J., Kageyama, G. H., Ha, D. H. & Yu, J. (1997) Specificity of attachment and neurite outgrowth of dissociated basal forebrain cholinergic neurons seeded on to organotypic slice cultures of forebrain. *Neuroscience*, 80(3), 741-52.

[270] Robinson, R. B. & Siegelbaum, S. A. (2003) Hyperpolarization-activated cation currents: from molecules to physiological function. *Annu Rev Physiol*, 65, 453-80.

[271] Rogóż, Z., Skuza, G., Dlaboga, D., Maj, J., & Dziedzicka-Wasylewska, M. (2001). Effect of

[272] Roohi-Azizi, M., Azimi, L., Heysieattalab, S. & Aamidfar, M. (2017) Changes of the brain's

bioelectrical activity in cognition, consciousness, and some mental disorders. *Med J Islam Repub Iran*, 31, 53.

[273] Roohi-Azizi, M., Azimi, L., Heysieattalab, S., & Aamidfar, M. (2017). Changes of the brain's bioelectrical activity in cognition, consciousness, and some mental disorders. *Medical Journal of the Islamic Republic of Iran*, *31*(1), 307–312. https://doi.org/10.14196/mjiri.31.53

[274] Roopun, A. K., Simonotto, J. D., Pierce, M. L., Jenkins, A., Nicholson, C., Schofield, I. S., Whittaker, R. G., Kaiser, M., Whittington, M. A., Traub, R. D. & Cunningham, M. O. (2010) A nonsynaptic mechanism underlying interictal discharges in human epileptic neocortex. *Proc Natl Acad Sci U S A*, 107(1), 338-43.

[275] Roopun, A. K., Traub, R. D., Baldeweg, T., Cunningham, M. O., Whittaker, R. G., Trevelyan, A., Duncan, R., Russell, A. J. & Whittington, M. A. (2009) Detecting seizure origin using basic, multiscale population dynamic measures: preliminary findings. *Epilepsy Behav*, 14 Suppl 1, 39-46.

[276] Rossetti, A. O. (2006). Prognosis of status epilepticus: Role of aetiology, age, and consciousness impairment at presentation. *Journal of Neurology, Neurosurgery & Psychiatry*,

[277] Rothman RB, Baumann MH. Therapeutic and adverse actions of serotonin transporter substrates. *Pharmacol Ther*. 2002;95:73–88.

[278] Rundfeldt, C. & Netzer, R. (2000) Investigations into the mechanism of action of the new anticonvulsant retigabine. Interaction with GABAergic and glutamatergic neurotransmission and with voltage gated ion channels. *Arzneimittelforschung*, 50(12), 1063-70.

S. D., Stanford, I. M. & Woodhall, G. L. (2017) Phase-amplitude coupled persistent theta and gamma oscillations in rat primary motor cortex in vitro. *Neuropharmacology*, 119, 141-156.

S. D., Stanford, I. M., & Woodhall, G. L. (2017). Phase-amplitude coupled persistent theta and gamma oscillations in rat primary motor cortex in vitro. *Neuropharmacology*, *119*, 141–156. https://doi.org/10.1016/j.neuropharm.2017.04.009

[279] Sabolek, H., Swiercz, W., Lillis, K., Cash, S., Huberfeld, G., Zhao, G., Ste. Marie, L., Clemenceau, S., Barsh, G., Miles, R. and Staley, K., 2012. A Candidate Mechanism Underlying the Variance of Interictal Spike Propagation. *Journal of Neuroscience*, 32(9), pp.3009-3021.

[280] Sakaguchi, T., Okada, M. and Kawasaki, K., 1994. Sprouting of CA3 pyramidal neurons to the dentate gyrus in rat hippocampal organotypic cultures. *Neuroscience Research*, 20(2), pp.157-164.

[281] Sakamoto, T., Arissian, K. & Asanuma, H. (1989) Functional role of the sensory cortex in learning motor skills in cats. *Brain Res*, 503(2), 258-64.

[282] SAMPAOLO, C. L., & SAMPAOLO, G. (1956). Organotypic cultures of chick embryo lung; some histologic and histochemical aspects. *Bollettino Della Societa Italiana Di Biologia Sperimentale*, *32*(7–8), 797–801.

[283] Sanes, J. N. & Donoghue, J. P. (1997) Static and dynamic organization of motor cortex. *Adv Neurol*, 73, 277-96.

[284] Sanes, J. N. & Donoghue, J. P. (2000) Plasticity and primary motor cortex. *Annu Rev Neurosci*, 23, 393-415.

[285] Sanz-Clemente, A., Gray, J. A., Ogilvie, K. A., Nicoll, R. A. & Roche, K. W. (2013a) Activated CaMKII couples GluN2B and casein kinase 2 to control synaptic NMDA receptors. *Cell Rep*, 3(3), 607-14.

[286] Schierhout, G. and Roberts, I., 2001. Antiepileptic drugs for preventing seizures following acute traumatic brain injury. *Cochrane Database of Systematic Reviews*,

[287] Schulte, J. T., Wierenga, C. J. & Bruining, H. (2018) Chloride transporters and GABA polarity in developmental, neurological and psychiatric conditions. *Neurosci Biobehav Rev*, 90, 260-271.

[288] Semple, B. D., Blomgren, K., Gimlin, K., Ferriero, D. M., & Noble-Haeusslein, L. J. (2013). Brain development in rodents and humans: Identifying benchmarks of maturation and vulnerability to injury across species. *Progress in Neurobiology*, *106–107*, 1–16. https://doi.org/10.1016/j.pneurobio.2013.04.001

[289] Sharma, A., Dahiya, N., Khanapure, A., & Kairi, J. (2016). Effect of tianeptine on seizure threshold and anticonvulsant activity of valproate, phenobarbitone and phenytoin in mice.

[290] Sherman, S. M. (2014) The function of metabotropic glutamate receptors in thalamus and cortex. *Neuroscientist*, 20(2), 136-49.

[291] Shetty, A. K., & Turner, D. A. (2001). Glutamic Acid Decarboxylase-67-Positive Hippocampal Interneurons Undergo a Permanent Reduction in Number Following Kainic Acid-Induced Degeneration of CA3 Pyramidal Neurons. *Experimental Neurology*, *169*(2), 276–297. https://doi.org/10.1006/exnr.2001.7668

[292] Shipp, S. (2007) Structure and function of the cerebral cortex. *Curr Biol*, 17(12), R443-9.

[293] Shmuely, S., Sisodiya, S. M., Gunning, W. B., Sander, J. W. & Thijs, R. D. (2016) Mortality in Dravet syndrome: A review. *Epilepsy Behav*, 64(Pt A), 69-74.

[294] Shorvon, S. & Ferlisi, M. (2011) The treatment of super-refractory status epilepticus: a critical review of available therapies and a clinical treatment protocol. *Brain*, 134(Pt 10), 2802-18.

[295] Sieghart, W., & Savić, M. M. (2018). International Union of Basic and Clinical Pharmacology. CVI: GABA $_A$ Receptor Subtype- and Function-selective Ligands: Key Issues in Translation to Humans. *Pharmacological Reviews*, *70*(4), 836–878. https://doi.org/10.1124/pr.117.014449

[296] Simoni, A., Griesinger, C. and Edwards, F., 2003. Development of Rat CA1 Neurones in Acute Versus Organotypic Slices: Role of Experience in Synaptic Morphology and Activity. *The Journal of Physiology*, 550(1), pp.135-147.

[297] Sirven, J. I. (2015). Epilepsy: A Spectrum Disorder. *Cold Spring Harbor Perspectives in Medicine*, *5*(9), a022848. https://doi.org/10.1101/cshperspect.a022848

[298] Smith, B. and Dudek, F., 2001. Short- and Long-Term Changes in CA1 Network Excitability After Kainate Treatment in Rats. *Journal of Neurophysiology*, 85(1), pp.1-9.

[299] Sokolova, S., Schmitz, D., Zhang, C. L., Loscher, W., & Heinemann, U. (1998). Comparison of Effects of Valproate and Trans-2-en-Valproate on Different Forms of Epileptiform Activity in Rat Hippocampal and Temporal Cortex Slices. *Epilepsia*, *39*(3), 251–258. https://doi.org/10.1111/j.1528-1157.1998.tb01369.x

[300] Stafstrom, C. and Carmant, L., 2015. Seizures and Epilepsy: An Overview for Neuroscientists. *Cold Spring Harbor Perspectives in Medicine*, 5(6), pp.a022426-a022426.

[301] Stafstrom, C. E. & Carmant, L. (2015) Seizures and epilepsy: an overview for neuroscientists. *Cold Spring Harb Perspect Med*, 5(6).

[302] Staiger, J. F., Flagmeyer, I., Schubert, D., Zilles, K., Kötter, R. & Luhmann, H. J. (2004) Functional diversity of layer IV spiny neurons in rat somatosensory cortex: quantitative morphology of electrophysiologically characterized and biocytin labeled cells. *Cereb Cortex*, 14(6), 690-701.

[303] Staiger, J. F., Zuschratter, W., Luhmann, H. J. & Schubert, D. (2009) Local circuits targeting parvalbumin-containing interneurons in layer IV of rat barrel cortex. *Brain Struct Funct*, 214(1), 1-13.

[304] Staley, K. J., & Dudek, F. E. (2006). Interictal Spikes and Epileptogenesis. *Epilepsy Currents*, *6*(6), 199–202. https://doi.org/10.1111/j.1535-7511.2006.00145.x

[305] Staley, K. J., Soldo, B. L. & Proctor, W. R. (1995) Ionic mechanisms of neuronal excitation by inhibitory GABAA receptors. *Science*, 269(5226), 977-81.

[306] Steward, O., & Scoville, S. A. (1976). Cells of origin of entorhinal cortical afferents to the hippocampus and fascia dentata of the rat. *The Journal of Comparative Neurology*, *169*(3), 347–370. https://doi.org/10.1002/cne.901690306

[307] Stoppini, L., Buchs, P. A. & Muller, D. (1991) A simple method for organotypic cultures of

nervous tissue. *J Neurosci Methods*, 37(2), 173-82.

[308] Stoppini, L., Buchs, P.-A., & Muller, D. (1991). A simple method for organotypic cultures of nervous tissue. *Journal of Neuroscience Methods*, *37*(2), 173–182. https://doi.org/10.1016/0165-0270(91)90128-M

[309] Su Liu, Candan Gurses, Zhiyi Sha, Michael M Quach, Altay Sencer, Nerses Bebek, Daniel J Curry, Sujit Prabhu, Sudhakar Tummala, Thomas R Henry, Nuri F Ince, Stereotyped high-frequency oscillations discriminate seizure onset zones and critical functional cortex in focal epilepsy, *Brain*, Volume 141, Issue 3, March 2018, Pages 713–730, https://doi.org/10.1093/brain/awx374

[310] Svenningsson, P., Bateup, H., Qi, H., Takamiya, K., Huganir, R. L., Spedding, M., Roth, B. L., McEwen, B. S., & Greengard, P. (2007). Involvement of AMPA receptor phosphorylation in antidepressant actions with special reference to tianeptine. *European Journal of Neuroscience*, *26*(12), 3509–3517. https://doi.org/10.1111/j.1460-9568.2007.05952.x

[311] Taylor, D. C. & Bower, B. D. (1971) Prevention in epileptic disorders. *Lancet*, 2(7734), 1136-8.

[312] Temkin, N., 2001. Antiepileptogenesis and Seizure Prevention Trials with Antiepileptic Drugs: Meta-Analysis of Controlled Trials. *Epilepsia*, 42(4), pp.515-524.

[313] Temkin, N., 2009. Preventing and treating posttraumatic seizures: The human experience. *Epilepsia*, 50, pp.10-13.

[314] Terranova, J. I., Ogawa, S. K., & Kitamura, T. (2019). Adult hippocampal neurogenesis for systems consolidation of memory. *Behavioural Brain Research*, *372*, 112035. https://doi.org/10.1016/j.bbr.2019.112035

[315] Terunuma, M., Xu, J., Vithlani, M., Sieghart, W., Kittler, J., Pangalos, M., Haydon, P. G., Coulter, *The Journal of Physiology*, *385*(1), 243–286. https://doi.org/10.1113/jphysiol.1987.sp016493

[316] Tiesinga, P. & Sejnowski, T. J. (2009) Cortical enlightenment: are attentional gamma oscillations driven by ING or PING? *Neuron*, 63(6), 727-32.

[317] Traub, R. D., Bibbig, A., Fisahn, A., LeBeau, F. E., Whittington, M. A. & Buhl, E. H. (2000) A model of gamma-frequency network oscillations induced in the rat CA3 region by carbachol in vitro. *Eur J Neurosci*, 12(11), 4093-106.

[318] Traub, R. D., Michelson-Law, H., Bibbig, A. E., Buhl, E. H. & Whittington, M. A. (2004) Gap junctions, fast oscillations and the initiation of seizures. *Adv Exp Med Biol*, 548, 110-22.

[319] Traub, R. D., Whittington, M. A., Colling, S. B., Buzsáki, G. & Jefferys, J. G. (1996a) Analysis of

gamma rhythms in the rat hippocampus in vitro and in vivo. *J Physiol*, 493 (Pt 2), 471-84.

[320] Traub, R. D., Whittington, M. A., Stanford, I. M. & Jefferys, J. G. (1996b) A mechanism for generation of long-range synchronous fast oscillations in the cortex. *Nature*, 383(6601), 621-4.

[321] Traynelis, S. F., Wollmuth, L. P., McBain, C. J., Menniti, F. S., Vance, K. M., Ogden, K. K., Hansen,

[322] Treiman, D. M., Walton, N. Y., & Kendrick, C. (1990). A progressive sequence of electroencephalographic changes during generalized convulsive status epilepticus. *Epilepsy Research*, *5*(1), 49–60. https://doi.org/10.1016/0920-1211(90)90065-4

[323] Trinka, E. (2012) Ideal characteristics of an antiepileptic drug: how do these impact treatment decisions for individual patients? *Acta Neurol Scand Suppl*(194), 10-8.

[324] Trinka, E., Cock, H., Hesdorffer, D., Rossetti, A. O., Scheffer, I. E., Shinnar, S., Shorvon, S. & Lowenstein, D. H. (2015) A definition and classification of status epilepticus--Report of the ILAE Task Force on Classification of Status Epilepticus. *Epilepsia*, 56(10), 1515-23.

[325] Trinka, E., Höfler, J. & Zerbs, A. (2012) Causes of status epilepticus. *Epilepsia*, 53 Suppl 4, 127-38.

[326] Turetsky, D., Garringer, E., & Patneau, D. K. (2005). Stargazin Modulates Native AMPA Receptor Functional Properties by Two Distinct Mechanisms. *The Journal of Neuroscience*, *25*(32), 7438–7448. https://doi.org/10.1523/JNEUROSCI.1108-05.2005

[327] Turrigiano, G. G. & Nelson, S. B. (1998) Thinking globally, acting locally: AMPA receptor turnover and synaptic strength. *Neuron*, 21(5), 933-5.

[328] Turrigiano, G. G. & Nelson, S. B. (2004) Homeostatic plasticity in the developing nervous system. *Nat Rev Neurosci*, 5(2), 97-107.

[329] Turrigiano, G. G. (2008) The self-tuning neuron: synaptic scaling of excitatory synapses. *Cell*, 135(3), 422-35.

[330] Turski, W. A., Cavalheiro, E. A., Schwarz, M., Czuczwar, S. J., Kleinrok, Z., & Turski, L. (1983). Limbic seizures produced by pilocarpine in rats: Behavioural, electroencephalographic and neuropathological study. *Behavioural Brain Research*, *9*(3), 315–335. https://doi.org/10.1016/0166-4328(83)90136-5

[331] Ueta, Y., Otsuka, T., Morishima, M., Ushimaru, M. & Kawaguchi, Y. (2014) Multiple layer 5 pyramidal cell subtypes relay cortical feedback from secondary to primary motor areas in rats. *Cereb Cortex*, 24(9), 2362-76.

[332] Uhlhaas, P. J. & Singer, W. (2006) Neural synchrony in brain disorders: relevance for cognitive dysfunctions and pathophysiology. *Neuron*, 52(1), 155-68.

[333] Uhlhaas, P. J. & Singer, W. (2011) The development of neural synchrony and large-scale cortical networks during adolescence: relevance for the pathophysiology of schizophrenia and neurodevelopmental hypothesis. *Schizophr Bull*, 37(3), 514-23.

[334] Uhlhaas, P. J., Pipa, G., Neuenschwander, S., Wibral, M. & Singer, W. (2011) A new look at gamma? High- (>60 Hz) γ-band activity in cortical networks: function, mechanisms and impairment. *Prog Biophys Mol Biol*, 105(1-2), 14-28.

[335] Uusi-Oukari, M., & Korpi, E. R. (2010). Regulation of GABAA Receptor Subunit Expression by Pharmacological Agents. *Pharmacological Reviews*, *62*(1), 97–135. https://doi.org/10.1124/pr.109.002063

[336] Uusi-Oukari, M., Kontturi, L. S., Kallinen, S. A. & Salonen, V. (2010) AMPA receptors serum-dependently mediate GABAA receptor alpha1 and alpha6 subunit down-regulation in cultured mouse cerebellar granule cells. *Neurochem Int*, 56(5), 720-6.

[337] Uva, L. and de Curtis, M., 2005. Polysynaptic olfactory pathway to the ipsi- and contralateral entorhinal cortex mediated via the hippocampus. *Neuroscience*, 130(1), pp.249-258.

[338] Vakilna, Y. S., Tang, W. C., Wheeler, B. C., & Brewer, G. J. (2021). The Flow of Axonal Information Among Hippocampal Subregions: 1. Feed-Forward and Feedback Network Spatial Dynamics Underpinning Emergent Information Processing. *Frontiers in Neural Circuits*, *15*. https://doi.org/10.3389/fncir.2021.660837

[339] Vitureira, N. & Goda, Y. (2013) Cell biology in neuroscience: the interplay between Hebbian and homeostatic synaptic plasticity. *J Cell Biol*, 203(2), 175-86.

W. (2006) Epileptogenesis in pediatric cortical dysplasia: the dysmature cerebral developmental hypothesis. *Epilepsy Behav*, 9(2), 219-35.

[340] Wagstaff, A. J., Ormrod, D., & Spencer, C. M. (2001). Tianeptine: A Review of its Use in Depressive Disorders. *CNS Drugs*, *15*(3), 231–259. https://doi.org/10.2165/00023210-

[341] Wang, S. J., Huang, C. C., Hsu, K. S., Tsai, J. J. & Gean, P. W. (1996) Presynaptic inhibition of excitatory neurotransmission by lamotrigine in the rat amygdalar neurons. *Synapse*, 24(3), 248-55.

[342] Watanabe, M., & Fukuda, A. (2015). Development and regulation of chloride homeostasis in the central nervous system. *Frontiers in Cellular Neuroscience*, *9*. https://doi.org/10.3389/fncel.2015.00371

[343] Wenthold, R. J., Petralia, R. S., Blahos J, I. I. & Niedzielski, A. S. (1996) Evidence for multiple AMPA receptor complexes in hippocampal CA1/CA2 neurons. *J Neurosci*, 16(6), 1982-9.

[344] Whalley, K. (2007). Balancing LTP and LTD. *Nature Reviews Neuroscience*, *8*(4), 249–249. https://doi.org/10.1038/nrn2123

[345] Whittington, M. A., Traub, R. D. & Jefferys, J. G. (1995) Synchronized oscillations in interneuron networks driven by metabotropic glutamate receptor activation. *Nature*, 373(6515), 612-5.

[346] Whitton, P. S., Sarna, G. S., Datla, K. P., & Curzon, G. (1991). Effects of tianeptine on stress-induced behavioural deficits and 5-HT dependent behaviour. *Psychopharmacology*, *104*(1), 81–85. https://doi.org/10.1007/BF02244558

[347] Wichmann, T. & DeLong, M. R. (1999) Oscillations in the basal ganglia. *Nature*, 400(6745), 621-2.

[348] Wilcox, K., Dixon-Salazar, T., Sills, G., Ben-Menachem, E., Steve White, H., Porter, R., Dichter, M., Moshé, S., Noebels, J., Privitera, M. and Rogawski, M., 2013. Issues related to development of new antiseizure treatments. *Epilepsia*, 54, pp.24-34.

[349] Wilde, M. I., & Benfield, P. (1995). Tianeptine. A review of its pharmacodynamic and pharmacokinetic properties, and therapeutic efficacy in depression and coexisting anxiety and depression. *Drugs*, *49*(3), 411–439. https://doi.org/10.2165/00003495-199549030-00007

[350] Williams, P., White, A., Clark, S., Ferraro, D., Swiercz, W., Staley, K. and Dudek, F., 2009. Development of Spontaneous Recurrent Seizures after Kainate-Induced Status Epilepticus. *Journal of Neuroscience*, 29(7), pp.2103-2112.

[351] Williams, S. R. & Stuart, G. J. (2000) Site independence of EPSP time course is mediated by dendritic I(h) in neocortical pyramidal neurons. *J Neurophysiol*, 83(5), 3177-82.

[352] WITTER, M. P., WOUTERLOOD, F. G., NABER, P. A., & HAEFTEN, T. V. (2000). Anatomical

[353] Wolf, M. K. (1970). Anatomy of cultured mouse cerebellum. II. Organotypic migration of granule cells demonstrated by silver impregnation of normal and mutant cultures. *The Journal of Comparative Neurology*, *140*(3), 281–297. https://doi.org/10.1002/cne.901400304

[354] Wong, M. (2009). The Window of Epileptogenesis: Looking beyond the Latent Period. *Epilepsy Currents*, *9*(5), 144–145. https://doi.org/10.1111/j.1535-7511.2009.01322.x

[355] Wright, A. & Vissel, B. (2012) The essential role of AMPA receptor GluR2 subunit RNA editing in the normal and diseased brain. *Front Mol Neurosci*, 5, 34.

[356] Wuarin, J.-P., & Dudek, F. E. (1996). Electrographic Seizures and New Recurrent Excitatory Circuits in the Dentate Gyrus of Hippocampal Slices from Kainate-Treated Epileptic Rats. *The Journal of Neuroscience*, *16*(14), 4438–4448. https://doi.org/10.1523/JNEUROSCI.16-14-

[357] Wyneken, U., Marengo, J. J., Villanueva, S., Soto, D., Sandoval, R., Gundelfinger, E. D. & Orrego,

[358] Yaari, Y., Selzer, M. E. & Pincus, J. H. (1986) Phenytoin: mechanisms of its anticonvulsant action. *Ann Neurol*, 20(2), 171-84.

[359] Yamada, K. A. & Turetsky, D. M. (1996) Allosteric interactions between cyclothiazide and AMPA/kainate receptor antagonists. *Br J Pharmacol*, 117(8), 1663-72.

[360] Yamawaki, N. & Shepherd, G. M. (2015) Synaptic circuit organization of motor corticothalamic neurons. *J Neurosci*, 35(5), 2293-307.

[361] Yamawaki, N., Borges, K., Suter, B. A., Harris, K. D. & Shepherd, G. M. (2014) A genuine layer 4 in motor cortex with prototypical synaptic circuit connectivity. *Elife*, 3, e05422.

[362] Yamawaki, N., Stanford, I. M., Hall, S. D. & Woodhall, G. L. (2008) Pharmacologically induced and stimulus evoked rhythmic neuronal oscillatory activity in the primary motor cortex in vitro. *Neuroscience*, 151(2), 386-95.

[363] Yang, S. S., Li, Y. C., Coley, A. A., Chamberlin, L. A., Yu, P. & Gao, W. J. (2018) Cell-Type Specific Development of the Hyperpolarization-Activated Current, Ih, in Prefrontal Cortical Neurons. *Front Synaptic Neurosci*, 10, 7.

[364] Yano, S., Tokumitsu, H. & Soderling, T. R. (1998) Calcium promotes cell survival through CaM-K kinase activation of the protein-kinase-B pathway. *Nature*, 396(6711), 584-7.

[365] Zapukhliak O, Netsyk O, Romanov A, Maximyuk O, Oz M, Holmes GL, et al. (2021) Mecamylamine inhibits seizure-like activity in CA1-CA3 hippocampus through antagonism to nicotinic receptors. *PLoS ONE* 16(3): e0240074. https://doi.org/10.1371/journal.pone.0240074

[366] Zaqout, S. & Kaindl, A. M. (2016) Golgi-Cox Staining Step by Step. *Front Neuroanat*, 10, 38.

[367] Zeng, L. H., Xu, L., Gutmann, D. H. & Wong, M. (2008) Rapamycin prevents epilepsy in a mouse model of tuberous sclerosis complex. *Ann Neurol*, 63(4), 444-53.

[368] Zenke, F., Agnes, E. J. & Gerstner, W. (2015) Diverse synaptic plasticity mechanisms orchestrated to form and retrieve memories in spiking neural networks. *Nat Commun*, 6, 6922.

[369] Zhang, D., Hou, Q., Wang, M., Lin, A., Jarzylo, L., Navis, A., Raissi, A., Liu, F., & Man, H.-Y. (2009). Na,K-ATPase Activity Regulates AMPA Receptor Turnover through Proteasome-Mediated Proteolysis. *The Journal of Neuroscience*, *29*(14), 4498–4511. https://doi.org/10.1523/JNEUROSCI.6094-08.2009

[370] Zhang, X. X., Min, X. C., Xu, X. L., Zheng, M. & Guo, L. J. (2016) ZD7288, a selective hyperpolarization-activated cyclic nucleotide-gated channel blocker, inhibits hippocampal

synaptic plasticity. *Neural Regen Res*, 11(5), 779-86.

[371] Zhou, F. M. & Hablitz, J. J. (1996) Morphological properties of intracellularly labeled layer I neurons in rat neocortex. *J Comp Neurol*, 376(2), 198-213.

[372] Ziburkus, J., Cressman, J., Barreto, E. and Schiff, S., 2006. Interneuron and Pyramidal Cell Interplay During In Vitro Seizure-Like Events. *Journal of Neurophysiology*, 95(6), pp.3948-3954.

[373] Zold, C. L., & Shuler, M. G. H. (2015). Theta Oscillations in Visual Cortex Emerge with Experience to Convey Expected Reward Time and Experienced Reward Rate. *Journal of Neuroscience*, *35*(26), 9603–9614. https://doi.org/10.1523/JNEUROSCI.0296-15.2015